Ecological principles of colonisation resistance in the gut microbiome



Frances Spragge

Magdalen College

University of Oxford

A thesis submitted for the degree of
Doctor of Philosophy
Michaelmas 2023

Statement of originality

I declare that this thesis was composed by myself, that the work contained herein is my own except where explicitly stated. This work has not been submitted for any degree or professional qualification except as specified.

Frances Spragge, Michaelmas term 2023

For Louise, Charles and Verity

Abstract

The mammalian gut is home to hundreds of species of microbes, collectively known as the gut microbiome. A key benefit conferred by the gut microbiome is protection against pathogens, known as colonisation resistance. The importance of colonisation resistance by the microbiome has been recognised for decades. A range of potential mechanisms underlying the protection against pathogens have been identified, including direct competition between the resident microbiota and pathogens. But when I started my research for this thesis, understanding how they work was restricted to specific communities and contexts and we lacked the ability to understand why one microbial community is protective while another is not. In this thesis I take an ecological approach to the human microbiota to seek general rules of colonisation resistance and discover two key ecological principles and the mechanism that underlies them.

I begin with an *in vitro* screen of 100 human gut strains to assess their individual ability to resist the growth of a critically antimicrobial-resistant model pathogen, *Klebsiella pneumoniae*. This screen shows that single species have negligible effects on pathogen growth. Next, I combine the best-ranked species from the screen and find that, together, colonisation resistance ability is greatly increased. To explore this community effect further, I randomly assemble gut communities of varying diversity and composition. Testing these communities against *K. pneumoniae* reveals that, in general, more diverse communities provide better colonisation resistance against the pathogen. A closer look at the data shows it is the communities that are both diverse and contain the competitor species *Escherichia coli* that have the greatest ability to suppress *K. pneumoniae* growth. Along with dropout experiments, where diverse communities are constructed without *E. coli*, it is deduced that species richness and community composition are both important for colonisation resistance. Diverse communities that do not contain *E. coli* are much less effective at resisting pathogen growth than those that do. The first general ecological principle of colonisation resistant communities is, therefore, the presence of a key competitor species closely related to the pathogen, such as *E. coli*. However, *E. coli* also needs to be part of a community of other gut species in order to exert strong suppression on *K. pneumoniae* growth. It follows that the second general principle of colonisation resistance is having an ecologically diverse community. To find out if these results apply in a more spatially complex host environment, I test the communities using a gnotobiotic mouse model. *In vivo*, I discover that I am able to reproduce the *in vitro* results.

Next, I turn to identifying the mechanism that underlies these two ecological principles. Comparing the nutrient use profiles of the communities and *K. pneumoniae* shows that the higher the nutrient use overlap is between a community and the pathogen, the greater the ability of the community to resist pathogen growth. This ability of a microbial community to resist pathogen growth by using the available nutrients is termed nutrient blocking. Supplementing the communities with a nutrient unique to *K. pneumoniae* removes suppression of pathogen growth, supporting the finding that nutrient blocking is the basis for colonisation resistance in these communities. Moreover, it is shown that predictions based on nutrient use or protein family overlap between gut communities and another pathogen, a clinical isolate of *E. coli*, can be made and experimentally validated. The ability to predict which combinations of gut bacteria will best suppress pathogen growth suggests a way to rationally design pathogen-protective communities ahead of time. I discuss the implications of my work for the current goal to engineer gut communities to prevent and treat infectious disease as a much-needed alternative to antibiotics.

Acknowledgments

I first would like to thank my DPhil supervisor, Kevin Foster. Since your lectures during my undergraduate and having you supervise my extended essay back in 2017, I knew I wanted to do my DPhil in your lab. You inspired me about science then, and continue to do so now. Thank you for always encouraging me, being there for guidance and for injecting fun and enthusiasm into the day-to-day. I will remember the many freezing outdoor meetings at the benches or in the park throughout the pandemic winters, and the ice throwing the day the experiments didn't work! To Olivier for teaching me so much in the lab at the very beginning of my DPhil, it was a blessing to work with you and I am so grateful. Erik, I am very glad to have been able to work with and learn so much from you, thank you. It has made the early mornings in the lab and trips up the hill much more fun! To Thomas, Signe and Kate for being wonderful co-DPhil students and Thomas for your advice, lunchbreaks and games of tennis. To the rest of the Foster Group past and present (Lou, Sean, Elisa, Holly, Jake, Martin, Bella, Rav, Will, Connor, Anna, Ryan and more), thank you for being the loveliest group of people and the most supportive and friendly team I could ever hope to work with!

To my family (mum, dad and Verity) for everything and for always being there, this is for you (and Daffy!). To Anne Spragge (Gran Gran), for always being interested in the science, and Naz for your support. To Laura and Maisie for being amazing friends and housemates over the last three years, for the countless delicious dinners, lockdown evenings and library sessions, I could not have done it without you. Ashna, my first friend on the DTP, I am so grateful that we have gone on this journey together and I have loved the lunches, bookshop browsing and ice cream trips. Maria, thank you for being a great friend and for all the Biochemistry coffees and catch-ups. To Laura, Ashna and Louis for the summer evenings spent playing tennis. Also, Issy, Kyra, Steve, Ercole, Annie, thank you for being wonderful friends in Oxford over the last few years. Lizzie, Tom and Rob, you are the best, and our annual holidays these past few years have been fantastic.

Thank you to Instituto Gulbenkian de Ciência in Portugal for organising and giving me the opportunity to attend the wonderful and inspiring SymbNET summer school on host-microbe symbiosis in July 2023 as I was writing my thesis. Last but not least, thank you to Esther Becker, Jen Massey and Lucy Taylor for your support at the DTP, and to the BBSRC for funding my DPhil and enabling me to present at and attend conferences in my final year.

Contributions

The data in Chapters 3, 4 and 5 are collaborative efforts though the majority of the work in each is my own. The contributions of others are summarised here.

The Heidelberg strains were a gift from Nassos Typas, EMBL Heidelberg. The AMR *E. coli* strain was from Nottingham University Hospitals Pathogen Bank. Kevin Foster conceived the study. Kevin Foster, Olivier Cunrath, Erik Bakkeren and I designed the experimental framework. The anaerobic culturing and general microbiome methods (detailed in Chapter 2) were developed alongside Olivier Cunrath, Erik Bakkeren, Xuedan Wang and Louise Pankhurst. I carried out the *in vitro* experiments at the Department of Biochemistry. I carried out the gnotobiotic mouse experiments at the germ-free facility in the Kennedy Institute of Rheumatology with the help of Erik Bakkeren, Claire Pearson and Elizete Araujo. Erik Bakkeren carried out the biolog analysis. Martin Jahn carried out the PGFam analysis. Kevin Foster has given comments on all Chapters.

The data presented in my thesis has been written up separately, alongside additional data that was generated in parallel by Erik Bakkeren and Olivier Cunrath using the pathogen *Salmonella enterica*, as part of a manuscript which is currently under review.

Contents

List of abbreviations

1 Introduction 1

1.1. The age of the microbiome……. 1
1.2. The gut……... 2
1.2.1 Abiotic gradients…… 3
1.2.2 Biotic gradients……... 4
1.3. Benefits of the gut microbiome…….…….. 8
1.3.1 Metabolic benefits…….……. 8
1.3.2 Immune system development……. 8
1.3.3 Colonisation resistance……... 9
1.3.4 Other functions…….. 12
1.4. The antimicrobial resistance crisis……... 14
1.5. An alternative to antimicrobials……... 16
1.6. Biology and significance of *Klebsiella pneumoniae*…….....……... 20
1.7. Producing resistance to *K. pneumoniae*……... 23
1.8. Thesis outline…….. 23

2 Methods and ways of working with many species of gut bacteria 26

2.1 Abstract…… 26
2.2 Introduction……. 26
2.3 Maintaining a diverse collection of gut bacterial strains……..... 28
2.4 Setting up an *in vitro* community experiment……. 33
2.5 Setting up an *in vivo* community experiment…….. 40
2.6 Working with *K. pneumoniae*……... 44
2.7 Discussion…… 47

3 Single strains of gut bacteria provide poor colonisation resistance 49

3.1 Abstract……..... 49
3.2 Introduction…….. 50
3.3 Results……..…..... 53
3.3.1 Screen of individual human gut symbionts……..... 53
3.3.2 Strains within Enterobacteriaceae are the strongest competitors……... 56
3.3.3 Single strains are not sufficient to resist pathogen growth *in vitro*…..… 58
3.3.4 *E. coli* is not sufficient to resist pathogen growth *in vivo*……...…….. 61
3.4 Discussion…… 64
3.5 Materials and Methods…….. 66

4 Ecological diversity promotes colonisation resistance by human gut bacteria **70**

4.1 Abstract……... 70
4.2 Introduction…… 70
4.3 Results……. 72
4.3.1 Diversity and key members are critical to colonisation resistance……. 72
4.3.2 Key members can sometimes be replaced by diversity……. 76
4.3.3 Other, but not all, closely related strains can drive strong colonisation resistance……. 77
4.3.4 Ecology of colonisation resistance in gnotobiotic mice…… 78
4.4 Discussion…… 83
4.5 Materials and Methods…….. 85

5 The role of nutrient blocking in colonisation resistance in the gut microbiome **91**

5.1 Abstract…… 91
5.2 Introduction……. 91
5.3 Results……..…… 94
5.3.1 Colonisation resistance is not explained by interference competition… 94
5.3.2. Carbon use overlap between the symbionts and pathogens explains colonisation resistance to *K. pneumoniae*……..… 96
5.3.3. Protein family overlap also predicts colonisation resistance…….…… 101
5.3.4. Nutrient blocking can be used to predict colonisation resistance to a novel strain……..……..…. 107
5.4 Discussion……..…..…….. 112
5.5 Materials and Methods……..…… 115

6 Conclusion **121**

Appendices

References

List of abbreviations

AMR…….. Antimicrobial Resistance

AMP…….... Antimicrobial Peptide

CFU…….... Colony Forming Units

DAPI……..4',6-diamidino-2-phenylindole

DSM……...Deutsche Sammlung von Mikroorganismen

ELISA……Enzyme-Linked Immunosorbent Assay

FDA……...United States Food and Drug Administration

HGT……..Horizontal Gene Transfer

LB……..Luria-Bertani

PBS……Phosphate Buffered Saline

PFA……Paraformaldehyde

PGFam…..Protein Global Family

WHO…….World Health Organisation

WT…….Wild Type

The majority of diseases begin in the digestive tract when "good" bacteria are no more able to control "bad" bacteria.

- Élie Metchnikoff (1845-1916)

Introduction

1.1 The age of the microbiome

Since I began my undergraduate degree in Biological Sciences in 2015, the field of microbiome science has exploded. Just under 7,000 articles containing the word "microbiome" were published on PubMed in 2015. In the year 2018, when I started my DPhil, 13,300 articles were published. Last year, this number reached 27,200. This near-exponential growth has made it a privilege to carry out my DPhil and write my thesis on the subject of the microbiome, as there has been a continual flow of new and highly relevant publications during my DPhil.

The microbiome is defined as the community of microorganisms (also known as microbes, or microscopic organisms, which may refer to bacteria, fungi or protists) that exists in a particular environment (National Institutes of Health). Animals spanning the phylogenetic tree, including sponges (Cleary et al. 2019) and corals (van Oppen and Blackall 2019) as well as mammals (de Jonge et al. 2022), are colonised by microbes. We are only just beginning to learn and appreciate that no region of the human body is truly free from microbial influence, either direct or indirect. The major benefits of the microbiome to the host are its contribution to metabolism, development of the immune system and protection against pathogens. More recently, the microbiome has been recognised as having even wider reaching impacts on the host in health and disease. This includes how the gut microbiota can influence behaviour via the gut-brain axis (Morais, Schreiber, and Mazmanian 2021). In addition, it has been found that microbes can colonise tumours, with implications for cancer development and its treatment (Elinav et al. 2019). In recognition of the rapidly increasing interest in the importance of the microbiome, a global initiative to conserve microbiota species in a vault in Switzerland, the Microbiota Vault, has been launched (Bello et al. 2018). This takes inspiration from Svalbard's Global Seed Vault.

The recent advances in microbiome research have also spiked commercial interest. The global microbiome therapeutics market was valued at $164.8 million in 2022 and is expected to expand at a compound annual growth rate of 54.8% between 2023 and 2027 to reach $1,465.3 million in 2027 (BCC Research). However, this is still small compared to other health sectors and the market is considered to be nascent. The clinical stage leading United States microbiome therapeutics

company, Seres Therapeutics, obtained approval from the Food and Drug Administration (FDA) in April 2023 for the first orally administered microbiota-based therapeutic, Vowst (previously SER-109). The publicly listed company's product had achieved successful results in a phase three trial in May 2022. Seres Therapeutics is currently valued at $563 million. In 2017 the British epidemiologist Tim Spector co-founded a microbiome-based nutrition start-up, ZOE, that currently reports as having 50,000 members and a further 250,000 people on its wait list. ZOE closed its latest Series B funding round at the end of 2022, leading to a valuation of £209 million.

1.2 The gut

This leads to the question of why, exactly, there is so much interest in the microbiome. To address this, I will first outline what the microbiome is, with a focus on the spatial structure of the gut and its microbiota, before delving into microbiome functions. All surfaces of the human body are colonised with microbes. For instance, we have skin, oral and vaginal as well as gut microbiomes. Containing hundreds of bacterial species (J. Yang et al. 2020) and an estimated order of 10^{13} microbial cells (Sender, Fuchs, and Milo 2016), the most densely colonised body site is the gastrointestinal tract. In particular, the colon carries the largest microbial density of all regions of the gut, with 10^{11}-10^{12} cells/mL, making it the highest recorded density in any microbial habitat (Ley, Peterson, and Gordon 2006). The mammalian gut spans from the mouth to the anus, with an average length of five metres in humans (Bellmann et al. 2015) and a total mucosal surface area of $32m^2$ (Helander and Fandriks 2014). Ingested food passes along the oesophagus, to the stomach, the small intestine (jejunum and ileum) and finally the large intestine (colon and rectum), before passing through the anus as faecal matter. The average transit time through the entire gut varies hugely among individuals, taking between 10 and 73 hours, with the majority of the time (10-59 hours) spent in the colon (Y.Y. Lee, Erdogan, and Rao 2014). The mammalian gut is highly spatially complex (Tropini et al. 2017). There is a multitude of microbial habitats within the gastrointestinal tract due to its varying conditions (Figure 1). Abiotic (physical and chemical) and biotic gradients exist along the length and breadth of the gut, acting as environmental filters that determine where each species lives. This process of selection by the local environment is known as ecological, or species, sorting (Langenheder and Szekely 2011).

1.2.1 Abiotic gradients

Physical or chemical gradients including mucus, pH, oxygen and antimicrobial gradients exist along the length and breadth of the gut. These conditions play a large role in determining the density and type of bacteria at different locations in the intestinal tract.

Mucus

Mucus is a slippery, aqueous gel that coats the epithelial lining of the gut. Goblet cells are single-celled glands in the lining of the gut that produce and secrete mucins, which are the high molecular weight, heavily glycosylated proteins that form a key component of mucus. The proportion of goblet cells in the lining increases from 4% of epithelial cells in the duodenum to 16% in the distal colon (Ermund et al. 2013). Consequently, the mucus layer is thinner in the small intestine and thickest in the distal colon (Chikina and Matic Vignjevic 2021). In addition to lubricating the gastrointestinal tract to allow for movement of food, the mucus acts as a physical barrier between the epithelium and the bacteria in the lumen. This helps to prevent overstimulation of the host immune system and to protect against pathogens.

pH

A longitudinal pH gradient exists along the gastrointestinal tract. The pH is lowest in the stomach (pH 1.5 – 2.0) due to the secretion of gastric acid (Fujimori 2020). In the proximal small intestine, the pH remains acidic (pH 1.7 – 2.0), but increases to pH 6.0 in the duodenum and pH 7.4 in the terminal ileum. The increase is due to the release of alkaline pancreatic juice in the duodenum. The pH drops suddenly to pH 5.7 in the caecum due to fermentation of fibre and production of short chain fatty acids, but rises again gradually along the large intestine to the rectum, where it reaches pH 6.7 (Fallingborg 1999). In addition, a transversal pH gradient is found between the epithelium and the lumen. A near-constant, close-to-neutral pH is maintained at the epithelium because the mucus traps hydrogen and bicarbonate ions (Chikina and Matic Vignjevic 2021).

Oxygen

A gradient of oxygen concentration exists longitudinally, becoming increasingly anaerobic along the length of the gut. The microbiota-independent mechanisms that cause hypoxia in the gut include chemical reactions, such as lipid oxidation, and oxygen consumption by gut epithelial cells (Friedman et al. 2018). In addition, it has been proposed that facultative anaerobes in the gut consume oxygen, creating a hypoxic environment suitable for obligate anaerobes. However, it has been found that the intestinal lumen in germ-free mice is also anaerobic, suggesting that the

formation of the oxygen gradient does not rely on the microbiota (Friedman et al. 2018). A radial gradient of oxygen concentration also exists due to the diffusion of oxygen into the gut from the highly vascularised intestinal mucosa, meaning that the lumen is more anaerobic than the gut lining. The partial pressure of oxygen in the caecal lumen has been measured as being extremely low, with an average of <1mmHg (Albenberg et al. 2014).

Antimicrobials

The mucus lining of the gut contains significant antibacterial activity compared with the lumen. Antimicrobial peptides (AMPs) with a broad spectrum of activity against both pathogenic and commensal bacteria are produced by the host and help protect the host from being exposed to the diverse bacteria present in the gut microbiota. A type of highly specialised secretory epithelial cell, Paneth cells, are located at the base of the crypts (the glands between the villi in the intestinal epithelium) of the small intestine. These cells are known to be an important source of AMPs in the gut. The crypt lumen, therefore, contains a high concentration of AMPs (Bevins and Salzman 2011). The AMPs also diffuse from the crypt into the mucus layer that overlies the epithelium, where they remain attached to the mucus rather than diffuse into the lumen (Dupont et al. 2014). One such AMP produced by Paneth cells is lysozyme, which is an enzyme that targets the peptidoglycan component of the bacterial cell wall (Mukherjee and Hooper 2015). Host-derived bile acids that are secreted in the duodenum also limit microbial activity. As a result, there is a gradient of decreasing AMP concentration along the length of the gut (Donaldson, Lee, and Mazmanian 2016).

1.2.2 Biotic gradients

Longitudinal and transversal gradients of microbial density and diversity exist along the two axes of the gastrointestinal tract (Donaldson, Lee, and Mazmanian 2016).

Longitudinal

The density of bacteria increases along the gastrointestinal tract, reaching the highest density in the colon. The density increases from 10^5 CFU/mL in the jejunum to 10^6 CFU/mL in the ileum, reaching 10^8 CFU/mL in the caecum. It is beneficial for the host to maintain a lower abundance of bacteria in the small intestine, where the microbiota is in competition with the host for uptake of nutrients. The nutrient supply for bacteria in the colon is reliant on the fibre that enters from the small intestine. The growth of bacteria is, therefore, highest in the proximal colon (Arnoldini,

Cremer, and Hwa 2018). The proportion of anaerobes also increases along the length of the gut. One study found that strict anaerobes represent 44% of faecal bacterial rRNA, but only 13% of caecal bacterial rRNA (Marteau et al. 2001). The ratio of the two dominant phyla in the gut, Firmicutes and Bacteroidetes, that represent over 90% of the total community (Magne et al. 2020), decreases from the small to the large intestine. The stomach and small intestine are enriched in Firmicutes (including the family Lactobacillaceae) and Proteobacteria (including the family Enterobacteriaceae), while the large intestine contains a higher proportion of Bacteroidetes (including families such as Bacteroidaceae, Prevotellaceae and Rikenellaceae) (Scheithauer et al. 2016).

Transversal

Across the breadth of the gut, different bacteria are found in the central lumen compared with the mucus layer. Certain bacteria species have been shown to adhere to mucins, the large glycoproteins that form part of the mucus, within the outer mucus layer, while the inner mucus layer remains essentially sterile (Donaldson, Lee, and Mazmanian 2016). For instance, *Lactobacillus* species can produce mucus-binding proteins that bind specifically to mucus (Sicard et al. 2017). Some bacteria, such as *Akkermansia muciniphila* and *Bacteroides thetaiotaomicron*, can metabolise mucus. *A. muciniphila* is considered to be a mucin specialist, while *B. thetaiotaomicron* is a generalist and is able to switch to metabolising mucus in the absence of dietary polysaccharides (Glover, Ticer, and Engevik 2022). Mouse studies (often used as a model for the mammalian microbiota), have shown that Lachnospiraceae and Ruminococcaceae, families belonging to the phylum Firmicutes, are enriched in the inter-fold region of the wall of the colon, which contains a greater amount of mucus. In contrast, families that belong to the Bacteroidetes, Prevotellaceae, Bacteroidaceae and Rikenellaceae, are enriched in the digesta of the lumen (Donaldson, Lee, and Mazmanian 2016).

Capturing microbial diversity within the gut

The spatial complexity of the gut can be visualised using fluorescence microscopy. There are different ways to do this. Cross sections of the gut can be taken from a conventional mouse, and stained with dyes that bind to, for instance, mucus or DNA, before imaging under a microscope, as was done by the Tropini Group (Tropini et al. 2017). Fluorescently tagged species-specific primers can also be used to bind to different bacteria *in situ*, as has been done in a gnotobiotic mouse colonised with a model 15-member human gut consortium (Mark Welch et al. 2017). Alternatively, libraries consisting of bacteria species that each express a different fluorescent colour can be made, as has been done by the Sonnenburg Group, with a library of six *Bacteroides* species.

Gnotobiotic mice colonised with these engineered strains can then be dissected and imaged (Whitaker, Shepherd, and Sonnenburg 2017).

The least invasive and most commonly used way to study the bacteria in the gut is by analysing faecal samples. However, it is important to be aware of the spatial complexity present within the mammalian gut and to understand that the faeces are not completely representative of other parts of the intestinal tract, such as the colonic mucosa or the ileum (Marteau et al. 2001; Kwon et al. 2021). The field of microbiome research would, therefore, benefit from the development of precise and minimally invasive sampling devices, such as ingestible capsules that can sample, for instance, colonic content (Tang et al. 2020).

The gut is considered a hospitable environment for bacteria to live in (Reese et al. 2018). It contains by far the majority of the body's microbiota and the colon is thought to be the most densely populated habitat on Earth (Whitman, Coleman, and Wiebe 1998). But the rate of supply of resources and finite amount of space necessarily limit bacterial growth in the gut, causing competition between species. What limits the growth of bacteria within the gut has not been studied in detail and remains open to speculation. However, it is thought to be largely determined by the nutrients supplied by the host's mucus secretions and diet (Pereira and Berry 2017). Rather than the growth of each species in the gut being limited by only one substrate, it is likely that most species can switch between using multiple substrates (Pereira and Berry 2017; Steeb et al. 2013). It is generally accepted that carbon is limiting for microbes living in the gut (Chang et al. 2004), but a recent report has shown that nitrogen can also be limiting (Reese et al. 2018). Moreover, it is thought that the host uses nutrient limitation to exert control over its associated community (Reese et al. 2018; McLoughlin et al. 2016; Schluter and Foster 2012).

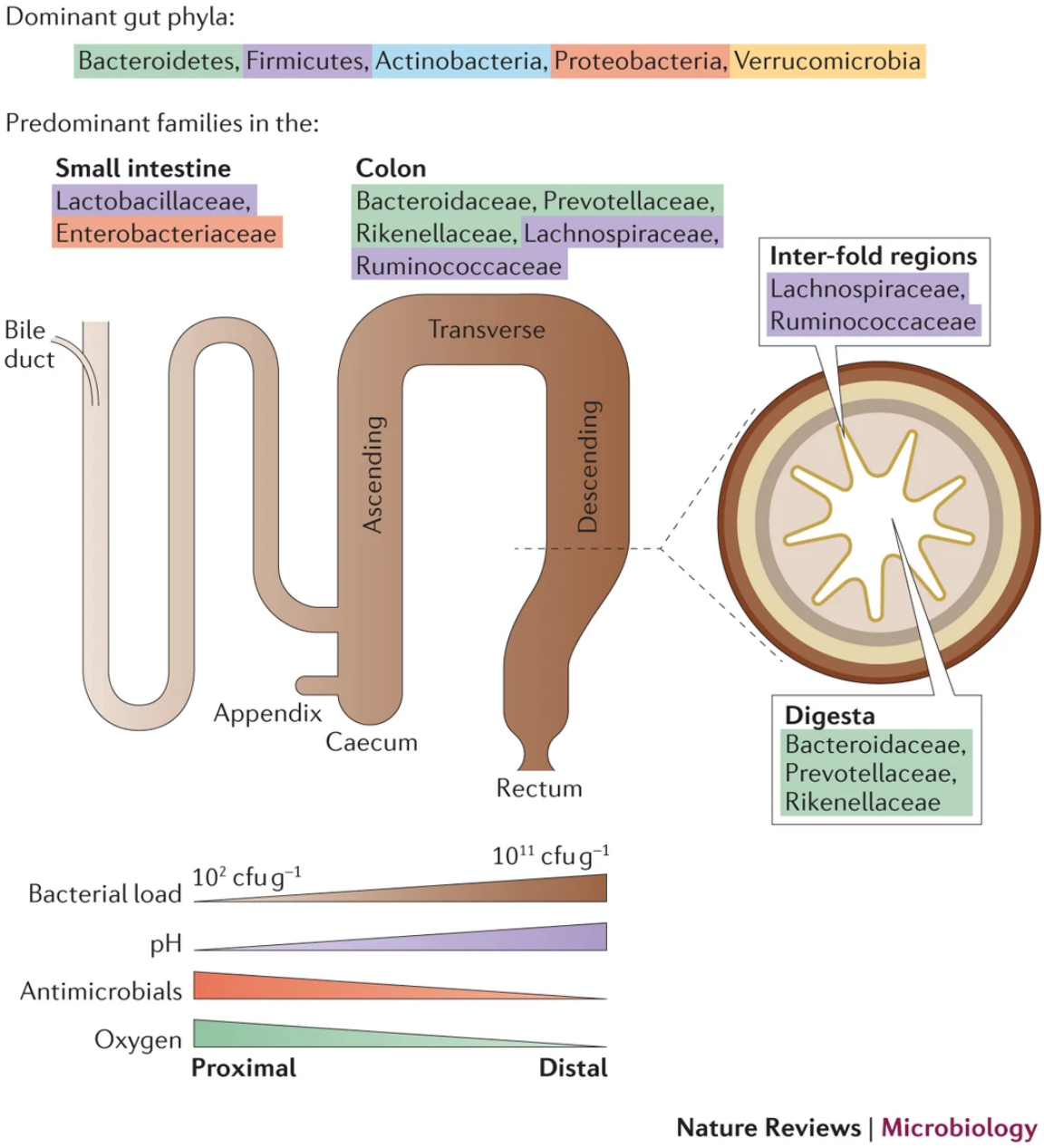


Figure 1. Anatomy of the human gut with corresponding abiotic gradients and dominant bacterial phyla. A cross-section of the colon shows the digesta and inter-fold regions of the lumen. (Donaldson, Lee, and Mazmanian 2016).

1.3 Benefits of the gut microbiome

The gut microbiome is known to confer a wide range of benefits on its host (Valdes et al. 2018), which I will review here. The main benefits are its contribution to host metabolism, the development of the host immune system, and protection against pathogens. In addition, a multitude of other ways in which the gut microbiome influences our health are being discovered.

1.3.1 Metabolic benefits

One of these benefits is the fermentation of non-digestible substrates into products that can be metabolised by the host. There are an estimated 2,000,000 bacterial genes in the gut compared with 20,000 human genes in the body (Gilbert et al. 2018). The 100-fold higher number of genes encoded by the gut microbiota allows it to undertake a variety of metabolic functions that humans are unable to or have limited ability to do (Bull and Plummer 2014). The human diet contains a mixture of three macronutrients: proteins, fats and carbohydrates. Simple carbohydrates, such as glucose and fructose, contain one or two sugars (monosaccharides or disaccharides) and are easily utilised by the host for energy. Complex carbohydrates (oligosaccharides or polysaccharides) contain three or more sugars. Starch is a common type of complex carbohydrate in the human diet that can be digested by the host into glucose subunits, which are absorbed from the gut into the bloodstream. Dietary fibres such as cellulose, resistant starch, inulin, lignins, beta-glucans and pectins are non-digestible complex carbohydrates that may be soluble or insoluble. Of these dietary fibres, fermentable fibres, including resistant starch and inulin, are fermented in the colon by the gut microbiota, producing short-chain fatty acids (SCFAs), including butyrate, acetate and propionate. Over 95% of microbial-produced butyrate is consumed by the colon (Oliphant and Allen-Vercoe 2019; Zhang et al. 2021). It has been found that 10% of our daily metabolic requirements are provided by SCFAs (den Besten et al. 2013). Moreover, decreased SCFA production is linked to metabolic diseases (Zhang et al. 2021). Another metabolic benefit of the gut microbiota is its ability to synthesise vitamins, such as vitamin K and the B-group vitamins riboflavin, niacin and cobalamin (Nysten and Van Dijck 2023). In fact, the gut microbiota is estimated to produce up to 30% of the recommended daily intake of vitamins for the host (Nysten and Van Dijck 2023).

1.3.2 Immune system development

A second major benefit is the contribution that the gut microbiota makes to the development of the host immune system (Zheng, Liwinski, and Elinav 2020). The host needs to be able to

determine which bacteria are pathogenic and which are harmless in order to mount appropriate immune responses. The gut microbiota plays a valuable role in training the immune system to protect the body against infection, while simultaneously maintaining tolerance to the gut microbiota, regulating immune homeostasis (Belkaid and Hand 2014; Barthels et al. 2017). For instance, dendritic cells (DCs), a type of antigen presenting cell, in the Peyer's patches of the gut produce high levels of the anti-inflammatory cytokine interleukin-10 (IL-10) compared with DCs of the spleen (Iwasaki and Kelsall 1999). Germ-free animals provide a useful model to study the effect of microbes on the immune system. There are striking differences between the immune systems of germ-free and conventional mice, some of which can be reversed upon colonisation of the germ-free animals with microbes. For example, germ-free mice contain much lower levels of intestinal intraepithelial lymphocytes than conventional mice, but these can be induced upon microbial colonisation (Umesaki et al. 1993). It is also known that immunoglobulin A antibody responses in the gut are induced by microbial colonisation of germ-free mice (Hapfelmeier et al. 2010). However, a few differences cannot be reversed by exposure to microbes once a critical time-window of host development has passed (Gensollen and Blumberg 2017). For instance, there are transcriptional differences in the intestines of germ-free mice that were conventionalised as adults compared to those conventionalised at birth (El Aidy et al. 2013).

1.3.3 Colonisation resistance

Another crucial benefit of the gut microbiota is its ability to protect the host from pathogen infection, via a phenomenon known as colonisation resistance (Caballero-Flores, Pickard, and Nunez 2022). In my research, I am particularly interested in the phenomenon of colonisation resistance. Due to colonisation resistance, the host is provided with a degree of natural protection against harmful pathogens such as *Klebsiella pneumoniae* and *Salmonella enterica*. Both germ-free and antibiotic-treated mice are much more vulnerable than conventional mice to colonisation by pathogens such as *Salmonella* spp. (Stecher et al. 2005). Taking antibiotics increases the risk of infection with *Clostridium difficile* by 7- to 10-fold (Centres for Disease Control and Prevention) due to the decimation of the gut microbiota. It is important to note that colonisation resistance did not evolve expressly to protect the host against harmful species. Strictly, colonisation resistance refers to the ability of resident microbial species to resist the growth of incoming, non-resident species, regardless of their pathogenic potential. However, colonisation resistance to pathogens is often studied, and is what I focus on in my research, as this is where the greatest health benefits lie. The protection conferred is a side effect of intense competition between microbes, which provides a strong selective pressure (Foster et al. 2017). The gut microbiota is a dense and diverse community

within which competitive interactions dominate (Palmer and Foster 2022a; Foster and Bell 2012). Colonisation resistance can take place via a myriad of mechanisms (Caballero-Flores, Pickard, and Nunez 2022), which may be direct, through interbacterial competition, or indirect, via the stimulation of the host immune system.

Direct, interbacterial competition

Bacteria live in dense communities in the gut and competition between strains and species is rife (Foster and Bell 2012; Coyte, Schluter, and Foster 2015). Resident intestinal microbial species compete directly with incoming species over shared resources such as nutrients and space (Maltby et al. 2013). Interbacterial competition may be "interference competition", where bacteria kill or inhibit one another with secreted toxins or contact-dependent weapons, such as bacteriocins or type six secretion systems (Granato, Meiller-Legrand, and Foster 2019). Alternatively, it can be in the form of "exploitative competition", with bacteria competing for shared resources such as nutrients. Both types of competition can be regarded as different strategies that evolve when bacteria face competition for shared resources. An analogy can be made to monkeys competing over a banana growing in a tree. Either one monkey kills the other monkey, thereby removing its competitor, or it climbs the tree faster to reach the banana first. However, this is a gross over-simplification and other fruit types, on other trees, with some fruits or trees preferred by different monkeys should be included, as well as alternative ways to climb the tree. At this point, the analogy becomes less useful, and it may be better to revert back to the bacteria (see Figure 2). Some studies have reported finding a role for nutrient competition in colonisation resistance (Pereira et al. 2020; Oliveira et al. 2020; Osbelt et al. 2021), while other studies find antagonism between bacteria (Buffie et al. 2015; Kim et al. 2019; Jacobson et al. 2018).

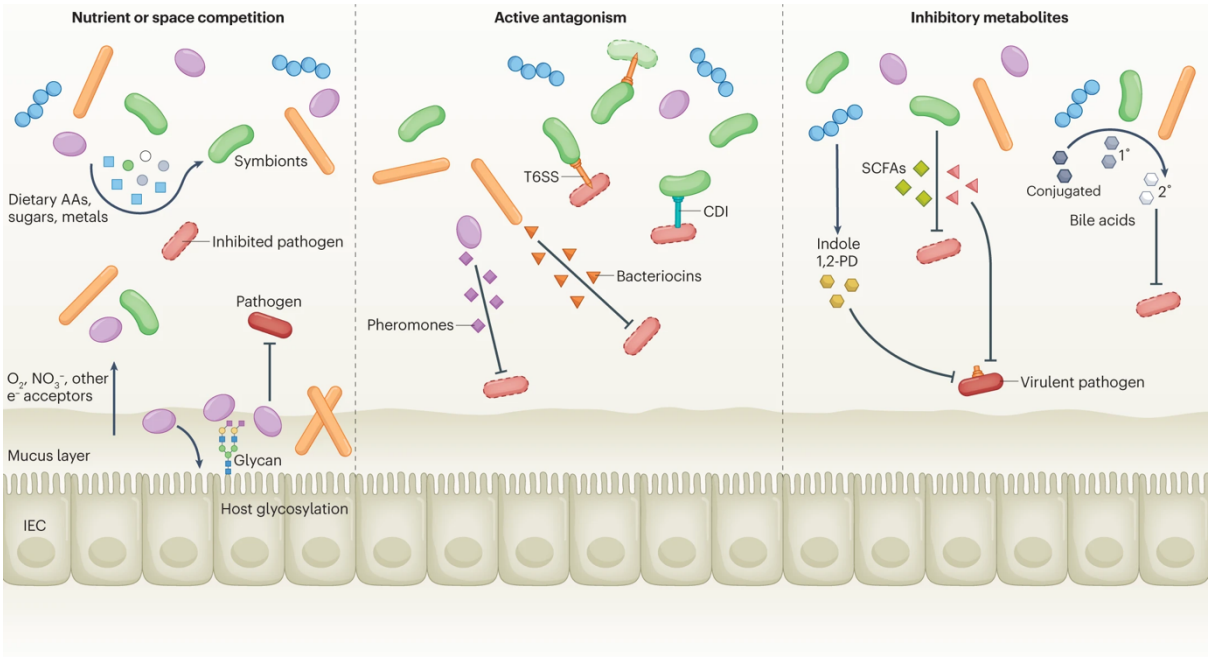


Figure 2. Direct, interbacterial mechanisms of colonisation resistance in the gut microbiome. (Caballero-Flores, Pickard, and Nunez 2022)

Immune system stimulation

The gut microbiota can also increase protection against pathogens indirectly by stimulating the host immune system (Caballero-Flores, Pickard, and Nunez 2022). For example, resident microbial species can stimulate host epithelial cell production of AMPs, such as RegIIIB and ReIIIy, that disrupt bacterial membranes (Caballero-Flores, Pickard, and Nunez 2022). In addition, stimulation of NOD2 receptors by gut microbiota-derived peptidoglycan leads to expression of cryptdins, a class of AMPs, that promote removal of, for example, the pathogen that causes listeria, *Listeria monocytogenes* (Kobayashi et al. 2005). Some studies have reported finding a role for stimulation of the host immune system in colonisation resistance (Sequeira et al. 2020; Byndloss et al. 2017).

History of colonisation resistance

The importance of colonisation resistance to the host has been recognised for a long time (Mackowiak 2013). Élie Metchnikoff (1845-1916) was a Russian biologist who was awarded the Nobel Prize in Physiology or Medicine in 1908 alongside Paul Ehrlich for his work on immunity. He advocated for the use of *Lactobacillus* for a long and healthy life (Podolsky 2012), attributing the longevity of Bulgarian peasants to their consumption of yoghurt. Metchnikoff also hypothesised that the differences between individuals in their susceptibility to cholera was due to differences in

gut microbes. To help understand this, he even drank a sample of cholera, and never became ill (Cavaillon and Levin 2022). Later, in the early 20th century, the German physician Alfred Nissle discovered that stool samples spiked with *Salmonella* strains varied in their ability to resist *Salmonella* growth. In most cases, *Salmonella* was able to outgrow the other faecal bacteria, but in a few cases, *Escherichia coli* dominated (Sonnenborn 2016). During the First World War, Nissle isolated an *E. coli* strain from the faeces of a German soldier who, unlike his comrades, did not develop diarrhoea or other intestinal diseases. As Nissle correctly suspected, this soldier carried an *E. coli* strain that was antagonistically strong against pathogenic enterobacteria (Sonnenborn 2016). This strain was named *E. coli* Nissle 1917. Regarded as the first probiotic, *E. coli* Nissle 1917 is now one of the best-studied strains of beneficial bacteria and is available commercially under the brand name Mutaflor.

However, despite having recognised the importance of colonisation resistance for human health for over a century, the principles that underlie it are less well understood. Why are some individuals more susceptible to colonisation by pathogens than others and what are the properties of pathogen-resistant communities? If we could uncover general ecological principles of resistance, it would aid in the ultimate challenge of engineering microbial communities to protect against pathogen infection. Moreover, many mechanisms have been implicated in colonisation resistance (Caballero-Flores, Pickard, and Nunez 2022), but it is not known which of the mechanisms are the key players in natural microbial communities such as the gut microbiome. Deciphering the mechanisms that explain the general ecological principles we hope to uncover would help in the rational design of protective probiotic communities. Here, I aim to apply an ecological perspective in order to better understand the interplay between symbiont and pathogen species in the gut microbiome that leads to colonisation resistance.

1.3.4 Other functions

Alongside the core benefits of metabolism, immune development and colonisation resistance, we are beginning to uncover additional roles of the microbiome for the host. The gut-brain axis is a developing field of study in which there is a proposed interplay between the gut microbiota and the brain. Many observational studies demonstrate a link between features of the gut microbiome and neurodegenerative disorders, psychiatric conditions and behavioural conditions (Shoubridge et al. 2022). It remains challenging to establish causality, however, and the most common strategy is to transplant the faeces of a human patient into a germ-free mouse. For example, it was found

that germ-free mice transplanted with faeces from Parkinson's disease patients developed increased motor dysfunction (Sampson et al. 2016). Another study found that transplantation of the faecal microbiota from human donors with autism spectrum disorder induces hallmark autistic behaviours in mice (Sharon et al. 2019), although it is important to note that mouse models of autism are controversial and other studies refute a causal relationship between autism and the gut microbiome. We are now beginning to develop our understanding of the mechanisms that might underlie the influence of the gut microbiome on the nervous system. Potential pathways include the production of microbial metabolites, which can diffuse through the gut epithelium and stimulate the vagus nerve, which is a long nerve that relays information directly to the brain (Shoubridge et al. 2022). In addition, it has recently been found that fragments of peptidoglycan, a key structural component of the bacterial cell wall, are shed by the gut microbiota and translocate across the intestinal epithelium into the bloodstream, where they disseminate to host organs including the brain (Wheeler et al. 2023). One role for these peptidoglycan fragments is that they can be directly sensed by a type of host neuron as a cue, in order to regulate appetite (Gabanyi et al. 2022).

Another, perhaps less obvious, way in which the gut microbiome can influence our health is through its two-way interaction with medicinal drugs. This field of study is gathering interest, as evidence is building for a strong impact of medication on the microbiome, either through a drug's mode of action or side effects (Maier and Typas 2017). Led by Lisa Maier, the Typas Lab developed a high-throughput screen of over 1,000 marketed, non-antibiotic drugs against representative human gut bacterial strains, and found that 24% of the drugs with human targets inhibited the growth of at least one gut strain *in vitro* (Maier et al. 2018). Certain classes of drugs, such as antipsychotics, were overrepresented within the 24%. On the other hand, the microbiome has potential to influence the host's response to a drug, by enzymatically altering the drug's structure. For instance, the effectiveness of chemotherapeutics in treating cancer varies among individuals and it is thought that microbes could play a role in this, by modulating the efficacy of the therapeutic. Gammaproteobacteria have been identified as key bacteria that can metabolise gemcitabine, a chemotherapeutic drug, into its inactive form (W.Y. Cheng, Wu, and Yu 2020). Selectively targeting these bacteria could, therefore, sensitise a tumour to gemcitabine treatment. On the other hand, multiple studies find that removal of the gut microbiota in fact reduces therapeutic efficacy (W.Y. Cheng, Wu, and Yu 2020). For example, the gut microbiota can positively impact an individual's response to immunotherapy in cancer treatment by stimulating the host immune system (Weersma, Zhernakova, and Fu 2020).

The significance of the gut microbiome for human health is evident from the numerous studies that highlight the negative consequences of taking antibiotics, which often not only kill or inhibit the intended pathogenic strain, but also inflict collateral damage by decimating the gut microbiome. As described in the section on colonisation resistance, the use of antibiotics is known to increase an individual's susceptibility to infection by pathogens such as *C. difficile* by decreasing colonisation resistance (Teng et al. 2019). However, there are other, additional negative impacts of antibiotics on human health that are beginning to be realised and the effect of different antibiotics on non-pathogenic human gut symbionts is being systematically investigated. The impact of 144 different antibiotics on 38 representative human gut microbial species was recently characterised *in vitro* (Maier et al. 2021). In particular, it was found that two classes of antibiotics, macrolides and tetracyclines, inhibited nearly all commensals tested and killed several species. Correlations have been found between gut microbial extinction, which has occurred in part due to the widespread use of antibiotics, and a rise in chronic, western diseases such as diabetes, obesity, asthma and allergy (Blaser 2017). Evidence shows that the negative side effects of antibiotic use in the first two years of a person's life are the most severe on health, suggesting a critical window for development (Blaser 2016). A mechanistic link between antibiotic use during this window and the subsequent development of asthma has recently been shown (Borbet et al. 2022).

The considerable importance of the gut microbiome is creating widespread interest and fuelling research into the potential for manipulating the microbiome to improve human health. Here, I will focus on how the microbiome could be engineered to increase protection against pathogens, through the phenomenon of colonisation resistance.

1.4 The antimicrobial resistance crisis

We are living in a time when the threat of antimicrobial resistance is rapidly increasing. More than ever, routine operations, caesarean sections and cancer treatments are associated with the risk of untreatable bacterial infection. The Lancet's 2022 report on the "Global burden of bacterial antimicrobial resistance in 2019" stated that 1,270,000 deaths worldwide in 2019 were directly attributable to antimicrobial resistance (AMR)(Antimicrobial Resistance 2022). The death rate is highest in sub-Saharan Africa, at 27.3 deaths per 100,000 people. The United Nations has estimated that by 2050, up to 10 million deaths could be attributable to antimicrobial resistance, matching the current annual global mortality due to cancer.

Antimicrobials are compounds that kill or inhibit microbes. They are produced in nature by bacteria and fungi, as a means of competing with one another. Some antibiotics are broad-spectrum, meaning that they target a wide range of microbes, whereas narrow-spectrum antibiotics have a much smaller range (Palmer and Foster 2022b). Their mechanisms of action vary. Beta-lactam antibiotics, including penicillins and cephalosporins, target bacterial cell wall synthesis by binding to enzymes (penicillin binding proteins, PBPs) involved in peptidoglycan cross-linking. Aminoglycosides, tetracyclines and chloramphenicol work by binding to the ribosome of the cell, inhibiting translation. Sulfonamides inhibit bacterial replication by competitively interfering with folic acid synthesis, due to their structural similarity to para-aminobenzoic acid. Folic acid is needed for DNA synthesis. Resistance mechanisms vary depending on the species of microbe and type of antimicrobial. For instance, resistance to beta-lactam antimicrobials may occur via the production of an enzyme, beta-lactamase, which is secreted by the bacterial cell, and degrades the antimicrobial by hydrolysing its beta-lactam bond. Alternatively, resistance to beta-lactams may also arise via the alteration of bacterial PBPs, preventing binding of the antimicrobial to the PBP. Another common mechanism of antimicrobial resistance is the production of efflux pumps, which span the bacterial membrane and pump solutes, including the antimicrobial, out of the cell (Soto 2013).

Resistance to antimicrobials has been evolving in an ongoing arms race between microbial strains and species for as long as they have existed in nature (Larsson and Flach 2022). The origin of many modern resistance genes is found in the environment, for example, in ancient permafrost samples and in caves (Perry, Waglechner, and Wright 2016), rather than originating in human pathogens *de novo*. Horizontal gene transfer (HGT) between bacteria plays an important role in the dissemination of antimicrobial resistance genes, which are often present on mobile genetic elements such as plasmids and integrons (Lerminiaux and Cameron 2019; Matlock et al. 2023; K. Lee et al. 2023). The relatively recent commercialisation, widespread use and overuse of antimicrobials in livestock, agriculture and human medicine, has increased the selection pressure on microbes to become resistant (Llor and Bjerrum 2014; K. Lee et al. 2023). In addition, sewage and waterway systems act as links between environmental reservoirs of bacteria, facilitating the spread of resistance genes (Matlock et al. 2023). The recently established One Health approach tackles the spread of antimicrobial resistance in the context of animals and our environment, as well as people (Velazquez-Meza et al. 2022). It is an integrated, unifying approach that calls for the collaboration of multiple disciplines to attain optimal health. Resistance is spreading, and many human pathogens are developing resistance even to last-line antimicrobials such as vancomycin (Figure 3).

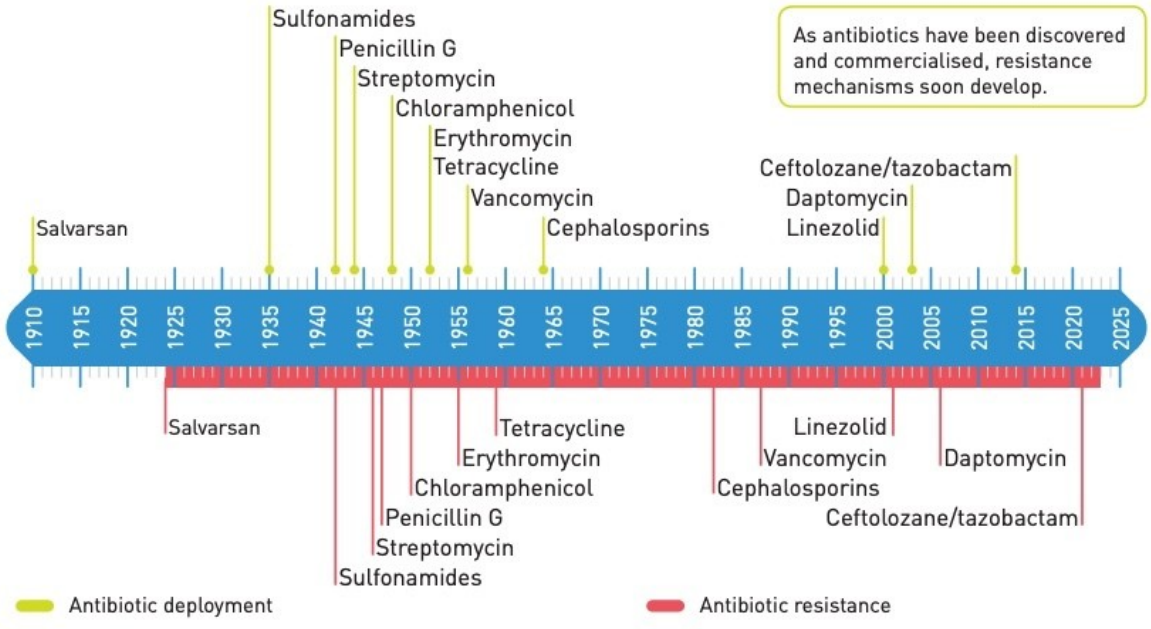


Figure 3. Commercial deployment of antibiotics and corresponding emergence of antibiotic resistance – a timeline. Taken from the United Nations Environment Programme (UNEP) 2023 report, "Bracing for Superbugs".

1.5 An alternative to antimicrobials

A solution to the antimicrobial resistance crisis is desperately needed. However, the speed of resistance development is equal to or outpacing the development of new antimicrobials (Wasan et al. 2023). Many large pharmaceutical companies, such as Norvartis and Sanofi in 2018, have left antimicrobial research due to the high likelihood of failure and the minimal return on investment into last-resort drugs that are supposed to be used sparingly and as one-offs. Most research into new antimicrobials is carried out by smaller companies and by academics, but they lack sufficient funding to bring new drugs to market. However, the resistance crisis has prompted governments and organisations to fund research into new antimicrobials and revive the dried-up development pipeline. This is known as "push funding". For instance, the global, charitable, non-governmental Wellcome Foundation has recently invested £175 million to fund early- and clinical-stage research and development into new antimicrobial drugs (Wasan et al. 2023).

Despite this, the annual World Health Organisation (WHO) 2022 report has stated that the development of new antibacterial treatments is inadequate to address the mounting threat of antibiotic resistance. Since 2017, only 12 new antibiotics have been approved, but 10 of these belong to pre-existing classes of antimicrobials that already face established mechanisms of resistance. In 2021, there were only 27 antibiotics in clinical development against priority pathogens (WHO, 2022). Of these 27, just six meet the WHO's requirements for innovation. The lack of innovation in current antimicrobial development quickly undermines the effectiveness of new drugs.

Developing new antimicrobials is not the only answer to the resistance crisis. New antimicrobial drugs have a limited lifespan before resistance ultimately emerges. One important way of slowing down the spread of resistance is to improve regulation of the use of antibiotics, by implementing Antimicrobial Stewardship programmes (Shrestha, Zahra, and Cannady 2023). Another approach is to combine antimicrobial drugs with adjuvant therapies that are designed to inhibit resistance mechanisms (Annunziato 2019). For instance, the adjuvant clavulanic acid is frequently used alongside the beta-lactam antibiotic amoxicillin for its ability to inhibit the resistance-conferring beta-lactamase enzymes that are secreted by bacteria. The combined clavulanic acid and amoxicillin therapy is known as Augmentin. Other adjuvant types include efflux pump inhibitors, which prevent expulsion of the antibiotic from the bacterial cell, and membrane permeabilisers, which increase penetration of the antibiotic across the cell membrane.

However, the approaches outlined above do not altogether solve the problem of resistance, they only act to slow its impact. In addition, the use of antimicrobials has significant detrimental effects on the host's health. Antimicrobials decimate the microbiome (Anthony et al. 2022), which increases susceptibility to infection by negatively impacting colonisation resistance to pathogens such as *C. difficile* (Patangia et al. 2022; de Nies, Kobras, and Stracy 2023). Alternatives to antimicrobials are needed. One such alternative to antimicrobials is to augment the microbiome with live bacterial therapeutics. This approach would boost colonisation resistance rather than break it, with the potential to prevent or treat infection. The original and crudest way to do this is via a faecal microbiota transplant (FMT). FMTs have existed for a long time, despite being relatively new to western medicine. The first known description of an FMT was in China, in 400 B.C., when "yellow soup", referring to a donor's faeces, was given to patients suffering from diarrhoea and food poisoning (de Groot et al. 2017). The first published account of an FMT in western medicine was in 1958, by Ben Eiseman and his colleagues, who used a faecal enema to

treat four patients with pseudomembranous enterocolitis (Khoruts 2017). They would almost certainly have been afflicted with *C. difficile* infection, although the cause was not known then. The first randomised controlled trial (RCT) of an FMT was published in 2013. In the trial, FMTs were used to treat recurrent *C. difficile* infection and the trial was stopped early when they found that the FMT was significantly more effective than vancomycin treatment for the recurrent infection (van Nood et al. 2013). FMT is currently recommended for patients with two or more recurrences of *C. difficile* infection (Bagdasarian, Rao, and Malani 2015). But the FDA treats FMT as a drug and requires that it undergoes an investigational new drug application in order to gain approval, meaning that large RCTs are necessary (Choi and Cho 2016; Sachs and Edelstein 2015). Evidence from clinical trials suggests that FMT prevents further recurrence in 80% of patients, compared with 20%-50% for standard antibiotic treatment (Mamoon and Olesen 2020). As the most common hospital-acquired infection in the United States, *C. difficile* is a major public health threat that causes 450,000 cases every year and was estimated to contribute $1 billion to healthcare costs in the United States in 2017 (Mamoon and Olesen 2020). The first FDA-approved FMT for recurrent *C. difficile* infection, Rebyota, was approved in November 2022, for patients who have previously completed antibiotic treatment. It is not known how widespread the use of FMT is, but it was recently estimated that 48,000 FMTs could be performed annually, preventing 32,000 *C. difficile* infection recurrences (Mamoon and Olesen 2020).

FMT involves transferring a complex, uncharacterised faecal community from donor to recipient. This is associated with many risks, for example, transfer of pathogens, which may be asymptomatic in the donor but cause infection in the recipient (Park and Seo 2021). Faecal communities need to be screened carefully before administration and this can be carried out at stool banks such as OpenBiome (Chen et al. 2021). However, stool banks do not currently screen for multidrug-resistant organisms and this has led to a series of recent adverse events (Park and Seo 2021). In addition, the longer-term health risks of receiving an FMT are currently unknown (Sachs and Edelstein 2015; Park and Seo 2021) and could include transfer of undesirable host phenotypes. Moreover, the response rates to FMT for infectious and chronic diseases other than recurrent *C. difficile* infection are much less striking, although somewhat encouraging, and do not support the more frequent implementation of FMT (Mikolasevic et al. 2021).

Designing refined and characterised microbial communities for use as prophylactics or therapeutics for infectious disease is a promising alternative strategy to FMT (Sbahi and Di Palma 2016; Wang, Nute, and Treangen 2023). These communities should contain the key species

required to obtain the desired health outcome, without transferring any unforeseen phenotypes. The risk associated with FMT would, therefore, be minimised. Moreover, the rational design of communities would allow targeted treatments of particular pathogens or other diseases. A handful of mouse gut microbial communities have been designed to confer colonisation resistance against pathogens in mice. For example, a minimal community designed to provide mice with colonisation resistance to the pathogen *Salmonella enterica*, is the OligoMM12 faecal microbiota community, which consists of 12 species of bacteria (Brugiroux et al. 2016). In addition, a mouse gut symbiont community comprising five species, BacMix, has been created to reduce *C. difficile* colonisation in mice. Some human gut consortia have also been designed with the aim of preventing pathogen growth. For instance (as briefly mentioned already), Seres Therapeutics has developed the live bacterial therapeutic, Vowst, which is designed to treat recurrent *C. difficile* infection in humans and succeeded in obtaining the first FDA approval of an oral microbiome therapeutic in April 2023. While they have not published their methods, further details can be found in their patents (patent number 20230125810, filed 2020, published 2023, *Designed bacterial compositions and uses thereof*; patent number 11666612, filed 2021, published 2023, *Network-based microbial compositions and methods*). Attempts at the rational design of bacterial therapeutics vary greatly and it remains to be determined which method is the most successful.

There are multiple challenges that need to be addressed in order for a probiotic to succeed as a prophylactic or treatment strategy, in addition to the probiotic's ability to block or eliminate a pathogen. One key challenge is that the probiotic has to be able to colonise, or engraft in the patient's gut, especially if the probiotic is designed to be taken once as opposed to daily over a longer period. Resident gut strains resist colonisation by any exogenous strain, including potential probiotics, in addition to pathogens. A microbiome therapeutics company established in 2015, Novome Biotechnologies, aimed to address this by engineering a putative probiotic *Bacteroides* strain so that it could metabolise a compound found in seaweed (Shepherd et al. 2018). If the host's diet was supplemented with this seaweed compound, the engineered strain was able to engraft in the gastrointestinal tract. Successful results of a Phase 1 clinical trial were published in late 2021 and Novome Biotechnologies raised $43.5 million in Series B financing in September 2022. However, at the time of writing this, in August 2023, the start-up has announced its decision to close after its failure to generate the data needed to develop their therapeutic approach. This illustrates the difficulty of translational research and of taking a drug to market, despite starting with a successful scientific basis. Another important challenge is ensuring that the strains comprising a probiotic community are able to co-exist within the host, rather than competing and

mutually excluding one another. Studying the ecological interactions between resident and exogenous gut microbiota strains as I aim to do here is, therefore, critical for the rational design of probiotics, not only for their ability to resist pathogens, but also to ensure the probiotic is able to successfully engraft.

1.6 Biology and significance of *Klebsiella pneumoniae*

One of the most significantly antimicrobial resistant pathogens is the species *K. pneumoniae*. It is a gram-negative, rod-shaped, non-motile facultative anaerobe that belongs to the family Enterobacteriaceae. *K. pneumoniae* has a wide distribution and is found in the environment as well as in human hosts (Wareth and Neubauer 2021). In the environment, *K. pneumoniae* is found in soil, water and vegetation (Wareth and Neubauer 2021). In humans, *K. pneumoniae* can be found in the gastrointestinal tract, nose and mouth as part of the normal microbiota. The National Institutes of Health's Human Microbiome Project was a research initiative launched in 2007 to improve the understanding of the human microbiota in health and disease. Under the initiative, healthy human microbiome samples were analysed and the presence of *K. pneumoniae* was detected in 3.8% of healthy stool samples (Conlan, Kong, and Segre 2012). It has been found that travel to Asia is a strong predictor for intestinal carriage of extended-spectrum cephalosporin resistant *K. pneumoniae* (Espenhain et al. 2018). Colonisation with *K. pneumoniae* is higher in low-income countries: a study of 911 pregnant women from Madagascar, Cambodia and Senegal detected an intestinal carriage rate of 56% (Huynh et al. 2020). Moreover, one third of these isolates harboured antimicrobial resistance genes (Huynh et al. 2020). Longitudinal studies of *K. pneumoniae* carriage are rare, but one study in Austria analysed stool samples from six healthy volunteers weekly over the course of a year. Five of the subjects were colonised with *K. pneumoniae* in at least one of the weekly stool samples. Up to five different strains were found in individual samples, and colonisation with a specific strain was found for no longer than two consecutive weeks, suggesting that colonisation was intermittent and of high clonal diversity. The authors of the study, Lepuschitz *et al*, suggested that food was a potential reservoir of *K. pneumoniae* for humans (Lepuschitz et al. 2020).

In the gastrointestinal tract of mono-colonised mice, *K. pneumoniae* has been found to occupy the duodenum, ileum and caecum. The highest density is found in the caecum (10^{10} CFU/g) and lowest in the duodenum (10^{6} CFU/g) (Caballero et al. 2015). Moreover, visualisation of *K. pneumoniae* localisation in the mouse colon, using fluorescence in situ hybridisation, showed that *K. pneumoniae* density is greatest adjacent to the colonic epithelium. Within the lumen, *K. pneumoniae* could also

be found associated with detached islands of mucus (Caballero et al. 2015). As facultative anaerobes, members of Enterobacteriaceae are known to be localised near the intestinal mucosa, due to their relatively higher tolerance of oxygen dispersed by the epithelium compared with other members of the gut microbiota (Zeng, Inohara, and Nunez 2017). The mammalian intestine is predominantly colonised by obligate anaerobes, which are hypothesised to suppress and maintain members of Enterobacteriaceae at a relatively low density in the healthy gut (Zeng, Inohara, and Nunez 2017). Compared with the stool, the duodenal microbiota contains relatively higher frequencies of the phylum Proteobacteria, to which *K. pneumoniae* belongs. At 21% relative abundance, Enterobacteriaceae has been found to be the second most abundant family in the small intestine (Leite et al. 2020). This is due to the overall lower microbial abundance in the small intestine, and its higher oxygen concentration, which favours facultative anaerobes (Leite et al. 2020).

In addition to colonising a subset of healthy humans, *K. pneumoniae* can also cause infection, especially in immunocompromised individuals. As such, *K. pneumoniae* is a particular problem in hospital settings, which act as a reservoir for *K. pneumoniae* strains (Gorrie et al. 2022). *K. pneumoniae* is considered the most common cause of hospital-acquired pneumonia in the United States (Ashurst and Dawson 2023). In addition, it is one of the most frequent causes of urinary tract infections, alongside *E. coli* (Behzadi et al. 2010). It has earned a place among the ESKAPE pathogens, six highly virulent and antibiotic resistant pathogens comprising *Enterococcus faecium, Stapylococcus aureus, K. pneumoniae, Acinetobacter baumannii, Pseudomonas aeruginosa* and *Enterobacter* spp.. *K. pneumoniae* is also one of the top priority pathogens on the WHO's priority pathogens list for research and development of new antibiotics. In particular, many *K. pneumoniae* strains have developed resistance to beta-lactam and carbapenem antibiotics.

For 30 years, *K. pneumoniae* isolates have been recognised as falling into two distinct categories. Classical *K. pneumoniae* strains (cKp) are usually found in immunocompromised patients and are not virulent in mouse models. On the other hand, hypervirulent strains (hvKp) are associated with community acquired (meaning that young, healthy individuals can be infected), invasive (meaning that they can establish infection in the liver) infections, and they are virulent in mouse models (Walker and Miller 2020). The classical strains have existed for longer and are more well studied than hvKp strains. Hypervirulent strains were first isolated in Taiwan in 1986 (Remya, Shanthi, and Sekar 2018). Classical strains tend to be more highly antimicrobial resistant than the

hypervirulent strains, however, the emergence of resistance among hvKp is a cause for concern (Remya, Shanthi, and Sekar 2018).

K. pneumoniae strains are known for their production of a polysaccharide capsule, which causes a mucoid phenotype (Figure 4). The capsule is an extracellular polysaccharide matrix that envelops the bacteria. It is considered to be a virulence factor during pathogenesis because it aids tissue invasion and protects cells from phagocytosis and toxins (Rendueles 2020). In mouse models, strains without a capsule are much less virulent than their isogenic encapsulated strains: mortality is lower, as is *K. pneumoniae* abundance in the lungs (Paczosa and Mecsas 2016). *K. pneumoniae* strains are sub-divided into 79 different capsular serotypes (K1-K79) (Hasani et al. 2020), of which serotypes K1 and K2 often comprise hypervirulent strains and are most associated with invasive infection (Remya, Shanthi, and Sekar 2018). Overproduction of the polysaccharide capsule and a hypermucoviscous colony phenotype is strongly associated with hypervirulence (Walker and Miller 2020). Other *K. pneumoniae* virulence factors include lipopolysaccharide (LPS), siderophores and fimbriae (Paczosa and Mecsas 2016).

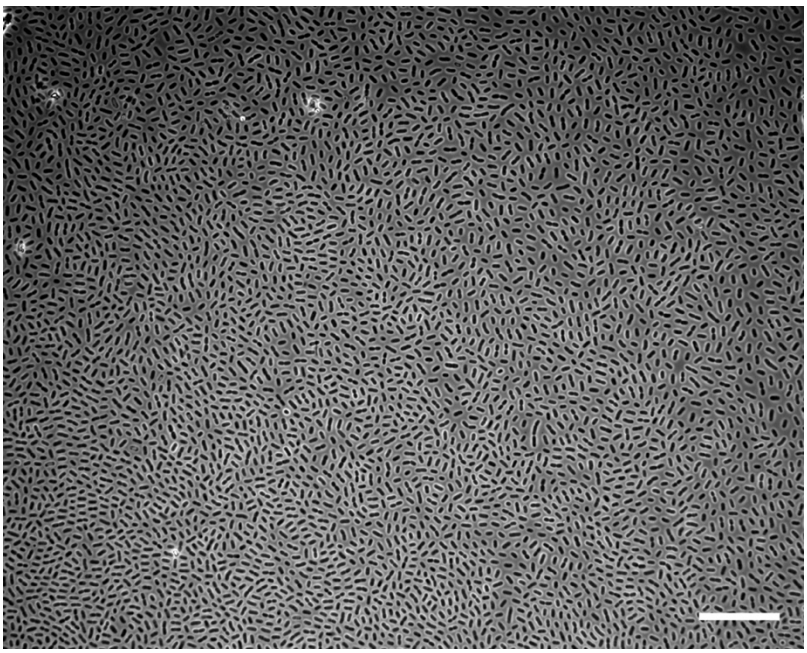


Figure 4. Phase-contrast image of *K. pneumoniae* DSM 30104 monoculture spotted on agar at high density. Scale bar: 20μm. Reproduced with kind permission from Dr Elisa Granato. Rod-shaped cells (in black) appear at regularly spaced intervals due to presence of a polysaccharide capsule surrounding each cell.

1.7 Producing resistance to *K. pneumoniae*: aims and approaches

Carriage of *K. pneumoniae* is a major risk factor for infection (Gorrie et al. 2017). One study of 498 intensive care unit (ICU) patients found that 49% of infections were caused by the patient's own unique *K. pneumoniae* strain (Gorrie et al. 2017). Carriage was also found to be higher among patients who had been in recent healthcare contact. 6% of ICU patients admitted direct from the community carried *K. pneumoniae*, compared with 19% of patients who had experienced recent healthcare contact, suggesting that exposure to healthcare settings is also a risk factor for colonisation and subsequent infection. Another study also found that *K. pneumoniae* carriage was higher among patients who had recently been in a hospital. The cohort study took place in geriatric wards in a specialised hospital and found that throat carriage of *K. pneumoniae* was 4.1% and rectal carriage 10.8%. Isolates were diverse and there was no evidence of transmission in the wards. However, the extended spectrum beta-lactamase (ESBL) *K. pneumoniae* strains were found to have been acquired in the referring hospital prior to the geriatric ward (Gorrie et al. 2018).

To date, no vaccines are available against *K. pneumoniae* infection. Producing a vaccine against *K. pneumoniae* based on its capsular polysaccharide is notoriously difficult due to the high diversity of capsular serotypes (Assoni et al. 2021). The absence of vaccine and high level of antimicrobial resistance means that there are limited therapeutic options for *K. pneumoniae*. This led me to choose to focus on *K. pneumoniae* as a model pathogen in my research. There is an increasing need to be able to prevent and treat *K. pneumoniae* infection, and I wanted to find out whether manipulating the gut microbiome to increase its colonisation resistance could act as a potential, alternative solution to antimicrobials and vaccines. In addition, I aim to uncover general principles that underlie colonisation resistance in the microbiome. What types of microbiomes are pathogen-resistant, and why? A better understanding of the ecological basis of colonisation resistance will be vital if we are to achieve the ultimate goal of engineering the microbiome to control infection.

1.8 Thesis outline

Chapter 2: Methods and ways of working with many species of gut bacteria

This Chapter outlines the methods developed for carrying out experiments using diverse, synthetic communities of human gut bacteria, ranging from two to 50 species in size. It is aimed as a guide for a newcomer to the field of microbiome science, to pass on the experimental knowledge that I have gathered over my DPhil. First, I discuss culturing and maintaining stocks of 100 human gut strains, many of which are sensitive to oxygen exposure and notoriously difficult to grow. Second, I recount how to assemble diverse microbial communities while avoiding contamination, for

experiments both *in vitro* and in germ-free mice. Finally, I detail a few tips for working with *K. pneumoniae*.

Chapter 3: Single strains of gut bacteria provide poor colonisation resistance

Here, I explore whether single strains are sufficient to provide colonisation resistance. I carry out an initial, high-throughput co-culture screen of 100 human gut symbiont strains for their individual ability to resist the growth of the human pathogen *K. pneumoniae*. Two assays are developed to simulate different conditions in the gut: the competition and the ecological invasion assays. The results of the two assays are combined and a subset of the 10 best-performing species from the screen is chosen. Another *in vitro* assay, the extended competition, is developed to more stringently test the ability of a single strain or a community to resist pathogen growth. The 10 best-performing species do not perform well individually. However, when combined into a 10-species community a striking non-additive effect is observed, where the community is able to resist *K. pneumoniae* growth by three logs compared with the single species. This effect is not seen when the equivalent experiment is performed with the community of 10 worst-performing species, suggesting that diversity and composition are both important for colonisation resistance. The results are validated *in vivo*, using gnotobiotic mice.

Chapter 4: Ecological diversity promotes colonisation resistance by human gut bacteria

In this Chapter I delve deeper into unravelling why some communities are more resistant to pathogens than others. I do this by randomly assembling communities of different diversity and composition and testing them in the extended competition assay for their ability to resist *K. pneumoniae* growth. The diversity of these communities ranges in size from two to 50 species. Higher-diversity communities display greater resistance to *K. pneumoniae* growth, but only when the species *E. coli* is present. This is validated in gnotobiotic mouse experiments. Two ecological principles of colonisation resistance are uncovered: diversity and the presence of a closely related key member species such as *E. coli*.

Chapter 5: The role of nutrient blocking in colonisation resistance in the gut microbiome

Here, I discuss the potential mechanisms of colonisation resistance in a community, and the experiments conducted to elucidate the underlying mechanism producing resistance to *K.*

pneumoniae growth. Spent media, nutrient supplementation and biolog assays are carried out. I hypothesise that inter-strain ecological competition for niche space plays a major role in determining the outcome of colonisation resistance. Based on this hypothesis, predictions are made about which combinations of human gut bacteria would provide the most and least colonisation resistance to a clinical isolate of AMR *E. coli*. Two sets of predictions are made. One is based on phenotypic profiling of the strains using biolog plates. The other approach calculates protein family overlap from the genome sequences of each strain. The predicted communities are next tested experimentally *in vitro*, to validate the predictions based on metabolic overlap. This work reveals that nutrient competition plays a key role in colonisation resistance in the gut microbiome.

2. Methods and ways of working with many species of gut bacteria

2.1 Abstract

The human gastrointestinal tract is home to hundreds of microbial species, collectively known as the gut microbiota. One of the key benefits of the gut microbiota to the host is its ability to protect the host against infectious disease. During my DPhil, I have carried out research on the ecological principles of colonisation resistance in the human gut microbiota. My key goal throughout has been to find out what sets of communities are more pathogen-resistant than others, and why. This work requires culturing a large number of human gut bacterial strains and species and combining them into diverse synthetic communities. The bottom-up approach allows investigation into the role of individual strains and strain combinations in colonisation resistance. However, this approach also represents a significant experimental challenge. One must successfully simultaneously culture diverse bacterial species that have diverse metabolic requirements, including many that are oxygen-sensitive, which requires working in anaerobic hoods that are not as sterile as the bench. A key contribution of my thesis, therefore, is the optimisation of methods and ways of working with diverse anaerobic bacterial communities. The aim of this Chapter is to put this knowledge in writing and pass on what I have learnt and developed during four years of establishing protocols for large-scale ecological experiments with gut bacteria. In addition, I will discuss working with *Klebsiella pneumoniae*, as an important pathogen and resident of the human gut microbiome.

2.2 Introduction

In order to carry out research on the ecology of colonisation resistance in the human gut microbiome, it is necessary to work with a large number of microbial strains and species. In particular, we carry out bottom-up experiments, where one assembles diverse communities from monocultures of individual strains. This can be contrasted with top-down experiments, where complex, natural communities are obtained and studied. Such top-down experiments are commonly found in the microbiome field (Osbelt et al. 2021; Pereira et al. 2020; Sequeira et al.

2020), however, the constituent strains in a complex community sample are often not well characterised, making it difficult to work out the contributions of individual strains to community function. In contrast, assembling defined communities with a bottom-up approach enables one to move more easily from making correlative to causative claims. However, these experiments represent a challenge, in that they require managing and simultaneously culturing a diverse collection of gut microbial species. I cultured over 100 different symbiont strains during this project, often at the same time. Many human gut microbial strains are anaerobic and notoriously tricky to grow and, with so many species, contamination with other bacterial species poses a significant risk to data quality. Contamination is a particular problem when carrying out anaerobic experiments because it is not possible to work next to a flame in the anaerobic chamber, as there is no oxygen. In this Chapter, I aim to set out the key lessons I have learned about working with communities of gut bacteria over the course of my DPhil. My hope is that this document will be helpful to future students and newcomers to the field.

The field of microbiome community ecology is relatively new, and there is no single agreed model microbial community for the field. Indeed, there is arguably a benefit from there being a range of different experimental systems, given the natural diversity of community compositions between individuals and host species. Nevertheless, one important model is the Oligo MM12 model community established in 2016 by Barbel Stecher's lab, which is a 12-member minimal gut community that provides colonisation resistance to *Salmonella enterica* serovar Typhimurium in gnotobiotic mice (Brugiroux et al. 2016) and has been widely adopted amongst microbiome researchers. However, this community consists of mouse gut as opposed to human gut bacteria, and does not contain *Escherichia coli*, a commonly found human gut symbiont. Our strategy was to work with a community of human gut bacteria to make our findings as relevant as possible to the human microbiome. Here, a handful of synthetic human gut consortia have recently been published, such as a 104-strain community composed of common taxa in the human microbiota ("hCom1") in 2022 (A.G. Cheng et al. 2022), or a community of 100 gut strains ("MCC100") in 2021 (Perez et al. 2021), but these have not yet been adopted by other labs and were not published when we began our work. In our experiments, we studied a wide range of different community compositions up to a maximum diversity of 50 non-pathogenic human gut species, which we studied both *in vitro* and to colonise gnotobiotic mice (see Table S1).

This Chapter is organised as an introduction to working with diverse gut communities. My goal is to take the reader on a journey, from maintaining stocks of gut bacteria to setting up community

experiments *in vitro* and *in vivo*. By the end, the reader should be equipped with the knowledge, tricks and tips to carry out large-scale ecological experiments on the gut microbiome, and, I hope, avoid a number of potential issues that one can run into when establishing these methods.

2.3 Maintaining a diverse collection of gut bacterial strains

The Foster Lab obtained a collection of human gut bacteria from Nassos Typas's group shortly before this project started. These are all type strains and can be individually ordered from a national strain collection. The rest of the bacteria we used in our experiments were type strains that were ordered from the German strain collection (DSM). These strains were chosen to be representative of the human gut microbiota. The names, internal IDs and collection IDs of all the strains can be found in Table S1 (Appendix). The Typas strains arrived with their own internal IDs from the Typas group, "NT…", which we continued to use in the Foster Lab. The strains that we ordered directly from DSMZ were given internal Foster Lab IDs. For instance, "A1" for *Bifidobacterium bifidum*. Members of the gram-positive phylum Actinobacteria were given IDs beginning with "A", whereas members of the gram-negative phylum Bacteroidetes were given IDs beginning with "B'. The members of the mostly gram-positive phylum Firmicutes, as well as *Akkermansia muciniphila* (a phylogenetic anomaly in the Foster collection, belonging to Verrucomicrobiota), were given IDs beginning with "F". Some strains in the Typas collection overlapped with the strains we had ordered for the Foster collection, leading to duplicate results for some of the symbiont strains in the screen (see Chapter 3). These were later merged, meaning that there were higher levels of experimental replication for some strains than others.

Upon receipt of bacteria from another lab or a strain collection, it is vital to make sequenced, well-labelled, uncontaminated freezer stocks of each strain for every person who uses the bacteria. The original stocks should never be used for lab experiments, except in order to make "working" stocks, from which cultures can be repeatedly inoculated. It is possible (and has happened on multiple occasions) that the original stocks are labelled incorrectly or contaminated with another strain, so this needs to be checked before embarking on any experiments.

Each new stock should first be sequenced to confirm strain identity, and duplicate "working" and back-up stocks made. This is best done by streaking the stock on an agar plate on the bench and transferring the plate to an anaerobic chamber until colonies grow. In the Foster Lab, we use mGAM agar (modified Gifu anaerobic medium), which is a nutrient-rich medium designed to support the growth of diverse anaerobic bacteria. Streaking should ideally take place on the bench,

where it can be done next to a flame, to avoid contamination of the stock. Transferring the stock to the anaerobic chamber runs the risk of contamination and defrosting of the stock. The latter can lead to bacterial death, shortening the stock's shelf-life. But some strains, such as *Roseburia* spps. are more sensitive to oxygen exposure than others, and in extreme cases it may be necessary to streak the stock anaerobically. However, we found that using a large amount of stock to streak from and quickly transferring the plate to the anaerobic chamber is usually sufficient. From my experience, the disadvantages of streaking in the anaerobic chamber outweigh the benefits, because the risk of contamination is too high. Not every anaerobic gut strain we used was able to grow on agar plates directly from freezer stock. A minority of strains only grew in liquid culture. If streaking directly from freezer stock proves tricky, I suggest inoculating the stock in liquid culture and letting it grow to stationary phase, before plating. Single colonies can then be sequenced and inoculated, and new stocks made.

It is important to make new stock from liquid culture that grew from a *single* colony. Either the colony, or the resulting liquid monoculture, should be sequenced in parallel, to verify the strain's identity. We sequenced the 16S rRNA gene of the strains using Sanger Sequencing provided by Source Bioscience. The universal primers 27F and 1492R were used for all the gut bacteria, except for *Bifidobacteria*, for which the *Bifidobacteria*-specific primers g-Bifid-F and g-Bifid-R were needed (see Table S4 for primers). Either a single bacterial colony was added to the PCR mix, or approximately 1.5μL overnight culture that had been inoculated from a single colony. Carrying out a PCR with liquid culture tended to be more reliable than the colony PCR. The PCR products were loaded into and run on a gel to ensure that the PCR had worked. DNA was extracted from successful PCR mixes using a simple PCR clean-up (NucleoSpin gel and PCR clean-up). A nanodrop was then used to measure the concentration of DNA in a 1.5μL sample. Ideally, DNA samples sent for Sanger Sequencing should be at a concentration of 20ng/μL. This can be achieved by diluting highly concentrated samples in nuclease-free water, or discarding samples that were below the required concentration of 20ng/μL. A total volume of at least 12μL is needed in order to send for sequencing. Chromatograms of the returned sequence can be visually inspected as an initial check for sequence quality. If the sequence quality is visibly poor, then a request can be made to Source Bioscience to re-run the sample. In my experience, this happened a few times and once the sequence had been re-run the quality was likely to improve, probably because Source Bioscience would, on a second attempt, take additional measures to clean the DNA sample before sequencing. Poor quality sequences should not be checked against a database. Otherwise, sequences can be checked against the Silva and NCBI databases to identify the strains, filtering for

strains that match the sequence with above 97% sequence identity. Ideally, full length alignments with a high proportion of identical bases against the target strain will be returned.

Freezer stock is made by adding 750μL overnight culture of the sequence-verified strain to be stocked, to 750μL of a mix of sterile 50% glycerol 50% mGAM. This mix can be sterilised by autoclaving or filter-sterilising. It is important to make a new glycerol and mGAM mixture each time strains are stocked, to avoid contamination. Despite many of the strains being anaerobic, we have found that it is best to make the stocks on the bench, next to the flame, and transfer them quickly to the minus 70 degrees Celsius freezer to avoid unnecessary oxygen exposure. Stocks are kept in cryotubes, which should be labelled with the strain name, internal ID, collection ID and date of the stock. Differently coloured caps can be used to code for groups or collections of strains. Multiple stocks should be made for each strain and kept in different freezers, to ensure there are back-ups for all the strains. Only one stock (the "working" stock) should be used at a time and switched to the back-up in case of contamination or de-frosting of the stock.

Making media

In our experiments, we used the nutrient-rich media mGAM to grow the gut microbial strains under anaerobic conditions. Anaerobic conditions are achieved by growing strains either in the anaerobic chamber, or in Hungate tubes. Hungate tubes are glass tubes which are filled with liquid media and anaerobically sealed with a rubber stopper and a plastic cap. Here, I will detail how the Hungate tubes are prepared. mGAM or mGAM agar powder mixes are ordered from Nissui (this turns out to be surprisingly important, as we noticed that mGAM purchased from different suppliers such as HiMedia varies greatly in appearance and how well different species grow across batches). The powder is dissolved in distilled water according to the instructions. To make 1L liquid media (equivalent to 200 Hungate tubes each containing 5mL media), we dissolve 41.7g mGAM powder and 21.3g MES buffer in around 800mL of distilled water, in a plastic 1L beaker, using a magnetic stirrer. While stirring, the pH can be measured using a pH probe. This pH is usually around 5.8 before buffering. NaOH 10M solution (40g NaOH in 100mL distilled H_2O) is then added drop-wise to the media, until it reaches a pH of 6.2. Take care not to overshoot the desired pH. If it does go above 6.2, concentrated HCl can carefully be added to lower the pH. 4mL of the oxygen-sensitive dye Resazurin (made up to a concentration of 0.025g/100mL and stored in the fridge) can also be added at this point. This allows a visual check of oxygen exposure (for instance, if the cap of the Hungate tube is not tightly enough fastened), as the dye will turn red upon exposure to oxygen.

Make the media up to a total volume of 1L with more distilled water, mix and distribute into two 500mL Duran bottles. Assemble clean, empty Hungate tubes into test tube racks and use the dispenser to add 5mL buffered media to every tube. This can be done on the bench. Next, transfer the filled tubes to the anaerobic chamber. The chamber should contain a gas mix of 2.5% H_2, 2.5% CO_2, 95% N_2, <20ppm O_2. This is provided by two types of gas canister attached to the chamber: one containing an anaerobic gas mix (5% H_2, 5% CO_2, 90% N_2) and the other containing pure N_2. When I first joined the lab, we used a H_2 and N_2 mix based on some initial advice, but not all the bacteria grew. Once we switched to a mix containing CO_2, many more strains were able to grow. The chamber is fitted with an air filter, which helps to reduce contamination. Leave the uncapped tubes in the chamber for at least 2-3 hours, for the media to de-gas. The colour of the media can be checked to ensure that it is no longer oxygenated. Once de-gassed, the filled tubes can be capped with a rubber stopper and a plastic screw-cap. Take care to ensure that the stopper and cap are firmly in place, in order to prevent gas exchange outside the chamber. If they are not correctly in place, some media may evaporate during the autoclave step and the tube cannot be used. The capped tubes can next be autoclaved (121 degrees Celsius, 20 minutes). Once autoclaved, tubes of media are stored in the fridge (4 degrees Celsius) until used.

Cleaning used Hungate tubes

Used Hungate tubes can be collected until there is a sufficient number to efficiently batch clean them. Firstly, use a 70% ethanol spray to remove the labels on the glass tubes. It is best to do this before autoclaving, as it is easier to remove the pen with ethanol when the glass is dry. Then, autoclave the tubes (121 degrees Celsius, 20 minutes) to kill any remaining bacteria. Let them cool, before emptying and rinsing the tubes at a sink. It is important to shake some water vigorously inside each tube (with a finger over the top of the tube to seal it), as sediment can build up inside the tube and prove tricky to shift. The tubes can be left to soak in a large bucket of water and thoroughly washed along with the caps and stoppers. The tubes are then ready to be filled with media again.

Inoculating cultures

A couple of different methods of inoculation were trialled. We began by inoculating in the anaerobic chamber, bringing multiple freezer stocks at a time into the chamber in a cold box. Doing so allowed us to inoculate directly into de-gassed falcon tubes containing mGAM, rather than into Hungate tubes, which was helpful when carrying out the initial high-throughput anaerobic screen of 100 strains (Hungate tubes are more time-consuming to prepare than falcon

tubes). But we found that this method of inoculation increased contamination because the anaerobic chamber is less sterile than working at the bench next to a Bunsen burner. In addition, despite the cold box, the freezer stocks quickly thawed when taken into the 37 degrees Celsius anaerobic chamber, and the cycles of thawing and re-freezing reduced their shelf-life. Therefore, we decided to follow a method of inoculating on the bench into Hungate tubes. Each tube is filled with 5mL buffered mGAM. Cultures can be inoculated or sampled on the bench using sterile needles (25G x 1") and 1mL syringes, which prevents gas exchange. To set up for inoculation on the bench, ensure that the Bunsen burner, needles and syringes, pipette and Eppendorfs are within easy reach. Label a fresh Hungate tube (these should be stored at 4 degrees Celsius) with the strain that is being cultured. The labels can rub off in an incubator, so it may be worth trying a few different pens and making sure that the label is clear. Sterilise the cap of the Hungate tube by dabbing it on a piece of cotton wool soaked in ethanol and passing it through a flame. Next to a flame, add 100µL sterile mGAM to an Eppendorf. Find the correct cryotube stock in the minus 70 degrees Celsius freezer and bring it to the bench in a cold box, to prevent thawing of the stock. Using a pipette tip, transfer a large crystal of freezer stock to the Eppendorf. Quickly, to minimise oxygen exposure, use the needle and syringe to transfer the mGAM plus dissolved crystal to the Hungate tube. To avoid injecting oxygen into the Hungate tube, try to only inject the 100µL of dissolved mixture and do not force the syringe all the way down. Take the stock back to the freezer immediately and incubate the Hungate tube in the 37 degrees Celsius shaking incubator. Bacterial strains differ in how long they take to reach stationary phase and also in the final optical density (OD-600) they reach. Some species, such as *Escherichia coli*, will reach stationary phase overnight, whereas other species, such as *Akkermansia muciniphila*, take three nights to grow. *Bacteroides* species reach a much higher OD-600 than *Lactobacilli*. For a list of the bacterial strains, how long they take to grow and their final OD-600s, see Table S2. OD-600 is most efficiently measured using a dedicated Hungate tube OD-600 reader (WPA Biowave C08000 Cell Density Meter), and using a tube of plain mGAM media as a blank. Previously, we would remove culture with a clean needle and syringe from every monoculture, and measure the OD-600 in cuvettes. This would take a long time, and the process was sped up by acquiring a machine that allows Hungate tubes to be inserted directly, rather than needing to sample culture for every measurement.

Notes on using needles and syringes

Safety: The use of Hungate tubes necessitates the use of needles and syringes for inoculation. These are obviously potentially hazardous, not only because of accidental injury but also the possibility of delivering bacteria with an injury. If a needle stick injury happens, run the injured finger under

water and clean the injury as much as possible (some suggest to try to squeeze anything out that may have entered the finger), before informing the department's health and safety officer. A needle-stick injury is especially problematic if the syringe contained any bacteria. I have given myself two needle-stick injuries during my DPhil, one with a sterile needle and another with a needle with a non-pathogenic strain of *E. coli*. I was fine both times, but it is easily done, particularly when one is starting. The needles must always be disposed of in a special sharps bin. Once full, the bin should be locked shut and autoclave tape labelled and then autoclaved and disposed of correctly. It is vitally important not to 're-cap' the needles after use. From experience, doing so is dangerous and is what is most likely to lead to needle-stick injuries.

Syringe technique: In order to draw up precise volumes of culture from the Hungate tube, the side of the syringe can be tapped gently with a finger to remove any air bubbles. If the Hungate tube with the needle and syringe inserted is held upside down while doing this, the syringe can be pushed slightly to release the air from the syringe back into the Hungate tube. Releasing the air from the syringe so that it contains only culture is also good practice to avoid injecting oxygen into a new Hungate tube.

2.4 Setting up an *in vitro* community experiment: from start to finish

The stages of an *in vitro* community experiment, also known as the extended competition assay, are outlined below (Figs. 1-3). The experiment is designed to incorporate an ecological invasion stage (Day 1) where the pathogen is inoculated into an already grown community, with a competition stage (Day 2) where the community and pathogen mix is passaged into fresh media and left to grow. We chose to inoculate the pathogen into a gut community at low density and subsequently supplement with fresh media in order to recapitulate the gut environment. When a pathogen enters the gut, it is likely to be at decreased density (depending partly on how much was ingested) as many cells will have been killed by the stomach acid (Rao et al. 2006). The pathogen is also likely to face a pre-established gut community, with many strains at stationary phase (Lim et al. 2023). As the host ingests more food, the nutrient supply will be replenished, giving the pathogen a chance to feed on new nutrients. This replenishing of nutrients is reflected in the passage stage of the experiment. In total, each experiment takes eight days, so it is worth planning ahead as going into the lab every day is required and some days are more time-intensive than others. I found that once I had improved my experimental technique, I could gradually build up to taking more experiments at a time, and started to run multiple experiments in parallel, each one staggered by a day.

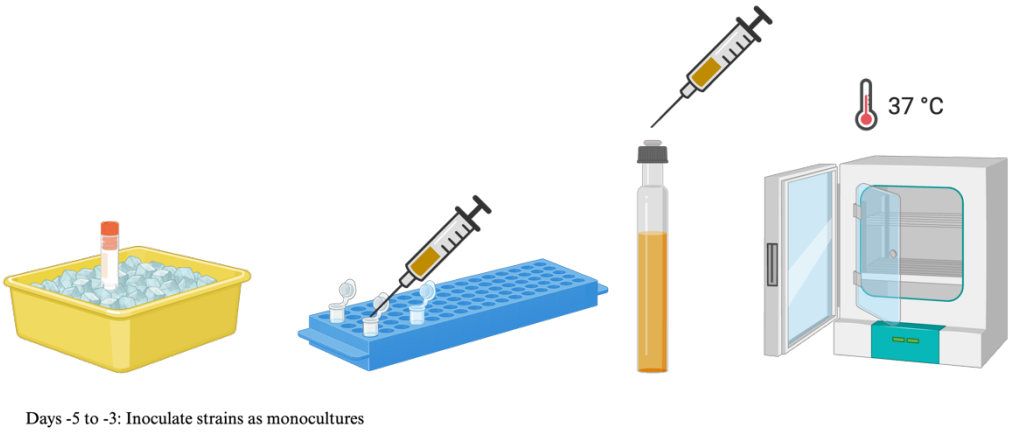


Figure 1. Days -5 to -3 of an *in vitro* community experiment. Inoculate monocultures of symbiont strains from freezer stock into Hungate tubes at the bench. Refer to Table S2 in the Appendix for how long each strain takes to grow and plan the timing of inoculation accordingly. Made with BioRender.

Day -5 to -3: Inoculate symbionts

Begin by inoculating the required symbiont strains as monocultures, as detailed in the "inoculating cultures" section above. As the symbiont strains take differing lengths of time to grow, it is best to calculate backwards which strains to inoculate on which day (see Table S2 and Fig. 1). Some strains are more difficult or unpredictable to grow than others, so usually we inoculate some of these tricky strains multiple times, to increase the likelihood that one of them grows. Quite a lot of freezer stock needs to be used to inoculate some of these strains. If they do not grow the first time, try again with more freezer stock. A quick initial check for contamination can be done by getting to know the characteristic growth of each strain and checking that it grows as expected. For example, how long the strain takes to grow, the density it grows to, whether it is 'clumpy' or if it produces gas (see Table S2). A more thorough check is done by streaking each individual strain on mGAM agar and incubating anaerobically. If there is no contamination, only one type of colony should grow.

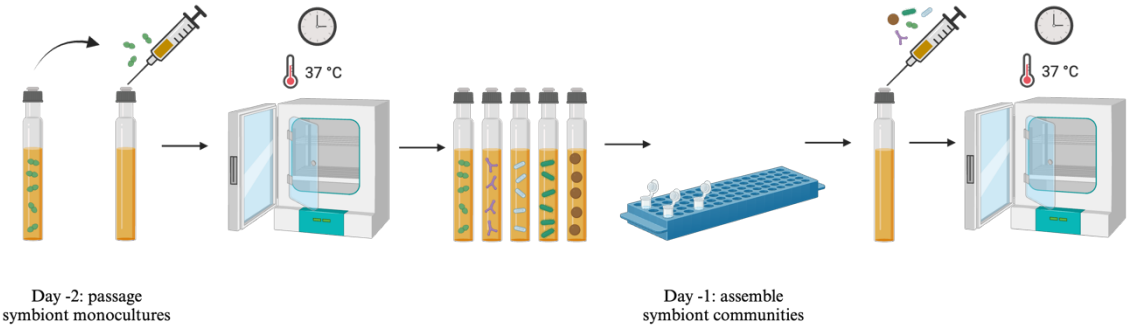


Figure 2. Days -2 and -1 of an *in vitro* community experiment. On Day -2, passage all symbiont monocultures. On Day -1 assemble communities under anaerobic conditions and incubate communities for 24 hours. Made with BioRender.

Day -2: Passage symbionts

Once all the symbiont monocultures reach stationary phase, passage the strains in parallel into fresh Hungate tubes (passage 100μL culture into 5mL media) and leave them to grow overnight (Fig. 2). Usually, I passage the strains at 5pm and they are ready to use at 10am the next day. It is critically important to passage the strains simultaneously before assembling them into communities in new media. Lag phase is the temporary period of non-replication that occurs when bacteria are introduced to fresh media and it varies in length depending on factors such as how long a strain has been at stationary phase and starved of new media, and the number of cells in the culture (Bertrand 2019). It is, therefore, important to ensure that no strain has been sitting at stationary phase for a long period of time before assembling the communities. Passaging the strains into fresh media the day prior to assembling the communities will help to avoid variation in lag phase between strains. If the strains are not passaged before community assembly, the resulting data will be highly variable to the extent that it is unusable.

Day -1: Assemble communities

Assemble the desired communities from the cultures of single strains (Fig. 2). Take the Hungate tubes out of the incubator and sterilise the caps at the bench by dabbing them on a cotton pad soaked in ethanol and passing them through the flame of the Bunsen burner. Transfer the tubes into the anaerobic chamber and "de-gas" each one with a sterile needle. A few of the strains produce gas, which, unless removed, builds up inside the Hungate tube, making it difficult to sample accurate volumes with a needle and syringe. Write a list of the communities to make. As

32 communities can be sampled per 96-well plate, it is best to make 16 or 32 communities per experiment, if possible. The formatting is obviously a personal preference but I find it easiest to set out a list like this:

T1 goes into TD3, TD9, TT2, TT8, TP8;
T2 goes into TD4, TD5, TT13, TP1;

And so on, where 'T1' and T2 are *strain* identifiers (for me T1 is the best-ranked strain from the luminescence screen, *B. breve*) and these are followed above by *community* identifiers, where for me 'TD#' are the two-strain, 'TT#' the three-strain, and 'TP#' the five-strain communities. Label Eppendorfs with the community code, such as TD3. Use a needle and syringe to sample one of the monocultures, and add 100μL culture to each of the Eppendorfs labelled with a community that contains that strain. Take care not to touch the needle to the inside of the Eppendorfs, and use a new needle and syringe for each strain. Keep the Eppendorf lids closed as much as possible, only opening them when adding a strain. It is sometimes possible to use the same needle and syringe for multiple communities, bypass the Eppendorf step, and transfer strains straight to the Hungate tube that is ultimate destination for these experiments. This is true in some cases, for example, those communities designed to resist the AMR *E. coli* strain (some example communities are listed below, see also Chapter 5, Table S7). Here, because the two-strain community is composed of a subset of the three- and five-strain communities, the same needle and syringe can be used to inoculate strain NT5077 directly into the Hungate tubes for all three communities, providing that they are inoculated from least ("Best two-strain Biolog") to most ("Best five-strain Biolog") diverse in order to prevent contamination between communities:

Best two-strain Biolog: NT5077, NT5037
Best three-strain Biolog: NT5077, NT5037, B11
Best five-strain Biolog: NT5077, NT5037, B11, NT14075, NT5041

Crucially, the needle can provide a source of contamination, and transfer different species of bacteria between Hungate tubes. It is important not to use the same needle between Hungate tubes that contain different species. Other methods we use to prevent contamination include adding *E. coli* last, as this is the most frequent contaminant, and wiping surfaces and the rubber gloves with Distil in between sampling each species. Ethanol cannot be used in the anaerobic chamber because

it evaporates in the air lock. Virkon is too harsh on the plastics of anaerobic chamber and cannot be used either. Distil or ChemGene can be used instead.

Once the communities have been made in the Eppendorfs, the mixes can be transferred to fresh, labelled Hungate tubes using a new, sterile needle and syringe for each community. These Hungate tubes are then incubated for 24 hours at 37 degrees Celsius in the shaking incubator.

In the afternoon of Day -1, inoculate the pathogen. The fluorescent *K. pneumoniae* is inoculated in the same way as the other strains, in anaerobic mGAM in a Hungate tube. Carbenicillin (50µg/mL) and kanamycin (50µg/mL) are added to select for *K. pneumoniae* and for plasmid retention, respectively.

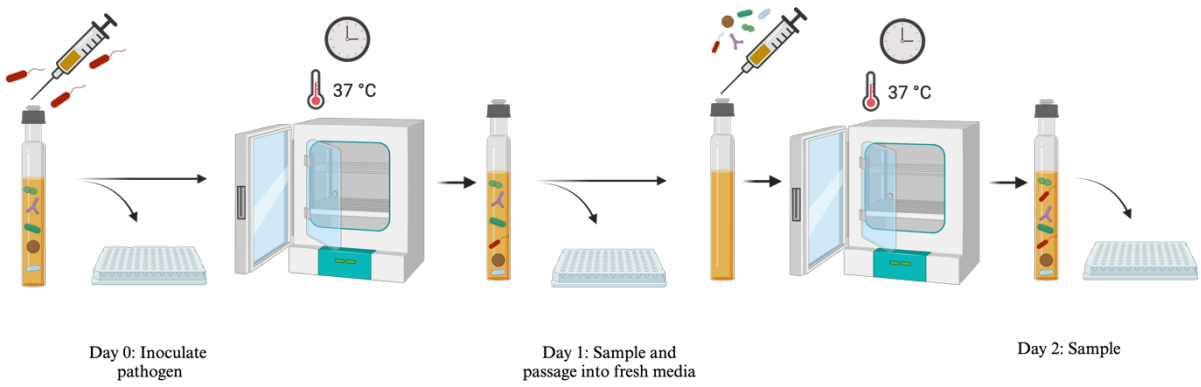


Figure 3. Days 0 to 2 of an *in vitro* community experiment. On Day 0, inoculate the communities with 10^6 cells/mL pathogen. Invert Hungate tubes to mix, then sample for flow cytometry. On Day 1, sample the cultures for flow cytometry and passage into fresh media. On Day 2, the endpoint of the experiment, sample for flow cytometry. Made with BioRender.

Day 0: Community invasion by pathogen or other strains

In the morning, take the Hungate tubes containing the grown community mixes out of the incubator, sterilise the caps with ethanol and de-gas them in the anaerobic chamber. Do the same with the Hungate tube containing the fluorescent *K. pneumoniae*. The rest of the experiment can be carried out on the bench using needles and syringes. With a sterile needle and syringe, remove 200µL PBS from a 5mL Hungate tube containing anaerobic PBS. Then, add 200µL of the fluorescent *K. pneumoniae* monoculture to the same tube, to reach an OD-600 of 0.05 and a corresponding concentration of 5×10^7 cells/mL. This protocol is based on the assumption that for members of Enterobacteriaceae, an OD-600 of 1.0 corresponds roughly to a density of

1×10^9 cells/mL. Initially, I measured the OD-600 of *K. pneumoniae* each time I carried out the experiment, and this is a good idea when starting. However, over time, I became confident that this strain reached a similar OD-600 each time, and so simply used a constant volume between experimental runs. Invert the tube containing PBS and 200μL of the fluorescent *K. pneumoniae* a few times to mix well. Next, add 100μL of the standardised *K. pneumoniae* mix to each of the community mixes (Fig. 3). Make sure to use a new, sterile needle and syringe for each tube, to prevent contamination (we tested this and found that not using a sterile needle and syringe will cause contamination). Invert the tubes with the pathogen added a few times to mix well. Sample each tube with a sterile needle and syringe. Do not use the same needle and syringe for sampling as for invading with *K. pneumoniae*, as the needle may contain a higher density of *K. pneumoniae* than is actually in the Hungate tube. Add the samples to a 96-well plate to fix and stain for flow cytometry, as detailed in the section on "Flow cytometry" below. Return the Hungate tubes to the 37 degrees Celsius shaking incubator.

Day 1: Community passage

After 24 hours (give or take an hour or two, as this is not strictly time-sensitive), take the invaded communities from the shaking incubator, sterilise the caps with ethanol and de-gas them in the anaerobic chamber. Back at the bench, remove roughly 300μL from each tube, add 100μL to labelled, fresh 5mL Hungate tubes, and the rest to a 96-well plate for fixing, staining and measuring in the flow cytometer (Fig. 3). Return the newly passaged Hungate tubes to the shaking incubator.

Day 2: Final day of extended competition

Then, 24 hours later, take the Hungate tubes out of the shaking incubator and sterilise the caps and de-gas as before. At this final time-point, the tubes do not need to be de-gassed under anaerobic conditions; it can be done on the bench. Sample the tubes with needles and syringes into a 96-well plate, taking care to use a new, sterile needle and syringe for each tube (Fig. 3). Fix, stain and measure the culture samples as before in the flow cytometer. To check for contamination in the end-point cultures, use a pipette tip to streak from each culture on an LB agar plate. The agar plates can be divided into four, so that four communities can be streaked per plate, to prevent unnecessary use of plates. Incubate the agar plates aerobically overnight. The fluorescence of *K. pneumoniae* means that ultraviolet light can be used to check for the presence of other, non-fluorescent, facultative anaerobic bacteria, such as *E. coli*, at high densities. We noticed that non-fluorescent bacteria are only seen on a plate if *E. coli* is present in a community. Otherwise, only the yellow fluorescent *K. pneumoniae* should be seen. This is a quick way to determine whether non-

E. coli containing communities are contaminated with *E. coli*, which is the most common contaminant.

Flow cytometry

Here, I outline some tips on how best to set up the flow cytometry part of the extended competition assay. These tips are intended to help make the set-up much more efficient and easier to run.

Firstly, prepare the stocks for the experiment. Make up a stock of PBS and chloramphenicol (300). The volume (in μL) needed for one experiment is (80μL + 90μL) * no. of samples * 3 days. Prepare the stock in a 50mL falcon tube and keep in the fridge. Also, prepare a stock of PBS/PFA 4%, triton and DAPI. The volume (in μL) needed for one experiment is 90μL * no. of samples * 3 days. Make the stock in a 50mL falcon tube and keep it in the fridge. Importantly, DAPI is light sensitive so it needs to be kept in the dark. If making 3mL of PBS/PFA, 12μL triton and 3μL DAPI stock is needed. The DAPI stock is kept in the fridge and is dissolved in DMSO (1 mg/mL). Next, label two 96-well plates as either 'sampling' or 'measuring' (see Fig. 4).

Secondly, prepare the 96-well plates. Add 90μL of the PBS and chloramphenicol (300) stock to the sample wells in the 'sampling' plate (blue wells in Fig. 4a) and 80μL of the PBS and chloramphenicol (300) stock to the sample wells in the 'measuring' plate (blue wells in Fig. 4b). Make sure that the sample wells in the measuring plate are spaced two wells apart, to avoid contamination between samples. A total of 32 samples can be recorded per 96-well plate.

Lastly, prepare the samples for flow cytometry. Sample 100-200μL culture directly into the empty wells in the sampling plate (red wells in Fig. 4a). Use a multichannel pipette to transfer 10μL of the cultures to the sample wells in the sampling plate (blue wells in Fig. 4a) and pipette up and down a few times to mix well. Then, use clean pipette tips to transfer 10μL from the sample wells in the sampling plate to the sample wells in the measuring plate (blue wells in Fig. 4b). Secure the measuring plate on a plate shaker and set it to shake for 15 minutes at room temperature. After 15 minutes, add 90μL PBS/PFA, triton and DAPI stock to each sample well in the measuring plate, using a new pipette tip for each sample. Put the measuring plate back on the shaker and ensure that it is not exposed to light by securing a cardboard box over the plate. (DAPI is light-sensitive.) After one hour, take the counting beads from the fridge and vortex, before adding 20μL beads to each sample well. Take care to pipette up and down to mix. Use a multichannel pipette to add

200µL PBS to the non-sample wells in the plate. Then, the plate is ready to run in the flow cytometer. Note that it is fine to store the measuring plate overnight in the dark in the fridge and run it in the flow cytometer the next day. But, ensure that the counting beads are only added just before measuring the plate, as they degrade upon exposure to light and at room temperature.

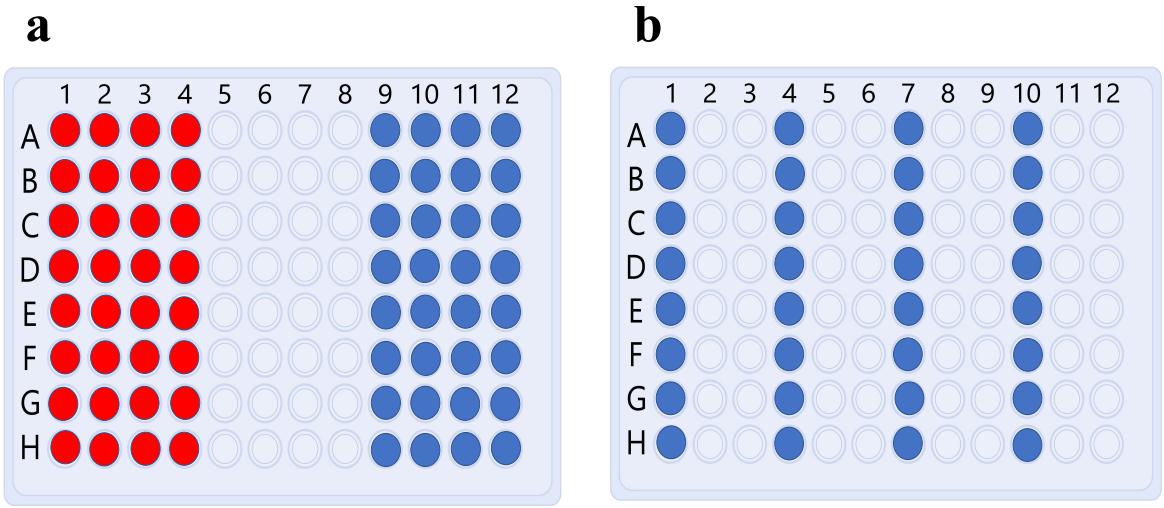


Figure 4. Layout of the sampling and measuring 96-well plates for flow cytometry in the extended competition assay. a). Sampling plate layout. b). Measuring plate layout. Pre-fill the blue wells in (a) with 90µL and the blue wells in (b) with 80µL PBS and chloramphenicol (300) stock. Directly sample cultures into the red wells in (a). Transfer 10µL to the corresponding blue wells in (a). Transfer 10µL to the corresponding blue wells in (b). After 15 minutes shaking at room temperature, add 90µL DAPI stock to the blue wells in (b). After one hour of shaking at room temperature in the dark, add 20µL counting beads to the blue wells in (b) and measure in the flow cytometer.

2.5 Setting up an *in vivo* community experiment: from start to finish

The aim of the *in vivo* community experiments is to test the communities already tested *in vitro* in a gnotobiotic mouse model, to find out whether the *in vitro* results can be reproduced *in vivo*. The same human gut bacteria strains that were used in the *in vitro* experiments are used to colonise germ-free mice. On gavage days, the communities of human gut species are assembled in the lab, each species having been grown independently as a monoculture. The OD-600 of each monoculture is measured, and the volume of each species added is calculated to ensure that each species is equally represented in the community being gavaged. Two weeks after colonisation with the symbiont communities, the mice are gavaged with the pathogen. Pathogen density is measured over the following four days by taking and plating faecal samples. Each experiment takes 23 days (just over three weeks) to carry out, so it is vital to plan well ahead, particularly as some days (such as Day -14 and Day 0) are very time intensive. One such experiment is detailed below. Some parts

of the experiment, for instance, inoculating and passaging the strains, have parallels to the *in vitro* counterpart.

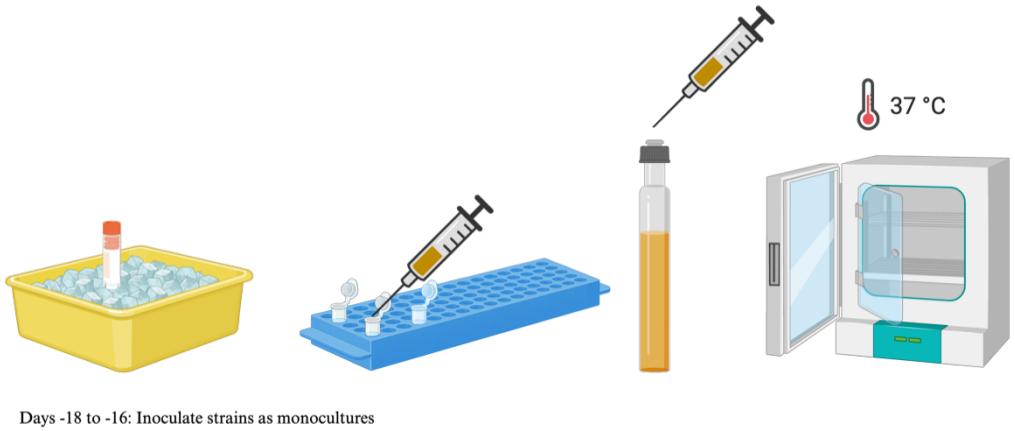


Figure 5. Days -18 to -16 of an *in vivo* community experiment. Inoculate monocultures of symbiont strains from freezer stock into Hungate tubes at the bench. Refer to **Table S2** in the Appendix for how long each strain takes to grow and plan the timing of inoculation accordingly. Made with BioRender.

Days -18 to -16: Inoculate symbiont strains

Inoculate monocultures of the symbiont strains anaerobically in Hungate tubes filled with mGAM, in the same way as described for the *in vitro* extended competition assay (Fig. 5).

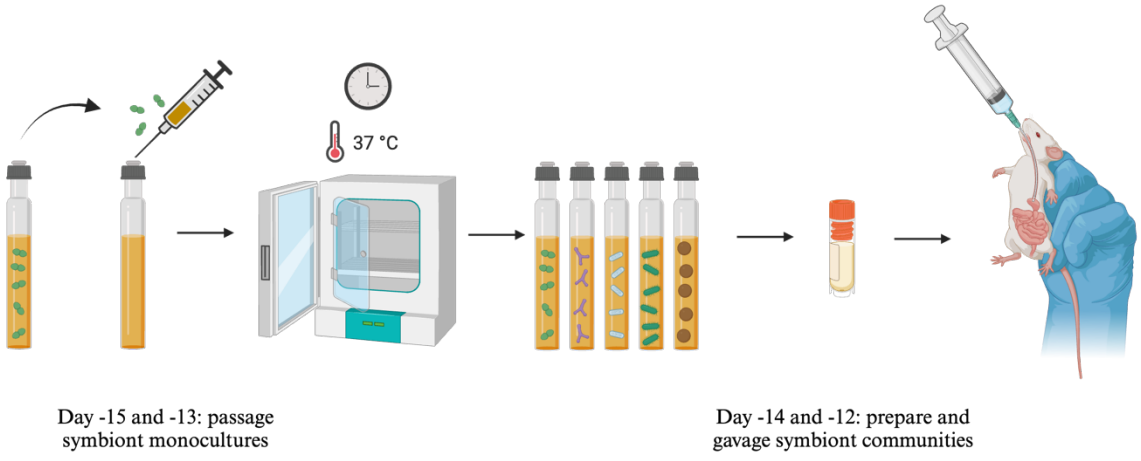


Figure 6. Days -15 to -12 of an *in vivo* community experiment. On Days -15 and -13, passage all symbiont monocultures. On Days -14 and -12 prepare communities from monocultures and gavage germ-free mice with communities. Made with BioRender.

Day -15: Passage symbiont strains

Passage 100μL culture into fresh 5mL mGAM Hungate tubes, in the same way as described for the *in vitro* extended competition assay. Do this around 3pm, if gavaging the mice at 9am the next day.

Day -14: First symbiont gavage

Arrive in the lab early to prepare the symbiont communities for gavage. Firstly, measure the OD-600 of every symbiont strain. Use the OD-600 and flow cytometry growth curve correlations (see Table S2) to calculate the required volume of each monoculture needed to obtain 10^9 cells (if gavaging one-10 strains) or 2×10^8 cells (if gavaging 49 or 50 strains). To make the communities, in the anaerobic chamber, use a sterile needle and syringe to remove the required volume from each constituent monoculture and add it to a falcon tube. As some strains reach only a very low OD-600, add up to a maximum volume of 5mL for each strain. To minimise the chance of contamination, add fast growing strains (like *E. coli* in our experiments) to the community mixes last.

When making the large communities (49 or 50 strains in our case), we found it is efficient to have two people work together: one person to read out the volumes of each strain, and another to measure the volumes of culture into the falcon tubes in the anaerobic chamber. Once the community mixes have been prepared, screw the lids on tightly to avoid oxygen exposure, and take the falcon tubes to the centrifuge. Spin down the community mixes for 10 minutes, 14000rpm, at room temperature. In the anaerobic chamber, discard the supernatant, add 2mL anaerobic PBS and resuspend. Set aside a small volume. Spin down some of this and freeze the resulting pellet for metagenomic sequencing. Dilute and plate the rest on mGAM agar under anaerobic conditions to check the inoculum density. Keep the remaining inoculum on ice and take it to the mouse facility. Gavage each mouse with 200μL. When gavaging the mice with different communities, begin with the lowest diversity community and end with the highest. If some communities contain fast growing strains like *E. coli*, carry out these gavages last to limit the chance of contamination.

Day -12: Second (repeat) symbiont gavage

In our experience, some strains do not establish in a mouse on the first gavage but do on the second and so experimental outcomes can be greatly improved by doing two gavage steps for all strains. Here, one simply repeats the protocol outlined above (Day -14). But rather than re-

inoculate all 50 symbiont strains from freezer stock, we passage the individual symbiont strains that were used for the first gavage and use these instead.

Day -1: Inoculate pathogen *in vitro*

Inoculate the wild-type *K. pneumoniae* DSM 30104 in an anaerobic Hungate tube containing mGAM and incubate in a 37 degrees Celsius shaking incubator (see Fig. 5). Add carbenicillin (50µg/mL) upon inoculation. Inoculate at ~3pm if gavaging at 9am the next day.

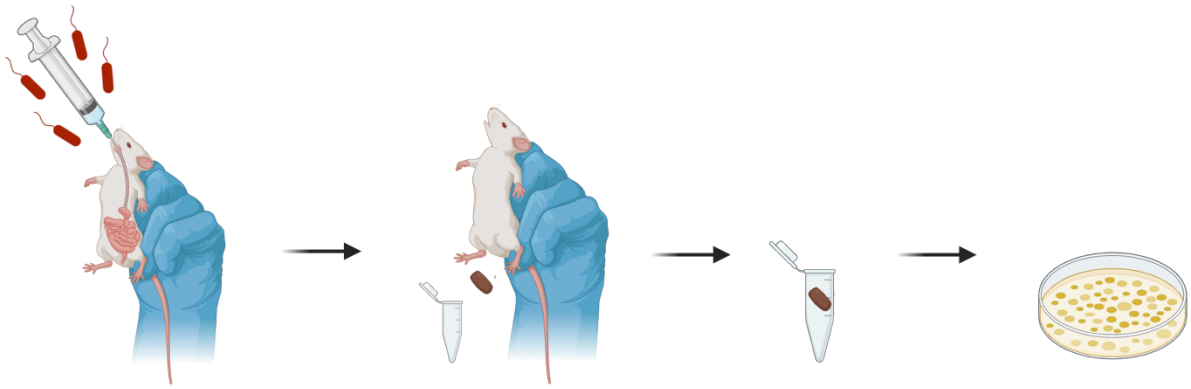


Figure 7. Days 0 to 4 of an *in vivo* community experiment. On Day 0, gavage the mice with *K. pneumoniae*. Sample faeces immediately and at 8 hours after gavage. Sample again at 24, 48, 72 and 96 hours post infection. Weigh and plate faeces on different types of agar to obtain cell counts of pathogen and symbiont species. Made with BioRender.

Day 0: Pathogen gavage

Measure the OD-600 of the pathogen culture. Transfer the 5mL pathogen culture to a falcon tube in the anaerobic chamber and spin down in the centrifuge (10 minutes, 14000rpm, room temperature). Resuspend in 2mL anaerobic, sterile PBS and spin down again. Wash three times in anaerobic, sterile PBS to remove the antibiotic and any spent media. Calculate the volume of culture needed to make 10^6 cells per 100µL (10^7 per 1mL). Dilute in anaerobic, sterile PBS. Set aside a small volume for plating on LB + carbenicillin (50µg/mL) and for flow cytometry. Keep the rest on ice. Gavage each mouse with 100µL. Weigh each mouse and take faecal samples at the same time as the gavage. Freeze a sample of each of these faeces for metagenomic sequencing. Plate the rest on mGAM and incubate in the anaerobic chamber. Take additional faecal samples 8 hours later and plate them (no need to keep for metagenomics). We found the data from selectively plating the pathogen at the 8-hour time point contained so much noise and no trend, that no conclusion could be drawn from them. This is likely to be due to variation between the mice

depending on when they had last fed before pathogen gavage. Therefore, we chose not to include these 8-hour time point results in later analysis.

Days 1-3: Faecal sampling

Weigh and sample faeces from each mouse every morning at the 24-, 48- and 72-hour time points post pathogen gavage. Freeze a part of every faecal sample for future metagenomic sequencing. Plate the faeces on LB, LB and carbenicillin (50μg/mL) and mGAM agar. We discovered that plating on mGAM at the bench and then incubating the plates anaerobically does not make a difference to the bacterial density, compared to when the plating was carried out in the anaerobic chamber.

Day 4: Mouse take-down

Take faecal samples from and take down the mice. Spray the mice with ethanol to disinfect. Remove the caecal contents, ileal contents and mesenteric lymph nodes (MLN). Make sure to remove the MLN first and caecal contents last, and to wash the dissection tools with ethanol in between each sample. Otherwise, bacteria from the caecal contents, where it is in high abundance, can contaminate other parts of the mouse body such as the MLN. This step was especially important when collecting organs such as the lungs, liver and spleen to check for systemic infection. As before, store some of each faecal pellet in the minus 70 degrees Celsius freezer for future metagenomic sequencing. Plate the remaining faeces, caecal content, ileal content and MLN on LB, LB plus carbenicillin (50μg/mL) and mGAM agar. Caecal content contains the highest density of bacteria, so only a small sized sample needs to be plated, and a 10-fold higher dilution than for the faeces can be used. Ileal content contains a lower abundance of bacteria, so a 10-fold lower dilution can be plated compared to the faeces. The MLN rarely contained many bacteria in my experiments, so no serial dilution was needed.

2.6 Working with *K. pneumoniae*

The key focus of this Chapter has been the development of protocols to perform ecological experiments with relatively large numbers of gut bacterial strains and species. However, another key feature of my work has been the focus on the pathogen *K. pneumoniae*. Here, I chose to use *K. pneumoniae* subsp. *pneumoniae* DSM 30104 in my experiments. This type strain is a category two opportunistic human pathogen. Its genome has been sequenced and is available online (J.H. Lee et al. 2012). It encodes 15 antibiotic resistance genes, including beta-lactamase genes. It is resistant to carbenicillin, which I used to select for *K. pneumoniae* when grown alone, or for selective plating

from a community. It is sensitive to kanamycin, which is partly why I chose it, so that kanamycin could be used as a selection marker when engineering the genome. *K. pneumoniae* DSM 30104 is serotype K3. The capsule type is linked to the virulence of a strain. There are 77 known K serotypes, of which K1 and K2 are recognised to be the most virulent (Brisse, Issenhuth-Jeanjean, and Grimont 2004) and cause liver abscesses (Liao et al. 2011). There are geographical differences in the spread of the serotypes, and liver abscesses due to *K. pneumoniae* infection are most prevalent in Taiwan (Liao et al. 2011). In order to cause liver abscesses, the pathogen must cross the gut epithelium and cause systemic infection. "Classical" *K. pneumoniae* strains are opportunistic and non-invasive, whereas invasive strains can be community-acquired and encode more virulence functions. Classical *K. pneumoniae* is more widespread and multi-drug resistance is currently of greater concern in these strains than in community-acquired *K. pneumoniae*.

Transformation of *K. pneumoniae* with luminescence and fluorescence plasmids

K. pneumoniae is well-known for its production of a polysaccharide capsule. Capsule production varies between strains, and hypervirulence is associated with overexpression of the capsule (Choby, Howard-Anderson, and Weiss 2020; Walker et al. 2019). Capsule production, however, can impede plasmid uptake by *K. pneumoniae* via electroporation. I initially found it difficult to retrieve many surviving transformed colonies of *K. pneumoniae*, and the capsule would often cause arcing during electroporation. But, when grown on the bench at room temperature, capsule production was lessened, making transformation of *K. pneumoniae* easier.

Measuring the cost of carrying the plasmid

The cost of the luminescence and fluorescence plasmids was measured by competing the isogenic wild type *K. pneumoniae* strain in liquid culture against its luminescent or fluorescent counterpart. The resulting co-cultures were plated to determine whether the final ratio was altered from the initial 50:50 ratio inoculated. We found that the final ratio was equivalent to the starting ratio; therefore, the cost of carrying the plasmid was minimal.

Checking for plasmid loss during the extended competition assay

Monocultures of the fluorescent *K. pneumoniae* were grown in kanamycin (50μg/mL) to ensure plasmid retention (kanamycin resistance is encoded on the plasmid). However, kanamycin could not be added to the communities during *K. pneumoniae* invasion as the symbiont strains are sensitive to the antibiotic. During the extended competition assay, the fluorescent *K. pneumoniae* grew in the absence of kanamycin for 48 hours. This is ample time for loss of the fluorescence-encoding

plasmid under strong competition. To ensure there was no plasmid loss during this time, we streaked the endpoint cultures on LB agar plus carbenicillin (50μg/mL) to select for *K. pneumoniae* and incubated the plates aerobically. Only fluorescent colonies were detected on the plates, meaning that there was no plasmid loss from *K. pneumoniae* during the experiment.

K. pneumoniae pathogenicity and invasiveness in mice

K. pneumoniae DSM 30104 is a category two pathogen, and the Kennedy Institute mouse facility had never used *K. pneumoniae* in experiments before, so I carried out some background research on *in vivo* infection with *K. pneumoniae* before it could be added to the project licence. As a K3 serotype, *K. pneumoniae* DSM 30104 should not cause systemic infection in mice. I tested this by gavaging germ-free mice with *K. pneumoniae* DSM 30104 and plating the spleen, liver and lungs upon take-down of the mice. No bacteria were found in the systemic sites of the mice, confirming that the strain is non-invasive. Some strains of *K. pneumoniae* cause inflammation in mice (Pope et al. 2019), whereas other strains do not (Lau, Huffnagle, and Moore 2008; Young et al. 2020; Calderon-Gonzalez et al. 2023). I carried out an ELISA on faecal lipocalin-2, a commonly used biomarker of inflammation, in mice colonised with *K. pneumoniae* DSM 30104, and found minimal, non-significant levels of lipocalin-2. In addition, no weight loss was observed during colonisation. These results show that *K. pneumoniae* DSM 30104, despite colonising the gastrointestinal tract, does not cause notable inflammation in mice.

Choosing the *K. pneumoniae* gavage dose

As *K. pneumoniae* had not been previously used in the Kennedy Institute mouse facility, there was no standard procedure to follow in terms of infection dose. *K. pneumoniae* strains are genetically diverse and vary in their ability to colonise the gastrointestinal tract (Calderon-Gonzalez et al. 2023). I read the literature to determine what dose of *K. pneumoniae* was commonly used in mouse models. This ranged widely from 10^5 to 10^{10} CFU (Pope et al. 2019; Lau, Huffnagle, and Moore 2008; Young et al. 2020; Sequeira et al. 2020) and also depended on whether the mice were germ-free or SPF, or if their gut microbiota had been depleted with antibiotics before the gavage. I tested a range of doses of *K. pneumoniae* DSM 30104 on germ-free mice and decided to use a dose of 10^6 CFU. All doses tested (10^4, 10^6 and 10^8 CFU) colonised the mice and had reached saturation by 24 hours. The mice remained healthy over four days, with no drop in weight or signs of inflammation during dissection. The 10^6 dose was high enough to colonise germ-free and pre-colonised mice (with a community of up to 50 strains), but not so unnaturally high as to completely overcome the colonisation resistance provided by the symbiont communities.

***K. pneumoniae* and antibiotic resistance**

The *K. pneumoniae* strain I used is naturally resistant to the semisynthetic penicillin, carbenicillin. Carbenicillin is bactericidal and interferes with cell wall synthesis by inactivating the transpeptidase enzyme. It targets mainly gram-negative bacteria. However, it is susceptible to degradation by beta-lactamases. I tested a range of carbenicillin concentrations in liquid culture to evaluate the minimal inhibitory concentration. Specifically, I wanted to choose an antibiotic concentration that was as high as possible, so as to select for *K. pneumoniae* from a diverse community of symbionts, whose antibiotic susceptibility had not been tested. Therefore, I initially chose to use a concentration of 200μg/mL, which is high but did not kill *K. pneumoniae* DSM 30104 in liquid culture *in vitro*. However, when I plated faeces from mice colonised with *K. pneumoniae* on LB agar and LB agar + carbenicillin (200μg/mL), I began to notice a difference between *K. pneumoniae* counts on LB and on LB + carbenicillin (200μg/mL) plates. Faecal *K. pneumoniae* seemed to have increased sensitivity to carbenicillin (200μg/mL): colonies took longer to grow and were less abundant compared to their counterparts on LB agar. However, when I replica-plated the LB agar colonies on to LB agar + carbenicillin (200μg/mL), all *K. pneumoniae* colonies were able to grow as normal. We hypothesised that the *K. pneumoniae* becomes stressed in the mouse gut and that this lowers its tolerance to carbenicillin, but that the colonies recover during growth on LB agar and the resistance phenotype is recovered. *In vivo* altered susceptibility is a known phenomenon and it has been suggested that an alternative to *in vitro* screening for resistance to clinically used antibiotics is needed (Ersoy et al. 2017). Therefore, I switched to using a lower concentration of carbenicillin (50μg/mL). This concentration of carbenicillin was high enough to eliminate *E. coli* IAI1, but low enough that it did not impact the survival of faecal *K. pneumoniae*. Interestingly, after the colonies have grown on LB agar and are left a day or two at room temperature, *E. coli* and *K. pneumoniae* become easily distinguishable from one another. *E. coli* looks yellow and matte, whereas *K. pneumoniae* colonies appear white and shiny. This could partially remove the need to use selective plating, except for when the *E. coli* density is much higher than the *K. pneumoniae* density and different dilutions need to be plated.

2.7 Discussion

In this Chapter I have outlined the methods for the *in vivo* and *in vitro* community experiments developed during my DPhil, alongside some suggestions about how best to carry them out. I have also gone into detail about the particular strain of *K. pneumoniae* that I used in my experiments, including why I chose it and whether a mouse experiences inflammation upon colonisation with this strain (it does not). Some studies use models of mouse gut bacteria to investigate colonisation

resistance in the gut microbiome (Jacobson et al. 2018; Sequeira et al. 2020; Pereira et al. 2020), while other studies, like our one, use human gut bacteria (Osbelt et al. 2021). It has been shown that, despite humans and mice harbouring different microbial species in nature, human gut bacteria are able to colonise the mouse gut (Seedorf et al. 2014). As our ultimate aim is to engineer human gut communities, we therefore decided to use human rather than mouse bacteria. The studies that colonise (or 'humanise') mice with human gut bacteria often begin with complex gut communities isolated from human stool samples as a top-down approach (Osbelt et al. 2021). The work presented here follows a bottom-up approach by assembling synthetic communities from individual human gut species. In doing so, we are able to build characterised communities and assess the contribution of individual species to colonisation resistance. Synthetic approaches have previously been used to study invasion resistance in plant communities or other (non-gut) microbial communities (Kennedy et al. 2002; Eisenhauer 2012; Bell et al. 2005). In addition, synthetic approaches have been used to study colonisation resistance in the gut using invertebrate animal models, such as the work of Nancy Moran on the honeybee (Steele et al. 2021) and that of Will Ludington on the fruit fly (Gould et al. 2018). But, invertebrates contain a much less complex microbiota than mammals; for instance, over 95% of the honeybee gut microbiota consists of just 10 microbial species (Steele et al. 2021) and the fruit fly gut microbiota consists of only 5 species (Gould et al. 2018). Here, we apply a synthetic approach to the complex human gut microbiota and test combinations of up to 50 species of bacteria, *in vitro* and *in vivo*.

3. Single strains of gut bacteria provide poor colonisation resistance

3.1 Abstract

The mammalian gastrointestinal tract is home to hundreds of species of bacteria, collectively known as the gut microbiome. A key benefit of the microbiome to the host is its ability to protect against harmful bacterial species and prevent infections, a phenomenon known as colonisation resistance. For many years, particular strains such as *Escherichia coli* Nissle 1917 have been heralded for their ability to promote colonisation resistance in the gut, but what determines whether certain bacteria are protective or not remains poorly understood. Here, we systematically study the ability of a diverse range of human gut bacteria to limit the growth of a major human bacterial pathogen, *Klebsiella pneumoniae*. To test the ability of individual human gut bacteria strains to compete with *K. pneumoniae*, an anaerobic screen of 100 gut strains was carried out *in vitro* using two complementary assays. Transformation of *K. pneumoniae* with a plasmid encoding luminescence production enabled the pathogen's growth to be measured during pair-wise interactions between *K. pneumoniae* and each gut symbiont. The 10 best- and 10 worst-ranked gut strains from the screen were then subjected to more detailed study in an extended competition assay designed to simulate invasion and subsequent growth in the mammalian gut. Here, symbiont monocultures are invaded with the pathogen and allowed to grow, before passage and further growth in fresh media. In this assay, *K. pneumoniae* consistently grew to a very high density in the presence of both the best performing and the worst performing strains from the screen, indicating that all strains provided poor colonisation resistance. In contrast to single strains, when we combined the 10 top ranked strains, this community was able to resist the growth of *K. pneumoniae*; something not seen for the 10 worst-performing strains from the screen. To validate the results *in vivo*, germ-free mice were colonised with the best performing single strain from the screen, *E. coli* IAI1, and challenged with *K. pneumoniae*. *K. pneumoniae* reached equivalent faecal densities in mice pre-colonised with *E. coli* IAI1 and in germ-free control mice, indicating that this strain provided no colonisation resistance. We conclude that single strains of gut bacteria provide very limited colonisation resistance. However,

our data indicate that diverse communities have the potential to perform much better in pathogen protection.

3.2 Introduction

Since the earliest days of microbiome research and the probiotic era, certain members of the microbiota have been singled out and focused on as key to the functioning of the microbiome in human health (Jacobson et al. 2018; Wotzka et al. 2018; Oliveira et al. 2020; Osbelt et al. 2021; Wotzka et al. 2019). Probably the best-known and earliest probiotic, *Escherichia coli* Nissle 1917, was isolated from the faeces of a German soldier who was fighting in the trenches during the First World War. This soldier was of particular interest because of his apparent resistance to *Shigella,* unlike his comrades, who were plagued by this and other diarrhoea-causing intestinal diseases (Sonnenborn 2016). *E. coli* Nissle 1917 is widely used both for its probiotic characteristics and in the study of the microbiome (M. Schultz 2017). Consistent with its potential importance, a clinical trial found that *E. coli* Nissle 1917 is as effective at maintaining remission of ulcerative colitis as the standard treatment, the anti-inflammatory drug mesalazine (Kruis et al. 2004). Moreover, a probiotic drug, Mutaflor, that consists of viable *E. coli* Nissle 1917 bacteria, is currently available on the market. Another intestinal species, *Akkermansia muciniphila*, is also a much discussed probiotic candidate, which was found to be at lower abundance in individuals with high BMI and blood cholesterol, than in healthy individuals (Naito, Uchiyama, and Takagi 2018) Daily administration of *A. muciniphila* for three months improved insulin sensitivity in overweight, insulin-resistant individuals, suggesting it may causally affect health (Depommier et al. 2019). In addition, there is a wealth of data on other species, including *Lactobacillus rhamnosus* and *Bifidobacterium animalis* subspp. Lactis, which have some positive indications (Dronkers, Ouwehand, and Rijkers 2020).

However, promising reports of probiotic strains represent only part of the story. Many bacterial strains have also been recorded as having little to no clinical impact (Derrien and van Hylckama Vlieg 2015; Kristensen et al. 2016; Singh et al. 2018; Barthow et al. 2022) and some even have harmful effects (Lerner, Shoenfeld, and Matthias 2019). A major issue is that there remains little understanding of what makes a beneficial strain distinctive from other strains. It seems likely that a lack of measured effect of probiotics in some cases is due to the difficulty in getting symbiont strains to colonise the human gut, also known as engraftment (Roselli et al. 2021; Shepherd et al. 2018). However, even this is debated and some challenged whether the purported health benefits of probiotics require the bacterial strain to survive and thrive in the intestinal tract (Suez et al.

2019). And even if compositional changes in the gut microbiota are observed, their effects are typically not well understood. Health effects have been assessed in a wide variety of ways but can be difficult to detect. Examples of the different types of health outcomes that have been measured in clinical studies of probiotics include treatment and prevention of pouchitis after surgery in ulcerative colitis patients (Nguyen et al. 2019), HbA1c (glycated haemoglobin) levels after six months in adults with pre-diabetes (Barthow et al. 2022) or the duration of respiratory infection in the elderly (Guillemard et al. 2010). There are also many variations confounding comparisons in clinical studies of probiotics, which include dose (which vary from 10^7 – 9 x 10^{11} CFU per day), age range of the participants (studies focus on children more than the elderly), whether the participant is healthy or not (43% of studies analysed included healthy participants (Dronkers, Ouwehand, and Rijkers 2020)), and the method of preparation of the probiotic, the description of which is often incomplete (Dronkers, Ouwehand, and Rijkers 2020). In sum, there is a great deal of variability in the literature in the effectiveness of probiotics. This variation could be due to the output measured, study conditions and the success of engraftment, or it may reflect true differences between strains.

Here, we investigate the potential for differences between the benefits provided by a diverse set of gut bacteria under controlled laboratory conditions. One of the major benefits conferred by the gut microbiome is colonisation resistance; the ability of resident bacteria to limit the growth of invading pathogens and prevent infection (McLaren and Callahan 2020). Evidence for this comes from germ-free animal work (Stecher et al. 2005) and the effects of antibiotic treatments, which can suppress the resident microbiota and leave the host highly susceptible to infection by pathogens such as *Clostridium difficile* (Theriot et al. 2014; Lewis et al. 2015). *C. difficile* infection can be successfully treated by a faecal microbiota transplant (FMT) from a healthy individual, replenishing the gut microbiota and its natural pathogen resistance (Nicholson et al. 2020). Many mechanisms of colonisation resistance by the gut microbiota have been proposed, including stimulation of the host immune system, interbacterial competition for nutrients and direct antagonism by toxins (Caballero-Flores, Pickard, and Nunez 2022; Sorbara and Pamer 2019). Moreover, experimental studies *in vitro* and in mice have highlighted the importance of certain symbiont strains for resisting pathogens (Jacobson et al. 2018; Velazquez et al. 2019; Wotzka et al. 2019; Sequeira et al. 2020; Oliveira et al. 2020; Osbelt et al. 2021; Buffie et al. 2015; Kim et al. 2019). For example, pre-colonisation of mice with the commensal strain *Klebsiella oxytoca* has been shown to speed up clearance of *Klebsiella pneumoniae* from the intestinal tract (Osbelt et al. 2021).

In another study, inoculating mice with the probiotic strain *E. coli* Nissle 1917 conferred resistance to *Salmonella enterica* serovar Typhimurium (Velazquez et al. 2019).

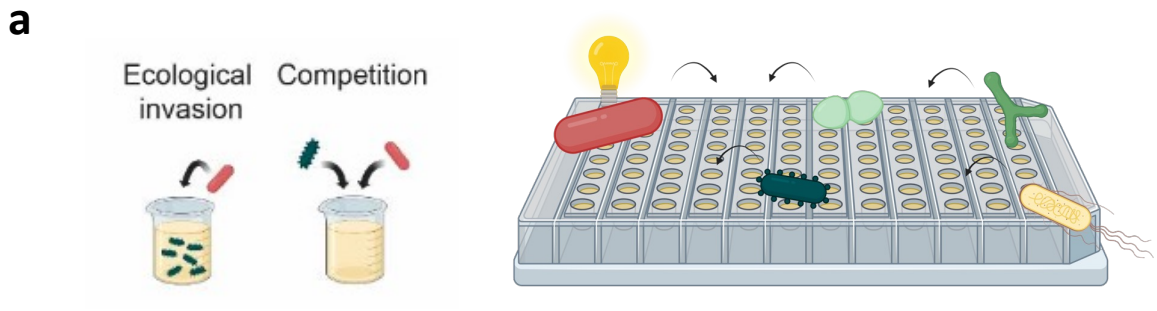
K. pneumoniae is an opportunistic pathogen that can colonise the human gut. The gut acts as an intestinal reservoir, from which *K. pneumoniae* can spread to other parts of the body and cause infection. *K. pneumoniae* is a common cause of hospital-acquired pneumonia (Torres et al. 2018), and the second most common cause of urinary tract infections worldwide (Caneiras et al. 2019). Due to its increasingly concerning levels of antimicrobial resistance, including to the last-resort antibiotics carbapenems, *K. pneumoniae* has earned a place among the ESKAPE group (an acronym for 6 highly virulent and antibiotic resistant bacterial pathogens) (De Oliveira et al. 2020) and is on the highest priority level ('critical') of the World Health Organisation's (WHO's) list of priority pathogens for research and development of new antibiotics (WHO 2017). Due to its developing resistance, there is an increasing number of reports of untreatable *K. pneumoniae* infections and outbreaks worldwide (Gomes et al. 2023; Z.Q. Yang et al. 2018; Gu et al. 2018). Colonisation of the gut by *K. pneumoniae* greatly increases the risk of infection. Recorded asymptomatic gut colonisation rates in the healthy population vary greatly, from 5% to 35% in Western populations, and between 19% and 88% in Asian populations (Russo and Marr 2019). *K. pneumoniae* is especially prevalent in hospital and healthcare settings, where the rate of gastrointestinal carriage has been recorded to increase (Gorrie et al. 2017). If a vulnerable individual's gut microbiome could be augmented by a symbiont bacterium that protects against colonisation with *K. pneumoniae*, this would greatly decrease the risk of infection and help circumvent the need for antibiotics. This strategy would be particularly important in patients upon admission to hospital, who are not already carriers, but face a higher risk of colonisation, and subsequent infection, with *K. pneumoniae*.

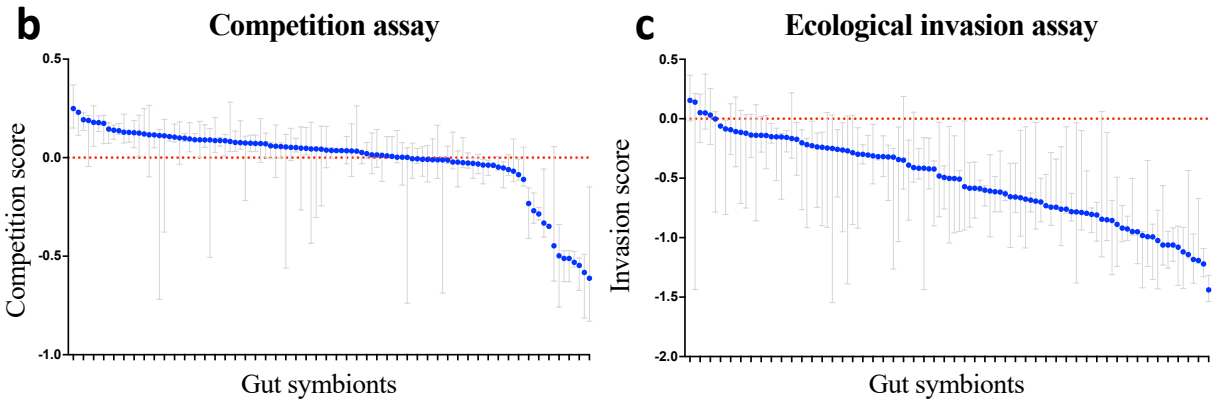
The gut microbiome contain a large diversity of strains and species and we lack a systematic understanding of the effects of single strains. Concerted effort to investigate the impacts of individual strains must be undertaken if we are to harness the natural colonisation resistance of the gut microbiome and use it, via the development of microbial therapeutics, to our benefit. In this Chapter, we set out to systematically identify individual members of the human gut microbiome that may or may not provide colonisation resistance to *K. pneumoniae*.

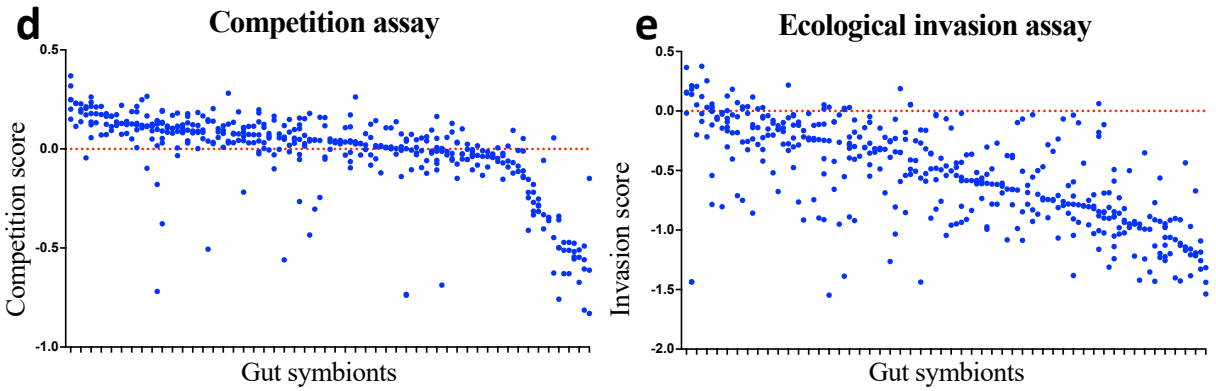
3.3 Results

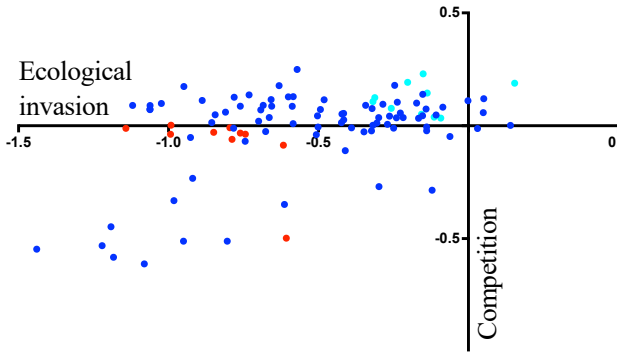
3.3.1 Screen of individual human gut symbionts

In order to identify which strains of human gut bacteria have the strongest inhibitory potential against the model pathogen *K. pneumoniae* DSM 30104, a screen of 100 human gut symbionts was carried out. *K. pneumoniae* was transformed with a plasmid that encodes constitutive expression of luminescence. Symbiont strains were pre-grown to stationary phase under anaerobic conditions and then co-cultured anaerobically with *K. pneumoniae* in 96-well plates. Two types of assay were developed and used: the competition assay and the ecological invasion assay (Fig. 1a). In the competition assay, equal volumes of symbiont and pathogen were inoculated concurrently and co-cultured. In the ecological invasion assay, symbiont strains were pre-grown in monoculture and invaded with the pathogen in a 19:1 symbiont to pathogen ratio. In both assays, after 6 hours of co-culture, the luminescence of *K. pneumoniae* was measured in order to characterise each pair-wise interaction. The luminescence measurements of *K. pneumoniae* in co-culture were normalised by the control luminescence of *K. pneumoniae* in monoculture and used as an approximation of the growth of *K. pneumoniae*. Pathogenic strains (category 2, as per the European classification) and multiples of strains from the same species were excluded from the selection. Many of the 10 best-performing strains, such as *Lactiplantibacillus plantarum*, are known to be potential probiotic strains (Seddik et al. 2017). The medians of the results from each assay in the luminescence screen are displayed in Fig. 1b-c. The full set of data for both assays is plotted in Fig. 1d-e. Strains with the most negative competition score were identified as being the best at resisting pathogen growth. The competition scores in the ecological invasion assay tended to be lower than those in the competition assay due to the design of the experiment: in the invasion assay, the symbiont strains are given the upper hand because they are already grown before the invasion, and only a relatively small volume of pathogen is inoculated. The values for *K. pneumoniae* growth in each of the competition and invasion assays were correlated against one another (Fig. 1f). From the ranked correlation, the 10 best- and 10 worst-performing symbiont strains were identified (Fig. 1g).









g

10 best-ranked	10 worst-ranked
Bifidobacterium breve	*Eubacterium rectale*
Holdemanella biformis	*Phocaeicola coprocola*
Ligilactobacillus ruminis	*Bacteroides clarus*
Bifidobacterium longum subsp. infantis	*Phocaeicola massiliensis*
Escherichia coli IAI1	*Phocaeicola vulgatus*
Lactobacillus acidophilus	*Blautia hydrogenotrophica*
Bifidobacterium animalis	*Roseburia intestinalis*
Lactobacillus plantarum	*Lactobacillus delbrueckii*
Limosilactobacillus fermentum	*Lactobacillus gasseri*
Ligilactobacillus salivarius	*Lachnoclostridium hylemonae*

Figure 1. Screen of individual human gut symbionts against the pathogen *K. pneumoniae*. (a) Schematic of luminescence screen set-up. The luminescent pathogen *K. pneumoniae* (shown in red) is inoculated in a 96-well plate containing either pre-grown symbiont monocultures (green, yellow) in a 19:1 ratio of symbiont to pathogen (ecological invasion assay) or symbiont monocultures in a 1:1 ratio with the pathogen (competition assay). Made with BioRender.com. (b-c) Results of the luminescence screen. The results of the competition assay shown in (b) and the ecological invasion assay in (e). Waterfall plots show the competition score (log of the ratio of luminescence of pathogen when grown with a symbiont vs when grown alone) of the worst-performing to the best-performing symbionts from left to right along the x-axis. Each blue circle represents the median value of a symbiont strain (n=3-10 replicates), the grey vertical bars depict the range. (d-e) The individual replicate values of the luminescence screen. The results of the competition assay are shown in (d) and the ecological invasion assay in (e). Each blue filled circle represents an independent replicate (n=3-10 replicates). The competition score (log of the ratio of luminescence of pathogen when grown with a symbiont vs when grown alone) of the worst-performing to the best-performing symbionts from left to right along the x-axis is plotted. (f) Correlation of the invasion (x-axis) and competition (y-axis) assay results. Each circle represents a symbiont strain. Red circles represent the 10 overall best-ranked symbionts and turquoise circles depict the 10 worst-ranked symbionts, excluding category 2 pathogens and multiple strains of the same species. The overall ranking was calculated by summing the ranks of the competition and ecological invasion assays. (g) The 10 best-ranked and 10 worst-ranked symbiont strains from the luminescence screen. Overall ranks were calculated by summing the ranks of the invasion and competition assays. Category level 2 pathogens were excluded from the selection, as were multiple strains from the same species (which is why, for instance, only the best-performing *E. coli* strain was selected).

3.3.2 Strains within Enterobacteriaceae are the strongest competitors of *K. pneumoniae*

A key tenet in ecology is that the strongest competitors of a given genotype are likely to be other genotypes that are ecologically and genetically similar. This effect occurs because these are individuals that are likely to share a similar niche and will, therefore, compete over shared resources such as nutrients. For example, a recent study from the lab of Karina Xavier found that the commensal species *Klebsiella michiganensis* is a strong competitor against pathogenic *E. coli* in the mouse gut. It was suggested that this was because the two species, both members of the same family, Enterobacteriaceae, share similar niches and compete directly over nutrients. To assess the extent to which phylogenetic relatedness predicts competitiveness, we made a phylogenetic tree of the human gut symbiont strains tested (Fig. 2a), where the competition scores for each strain from both competition and invasion assays is coloured on a gradient from red (most competitive) to white (least competitive). The strains belonging to the family of bacteria Enterobacteriaceae visually appear to have the strongest competitive tendency against *K. pneumoniae*. This effect is also supported by an analysis that directly compares the scores for the competition assay between Enterobacteriaceae and non-Enterobacteriaceae (Fig. 2b). A wider study of strains and species across the bacterial phylogeny would be needed to fully assess this pattern. Nevertheless, within our data set, there is evidence of stronger competition driven by close relatives. *K. pneumoniae* supports the hypothesis that closely related strains are more competitive. *K. pneumoniae* belongs to Enterobacteriaceae and its strongest competitors in the screen include other members of the family, such as *E. coli* and *Salmonella enterica* serovar Typhimurium.

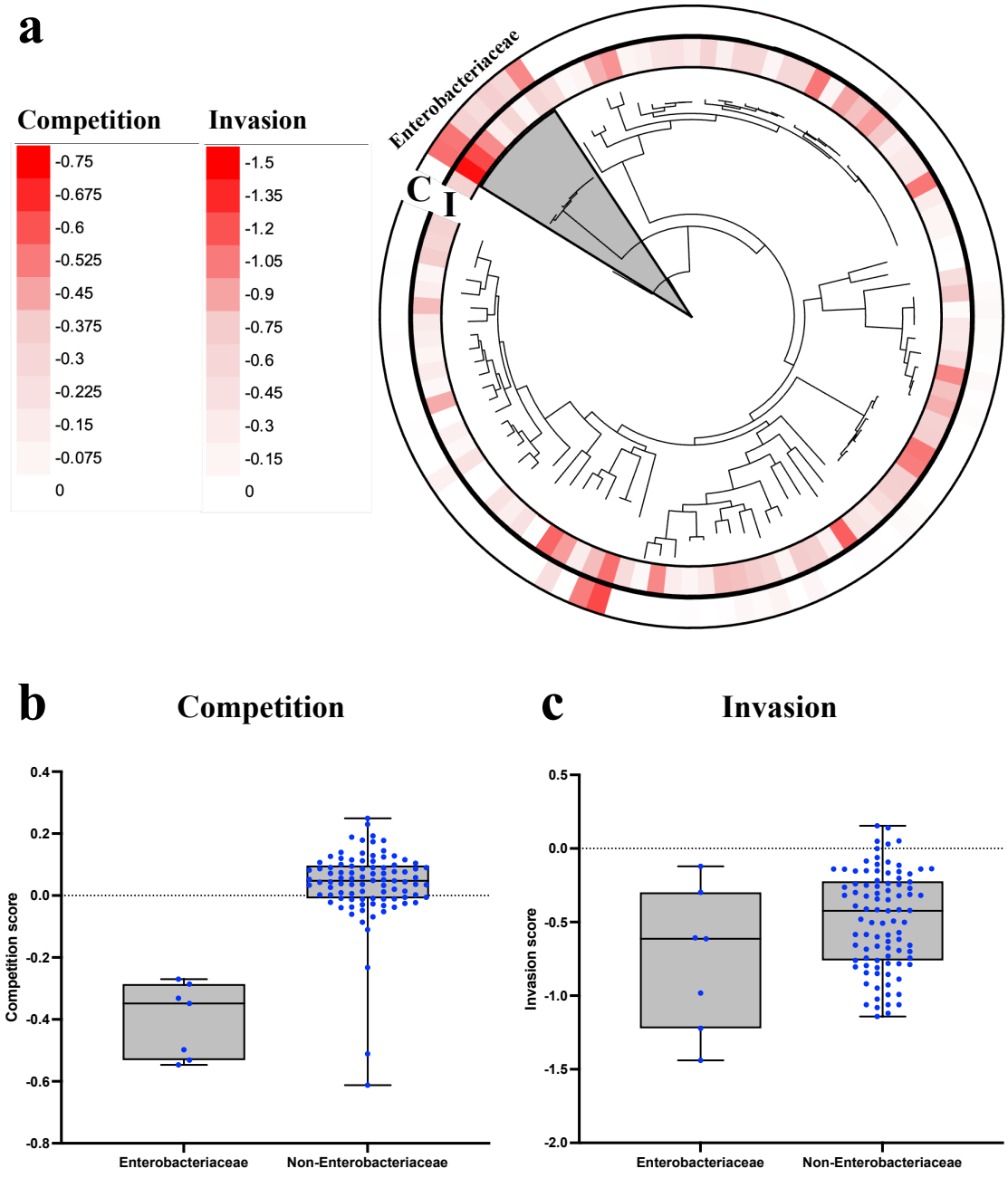


Figure 2. Close relatives (other Enterobacteriaceae) tended to be the strongest competitors of *K. pneumoniae* in the luminescence screen. (a) Phylogenetic tree, rooted on *Akkermansia muciniphila*, of all 100 symbiont strains tested in the luminescence screen. Area shaded in grey depicts the family Enterobacteriaceae, which contains *K. pneumoniae*, *E. coli* and *S. enterica*. The rings around the tree represent the results of the competition assay ('C', outer ring) and ecological invasion assay ('I', inner ring). The darker red, the stronger the inhibition of growth of *K. pneumoniae*. (b-c) Box and whisker plots comparing the results of the luminescence screen between Enterobacteriaceae and non-Enterobacteriaceae. Results of the competition assay in (b) and invasion assay in (c). Each circle represents the median value of a single symbiont strain (n=3-10). Mann Whitney U tests on (b-c) show that the inhibition values were significantly different between Enterobacteriaceae and non-Enterobacteriaceae for the competition assay ($p<0.0001$), but not for the ecological invasion assay ($p=0.1762$).

3.3.3 Single strains are not sufficient to resist pathogen growth *in vitro*

We next applied a more stringent *in vitro* test of colonisation resistance to the 10 best- and 10 worst-performing symbiont strains from the luminescence screen. This test, called the extended competition assay, was designed to combine aspects of the invasion and the competition assays from the screen (Fig 3a). Specifically, symbiont strains were pre-grown anaerobically as monocultures and invaded with *K. pneumoniae* to reach an initial pathogen density of 10^6 cells/mL. The mixture of single symbiont strain and pathogen was allowed to grow for 24 hours (the *invasion* stage of the assay). At this time, 100μL of the culture was passaged into 5mL fresh media and left to grow for a further 24 hours (the *competition* stage). Samples were taken before passage (Day 1) and at the endpoint of the assay (Day 2). The ecological invasion is followed by passage because, in the mammalian intestine, a pathogen is likely to arrive and grow from a small density relative to the symbiont, which has already colonised the gut. However, in the intestine, there is a regular influx of nutrients as the host ingests food. This influx gives the pathogen an opportunity to compete with the symbiont for new, incoming nutrients (not just those that are leftover) and explains why passage into fresh media is an important stage of the extended competition assay. As a result, we focus most attention here on the Day 2 data, because this takes into account both stages of the extended competition assay.

To follow its frequency, *K. pneumoniae* was transformed with a plasmid that confers constitutive expression of fluorescence via the YPet protein. Samples were also fixed and stained with DAPI, a dye that binds to DNA. The YPet and DAPI allowed *K. pneumoniae* and total cell density to be measured using flow cytometry, respectively. The *K. pneumoniae* density for the 10 best-performing symbiont strains on Days 1 and 2 is shown in Fig. 3b-c. The *K. pneumoniae* density for the 10 worst-performing symbiont strains on Days 1 and 2 is shown in Fig. 3d-e. Out of the individual 10 best-performing strains from the luminescence screen, *Bifidobacterium breve* is able to resist the growth of the pathogen significantly more than the no symbionts control on Day 1, keeping *K. pneumoniae* density at 10^6 cells/mL (Fig. 3b). However, this effect is lost after the passage that takes the assay to Day 2, when *K. pneumoniae* grows to its maximum density of 10^9 cells/mL (Fig. 3c). *Escherichia coli* IAI1 maintains *K. pneumoniae* at a similar level before and after passage, at 10^8 cells/mL. On Day 2, the other, non-*E. coli* IAI1, symbiont strains individually allow *K. pneumoniae* to reach a density equivalent to when it is growing in monoculture, of around 10^9 cells/mL. In contrast, we find that when the 10 best-performing symbionts are grouped together in a community, they outperform all the single strains and maintain *K. pneumoniae* density at around 10^6 cells/mL on both Day 1 and Day 2 (Fig. 3b-c). Throughout these experiments, none of the strains reduce *K.*

pneumoniae to a density below the inoculum size, suggesting that pathogen cells are not actively killed. Or, if they are, the killing rate does not exceed the growth rate of the pathogen. This finding suggests that interference competition does not play a significant role in the experiments.

Some of the 10 worst-performing symbionts also show some ability to limit growth of the pathogen before passage, such as *Roseburia intestinalis*, which maintains *K. pneumoniae* at 10^7 cells/mL on Day 1 (Fig. 3d). However, this ability is again lost after passage when *K. pneumoniae* grows to 10^9 cells/mL by Day 2 (Fig. 3e). A benefit to diversity is again also seen. When the 10 worst-performing strains are grouped together, the resulting community performs well on Day 1, maintaining *K. pneumoniae* density at 10^6 cells/mL (Fig. 3d). However, on Day 2 *K. pneumoniae* grows to 10^9 cells/mL (Fig. 3e).

In sum, therefore, we find that single strains perform poorly in their ability to resist pathogen growth under extended competition.

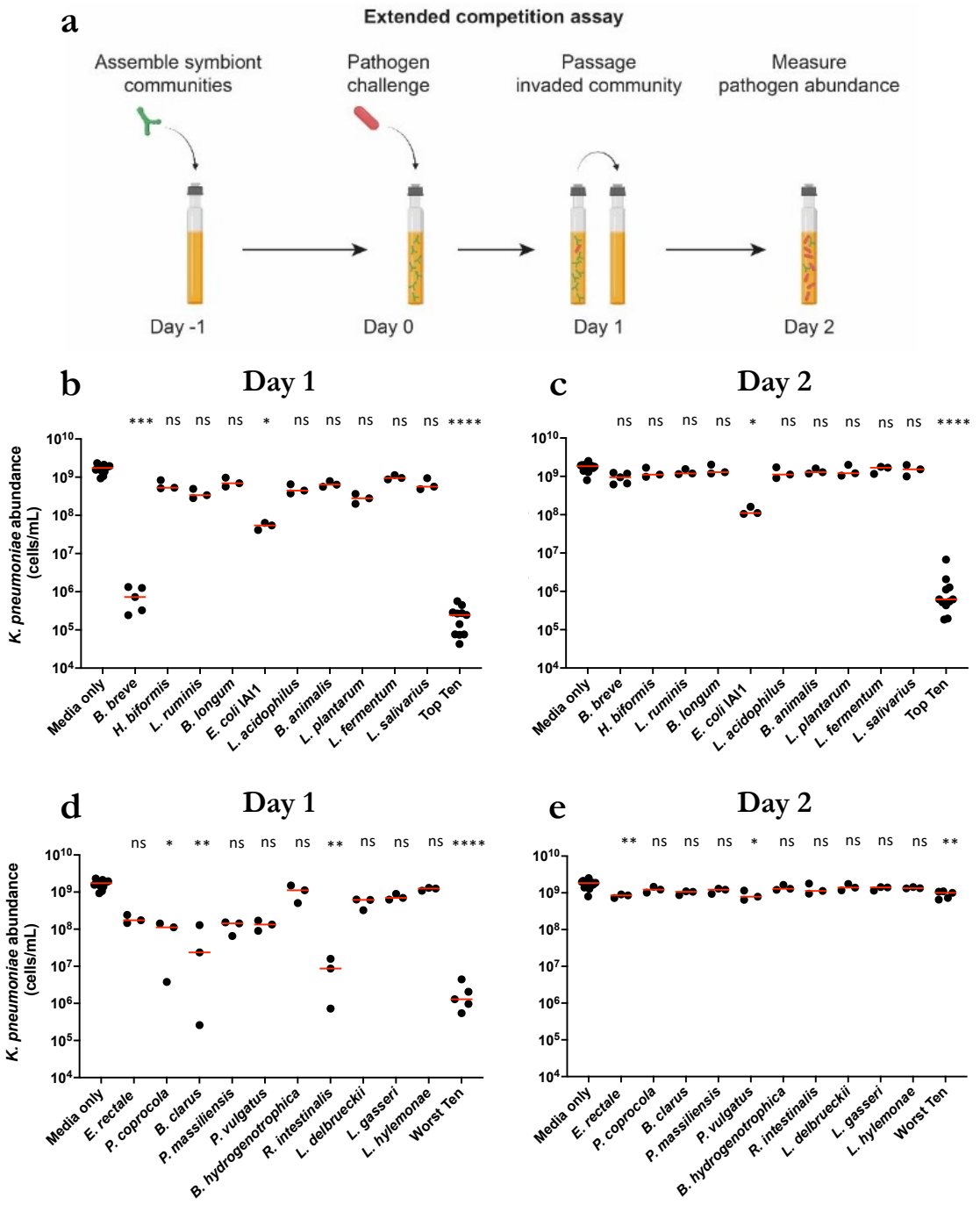


Figure 3. Single symbiont strains are unable to resist invasion by *K. pneumoniae* in the extended competition assay. (a) Schematic of the extended competition assay. Symbiont strains (green) are pre-grown as monocultures before invasion with 10^6 cells/mL of the fluorescent *K. pneumoniae* strain (red). Invaded symbiont cultures are grown for a further 24 hours, then passaged and grown for 24 hours. Samples are taken and measured by flow cytometry. (b-e) *K. pneumoniae* density (cells/mL) as measured by flow cytometry on Day 1 (b, d) and Day 2 (c, e) of the extended competition assay. Results for the 10 best ranking strains from the luminescence screen are shown in (b, c) and for the 10 worst ranking strains in (d, e). Each circle represents a replicate measurement (n=3-15), and the horizontal red lines represent the median value for each strain. Kruksal-Wallis tests with Dunn's multiple test correction compare each group in (b-e) to the no-symbionts control ($p>0.05$=ns; $p<0.05$=*; $p<0.01$=**; $p<0.0001$=****).

3.3.4. The single strain *E. coli* is not sufficient to resist pathogen growth *in vivo*

Our work suggests that single strains perform poorly in pathogen protection. However, so far, we have relied on *in vitro* data. In the mammalian intestine, compared to a Hungate tube, there is a great degree more spatial complexity, which may impact the outcomes of competition (Tropini et al. 2017). In addition, *in vivo*, the interaction between the microbiota and the host immune system has the potential to influence colonisation resistance (Leshem, Liwinski, and Elinav 2020). Therefore, there are many more factors influencing the outcome of colonisation resistance in the mammalian host, making *in vivo* validation of the *in vitro* results crucial. We, therefore, decided to study the best performing competitor from the *in vitro* screen, which was a strain of *E. coli*, in an *in vivo* assay and assess its ability to confer colonisation resistance.

To do this, germ-free mice were first gavaged with 2 doses of live bacteria each consisting of 10^8 colony forming units (CFU) of *E. coli* IAI1. The mice were given 2 identical doses of the symbiont, 48 hours apart, to ensure colonisation (see Chapter 2). The mice were left for a period of 2 weeks to allow full colonisation by the bacteria and adjustment of the host immune system. 14 days after the first gavage, mice were given a gavage containing 10^6 CFU of *K. pneumoniae*. Faecal samples were taken on Days -12, 0, 1, 2, 3 and 4 and the pathogen and symbiont faecal density were measured at each time point by plating on agar. At the take-down of the mice on Day 4 post-pathogen gavage, samples of ileal content, caecal content and the mesenteric lymph nodes (MLN) were taken in addition to the faecal samples. The outline of the mouse experiments is shown in Fig. 4a.

The germ-free control mice that were not pre-colonised by a symbiont strain reached the final carrying capacity of just under 10^{10} *K. pneumoniae* CFU/g faeces by 24 hours after pathogen gavage (Fig. 4b). The mice that were pre-colonised by *E. coli* IAI1 displayed an increase in *K. pneumoniae* density to just under 10^9 CFU/g faeces by 24 hours after pathogen gavage. This suggested a very modest impact of *E. coli* on *K. pneumoniae* comparable to that seen *in vitro*. However, this difference had gone by Day 2 and after the carrying capacity of *K. pneumoniae* was indistinguishable to that of the control mice. *E. coli* IAI1 faecal density was at 10^{10} CFU/g at the point of pathogen gavage (time = 0) and decreased by nearly 2 logs over the course of the experiment as *K. pneumoniae* density increased (Fig. 4c).

The data shown here, therefore, indicate that *E. coli* IAI1 is able to slightly slow the colonisation of the mouse gut by *K. pneumoniae* (there is, on average, 1 log lower faecal *K. pneumoniae* load 24

hours after pathogen gavage), but that the final carrying capacity of *K. pneumoniae* is unchanged by the presence of *E. coli* IAI1. It is important to note that colonisation resistance can be measured by final carrying capacity and also by the speed of colonisation. Colonisation resistance is on a spectrum that can vary depending on the dose given in the gavage; so, this is something to take into account when evaluating the effectiveness of colonisation resistance. Here, the final carrying capacity is the same for both germ-free mice and mice pre-colonised with *E. coli* IAI1, but the mice pre-colonised with *E. coli* IAI1 reach the carrying capacity slightly more slowly. There is some colonisation resistance, therefore, but the single strain *E. coli* IAI1, which was shown to be the best-performing strain against *K. pneumoniae in vitro*, does not provide effective colonisation resistance.

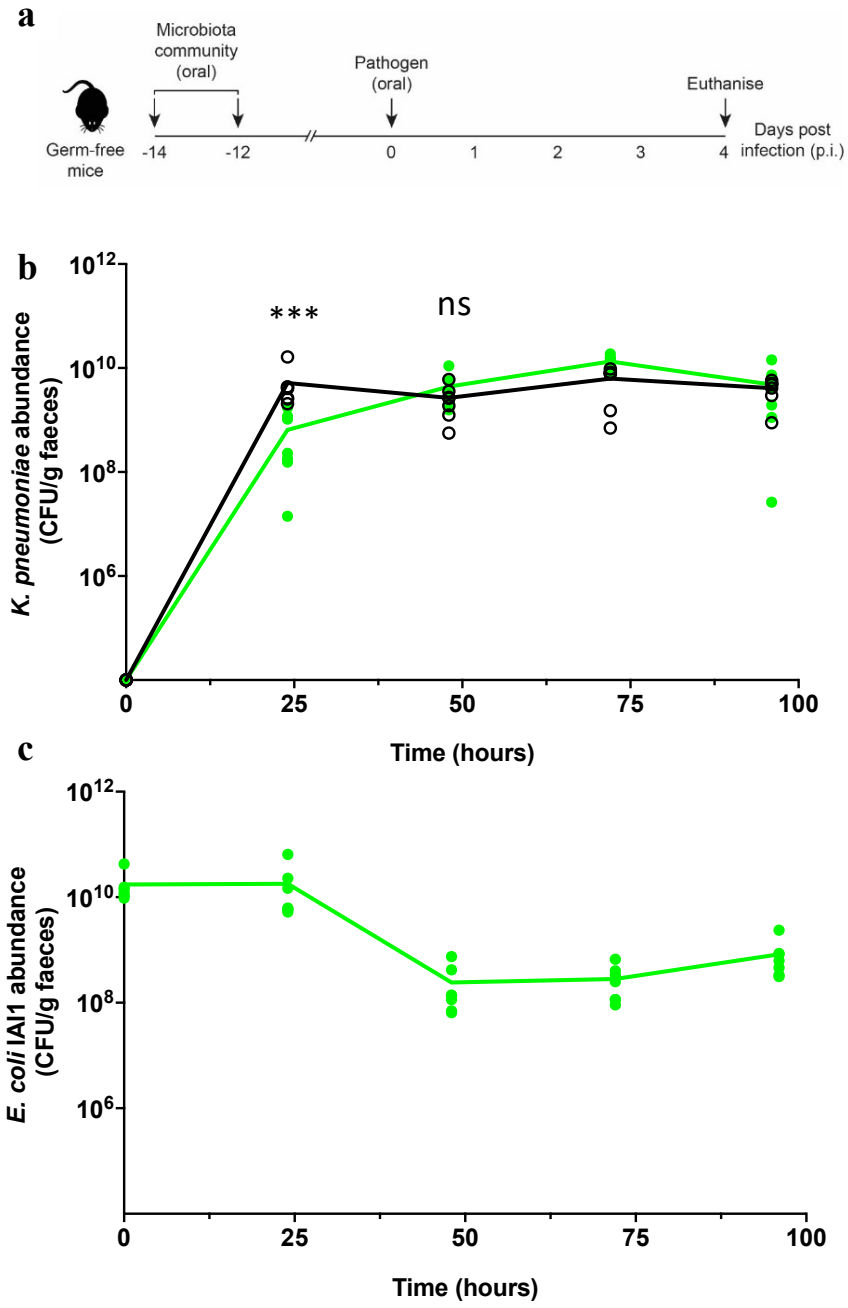


Figure 4. *E. coli* alone does not provide effective colonisation resistance in mice. (a) Schematic of the *in vivo* experiments. Germ-free mice are repeat gavaged with 10^8 CFU of the commensal strain on Days -14 and -12, before gavage with 10^6 CFU of the wild type pathogen *K. pneumoniae* on Day 0. Daily faecal samples are taken post infection before mice take-down on Day 4. Faeces are plated in the laboratory to measure abundance of the pathogen and commensal. Abundance of the pathogen over time post infection is shown in (b) and of the commensal in (c). Each circle represents a faecal sample from a different mouse (n=7). The lines join the median values for each treatment at each time point. The green lines in (b,c) represent the mice pre-colonised with *E. coli*. The black line in (b) represents the control mice not pre-colonised with a symbiont. Mann-Whitney tests comparing pathogen abundance in the control and *E. coli* IAI1 mice at 24h and 48h are shown in (b) ($p>0.05$=ns; $p<0.001$=***).

3.4 Discussion

Colonisation resistance describes the ability of the microbiome to protect a host against colonisation by new microorganisms (Sorbara and Pamer 2019; Caballero-Flores, Pickard, and Nunez 2022). While this effect likely evolved due to competition between strains of bacteria for niche space, the outcome is a major benefit to the host because it helps to prevent infection by harmful microbes (McLaren and Callahan 2020). Individual strains of bacteria, such as *E. coli* Nissle 1917, have long been singled out as key to gut health. Some of these strains are commercially available as probiotics, however, clinical trials provide mixed and inconclusive evidence of strains that provide a particular benefit to the host (Lerner, Shoenfeld, and Matthias 2019; Suez et al. 2019; Singh et al. 2018; Kristensen et al. 2016; Derrien and van Hylckama Vlieg 2015). In this Chapter, we sought to identify which common human gut symbionts have the strongest inhibitory potential against the pathogen *K. pneumoniae* under controlled laboratory conditions. To do this, we screened 100 human gut bacteria strains in pairwise competition with K. *pneumoniae*, using two types of experimental assay: the competition and the ecological invasion assays (Fig. 1). It was revealed that the best competitors often belonged to Enterobacteriaceae, which is the same family of bacteria that *K. pneumoniae* belongs to (Fig. 2). This fits with other data showing the importance of phylogenetic similarity for competition (Osbelt et al. 2021; Oliveira et al. 2020). The strongest competitors also tended to be pathogenic (the initial screen included some category two gut pathogens).

We next chose a sub-group of the best- and worst-performing bacteria from the screen and tested the ability of these individual symbiont strains to resist *K. pneumoniae* growth in a different experiment: the extended competition assay (Fig. 3). This assay was designed to incorporate elements of competition and invasion, in order to model both these aspects of the gut environment. During the ecological invasion stage, (Day 1), some individual strains such as *B. breve* were able to resist *K. pneumoniae* growth to an extent, but there was no evidence of an effect of interference competition because no overall reduction in pathogen cell density was observed. It is possible that the observed lack of interference competition in these experiments is because we are seeking to understand competition between species (interspecific) rather than within species. Evidence of interference competition is often found within species (intraspecific) as strains of the same species are more closely related and their niches overlap the most strongly. This is supported by findings from other studies, for instance it has been widely documented that strains belonging to the gut species *Bacteroides fragilis* compete with one another using type six secretion systems (Attar 2016; Hecht et al. 2016).

After passage into fresh media, when in combination with any of the individual 10 best-ranked symbiont strains except for *E. coli* IAI1, *K. pneumoniae* grew to a density equivalent to its growth in monoculture. When in combination with *E. coli* IAI1, *K. pneumoniae* grew to a final density of 10^8 rather than 10^9 cells/mL This demonstrates that, although *E. coli* IAI1 is slightly better than the other single strains, single symbiont strains cannot successfully resist growth of *K. pneumoniae in vitro*.

To validate these results *in vivo*, germ-free mice were pre-colonised with *E. coli* IAI1 before challenge with *K. pneumoniae* (Fig. 4a). 24 hours after gavage with *K. pneumoniae*, mice pre-colonised with *E. coli* IAI1 had slightly lower faecal density of the pathogen, although the final carrying capacity of *K. pneumoniae* was no different from the germ-free control (Fig. 4b). This suggests that, while *E. coli* IAI1 can provide a small degree of pathogen resistance in germ-free mice by slightly slowing the speed of colonisation, colonisation resistance by single strains *in vivo* is minimal.

Overall, in our systematic screen of 100 human gut symbionts, we found no evidence of single strains that were strongly competitive against *K. pneumoniae*. This was confirmed by further investigation of a sub-group of selected strains in the extended competition assay. *In vivo* validation in gnotobiotic mice showed that there was little to no effect of prior colonisation with *E. coli* IAI1 on *K. pneumoniae* invasion. This is not out of keeping with the wider, mixed conclusions of analyses of clinical studies (Suez et al. 2019; Kristensen et al. 2016; Derrien and van Hylckama Vlieg 2015). However, our results are in contrast with individual experimental studies that hail certain strains as putative probiotics for pathogen resistance (Wotzka et al. 2019; Osbelt et al. 2021; Velazquez et al. 2019; Jacobson et al. 2018; Sequeira et al. 2020; Buffie et al. 2015; Kim et al. 2019; Oliveira et al. 2020). It is possible that our screen did not encompass any of these 'magic bullet' strains. Alternatively, perhaps a more complex explanation is required. We found that the community formed from the 10 best ranking strains kept *K. pneumoniae* abundance three logs lower than the single strains were able to. This suggests that in the 10 species community, a higher-order, non-additive effect comes in to play. This will be explored in more detail in the following Chapters.

3.5 Materials and Methods

Bacterial strains

A full list of bacterial strains used in this study is provided in Table S1. The plasmids used in this study are listed in Table S3. *Klebsiella pneumoniae* subsp. *pneumoniae* purchased from DSMZ (stock number 30104) was used in all experiments containing *K. pneumoniae*. Symbiont strains were chosen based on those commonly isolated from the human gut microbiota. Strains were provided by Nassos Typas (EMBL Heidelberg, Germany), or were ordered from strain collections (e.g. the German Collection of Microorganisms; DSMZ).

Culturing of anaerobes

All symbionts were cultured under anaerobic conditions (5% H_2, 5% CO_2, 90% N_2, <20ppm O_2) in modified Gifu Anaerobic Medium (mGAM; Nissui Pharmaceuticals) broth buffered to pH 6.2 with 100mM 2-(N-morpholino)ethanesulfonic acid (MES). The redox indicator dye Resazurin (1g/L media) was added as a quality control check for the presence of oxygen (turns red when conditions are not sufficiently anaerobic). To prepare glycerol stocks, individual strains were first streaked onto mGAM agar and grown under anaerobic conditions (if possible, as not all strains can grow as single colonies on agar-based media). The identity of each strain was confirmed using 16S rRNA sequencing (Sanger sequencing; Source Biosciences) using universal primers 27F and 1492R (Table S4). Single colonies were then inoculated in mGAM broth and stored at -80 degrees Celsius in mGAM with a final concentration of 25% glycerol.

Genetic engineering of bacterial strains

Luminescence and fluorescence plasmids were transformed into *K. pneumoniae* using electroporation. Briefly, 5mL overnight culture was washed 3x with cold miliQ water, before being concentrated in 500µl cold miliQ water. 2µl of plasmid was mixed with 50µl of concentrated cells and electroporated (1.8kV; 0.1cm gap cuvettes) before recovery in 1ml pre-warmed LB (1h at 37°C, shaking at 220rpm) and plating on LB with the appropriate antibiotics.
Plasmids used for genetic engineering are listed in Table S3.

Luminescence screen

K. pneumoniae (DSM 30104) carrying a low copy number plasmid with P_{nptII} promoter-driven expression of *lux*CDBAE (pIJ11282; also known as the improved lux operon plasmid(Soldan et al. 2021)) was used for the luminescence screen. Symbiont strains were tested in pairwise co-culture

with the pathogen. All strains tested were first grown in monoculture anaerobically in static de-gassed mGAM broth buffered to pH 6.2 with 100mM MES (Sigma-Aldrich) at 37 degrees Celsius. *K. pneumoniae* WT carrying the luminescence plasmid pIJ11282 was separately incubated in the same media overnight.

Competition assay: once all strains had reached stationary phase (12-72 hours of growth depending on the species), 20µL of each symbiont strain was dispensed in technical triplicates in a 96-well plate containing 160µL of mGAM broth. 20µL of *K. pneumoniae* pIJ11282 overnight culture was then added to each well.

Ecological invasion assay: 180µL of each symbiont strain was dispensed in technical triplicates in a 96-well plate and 20µL *K. pneumoniae* pIJ11282 overnight culture was added to each well.

96-well plates from both assays were incubated anaerobically for 6 hours at 37 degrees Celsius. Before luminescence measurement, 96-well plates were brought out of the anaerobic chamber and exposed to O_2 for 10 minutes because, critically, O_2 is needed for light production catalysed by the enzyme luciferase. Luminescence at 515-575nm and OD-600nm were measured using a CLARIOstar Plus spectrometer (BMG Labtech). The average of each technical triplicate was taken. Each data point (Figure 1c-d) represents the median of at least 3 independent biological replicates (that is, using different overnight cultures of the same strain in different 96-well plates).

Selection of the 'top' and 'bottom' 10 symbiont strains

For each of the assays, symbiont strains were ordered from best- to worst-performing. Symbiont strains were given two rankings: one from the competition assay and one from the invasion assay. The two rankings were summed and ordered from lowest sum (best overall performing) to highest sum (worst overall performing). From these ranks, the top 10 and bottom 10 strains were chosen, with the added selection criteria that biosafety level 2 strains and repeat strains of the same species were removed.

Extended competition assay

Symbiont strains were grown to stationary phase anaerobically (12-72 hours, depending on the species), in Hungate tubes containing 5mL mGAM broth (HyServe-05433) and 100mM MES (Sigma Aldrich) and buffered to pH 6.2. (225rpm, 37 degrees). *K. pneumoniae* carrying the fluorescence plasmid pBC11 (YPet)(Cunrath and Bumann 2019) was incubated overnight under the same conditions, with the appropriate antibiotics (Table S1).

Once in stationary phase, monocultures of symbionts were passaged (100µL culture into a new 5mL tube of media) and grown for ~17 hours. Once grown, strains were invaded with 100µl of the pathogen (10^6 cells/mL final concentration) in each 5mL Hungate tube. Samples were taken immediately after pathogen invasion and prepared for measurement using flow cytometry (Day 0). Invaded commensals were incubated in a shaking incubator (37 degrees Celsius, 225rpm). After 24 hours, the invaded commensals were sampled for flow cytometry (Day 1) and 100µL was passaged into new 5mL tubes of mGAM broth. After a further 24 hours, the end-point co-cultures were sampled and measured a final time (Day 2).

Flow cytometry

Hungate tubes containing culture to be sampled were de-pressurised under anaerobic conditions using needles. Samples were removed using needles and syringes. 10µL of each sample was diluted in 90µL PBS + chloramphenicol 200µg/ml then 10µL added to a 96-well flat-bottomed plate already containing 80µL PBS + chloramphenicol 200µg/ml. The 96-well plate was left to shake at room temperature on the bench for 15 minutes to allow oxygen-dependent folding of YPET, while preventing further growth of the sample with the bacteriostatic antibiotic chloramphenicol. Next, all bacterial cells were fixed, permeabilised and fluorescently stained by adding 90µL PBS containing 4% paraformaldehyde, 0.4% Triton X-100 and 1µg/mL 4',6-diamidino-2-phenylindole (DAPI) to each sample well and incubating the plate in the dark for 1 hour at room temperature on a microplate shaker. Prior to the measurement, 20µL AccuCheck counting beads (ThermoFisher- PBC100) was added to every sample well. Two wells containing 200µL PBS were left between sample wells, in order to prevent cross-contamination between samples. 96-well plates were run in a flow cytometer set to: acquisition volume 50µL, total draw volume 80µl, total sample volume 200µL, at a speed of 100mL/minute. Relevant spectral parameters were recorded in a flow cytometer (Attune NxT Autosampler) equipped with 405nm, 488nm and 561nm lasers (ThermoFisher). The following channels were used: DAPI staining, excitation 405nm, emission 415-465nm ('blue'); YPet fluorescence, excitation 488nm, emission 505-515nm and 525-555nm ('green').

Flow cytometry data was processed using FlowJo v10.8.1 software. 'Beads' were gated on a linear (FSC-H; SSC-H) axis. 'Bacteria' were gated on a logarithmic (FSC-H; SSC-H) axis. DAPI was gated within the 'Bacteria' gate, on a logarithmic (Ex405-417; Ex405-495) axis. Within the DAPI gate, YPet was gated on a logarithmic (Ex488-503; Ex488-555) axis. Count statistics for beads, DAPI and YPet were exported to Excel. Pathogen density (cells/mL) was calculated.

Mouse husbandry and experiments

Mouse experiments were performed with 6-8 weeks old germ-free C57BL/6J female mice that were bred and maintained in germ-free isolators at the Kennedy Institute, University of Oxford. During experiments, mice were housed as pairs or trios in sterile, individually ventilated cages with irradiated food and autoclaved water. Cages of mice were disinfected in hydrogen peroxide and peracetic acid solution (TecCare Ultra, pH 1) before mice were handled using individually sterilised gloves (single use for each cage) in a biosafety cabinet that was disinfected with hydrogen peroxide and peracetic acid solution (TecCare Ultra, pH 1) in between each treatment group. Mouse experiments were performed in accordance with the UK Animal Scientific Procedures Act (1986) under a Project Licence (PPL; PP9127884 to Fiona Powrie) authorised by the UK Home Office.
To prepare the inocula for the mice, a monoculture of *E. coli* IAI1 was grown, then OD-600 measured. 5mL culture was centrifuged (10 minutes, room temperature, 14000rpm) and the resulting pellet resuspended in 1mL anaerobic PBS and kept on ice. The volume of culture containing 10^9 cells was calculated for *E. coli* IAI1, based on a standard curve of OD-600 and flow cytometry quantification. 200µl was gavaged into each mouse corresponding to 10^8 cells of *E. coli* IAI1. For all inoculums, samples were taken for plating anaerobically on mGAM agar to confirm the cell density. The same protocol was carried out for *K. pneumoniae,* except that the inocula prepared had 2 logs lower cell density.

Germ-free mice were gavaged with 200µL inoculum of symbionts at Day -14 of the experiment and again on Day -12 of the experiment (see scheme Fig. 4a). On Day 0, overnight cultures of the pathogen (*K. pneumoniae)* grown aerobically in LB containing the appropriate antibiotics were washed 3x with PBS and diluted. 10^6 CFU of the pathogen was given to each mouse as a 100µl gavage. Faeces were sampled daily after gavage of the pathogen. Faecal pellets were weighed and homogenised with a 5mm stainless steel bead in 1ml PBS (samples were shaken vigorously in 2ml Eppendorf tubes). CFUs were enumerated using selective plating (LB + carbenicillin 50 µg/mL for *K. pneumoniae*). *K. pneumoniae* can be differentiated by colour from *E. coli* on LB agar (*K. pneumoniae* appears shiny and white whereas *E. coli* appears yellow) or morphology (*K. pneumoniae* produces a capsule). Mice were euthanised 4 days after infection with the pathogen.

Statistical analysis

All graphs were made and statistical analysis carried out in Prism v9.4.1. Figure legends indicate the statistical test used and the sample sizes.

4. Ecological diversity promotes colonisation resistance by human gut bacteria

4.1 Abstract

The potential health benefits of a species-rich microbiome are much discussed. However, the majority of evidence for the role of species diversity on health comes from association and correlation, where cause and effect can be difficult to distinguish. Here, we explore the effects of species diversity on microbiome function experimentally. Symbiont communities of varying diversities were assembled up to a maximum of 50 species and their ability to resist the pathogen *Klebsiella pneumoniae* was tested in an *in vitro* assay designed to capture the process of colonisation and establishment of a pathogen in the gut. These experiments indicated a positive association between diversity and the ability of a community to suppress pathogen growth, but the data were highly variable based upon community composition. Further study revealed that a large amount of this variability was explained by the presence of key species, particularly *Escherichia coli* IAI1 but also *Bifidobacterium breve*. While individual species were important, we also found that a community of eight other symbiont strains can replace the role of *B. breve*. This observation suggested that increasing ecological diversity can eventually overcome the role of key member species. We also found that key role of *E. coli* IAI1 in the 10-species community could be performed by several other *E. coli* strains tested, albeit not by more distantly related Enterobacteriaceae, indicating that the effects of *E. coli* were relatively general. In sum, we find that community composition matters for colonisation resistance as well as ecological diversity. Non-additive, or higher-order, effects are at play between the strains in a community, thereby adding ecological complexity to our understanding of colonisation resistance.

4.2 Introduction

The human microbiome is a diverse ecological system, containing many strains and species. A key goal of microbiome science is to identify single strains and species that are particularly important for health. However, microbial diversity itself is also thought to be important for health. People

living in developed countries and eating a Western diet high in sugar and fat but low in fibre appear to have lost a large number of bacterial species, which were present in ancestral populations (Sonnenburg et al. 2016; Merrill et al. 2022; Mosca, Leclerc, and Hugot 2016). At the same time, there has been a rise in so-called Western diseases, including immune-related diseases such as allergies and inflammatory bowel disease, as well as metabolic disorders, like obesity and type two diabetes (Mosca, Leclerc, and Hugot 2016). Low intestinal microbial diversity is correlated with obesity, type two diabetes and indicators of poor bowel health (frequent diarrhoea, nausea and acid reflux) as well as anxiety and stress (Manor et al. 2020; K.V. Johnson 2020; Deng, Li, and Zhao 2019). In addition to disease, changes in diversity of the gut microbiome are also associated with changes in microbial composition (Manor et al. 2020). In an observational human study, gut microbiome diversity was negatively correlated with relative abundance of the phylum Bacteroidetes, but positively correlated with Firmicutes (Manor et al. 2020).

There are many associations, therefore, between microbiome diversity and health. However, observational studies only provide correlations, and causality between diversity and disease cannot be inferred in either direction. Moreover, evidence for the importance of diversity is not always forthcoming. A systematic analysis of randomised controlled trials that was carried out to compare the effects of single-strain and multi-strain probiotics found that, on average, multi-strain mixes were no more effective than single-strain probiotics (McFarland 2021). Here, I use an experimental approach to study the relationship between species diversity and one of the key health benefits provided by the microbiota: its ability to prevent pathogen invasion and subsequent infection, or colonisation resistance (McLaren and Callahan 2020; Caballero-Flores, Pickard, and Nunez 2022; Sorbara and Pamer 2019). The potential for species diversity to promote colonisation resistance has been raised by theoretical work (Galland et al. 2019; Turnbull et al. 2010). Moreover, the importance of diversity for colonisation resistance is supported by the vulnerability of antibiotic-treated patients to recurrent *Clostridium difficile* infection and the success of its treatment with faecal microbiota transplants that contain hundreds of species of bacteria (Rohlke and Stollman 2012). Additionally, there is evidence that in some cases colonisation resistance depend upon the effects of multiple species. For example, colonisation resistance against vancomycin-resistant *Enterococcus faecium* (VRE) was shown to rest upon a community of four symbiont strains, where the consortium's members did not produce this effect individually (Kim et al. 2019). While there is evidence that diversity can be important for colonisation resistance, however, there is a need for direct tests that systematically vary diversity and study its impact (Sonnenburg et al. 2016).

In our work, we found that single strains of human gut bacteria provided poor protection against the important pathogen *K. pneumoniae,* both *in vitro* and in a gnotobiotic mouse model. However, when we combined a set of 10 strains together in a single community, we found that these strains collectively limited the growth of *K. pneumoniae* to a far greater extent than any of the individual symbiont strains (Chapter 3, Fig. 3c). This points to a higher-order, or non-additive, effect at play among the individual strains (Mayfield and Stouffer 2017). In this Chapter, we explore the effect of diversity on colonisation resistance, by systematically testing pathogen growth in symbiont communities of differing diversities and compositions.

4.3 Results

4.3.1 Diversity and key members are critical to colonisation resistance.

In order to systematically explore the role of diversity in colonisation resistance, we assembled symbiont communities of increasing diversity and tested them against *K. pneumoniae* in the extended competition assay. We based our experiments on the results of the luminescence screen and associated competition assays discussed in Chapter 3. Specifically, there we found that individually, the best-ranking strains in the luminescence screen offered little or no colonisation resistance to *K. pneumoniae* but when combined together in a 10-strain community, *K. pneumoniae* abundance was greatly suppressed across a two-day extended competition assay. To explore this pattern in more detail, communities of two, three or five strains were selected at random from the 10 best-ranking strains in the luminescence screen, and compared to the performance of each of the single strains when alone with *K. pneumoniae* (Chapter 3). In addition, to assess the potential impacts of higher diversity levels, we assembled a community of 50 species chosen from the initial screened set of 100 strains. This 50-species community included the 10 best and 10 worst ranked strains from the screen but excluded all category two strains as well as any multiples of strains from a particular species. Symbiont strains were grown to stationary phase as monocultures, then combined into communities that contained equal volumes of each symbiont. Communities were left to grow overnight before being invaded with the fluorescent strain of *K. pneumoniae. K. pneumoniae* density was measured by flow cytometry on Days 1 and 2 of the assay. The results of this initial test of diversity are shown in Fig. 1a-b. Overall, pathogen resistance monotonically increased as symbiont community diversity increased (Fig. 2a). However, we also observed a large amount of variability across diversity levels.

In order to better understand this variability, we looked at the composition of communities that performed well in colonisation resistance as compared to those that performed poorly for each

level of diversity. This revealed that the best-performing communities always contained *E. coli* IAI1 (results for *E. coli* IAI1 and non-*E. coli* IAI1 communities differ, see Fig. 2a). It makes sense that *E. coli* plays a key role in the communities, because *E. coli* is, like *K. pneumoniae*, a member of the family Enterobacteriaceae, and therefore is considered a close relative of the pathogen. *E. coli* IAI1 was also shown to be the best-performing single strain out of the 10 best-ranked strains from the initial screen (Chapter 3, Fig. 3c). However, it is clear from the results that diverse communities containing *E. coli* IAI1 perform better than *E. coli* IAI1 when it is alone. *E. coli* IAI1 appears to play an important role in colonisation resistance, but, critically, only when it is in the context of a community of other gut strains. As a further test of the observation that the best-performing communities contain *E. coli* IAI1, we performed further competition experiments with additional randomly selected communities containing *E. coli* IAI1 at each diversity level (Fig. 1c-d). Together, the data showed that gut communities containing *E. coli* IAI1 (depicted in green) displayed increased colonisation resistance to *K. pneumoniae* relative to those that do not contain *E. coli* IAI1 (shown in black). This strengthens the conclusion that *E. coli* IAI1 plays a critical role in colonisation resistance, but that its role is context-dependent on *E. coli* IAI1 being part of a diverse community and not alone, showing that there is a higher-order effect between the species. Construction of a null model demonstrates that at higher diversities, pathogen abundance deviates strongly from what would be expected if the effects of the species were simply additive (Fig. 2b). In the *E. coli* IAI1-containing communities there was a strong relationship between the number of symbiont species in a community and colonisation resistance (Fig. 1d). This contrasted with communities that did not contain *E. coli* IAI1, where this pattern was weaker on Day 1 and absent on Day 2. At the maximum colonisation resistance, the 50-strain community was able to maintain *K. pneumoniae* abundance at four logs (10,000-fold) below that of the non-*E. coli* IAI1 single strains, and at three logs (1,000-fold) below that of *E. coli* IAI1 alone. To further test the role of *E. coli* IAI1 in colonisation resistance, we assembled the 10 and 50 species communities without *E. coli* IAI1 present, to create nine and 49 species communities (Fig. 1c-d). Strikingly, this revealed that the colonisation resistance seen at Day 2 by these high diversity communities was completely lost in the absence of *E. coli* IAI1 (nine and 49 species communities, in black, compared to 10 and 50 species communities, in green, Fig. 1d). Taken together, these results, therefore, suggest that *E. coli* IAI1 is a key member of symbiont communities that are resistant to *K. pneumoniae*. Further inspection of the data suggested another key species within the communities (Fig. 1e-f). Specifically, communities that contained both *E. coli* IAI1 and *B. breve* performed better than communities that contained just *E. coli* IAI1, suggesting that *B. breve* is also key to colonisation resistance, but less so than *E. coli* IAI1. The *B. breve* effect is particularly striking on Day 1 of the

extended competition, where even communities containing *B. breve* but not *E. coli* IAI1 performed well (Fig. 1e). The effect of *B. breve* can also be seen on Day 2, where it greatly improves colonisation resistance in some cases. (Fig. 1f). However, the presence of *E. coli* IAI1 or *B. breve* alone is not enough to resist *K. pneumoniae* growth. A backdrop of other symbiont strains must also be present. Therefore, both community diversity and key members are critical to colonisation resistance.

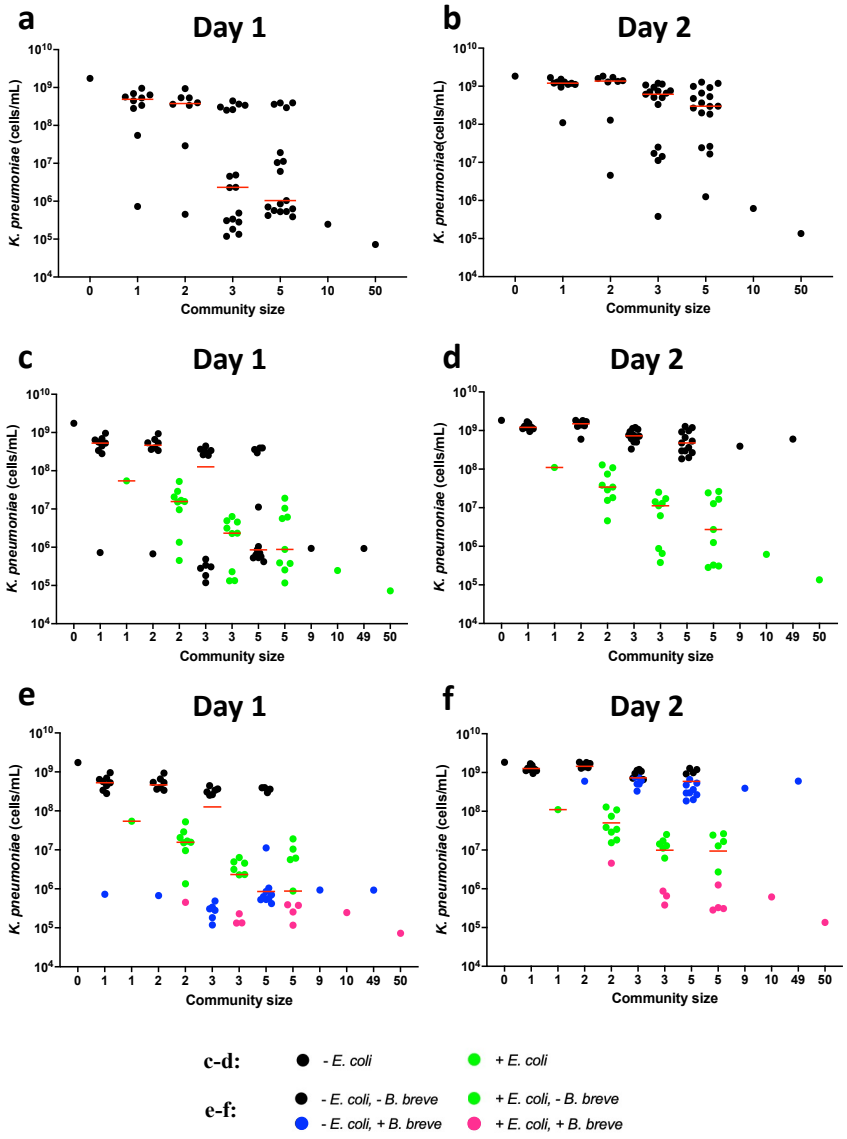


Figure 1. Diversity and key members are critical to colonisation resistance. *K. pneumoniae* abundance as measured by flow cytometry on Day 1 (a,c,e) and Day 2 (b,d,f) of the extended competition assay. Horizontal red lines depict median values at a diversity level. Each circle represents the median value of a particular community (n=3-11). (a-b) shows the initial randomly selected set of communities. (c-f) shows the augmented set of communities, with additional, randomly selected communities containing *E. coli.* In (c-d), communities in black do not contain *E. coli,* communities in green contain *E. coli.* In (e-f), communities in black do not contain *E. coli* or *B. breve,* communities in green contain *E. coli* but not *B. breve*, communities in blue contain *B. breve* but not *E. coli*, communities in pink contain *E. coli* and *B. breve.*

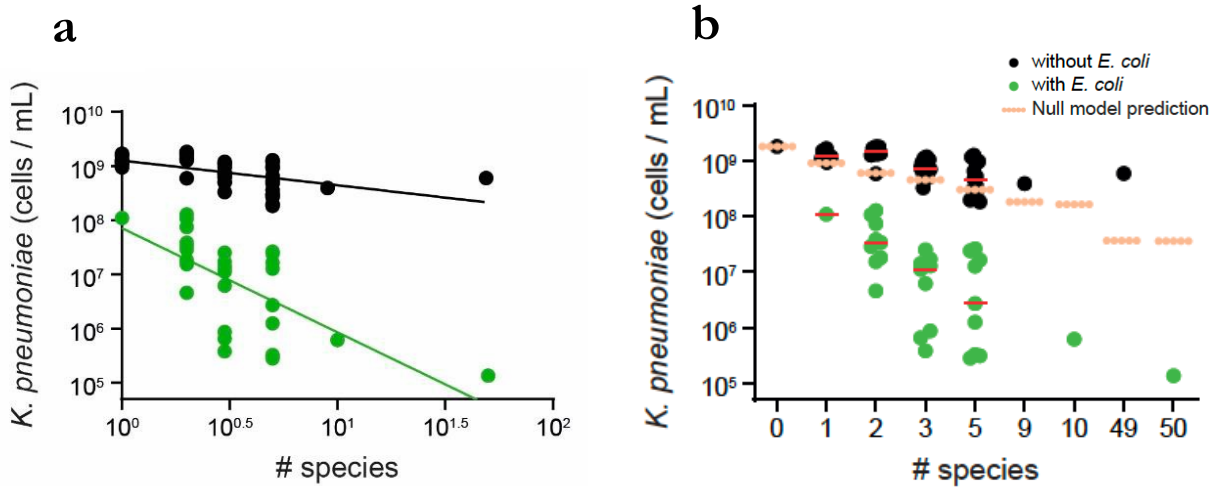


Figure 2. (a) Community diversity negatively correlates with pathogen abundance. As the number of symbiont strains increases, *K. pneumoniae* density on Day 2 of the extended competition decreases (x axis on log scale). Each circle represents the median value of a community tested in the extended competition assay (data from Fig. 1d). Communities in green contain *E. coli* IAI1, communities in black do not contain *E. coli* IAI1. Linear regression of log-transformed data: R^2 = 0.4296, non-zero slop for *E. coli* communities (F test, $p<0.0001$). R^2 = 0.3103, non-zero slope for communities without *E. coli* (F test, $p<0.0001$). Moreover, slopes of the two regressions are significantly different from each other (F test, $p=0.0001$). **(b) As community diversity increases, pathogen abundance deviates strongly from the null model.** Predictions from a simple null model, where pathogen abundance scales with 1/n, where n is the total number of species (community plus pathogen), are plotted alongside the results from Fig. 1d. As our findings deviate strongly from this null model at higher diversities, it supports the conclusion that the effects of diversity are non-additive. Statistics comparing the difference between the null model and the observed data show that $p<0.0001$ for 1 vs. 10 species and $p=0.007$ for 1 vs. 50 species (Mann-Whitney test on the ratios of the null to the observed data at (1+1) species to (1+10) and (1+50) species.)

4.3.2 Key members can sometimes be replaced by diversity

In order to further understand the roles of the key members *E. coli* IAI1 and *B. breve* in colonisation resistance, we carried out further community drop-out experiments, where communities were assembled with and without *E. coli* IAI1 and *B. breve* present. Communities were assembled as before: strains were grown individually before combining equal volumes of each monoculture into communities and allowing them to grow for 24h before pathogen invasion. As discussed above, neither *E. coli* IAI1 or *B. breve* is able to strongly resist the growth of *K. pneumoniae* alone. However, together the pair is able to suppress growth of *K. pneumoniae* by nearly three logs to 5×10^6 cells/mL (Fig. 3). This level of suppression is similar to that of the community formed from the top 10 best-ranked strains minus *B. breve* (Fig. 3), suggesting that, when in combination with *E. coli* IAI1, the combined effect of the other eight strains is functionally equivalent to the effect of *B. breve*.

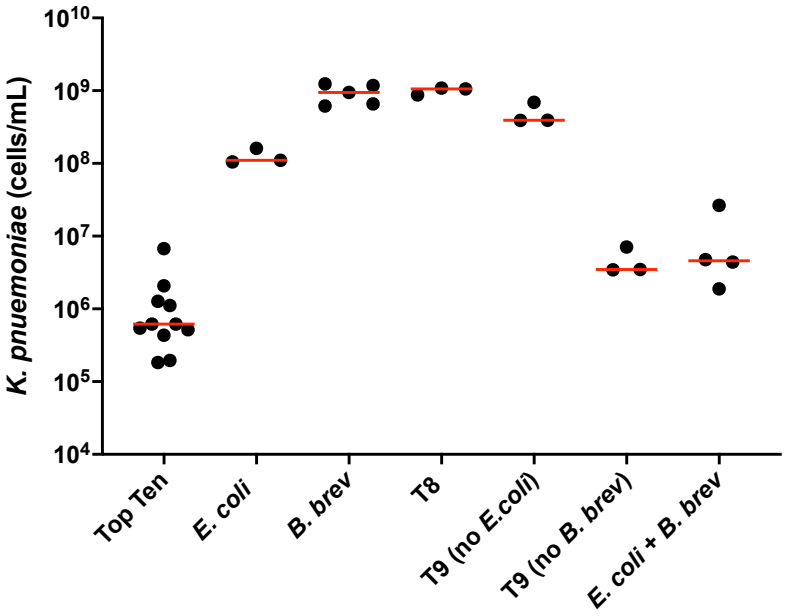


Figure 3. The role of key species *B. breve* in resisting *K. pneumoniae* growth is functionally replaced by a community of eight symbionts when in combination with *E. coli* IAI1. Red horizontal lines depict median values. Each black circle represents a replicate (n=3-11). Pathogen density (cells/mL) measured by flow cytometry on Day 2 of the extended competition is shown. Community T8 is the top 10 ranked strains from the luminescence screen minus *E. coli* IAI1 and *B. breve*. T9 (no E. coli) is the top 10 ranked strains minus *E. coli* IAI1. T9 (no *B. brev*) is the top 10 ranked strains minus *B. breve*.

4.3.3. Other, but not all, closely related strains can also drive strong colonisation resistance

Our work shows that a particular strain of *E. coli,* when in the context of a community of other gut symbionts, is key to providing colonisation resistance against *K. pneumoniae*. This raises the question of whether different strains of *E. coli*, and even other, closely related species of the same genus or family, would be able to provide a similar role in resisting pathogen colonisation. To test this, we substituted *E. coli* IAI1 from the 10 best-ranked community with each of four other non-pathogenic *E. coli* strains (Fig. 4a). Only the addition of one of the four strains, *E. coli* HS, to the nine best-ranked strains caused a significant decrease in *K. pneumoniae* growth compared with the nine best-ranked strains. In particular, *E. coli* strain Z1331 performed poorly in the sense that the resulting community did not resist *K. pneumoniae* growth well (*K. pneumoniae* only grew to a 10-fold lower abundance than in the media-only control). This result suggests that not all strains of *E. coli* perform equally well in the context of the nine best-ranked species against *K. pneumoniae*. Next, to test a broader range of non-*E. coli* species, we substituted *E. coli* IAI1 for other members of Enterobacteriaceae or members of Enterococcaceae (Fig. 4b). The substituted species included one other member of the genus *Escherichia* (*Escherichia marmotae*) as well as the closely related pathogen *Salmonella enterica* Typhimurium. Only the addition of *S.* Typhimurium or *E. marmotae* significantly increased the collective ability of the nine best-ranked species (that is, the 10 best-ranked, minus *E. coli* IAI1) to resist the growth of *K. pneumoniae*. The addition of *Enterobacter cloacae, Proteus mirabilis, Plesiomonas shigelloides, Enterococcus faecalis* or *Enterococcus faecium* did not significantly alter the ability of the nine species to resist *K. pneumoniae* growth. The community of three Enterobacteriaceae (*E. coli* IAI1, the non-fluorescent wild type *K. pneumoniae,* and *S.* Typhimurium), was able to resist growth of *K. pneumoniae* to a similar degree as the community of the 10 best-ranked strains (Fig. 4b).

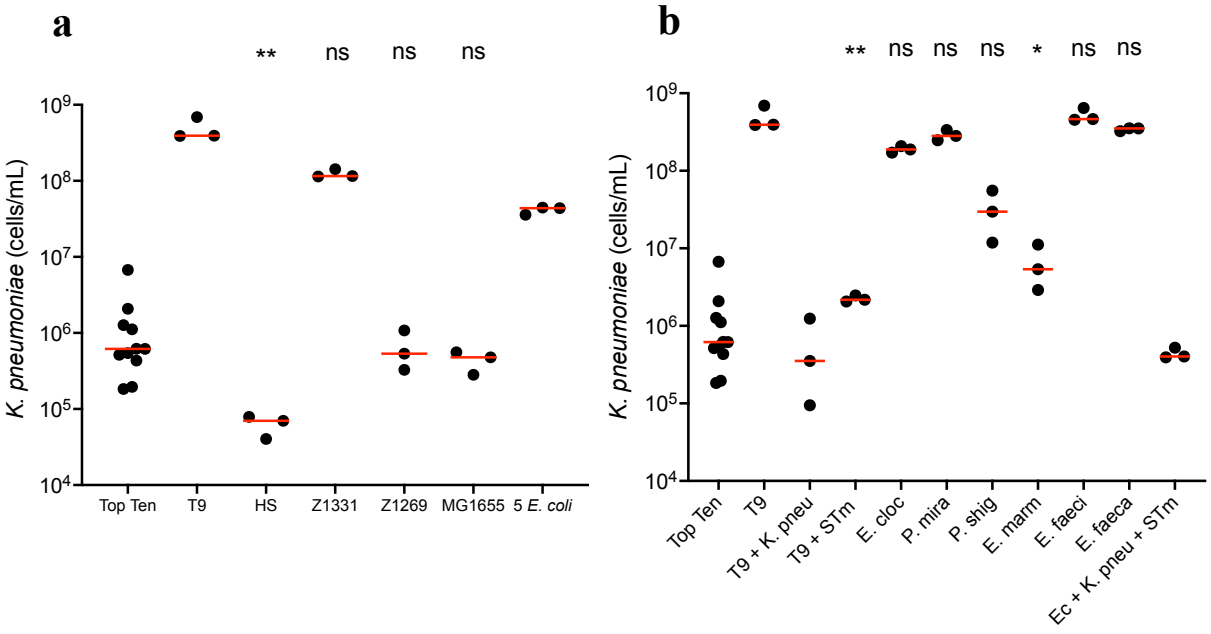


Figure 4. Substitution of *E. coli* IAI1 in the 10 best-ranked species with other strains of *E. coli* and other species of Enterobacteriaceae and Enterococcaceae. *K. pneumoniae* abundance as measured by flow cytometry on Day 2 of the extended competition. Red bars depict median values. Each black circle represents a replicate (n=3-11). In (**a**), *E. coli* IAI1 was substituted from the top ten community with other strains of *E. coli*. T9 refers to the 10 best-ranked strains without *E. coli* IAI1. In the five *E. coli* treatment, all five strains of *E. coli* were mixed as a community (*E. coli* IAI1, HS, Z1331, Z1269, MG1655). In (**b**), *E. coli* IAI1 was substituted from the top 10 community with other species of Enterobacteriaceae (the non-fluorescent wild type *K. pneumoniae* strain DSM 30104, *S.* Typhimurium, *Enterobacter cloacae*, *Proteus mirabilis, Plesiomonas shigelloides, Escherichia marmotae*) or Enterococcaceae (*Enterococcus faecium, Enterococcus faecalis*). A Kruksal-Wallis test with Dunn's multiple test correction is used to compare the indicated groups with T9 in both graphs ($p>0.05$=ns; $p<0.05$=*; $p<0.01$=**).

4.3.4 Ecology of colonisation resistance in gnotobiotic mice

We have already shown that diversity is important for colonisation resistance to the pathogen *K. pneumoniae*. In particular, both species richness and species composition (the presence of *E. coli* IAI1) are crucial for colonisation resistance and both must be present to ensure maximum resistance to the pathogen (Fig. 1d). However, so far, we have only shown these ecological principles *in vitro*. It is important to validate the *in vitro* results *in vivo*, because the host adds further complexity to the system. For instance, the host's immune system may interact with the symbionts, which can contribute indirectly to colonisation resistance against a pathogen (Sequeira et al. 2020). The gastrointestinal tract of a mouse is much more spatially complex than the *in vitro* model (Tropini et al. 2017; Meier et al. 2023), and this may also affect the outcome of colonisation resistance. The spatial structure of the gut plays an important role in determining whether the pathogen and symbiont are in the same physical location and can directly interact with one another, allowing the symbiont to provide colonisation resistance. Therefore, we next turn to testing our communities in a gnotobiotic mouse model.

Germ-free mice were gavaged twice over two days with a human gut symbiont community, then left for 14 days while the colonising symbionts established in the mouse gut. The symbiont communities were assembled by growing the constituent strains individually *in vitro,* before combining standardised volumes of each symbiont to form the community. Strains were not grown together before the gavage. 14 days after the first symbiont gavage (Day 0 post infection), mice were gavaged with 10^6 cells of *K. pneumoniae* and their faeces sampled at 0, 24, 48, 72 and 96 hours. Metagenomic sequencing was carried out on the symbiont community inocula and mouse faeces 14 days after symbiont gavage (Day 0 post infection). Germ-free mice that were gavaged

with more diverse symbiont communities became colonised with a more diverse set of bacteria. For mice that were gavaged with the 50-strain symbiont community, an average of 44 strains were detected in the inoculum, while an average of 23.5 strains were detected (above a 0.1% relative abundance threshold) in the faeces two weeks later (Fig. 5). Despite the number of strains being lower *in vivo* than in the 50-strain inoculum, this was more diverse than the number of strains from the 10-strain inocula that were detected *in vivo* (an average of 6.5 strains). We concluded, therefore, that our experiment represents a good test of the impacts of diversity on colonisation resistance *in vivo*.

Pathogen abundance and *E. coli* IAI1 abundance (if present) were quantified by plating mouse faeces. The abundance of faecal *K. pneumoniae* 24 hours after gavage with the pathogen is shown in Fig. 6a. This work revealed the same key ecological patterns *in vivo* as was seen *in vitro*. As symbiont community diversity increases, pathogen resistance increases. At 24 hours post infection, the 50-species community maintains *K. pneumoniae* abundance at over two logs (100-fold) below the *K. pneumoniae* abundance when mice are pre-colonised with the 10-species community. Moreover, the presence of *E. coli* IAI1 in the 50-species community has an important role in resisting pathogen growth: at 24 hours post infection, *K. pneumoniae* growth is suppressed to two logs lower when in the presence of the 50-strain community than when in mice pre-colonised with the 49-strain community, that is, when *E. coli* IAI1 is absent. The effect of *E. coli* IAI1 is also significant at the 10-species diversity level, where the abundance of *K. pneumoniae* is roughly 10-fold lower compared to the nine-species, *E. coli* IAI1 dropout community at 24 hours post infection. When comparing the observed data to a simple null model, pathogen abundance deviates strongly from the null model at higher diversities, showing that, as with the *in vitro* results, the effects of diversity are non-additive (Fig. 6b).

Colonisation resistance can be measured in two ways: the speed of colonisation, or the final carrying capacity of the pathogen. Pathogen abundance was tracked over time after gavage with *K. pneumoniae*. Faeces were sampled daily for 4 days and selectively plated to distinguish *K. pneumoniae* (Fig. 7a). Differences in pathogen abundance between treatments were most striking on Day 1 (24 hours post infection) and reduced over time. However, colonisation resistance was indeed increased in the more diverse communities (*K. pneumoniae* abundance significantly reduced in mice pre-colonised with 50 species compared with 10 species at 24 hours post infection, see Fig. 6a). Colonisation resistance was also significantly greater in communities containing *E. coli* IAI1 (*K. pneumoniae* abundance significantly reduced in mice pre-colonised with 50 species compared with

49 species, or 10 species compared with nine species, at 24 hours post infection, see Fig. 6a). These two ecological principles of colonisation resistance, diversity and the key member *E. coli* IAI1, line up with the *in vitro* results (Fig. 1d), showing that the *in vitro* results can be reproduced *in vivo*. To determine whether a community's performance was simply explained by the abundance of *E. coli* IAI1 in that community, we also tracked *E. coli* IAI1 abundances *in vivo* (Fig. 7b). *E. coli* IAI1 abundance was shown to be consistently high in all *E. coli* IAI1 - containing symbiont communities (Fig. 7b). Therefore, while communities containing *E. coli* IAI1 differed in their success at resisting *K. pneumoniae* growth, this is not due to variation in abundance of *E. coli* IAI1.

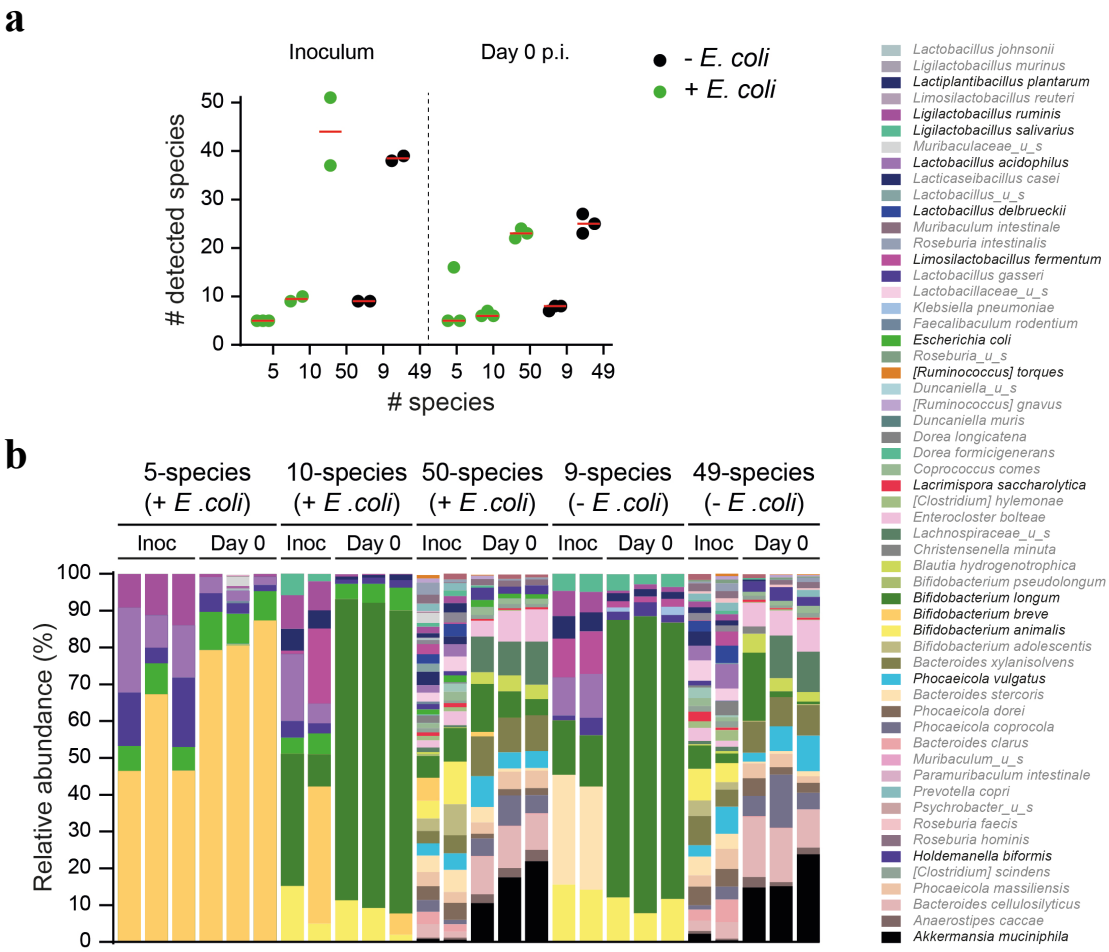


Figure 5. Metagenomic sequencing data for *in vivo* experiments showing that mice gavaged with more gut species became colonised with higher diversity communities. (a) Number of detected species in the symbiont inoculum given to germ-free mice via oral gavage and in mouse faeces 14 days after symbiont gavage (the day of pathogen gavage). Each circle represents an independent replicate. Red lines represent median values. Green symbols depict communities that contain *E. coli* IAI1, black symbols represent communities that do not contain *E. coli* IAI1. Species were detected if they were above a threshold relative abundance of 0.1%. (b) Relative abundances of symbiont strains detected above a 0.1% threshold in inocula given to germ-free mice and in mouse faeces 14 days after symbiont gavage (Day 0 post infection). Different colours represent different strains of bacteria.

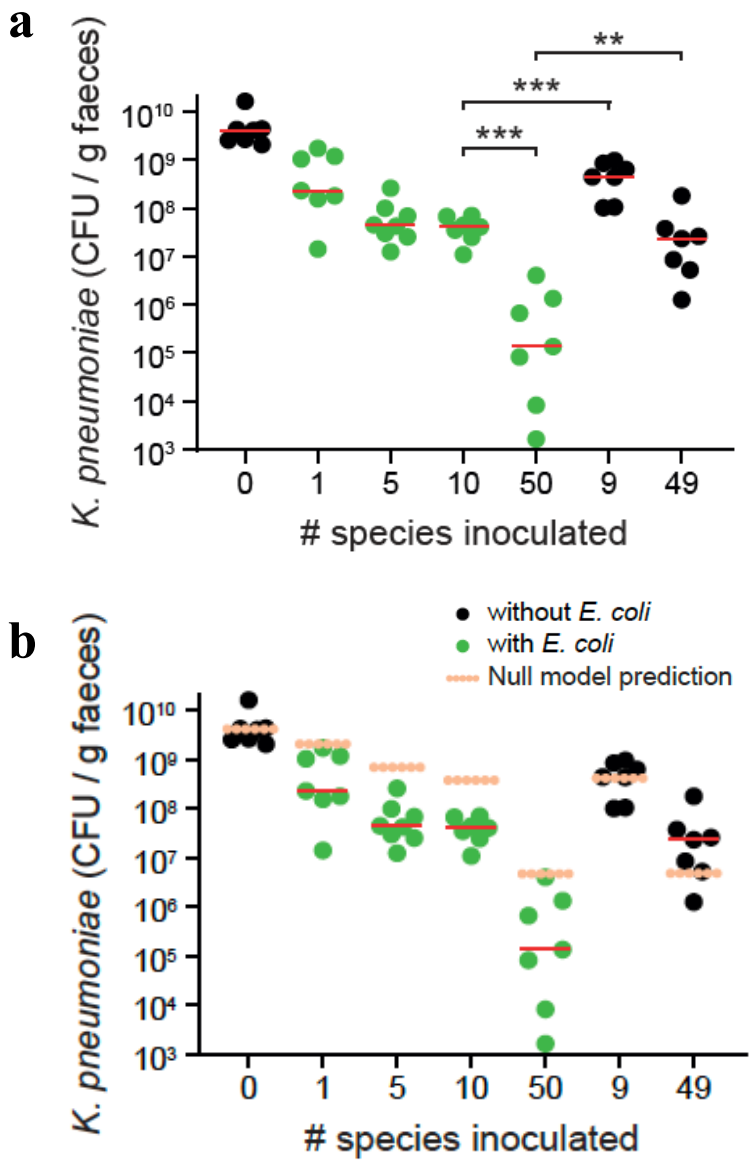


Figure 6. (a) The ecological patterns of colonisation resistance seen *in vitro* are upheld in gnotobiotic mice. Each symbol represents an independent mouse colonised with a particular symbiont community at each diversity level (n=7-8 mice per group in cages of 2-3 mice; 2-3 independent experiments). Red lines indicate the medians. One community composition was tested at each diversity level. Mouse faeces were sampled at 24 hours post infection with *K. pneumoniae* and *K. pneumoniae* abundance quantified by selective plating on LB + carbenicillin (50μg/mL). A two-tailed Mann-Whitney test is used to compare the indicated groups ($p>0.05$=ns; $p<0.05$=*; $p<0.01$=**; $p<0.001$=***). **(b) As community diversity increases, pathogen abundance deviates strongly from the null model for *E. coli* IAI1-containing communities.** Predictions from a simple null model, where pathogen abundance scales with 1/n, where n is the total number of species (community plus pathogen), are plotted alongside the results from (a). As our findings deviate strongly from this null model at higher diversities, it supports the conclusion that the effects of diversity are non-additive. Statistics comparing the difference between the null model and the observed data show that $p=0.62$ for 1 vs. 10 species and $p=0.0041$ for 1 vs. 50 species (Mann-Whitney test on the ratios of the null to the observed data at (1+1) species to (1+10) and (1+50) species.)

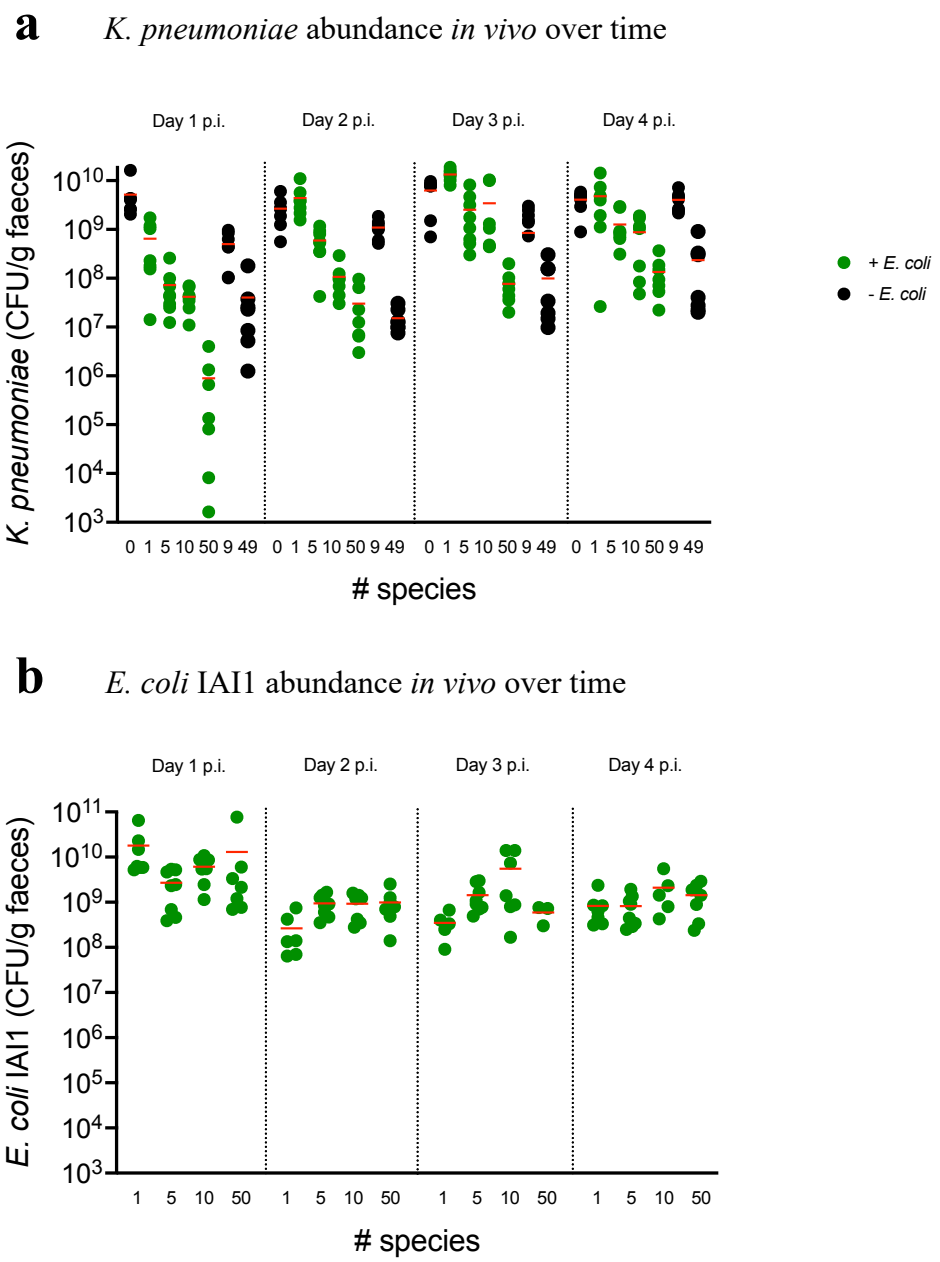


Figure 7. *K. pneumoniae* abundance and *E. coli* IAI1 abundance in mouse faeces for four days after pathogen gavage (p.i. = post infection). Each circle represents a faecal sample from a mouse (n=7-8 mice per group in cages of 2-3 mice; 2-3 independent experiments). The bacterial abundance at each diversity level is plotted. Horizontal red bars depict median values. Abundances measured by selective plating of faeces. *K. pneumoniae* grown on LB (carbenicillin 50µg/mL) agar (a) and *E. coli* IAI1 grown on LB agar (b). Circles in green represent mice colonised with symbiont communities containing *E. coli* IAI1, those in black represent mice not colonised by *E. coli* IAI1.

4.4 Discussion

In this Chapter, we set out to investigate the impact of diversity on the pathogen resistance of a community. Overall, as diversity of a community increases, its pathogen resistance also increases. A more diverse community may perform well due to higher species richness or due to the increased likelihood of certain important species being included in a community (species composition). These two factors are often found to be confounding in studies on the importance of ecological diversity (Bell et al. 2005). To separate out the contributions of species richness and species composition to the beneficial effects of diversity, we tested multiple, randomly selected community combinations at different diversity levels (Fig. 1d). Once *E. coli* IAI1 was identified as being present in the best-performing communities, dropout communities were constructed without *E. coli* IAI1 to validate its role as a key member species (nine and 49 species communities, Fig. 1d). This led to the identification of the first ecological principle of colonisation resistance: the presence of a key competitor species that is closely related to the pathogen, such as *E. coli*. Moreover, another strain of *E. coli* (*E. coli* HS) was also able to significantly increase the colonisation resistance ability of the 9 best-ranked species (Fig. 4a), suggesting that the effect of *E. coli* is not specific to strain IAI1. However, *E. coli* IAI1 alone was not sufficient to produce colonisation resistance to *K. pneumoniae* (Fig. 1d). The presence of other gut species alongside *E. coli* IAI1 was also required to attain maximum colonisation resistance. This revealed the second ecological principle of colonisation resistance: species richness.

The finding that diversity promotes colonisation resistance to the pathogen *K. pneumoniae* supports the suggestion that multi-strain microbiome therapeutics would be more effective than single strain products. Indeed, the first approved microbiome therapeutic, Vowst, which is designed to treat *C. difficile* infection, is based on a (undisclosed) combination of diverse symbiont strains (Jain et al. 2023). In addition, our results are also in line with recent work that finds that a backdrop of additional strains is needed, alongside a symbiont strain already identified as protective, to provide full colonisation resistance. The non-pathogenic strain *Klebsiella oxytoca* was found to promote resistance to *K. pneumoniae* in antibiotic-treated mice, but it required three other gut strains, chosen from the Oligo-MM12 community, to provide full colonisation resistance (Osbelt et al. 2021).

A key question surrounding this work is how the diversity effect we have found here relates to current debate on the importance of a diverse gut microbiome for health. Gut microbial diversity is generally accepted to be important for health (for example, the epidemiologist Tim Spector is well known for advocating the consumption of 30 different plants per week to encourage a diverse

range of bacteria in the gut (McDonald et al. 2018)), but the question of exactly how much microbial diversity is required is currently unanswered. Here, we focus on colonisation resistance to pathogens as a major health benefit of the microbiome and find that diversity of the microbiota is key for pathogen-protection. Based on previous research on the relationship between microbial diversity and community function, it seems likely that, at some level, the effect of diversity on colonisation resistance will be saturating. For instance, it was found that the respiration rate of a community increased with species richness, but at a decelerating rate, in communities containing up to 72 microbial species (Bell et al. 2005). Importantly, while here we study combinations of up to 50 species of bacteria, we would need to construct more diverse communities to find out the level of diversity at which maximum colonisation resistance will be achieved. In addition, it is unclear whether the level of diversity required for colonisation resistance is different from the level of microbial diversity that may be needed to maintain other health benefits of the microbiome.

It is possible that high levels of diversity in the microbiome may also be able to replace the need for key members in a community. This is based on the finding that the 10 species community minus *B. breve* performed at a similar level of colonisation resistance to the two species combination of *E. coli* IAI1 and *B. breve* (Fig. 3). Here, a species already identified to be important for colonisation resistance (*B. breve*) effectively replaced eight other species in terms of their contribution to colonisation resistance. In addition, there was a 100-fold decrease in *K. pneumoniae* abundance between the two *E. coli* dropout treatments *in vivo* (nine and 49 species communities, Fig. 6a), although no parallel decrease in pathogen abundance was observed *in vitro*. However, the 49 species still performed significantly less well, by which I mean that *K. pneumoniae* grew to a greater abundance when added to this community, than the 50 species treatment (Fig. 6a). An interesting next experiment would be, therefore, to test the colonisation resistance ability of more highly diverse gut communities, both with and without *E. coli*. One way to do this would be to compare the ability of different lab strains of mice, which vary in their microbiome composition, to resist colonisation by *K. pneumoniae*. Jackson Laboratories (JAX) mice are known to not harbour *E. coli* in their complex microbiotas, while most other laboratory mice do (Alegre 2019). A recent study has in fact shown that JAX mice are more susceptible to infection with *S.* Typhimurium, another pathogenic Enterobacteriaceae species, than *E. coli*-containing mice from other vendors (Velazquez et al. 2019). This suggests that the role of *E. coli* in resisting pathogenic Enterobacteriaceae continues to be critical in mice colonised with even more diverse microbiomes than those tested here.

Studies show that western societies are currently experiencing a rapid decline in gut microbial diversity, as we consume less fibre, take antibiotics and live a more sterile lifestyle (Sonnenburg et al. 2016; Merrill et al. 2022). The consequences of this loss of diversity are yet to be fully understood but have been proposed to play a role in the rise of chronic diseases that are correlated with decreased diversity, such as obesity, type two diabetes and immune disorders (Sonnenburg and Sonnenburg 2019; Blaser and Falkow 2009; Blaser 2017; Manor et al. 2020). Therefore, deciphering the role of diversity in producing key benefits such as colonisation resistance will be key to understanding the consequences of diversity loss in the gut microbiome (which could be due to, for instance, antibiotics or diet) and working out what can be done to alleviate it.

4.5 Materials and Methods

Bacterial strains and plasmids

A full list of bacterial strains used in this study is provided in Table S1. The plasmid used in the extended competition assay is listed in Table S3. *Klebsiella pneumoniae* subsp. *pneumoniae* purchased from DSMZ (stock number 30104) was used in all experiments containing *K. pneumoniae*. Symbiont strains were chosen based on those commonly isolated from the human gut microbiota. Strains were provided by Nassos Typas (EMBL Heidelberg, Germany), or were ordered from strain collections (e.g. the German Collection of Microorganisms; DSMZ). The *Lactobacillus plantarum* strain was provided by the Department of Food and Nutritional Sciences, University of Reading. *Escherichia coli* strains Z1331 and Z1269 were isolated from the faeces of two healthy human donors in Switzerland (Wotzka et al. 2018).

Culturing of anaerobes

For engineering of *K. pneumoniae*, strains were grown aerobically in Lysogeny broth (LB) with the appropriate antibiotics (Table S1) at 37°C, shaking at 225 rpm. All symbionts were cultured under anaerobic conditions (5% H_2, 5% CO_2, 90% N_2, <20ppm O_2) in modified Gifu Anaerobic Medium (mGAM; Nissui Pharmaceuticals) broth buffered to pH 6.2 with 100mM 2-(N-morpholino)ethanesulfonic acid (MES). The redox indicator dye Resazurin (100µg/L media) was added as a quality control check for the presence of oxygen (turns red when conditions are not sufficiently anaerobic). To prepare glycerol stocks, individual strains were first streaked onto mGAM agar and grown under anaerobic conditions (if possible, as not all strains can grow as single colonies on agar-based media). The identity of each strain was confirmed using 16S rRNA sequencing (Sanger sequencing; Source Biosciences) using the universal primers 27F and 1492R

for most species, or the Bifidobacteria-specific primers g-Bifid-F and g-Bifid-R for Bifidobacteria (Table S4). Single colonies were then inoculated in mGAM broth and stored at -70 degrees Celsius in mGAM with a final concentration of 25% glycerol.

Genetic engineering of bacterial strains

The fluorescence plasmid was transformed into *K. pneumoniae* using electroporation. Briefly, 5mL overnight culture was washed 3x with cold milliQ water, before being concentrated in 500µl cold milliQ water. 2µl of plasmid was mixed with 50µl of concentrated cells and electroporated (1.8kV; 0.1cm gap cuvettes) before recovery in 1ml pre-warmed LB (1h at 37°C, shaking at 220rpm) and plating on LB with the appropriate antibiotics.
Primers used for genetic engineering are listed in Table S4.

Extended competition assay

Symbiont strains were grown to stationary phase anaerobically (12-72 hours, depending on the species), in Hungate tubes containing 5mL mGAM broth (HyServe-05433) and 100mM MES (Sigma Aldrich) and buffered to pH 6.2. (225rpm, 37 degrees). *K. pneumoniae* carrying the fluorescence plasmid pBC11(Cunrath and Bumann 2019) (YPet) was incubated overnight under the same conditions, with the appropriate antibiotics (Table S1).

Once in stationary phase, monocultures of symbionts were passaged (100µL culture into a new 5mL tube of media) and grown for ~17 hours. Communities were assembled under anaerobic conditions into new 5mL Hungate tubes (see section "community preparation") and grown for 24 hours. Once grown, communities were invaded with 100µl of the pathogen (10^6 cells/mL final concentration) in each 5mL Hungate tube. Samples were taken immediately after pathogen invasion and prepared for measurement using flow cytometry (Day 0). Invaded communities were incubated in a shaking incubator (37 degrees Celsius, 225rpm). After 24 hours, the invaded communities were sampled for flow cytometry (Day 1) and 100µL was passaged into new 5mL tubes of mGAM broth. After a further 24 hours, the end-point communities were sampled and measured a final time (Day 2).

Community preparation

Constituent monocultures were grown to stationary phase, passaged into new media and grown overnight for approximately ~17 hours, and then combined into communities. The OD-600 of the single strains was measured and the cultures were streaked anaerobically on mGAM agar to

check for contamination. Communities ranged from two to 50 strains in size and were assembled under anaerobic conditions. Community IDs are detailed in Table S5-6.

In vitro: For the communities containing two-10 strains, equal volumes (100µL) of each overnight were combined in a Hungate tube containing 5mL mGAM to form a community. For the 49- and 50-strain communities, 20µL of each single strain was added, equating to a total volume of 1mL. The communities were made by adding 1mL of each strain anaerobically to a 50mL falcon tube, mixing, and removing 1mL to add to a fresh Hungate tube of 5mL mGAM broth. Communities were grown in the shaking incubator (37 degrees, 225rpm) for 24 hours before being invaded with 10^6 cells/mL of the pathogen.

Communities containing two-10 strains were selected at random from the best-ranked 10 strains from the luminescence screen (see Fig. 1 in Chapter 3). The experiment was then augmented with additional communities selected at random, but under the condition that they contain *E. coli* IAI1 (original communities in Fig. 1a-b, with additional communities in Fig. 1c-f, see Table S5 for community compositions).

In vivo: Strains were grown separately, then OD-600 of each culture was measured. For communities containing two-10 strains, the volume of culture containing 10^9 cells was calculated for each individual strain, based on a standard curve of OD-600 and flow cytometry quantification. This was added to a large falcon tube. The community mix was centrifuged (10 minutes, room temperature, 14000rpm) and the resulting pellet resuspended in 2mL anaerobic PBS and kept on ice. 200µl were gavaged into each mouse corresponding to 10^8 cells for each strain. For the 49- or 50-strain communities, we used fewer cells for each strain to avoid gavaging a large total cell density into mice (as done for the *in vitro* experiments). The volume of culture containing 2×10^8 cells was calculated for each constituent strain and they were combined. The mixture was centrifuged and the pellet resuspended in 2mL PBS. Mice were gavaged with 200µL of the inoculum. Therefore, the density of bacteria in the 200µL gavage was equivalent for the 50-strain community as for the 10-strain community. For all inoculums, samples were taken for plating anaerobically on mGAM agar to confirm the cell density.

One community at each diversity level (five, 10, 50 strains) was selected to test *in vivo*. Community compositions are detailed in Table S6.

Flow cytometry

Hungate tubes containing culture to be sampled were de-pressurised under anaerobic conditions using needles. Samples were removed using needles and syringes. 10μL of each sample was diluted in 90μL PBS + chloramphenicol 200μg/ml then 10μL added to a 96-well flat-bottomed plate already containing 80μL PBS + chloramphenicol 200μg/ml. The 96-well plate was left to shake at room temperature on the bench for 15 minutes to allow oxygen-dependent folding of YPet, while preventing further growth of the sample with the bacteriostatic antibiotic chloramphenicol. Next, all bacterial cells were fixed, permeabilised and fluorescently stained by adding 90μL PBS containing 4% paraformaldehyde, 0.4% Triton X-100 and 1μg/mL 4',6-diamidino-2-phenylindole (DAPI) to each sample well and incubating the plate in the dark for 1 hour at room temperature on a microplate shaker. Prior to the measurement, 20μL AccuCheck counting beads (ThermoFisher- PBC100) was added to every sample well. Two wells containing 200μL PBS were left between sample wells, in order to prevent cross-contamination between samples. 96-well plates were run in a flow cytometer set to: acquisition volume 50μL, total draw volume 80μl, total sample volume 200μL, at a speed of 100mL/minute. Relevant spectral parameters were recorded in a flow cytometer (Attune NxT Autosampler) equipped with 405nm, 488nm and 561nm lasers (ThermoFisher). The following channels were used: DAPI staining, excitation 405nm, emission 415-465nm ('blue'); YPet fluorescence, excitation 488nm, emission 505-515nm and 525-555nm ('green').

Flow cytometry data was processed using FlowJo v10.8.1 software. 'Beads' were gated on a linear (FSC-H; SSC-H) axis. 'Bacteria' were gated on a logarithmic (FSC-H; SSC-H) axis. DAPI was gated within the 'Bacteria' gate, on a logarithmic (Ex405-417; Ex405-495) axis. Within the DAPI gate, YPet was gated on a logarithmic (Ex488-503; Ex488-555) axis. Count statistics for beads, DAPI and YPet were exported to Microsoft Excel and pathogen density (cells/mL) was calculated.

Mouse husbandry and experiments

Mouse experiments were performed with 6-8 weeks old germ-free C57BL/6J female mice that were bred and maintained in germ-free isolators at the Kennedy Institute, University of Oxford. During experiments, mice were housed as pairs or trios in sterile, individually ventilated cages with irradiated food and autoclaved water. Cages of mice were disinfected in TecCare Ultra Hydrogen peroxide, peracetic acid solution before mice were handled using individually sterilised gloves (single use for each cage) in a biosafety cabinet that was disinfected with the same acid solution in between each treatment group. Mouse experiments were performed in accordance with the UK

Animal Scientific Procedures Act (1986) under a Project License (PPL; PP9127884 to Fiona Powrie) authorised by the UK Home Office.

Germ-free mice were gavaged with a 200µL inoculum of symbionts (see "community preparation") at Day -14 of the experiment and again on Day -12 of the experiment (see scheme Fig. 4a in Chapter 3). On Day 0, overnight culture of the pathogen (*K. pneumoniae*) grown aerobically in LB containing the appropriate antibiotics was washed 3x with PBS and diluted. 10^6 CFU of the pathogen was given to each mouse as a 100µl gavage. Faeces were sampled daily after gavage of the pathogen. Faecal pellets were weighed and homogenised with a 5mm stainless steel bead in 1ml PBS (samples were shaken vigorously in 2ml Eppendorf tubes). CFUs were enumerated using selective plating (LB + carbenicillin 50µg/mL for *K. pneumoniae*, LB for *E. coli* IAI1). *E. coli* and *K. pneumoniae* can be differentiated by colour on LB agar after a couple of days of growth on the bench at room temperature (*K. pneumoniae* appears whiter and shiny due to capsule production, *E. coli* appears yellow). Mice were euthanised four days after infection with the pathogen.

DNA isolation from faeces and metagenomic sequencing

Aliquots of the faeces were frozen immediately after collection (prior to homogenisation in PBS) and stored at -70°C until use. Faecal samples were thawed and resuspended in nuclease-free water, before being transferred to a lysing matrix B tube (MP Biomedicals). Three rounds of bead beating were performed at 6 m/s for 40s. Samples were centrifuged at high speed and DNA in the supernatant was precipitated by adding sodium acetate (1/10 volume) and ice-cold ethanol (96-100%; equal volume) and left at -20°C overnight. Samples were centrifuged at high speed and the pellet was washed twice with 70% ethanol, before being dried and resuspended in nuclease-free water.

Samples were further purified using an AMPure clean-up protocol. The samples were mixed with AMpure XP beads (Beckman Coulter) incubated at room temperature for 5 minutes, before being washed twice with 70% ethanol, using a magnet avoid removing the DNA bound to the AMPure beads. After air drying, nuclease-free water was added to the beads, to allow collection of the purified DNA in the supernatant.

CosmosID performed metagenomic sequencing on isolated DNA. DNA libraries were prepared using the Nextera XT DNA Library Preparation Kit (Illumina) and IDT Unique Dual Indexes

with total DNA input of 1ng. Genomic DNA was fragmented using a proportional amount of Illumina Nextera XT fragmentation enzyme. Unique dual indexes were added to each sample followed by 12 cycles of PCR to construct libraries. DNA libraries were purified using AMpure magnetic Beads (Beckman Coulter) and eluted in QIAGEN EB buffer. DNA libraries were quantified using Qubit 4 fluorometer and Qubit dsDNA HS Assay Kit. Libraries were then sequenced on Illumina NovaSeq platform 2x150bp (3M reads per sample). CosmosID performed bioinformatic analysis according to proprietary methods on the raw data to generate fine-grained taxonomic and relative abundance estimates (Fig. 5).

Statistical analysis

All graphs were made and statistical analysis carried out in Prism v9.4.1. Figure legends indicate the statistical test used and the sample sizes.

5. The role of nutrient blocking in colonisation resistance in the gut microbiome

5.1 Abstract

The ability of gut communities to protect their host from infection by incoming pathogens, known as colonisation resistance, has multiple potential underlying mechanisms. These include stimulation of the host immune system, direct killing of the pathogen by resident bacteria, and outcompeting the pathogen for nutrients in the gut. It is not known which of these mechanisms is generally the most important in the natural gut ecosystem, but we need this information if we are to understand why certain combinations of gut bacteria successfully resist pathogen colonisation, while others do not. Here, we show that the ability of communities of gut bacteria to block colonisation by *Klebsiella pneumoniae* lies in nutrient competition. Furthermore, we show that we can use the simple principle of nutrient blocking, whereby resident species use the nutrients that would otherwise be available to the pathogen, to successfully predict, *in silico*, communities to resist a novel target strain, an antimicrobial resistant strain of *Escherichia coli*. Nutrient blocking explains why both diversity and community composition can be critical to colonisation resistance in the gut microbiome.

5.2 Introduction

Colonisation resistance, or the ability of the microbiome to resist colonisation by exogenous bacteria and thereby protect the host from pathogens, is a vital benefit of the gut microbiome. There are multiple potential mechanisms that can promote colonisation resistance (Sorbara and Pamer 2019; Caballero-Flores, Pickard, and Nunez 2022). These mechanisms include the potential to modulate host physiology. Some studies, for example, have highlighted the importance of the host immune system in microbial defence against pathogens. Sequeira *et al* found that IL-36 signalling primed by the presence of Bacteroidetes in the intestinal microbiota was able to protect against *K. pneumoniae* colonisation (Sequeira et al. 2020). Byndloss *et al* discovered that the resident microbiota induces PPAR-y signalling, thereby reducing the bioavailability of respiratory electron

acceptors in the colonic lumen and preventing the expansion of potentially pathogenic and facultatively aerobic Enterobacteriaceae (Byndloss et al. 2017). The resident microbiota achieves this by producing the short chain fatty acid (SCFA) butyrate, which is a product of fermentation that is sensed by the host colonocyte PPAR-y receptor.

Another key way in which colonisation resistance can arise is via interbacterial interactions, where resident strains compete against incoming strains. One way that this can occur is via the release of antimicrobial toxins and other related mechanisms of interference competition. For example, Kim *et al* found that a symbiont *Lactococcus lactis* strain produces a lantibiotic (a type of antibacterial peptide) that inhibits vancomycin-resistant *Enterococcus faecium* growth. The commensal *E. coli* strain Mt1B1 has been discovered to harbour two type six secretion systems (T6SSs), which are a type of contact-dependent machinery that injects toxins directly into the cells of target bacteria, in this case pathogenic *Citrobacter rodentium* in the mouse gut (Serapio-Palacios et al. 2022). In other cases, the compound mediating colonisation resistance is not a dedicated bacterial toxin. Jacobson *et al* showed that intestinal *Bacteroides* species mediate colonisation resistance to *Salmonella enterica* serovar Typhimurium by producing the SCFA propionate, which inhibits the pathogen's growth by disrupting intracellular pH. Similarly, Buffie *et al* found that the intestinal bacterium *Clostridium scindens* modifies host-derived bile salts, producing secondary bile acids that inhibit the pathogen *Clostridium difficile* (Buffie et al. 2015).

Perhaps the most fundamental potential mechanism underlying colonisation resistance is resource competition, and in particular, competition over nutrients. A handful of studies published over the past few years have discovered nutrient competition to be the primary mechanism for resisting pathogens in the gut microbiome. Two studies published in consecutive years (2020 and 2021) took a similar, top-down approach, where they studied the root cause of variation in colonisation resistance ability among complex gut communities (Oliveira et al. 2020; Osbelt et al. 2021). The study led by Rita A Oliveira was in mice, whereas the study led by Lisa Osbelt looked at faecal samples from healthy human donors. Each study identified a symbiont *Klebsiella* species from the resistant communities as key for protection against a pathogenic Enterobacteriaceae. Oliveira *et al* found a strain of *Klebsiella michiganensis* to be protective against pathogenic *E. coli*, whereas Osbelt *et al* found *Klebsiella oxytoca* to be protective against *K. pneumoniae*. Both studies found that the respective symbiont strain was able to outcompete the pathogen strain for various carbon sources. Each study identified a private nutrient (galactitol or lactulose, by Oliveira *et al* and Osbelt *et al* respectively), by which I mean a nutrient that is unique to the pathogen and cannot be metabolised

by the symbiont. Upon supplementation of this nutrient *in vivo* during pathogen challenge, both studies found that colonisation resistance was abolished, providing strong support for competition over nutrients as the main mechanism of colonisation resistance. Nutrient competition has also been found to be important for resisting a different gut pathogen, *C. difficile* (Pereira et al. 2020). In this study, a top-down approach was again taken. Colon contents were extracted from mice and screened for individual microbial cells that could metabolise O-glycan monosaccharides, which are compounds that are found in mucus in the gut, a known source of food for bacteria. The identified cells were then sequenced and used to design a consortium of five microbial species able to forage on the monosaccharides. The authors demonstrated that this consortium was able to impair colonisation by *C. difficile in vivo*, providing evidence for nutrient competition as the primary mechanism of colonisation resistance against *C. difficile* in the mouse gut.

Our previous work revealed that community diversity is necessary for colonisation resistance to the problematic pathogen *K. pneumoniae*, both *in vitro* and *in vivo* (Chapters 3 and 4). However, we also found that diversity alone is not sufficient to provide colonisation resistance. The combination of species in a community also matters, with certain species playing a key role in colonisation resistance. *E. coli* was found to be particularly important for colonisation resistance to *K. pneumoniae*. This finding fits with the general importance of competition with ecologically similar strains and species (Palmer and Foster 2022a; Granato, Meiller-Legrand, and Foster 2019). As closely related strains are more likely to occupy overlapping niches and share similar resources, it is expected that they will often be strong competitors with one another (Palmer and Foster 2022b). This effect can be observed among strains of *Bacteroides* in the gut, for example, which have overlapping nutrient niches and carry toxins that target one another (Shumaker et al. 2019). It is also observed in the studies by Oliveira *et al* and Osbelt *et al* that find two non-pathogenic *Klebsiella* species are key for protection against the closely related pathogens *E. coli* and *K. pneumoniae*, respectively (Oliveira et al. 2020; Osbelt et al. 2021). However, interestingly, our work also identified an important role in colonisation resistance for species that are not a close phylogenetic relative of *K. pneumoniae*. This finding suggests that phylogenetic similarity, either associated with toxins or nutrient competition, is not sufficient to explain the colonisation resistance observed (Chapters 3 and 4).

Here, we seek to understand the mechanism underlying these ecological patterns of colonisation resistance. Specifically, our goal is to understand why some communities perform well in resisting pathogen growth while others do not. With this information, we hope not only to better

understand colonisation resistance but also, critically, have the potential to predict ahead-of-time, which communities will be protective against a given problem strain.

5.3 Results

5.3.1 Colonisation resistance is not explained by interference competition

Studies have proposed multiple potential mechanisms of colonisation resistance, including host immune system stimulation, nutrient competition, and interference competition. However, it is still not clear which one of these is the primary mechanism underlying pathogen-protection. In our experiments so far, it has been found that diverse microbial communities that contain a key competitor species are the types of communities that are best at resisting pathogen colonisation. We uncovered the same pattern of colonisation resistance *in vivo* as *in vitro*, which suggests that host effects, such as immune system stimulation, are not critical for achieving colonisation resistance. The two other types of colonisation resistance, that occur as a direct result of interbacterial interactions, are nutrient competition and interference competition. I now aim to uncover which of these mechanisms can explain pathogen-resistance in our communities. To do so, experiments are carried out that take place *in vitro*, because this is where we have the most power to understand mechanisms. However, future work should also investigate the mechanisms outlined here *in vivo*.

During interference competition, the symbiont community directly kills or inhibits the pathogen, for example by secreting toxins into the local environment, lowering the pH, or by using a T6SS to directly inject an opponent cell with toxic proteins (which requires contact between cells). In our experiments, we did not find any evidence for killing of the pathogen. While the growth of *K. pneumoniae* can be strongly suppressed, the abundance of *K. pneumoniae* does not decrease below the level at which it was inoculated (see Chapter 4, Fig. 1c-d). However, it is possible that there could be a combination of killing and growth of the pathogen that leads to the *K. pneumoniae* densities observed. In order to seek evidence for interference competition, we carried out experiments *in vitro,* where we grew *K. pneumoniae* in cell-free ('spent') media collected from the cultures of different single strains and communities. If the presence of the symbiont cells is necessary to prevent pathogen growth (for instance, if contact-dependent inhibition occurred), this supernatant alone should not provide colonisation resistance. In a further set of treatments, we added back nutrient to the spent media to minimise any effects of nutrient limitation. In this case, if toxins are produced by the symbiont strains and released into the media, they should limit pathogen growth even though nutrients are not limiting. More specifically, to perform these tests, we grew *E. coli* IAI1,

the 10 best-ranked strains from the screen together as a community, and the isogenic wild type *K. pneumoniae* strain for 96 hours in Hungate tubes containing nutrient-rich mGAM media buffered to pH 6.2. Then, we centrifuged and filter-sterilised the cultures under anaerobic conditions. To rule out the possibility of any bacteria still being present in the supernatants, we inoculated sterile media with supernatant and confirmed absence of growth. Fluorescent *K. pneumoniae* cell density was measured via flow cytometry 24 hours after pathogen inoculation.

Growth of *K. pneumoniae* was inhibited by the spent media, as compared to when the spent media was re-supplemented with fresh mGAM media (Fig. 1a). This result suggests that the symbiont cells do not need to be physically present in the culture to be able to inhibit pathogen growth, which does not support a role for contact dependent mechanisms of inhibition. Additionally, the pathogen was able to grow when supplemented with new nutrients. This result suggests that toxins released into the media are also not important for colonisation resistance, because if toxins were present, they should continue to inhibit pathogen growth upon the addition of nutrients to the spent media.

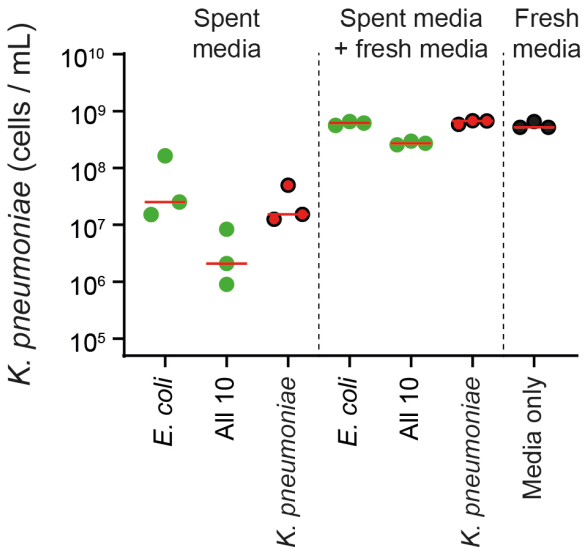


Figure 1. Spent media experiments show that colonisation resistance is not explained by toxin production. *E. coli* IAI1, the 10 best-ranked strains ('All 10') and *K. pneumoniae* were grown for 96 hours, supernatants were prepared, then the fluorescent strain of *K. pneumoniae* was inoculated in the spent media (either in 100% spent media, or in 50% spent media 50% fresh media) and its density measured 24 hours later via flow cytometry. Each symbol represents a replicate (n=3), green circles indicate presence of *E. coli* IAI1, red circles indicate the isogenic wild type *K. pneumoniae*, black circles indicate the no symbiont control. Red bars indicate medians.

5.3.2 Carbon use overlap between the symbionts and the pathogen explains colonisation resistance to *K. pneumoniae*.

The spent media experiments suggest that contact dependent mechanisms do not explain colonisation resistance. Instead, the data suggests a central role for nutrient competition. However, there are scenarios where toxins could explain some of the patterns seen in the spent media experiments. For example, toxins in the media may only be effective in spent media where no supplemented nutrient have been added. In order to further test for the role of nutrient competition, therefore, we profiled the carbon sources that each of the 10 symbiont species used, along with those used by *K. pneumoniae,* using Biolog AN MicroPlates. Six additional symbiont species were profiled on Biolog AN MicroPlates, and the choice of these six strains comes from the experiments that were carried out in parallel by another member of the lab working on *S.* Typhimurium, Erik Bakkeren (unpublished work). In brief, the 16 symbiont species profiled here are the 10 best-ranked strains from the initial screen (Chapter 3) for *K. pneumoniae,* plus the 10 best-ranked species for *S.* Typhimurium, some of which were the same for both pathogens.

Each 96-well Biolog AN MicroPlate contained 95 different single sugars (one sugar per well) in minimal media. If a strain was able to grow on a particular sugar alone under anaerobic conditions, it indicates that the strain is able to utilise that sugar. We assessed which sugars the strains could use (Fig. 2a-b, also see Materials and Methods). Our data shows that as community diversity increases so too does colonisation resistance. If competition over nutrients is important, therefore, one might expect an increase in the importance of nutrient competition as diversity increases. To look for evidence of this computationally, we calculated the carbon source percentage overlap between symbiont communities (size two-10 strains, picked at random from the 10 best-ranked strains) and *K. pneumoniae*. Specifically, we simply calculated the number of carbon sources that could be used by the constituent strains in a community as a percentage of the number of carbon sources that *K. pneumoniae* could use (see Materials and Methods). Consistent with a link between nutrient use and colonisation resistance, this analysis showed that, as community diversity increased, carbon source utilisation overlap between communities and the pathogen also increased (Fig. 2c).

To explore the potential link between carbon source use and colonisation resistance more directly, we next explored the relationship between this carbon source overlap measure and the colonisation resistance of the communities measured in Chapter 3. This revealed a strong relationship between the two measures, whereby as carbon source percentage overlap with the pathogen increased, the

abundance of *K. pneumoniae* initially remained high, at around 10^9 cells/mL, before decreasing more and more steeply with increased overlap, until reaching around 10^5 pathogen cells/mL (Fig. 2d). At the extreme of overlap, therefore, this suggests that the resident community is, in some cases, utilising the available nutrients in the media to the extent that the growth of *K. pneumoniae* was blocked. Hereafter, we use the term nutrient blocking to describe this effect.

The highest level of colonisation resistance was provided by the 50 species community, which has a carbon utilisation overlap of 71.2% with *K. pneumoniae*, and resisted *K. pneumoniae* growth so that it grew to an abundance of only 10^5 cells/mL. But how much growth of *K. pneumoniae* in the community does this cell density imply? In the extended competition assay, we inoculate the symbiont community with a final concentration of 10^6 cells/mL *K. pneumoniae*, leave it to grow for 24 hours, then passage 100μL into 5mL fresh media. If there was no growth of *K. pneumoniae*, therefore, then we can expect the starting *K. pneumoniae* density of 10^6 cells/mL to be diluted 50-fold, to 2×10^4cells/mL. With the final *K. pneumoniae* concentration in the 50 species treatment at 10^5 cells/mL, therefore, this calculation suggests that there was very little overall growth of the pathogen. Indeed, this outcome implies even less growth than in our positive control, which is when we inoculate the fluorescently distinct *K. pneumoniae* into an isogenic *K. pneumoniae* population (red dot, Fig. 2d). That is, we observe more growth of *K. pneumoniae* in this treatment (averaging 10^6 cells/mL *K. pneumoniae*) than in the 50 species treatment, despite there being a 100% carbon use overlap between the two *K. pneumoniae* strains. If nutrient competition is the only determinant of competition in our experiments, one might expect the isogenic wild type *K. pneumoniae* should produce the strongest growth inhibition of the fluorescent *K. pneumoniae*. Therefore, there may be a factor at play in addition to nutrient competition in some of the community experiments. Nevertheless, the strong association between carbon source utilisation and colonisation resistance suggests again that nutrient competition is the central driving process.

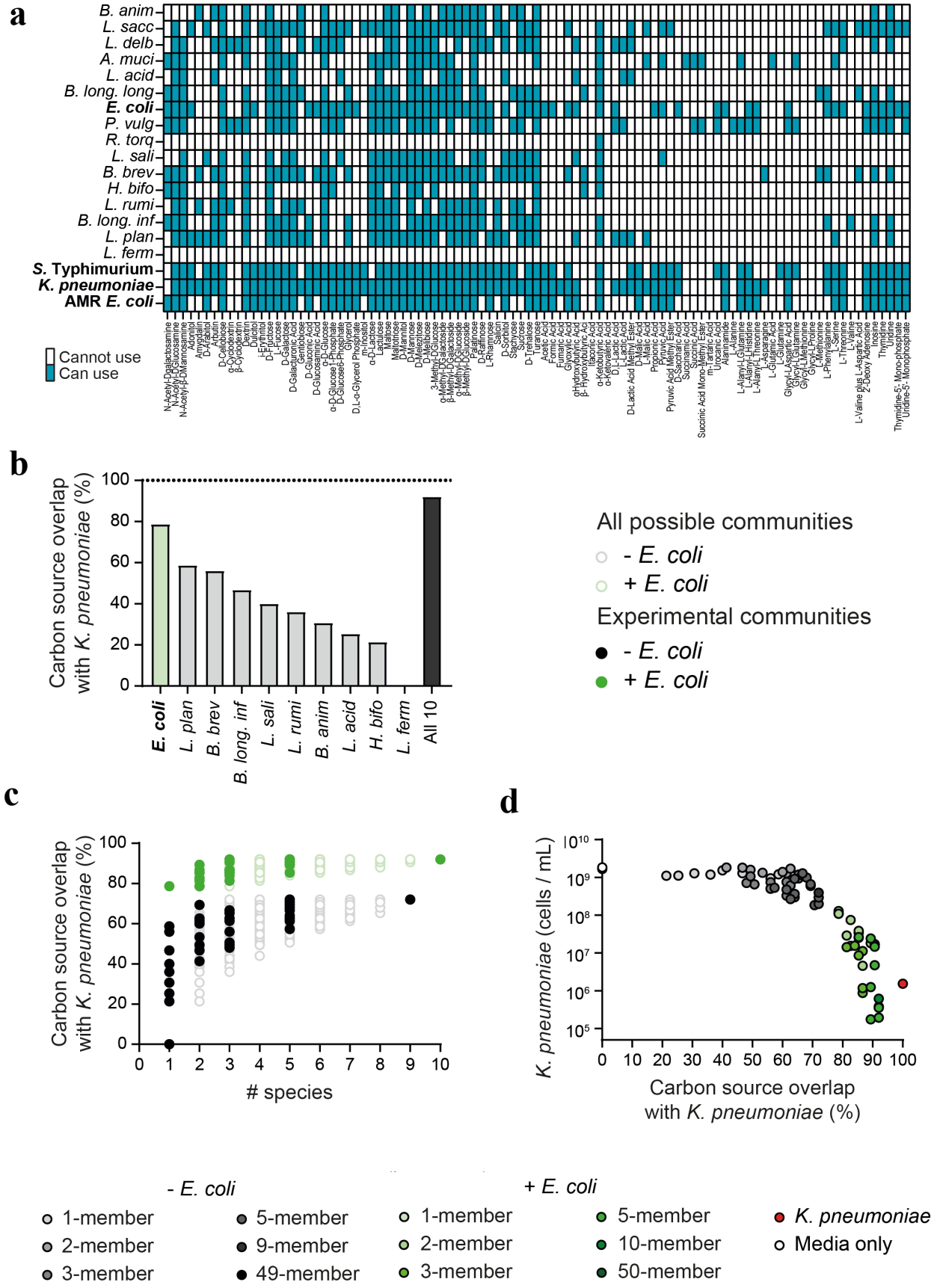

a
B. anim
L. sacc
L. delb
A. muci
L. acid
B. long. long
E. coli
P. vulg
R. torq
L. sali
B. brev
H. bifo
L. rumi
B. long. inf
L. plan
L. ferm
S. Typhimurium
K. pneumoniae
AMR E. coli
Cannot use
Can use
b
Carbon source overlap with K. pneumoniae (%)
E. coli
L. plan
B. brev
B. long. inf
L. sali
L. rumi
B. anim
L. acid
H. bifo
L. ferm
All 10
All possible communities
- E. coli
+ E. coli
Experimental communities
- E. coli
+ E. coli
c
Carbon source overlap with K. pneumoniae (%)
species
d
K. pneumoniae (cells / mL)
Carbon source overlap with K. pneumoniae (%)
- E. coli
1-member
2-member
3-member
5-member
9-member
49-member
+ E. coli
1-member
2-member
3-member
5-member
10-member
50-member
K. pneumoniae
Media only

Figure 2. Overlap in carbon source use explains which communities have high colonisation resistance to *K. pneumoniae*. (a) Profile of carbon source use for each of the 16 symbiont strains tested, and the three pathogens *K. pneumoniae*, *S.* Typhimurium and a strain of AMR *E. coli*. Each of the 95 single carbon sources in AN biolog plates is listed along the X-axis. Blue coloured boxes indicate that a strain is able to use that sugar, based on a thresholding approach. (b) % carbon source overlap (out of a total of 95 carbon sources tested) with *K. pneumoniae*. All of the top 10 best-ranked strains were tested individually. *E. coli* is shown in green, the top 10 best-ranked strain community in black. The nutrient use for the 10 species community was calculated using an additive approach. (c) Communities of differing diversity and composition formed from the 10 best-ranked strains from the screen. Each circle represents a community of a different composition. Filled circles represent communities that were chosen at random and experimentally tested in the extended competition assay, empty circles represent potential communities that were not tested. Green circles represent communities that include *E. coli* IAI1, black circles represent communities that do not. (d) Correlation of the results of the communities experimentally tested in the extended competition assay with the carbon source overlap calculated based on measuring the single strains in biolog plates. Each circle represents a different community. Communities in green contain *E. coli* IAI1, those in black do not. The circle in red represents the isogenic wild type *K. pneumoniae*. The colour intensity of the circles indicates the community diversity (higher colour intensity correlates with higher diversity).

Our work supports the central role of nutrient competition. As a further test of its importance, we next turned to experiments that supplement the culture with a single known nutrient, the sugar alcohol known as galactitol. Galactitol was chosen because, as is shown in the Biolog nutrient profiles under its alternate name of dulcitol (Fig. 2a), it can only be utilised by *E. coli* IAI1 and *K. pneumoniae*, but not by any of the other symbionts. The *E. coli* gatABC deletion mutant was engineered (see Methods), to remove the ability of *E. coli* IAI1 to utilise galactitol. We hypothesised that, if nutrient limitation is the key reason why pathogen growth is suppressed in the most resistant communities, addition of a nutrient that is private to the pathogen will allow the pathogen to grow. Therefore, in the communities where the *E. coli* gatABC mutant has been substituted in for the wild type *E. coli*, and galactitol is supplemented, it is expected that colonisation resistance to *K. pneumoniae* will be abolished, because the galactitol will only be available to *K. pneumoniae*. As an important control, if galactitol is supplemented to communities containing the wild type *E. coli*, the resident *E. coli* will be able to use the galactitol and colonisation resistance to *K. pneumoniae* should be maintained.

Galactitol was supplemented to the cultures at concentrations of 0.1% and 1%, in addition to a 0% (no galactitol) control. First, to test for a direct effect of galactitol on the the growth of *K. pneumoniae*, we grew *K. pneumoniae* alone in the presence and absence of galactitol (see data at far left of Fig. 3). At both concentrations, *K. pneumoniae* grew to the same abundance, showing that

the addition of galactitol to the media does not directly impact *K. pneumoniae* growth. At 1% galactitol concentration, the 10 species community containing the mutant *E. coli* strain was unable to resist pathogen growth, allowing *K. pneumoniae* to grow significantly higher, to nearly three logs (1,000-fold) greater abundance than when the isogenic wild type *E. coli* IAI1 was present in the 10 species community ($p=0.0286$, dark blue symbols, Fig. 3). At 0% and 0.1% galactitol concentrations, the 10 species communities attained similar levels of colonisation resistance (just over 10^6 cells/mL) whether or not they contained the wild type or mutant *E. coli*. This result suggests that a galactitol concentration of 1% is needed to observe the decrease in colonisation resistance for the 10 species community containing the *E. coli* mutant, as the 0.1% concentration is not high enough to produce this effect. Importantly, the presence of the nine symbiont species was needed alongside *E. coli* to produce the change in colonisation resistance between the wild type and mutant *E. coli* strains. As previously observed (see Chapter 3), the single strain *E. coli* does not confer a high level of protection against *K. pneumoniae*, allowing it to grow to nearly 10^8 cells/mL. This suggests, as supported by the Biolog carbon use profiles in Fig. 2, that as the nutrient use overlap between *E. coli* and *K. pneumoniae* is not great enough to provide full colonisation resistance, the addition of a nutrient unique to *K. pneumoniae* does not make a difference to the ability of *E. coli* to suppress its growth. The 1% galactitol concentration is not shown for the single strain data or the no symbionts control, because in these treatments the higher galactitol concentration caused extensive fermentation and acidification of the media, interfering with the flow cytometry. In sum, our data from spent media, Biolog and nutrient supplementation experiments support the hypothesis that nutrient competition is the basis for colonisation resistance in our experiments.

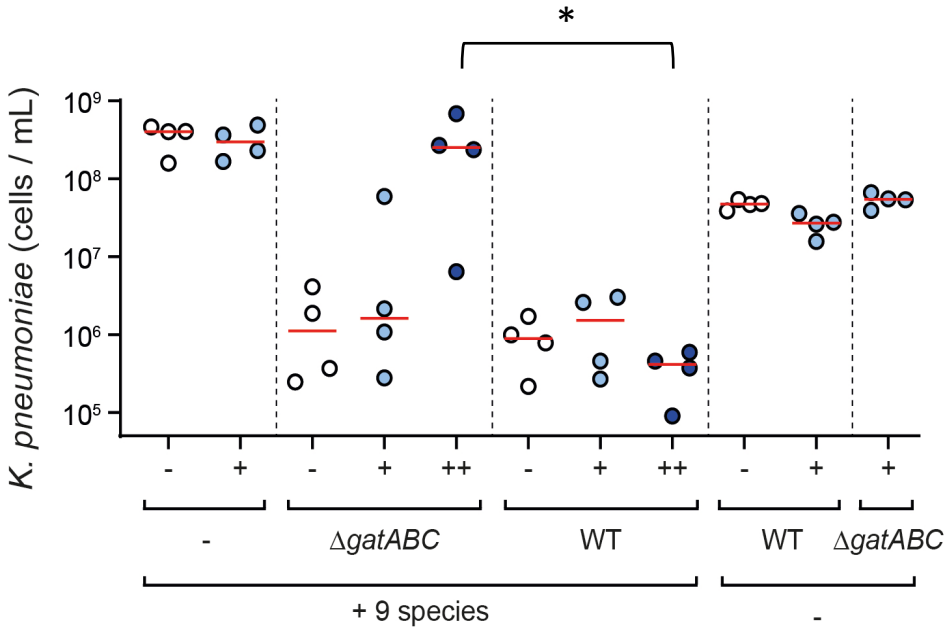


Figure 3. A private nutrient, galactitol, that could only be used by *E. coli* IAI1 wild type and *K. pneumoniae*, but not the symbionts nor an *E. coli* gatABC mutant, was supplemented to the media and extended competition performed as before. '-' (white circles) indicates no galactitol, '+' (blue circles) indicates 0.1% galactitol, '++' (black circles) indicates 1% galactitol. n=4 replicates per treatment. In all treatments, pathogen abundance was measured by flow cytometry after 48h of growth post-passage instead of the usual 24 hours. This change did not influence the control experiments without galactitol, but proved informative because we found the growth impacts of galactitol were relatively slow. A Mann-Whitney test was carried out to make the indicated comparison, n=4, p=0.0286. (p>0.05=ns; p<0.05=**; p<0.01=**).

5.3.3 Protein family overlap also predicts colonisation resistance

So far, we have found that nutrient blocking is central to explaining what makes a community of bacteria able to resist growth of the pathogen *K. pneumoniae*. Nutrient blocking describes the mechanism by which symbiont bacteria metabolise the nutrients that would otherwise be available to the pathogen and in doing so, prevent the pathogen from growing. Here, we used Biolog MicroPlates to profile the carbon sources that can be metabolised by *K. pneumoniae* and 16 different gut symbiont species, including *E. coli* (Fig. 2a). We used these data to show that the higher the nutrient use overlap between a symbiont community and *K. pneumoniae*, the more strongly the community is able to resist *K. pneumoniae* growth.

These data on carbon source overlap are consistent with the importance of the degree of niche overlap between a community and a focal pathogen for colonisation resistance. Specifically, it suggests that a species is only able to colonise the gut if there is a niche available to it. While the concept of niche is complex and difficult to define, especially for host-associated microorganisms such as gut bacteria, a niche can be conceptualised as a multidimensional space encapsulating the environmental factors that influence species survival, including nutrients, pH and oxygen (Ashby et al. 2017). Bacteria with strongly overlapping niches are predicted to compete over shared resources, which can result in the exclusion of the lesser competitor. The data presented here suggest that nutrient availability is particularly critical in determining whether a species can colonise. In practice then, to put it simply, a niche in the gut means there is at least one nutrient available to the colonising species, that it can grow on. If the nutrients that could potentially be used by an incoming pathogen are effectively "blocked" by the resident bacteria, meaning that they feed on and use up those nutrients, there are no nutrients left over for the exogenous species and, therefore, no available niche. As a result, the incoming bacteria are unable to colonise the gut. Our data, therefore, fit with a model where the nutrient landscape of the gut is carved into nutrient

niches by the bacteria inhabiting it, as first put forward by Rolf Freter in his nutrient niche theory (Pereira and Berry 2017).

Based on this, we hypothesised that other measures of niche overlap may also serve to predict which communities are protective against the pathogen. Specifically, we turned to the strains' genomes to see whether a metric based on overlap with the pathogen could also explain the extent of growth inhibition of the pathogen. Here, we used a computational cluster-based analysis approach to identify all of the proteins present in each of 50 symbiont strains (the same strains as in the 50 species community used in Chapter 4, see Table S1) and *K. pneumoniae*. Genomic information for the 50 symbiont strains and *K. pneumoniae* was retrieved from the PATRIC database. Next, proteins were clustered by function into groups, or protein global families, called PGFams (Davis et al. 2016).

To establish that the protein family overlap method was appropriate for use in this study, we first checked the distribution of distinct protein global families within the subset of 50 symbiont strains used in the genomic analysis. From the perspective of the strains, the *K. pneumoniae* genome for example contained a total of 5250 annotated protein families (out of a total of 5259 coding sequences). From the perspective of the proteins, we found that any particular protein family is shared by, on average, 2.44 strains (Fig. 4a). Within a protein family, there are, on average, 3.22 proteins, and 141 protein families are shared between all 50 symbiont strains. The distribution of unique protein families among the 50 genomes analysed was plotted (Fig. 4a). The even distribution validates the use of the protein family method, because it means that as symbiont species are systematically added to a community, the number of protein families in the community increases. If the number of protein families unique to a strain was too low, then the increase in the total number of protein families would not increase with symbiont community diversity. We show that as the number of symbiont species increases, the total number of unique protein families increases linearly (Fig. 4b). This holds true whether or not *E. coli* IAI1 is present in the symbiont community.

Once it had been ascertained that the protein family method was appropriate to use to analyse the 50 species, we next sought to model niche overlap between the symbionts and the pathogen based on the number of shared protein families. Ultimately, we wanted to find out whether we could explain the observed variation in colonisation resistance among the tested communities by calculating how many protein families each of the different communities have in common with *K.*

pneumoniae. If protein family overlap can model niche overlap, we predicted we would discover that the communities with the highest protein family overlap with *K. pneumoniae* would provide the greatest colonisation resistance. To do this, protein family percentage overlap between each of the 10 individual symbiont strains and *K. pneumoniae* was first calculated (Fig. 5a). As expected, due to high phylogenetic relatedness, *E. coli* IAI1 has the highest protein family overlap with *K. pneumoniae*, at 64.34%. Moreover, as expected, the total protein family overlap of the 10 best-ranked strains collectively, which include *E. coli* IAI1, was higher than for *E. coli* IAI1 alone, at 67.72% (Fig. 5a). This finding is consistent with our observation that the community of the 10 best-ranked species limits pathogen growth more than *E. coli* IAI1 alone. Next, from the subset of the 10 best-ranked symbiont species, all possible communities containing up to a total of 10 species, including the ones tested *in vitro* (corresponding to Fig. 1c-f, Chapter 4), were assembled *in silico*, and the protein family overlap with *K. pneumoniae* was calculated for each community. Fig. 5b shows these communities, where those that were tested *in vitro* are depicted by filled symbols, which suggests that the experimentally tested communities are a reasonable and representative subset of the *in-silico* communities.

As was seen for carbon source utilisation (Fig. 2c), average protein family overlap between communities and *K. pneumoniae* increased as the number of strains in a community increased from one to 50 strains (Fig. 5c-d). In addition, as expected, protein family overlap was much greater if the community contained *E. coli* IAI1. We next asked how protein family overlap between the pathogen and a community relates to colonisation resistance provided by the community. Here, again as was seen for carbon source utilisation (Fig. 2d), we observe a negative relationship between overlap and *K. pneumoniae* abundance (Fig. 5e-f). This effect is clearest when one plots only *E. coli* IAI1 - containing communities (Fig. 5f), because the presence or absence of *E. coli* IAI1 has a dominant effect on the measure of overlap when plotting all community types (Fig. 5e).

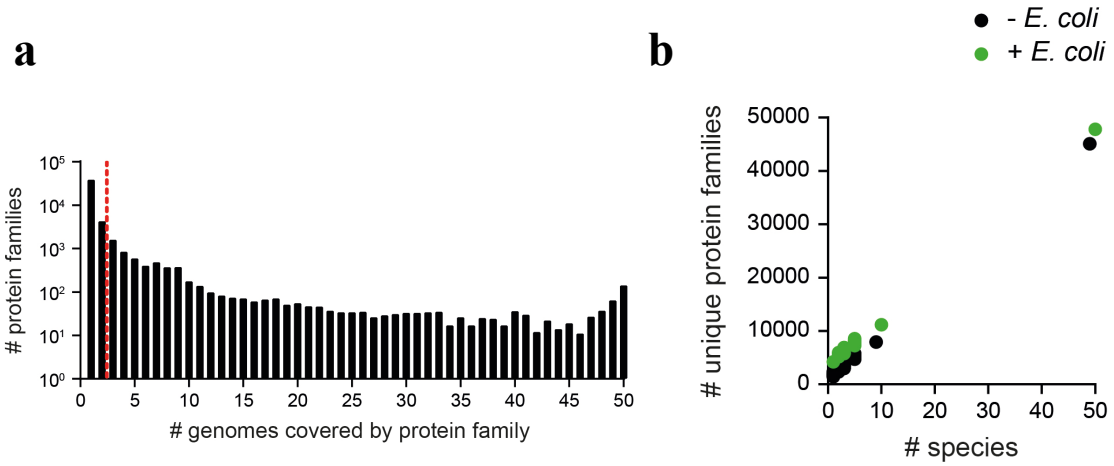


Figure 4. The number of protein families increases with community diversity. (a) Histogram showing how unique protein families are among the 50 species subset used for protein family analysis. The vertical red dashed line represents the mean average number of genomes out of the 50 strains that share a particular protein family (2.44 genomes). There is an average of 3.22 proteins in each PGFam. The histogram shows that many protein families are unique to a strain while others (141) are shared between all 50 strains. (b) The number of protein families covered by a community increases as the number of strains in the community increases. Community IDs taken from Fig. 1d in Chapter 4. Each circle represents a different community. Green circles depict communities containing *E. coli*, while black circles are communities without *E. coli*.

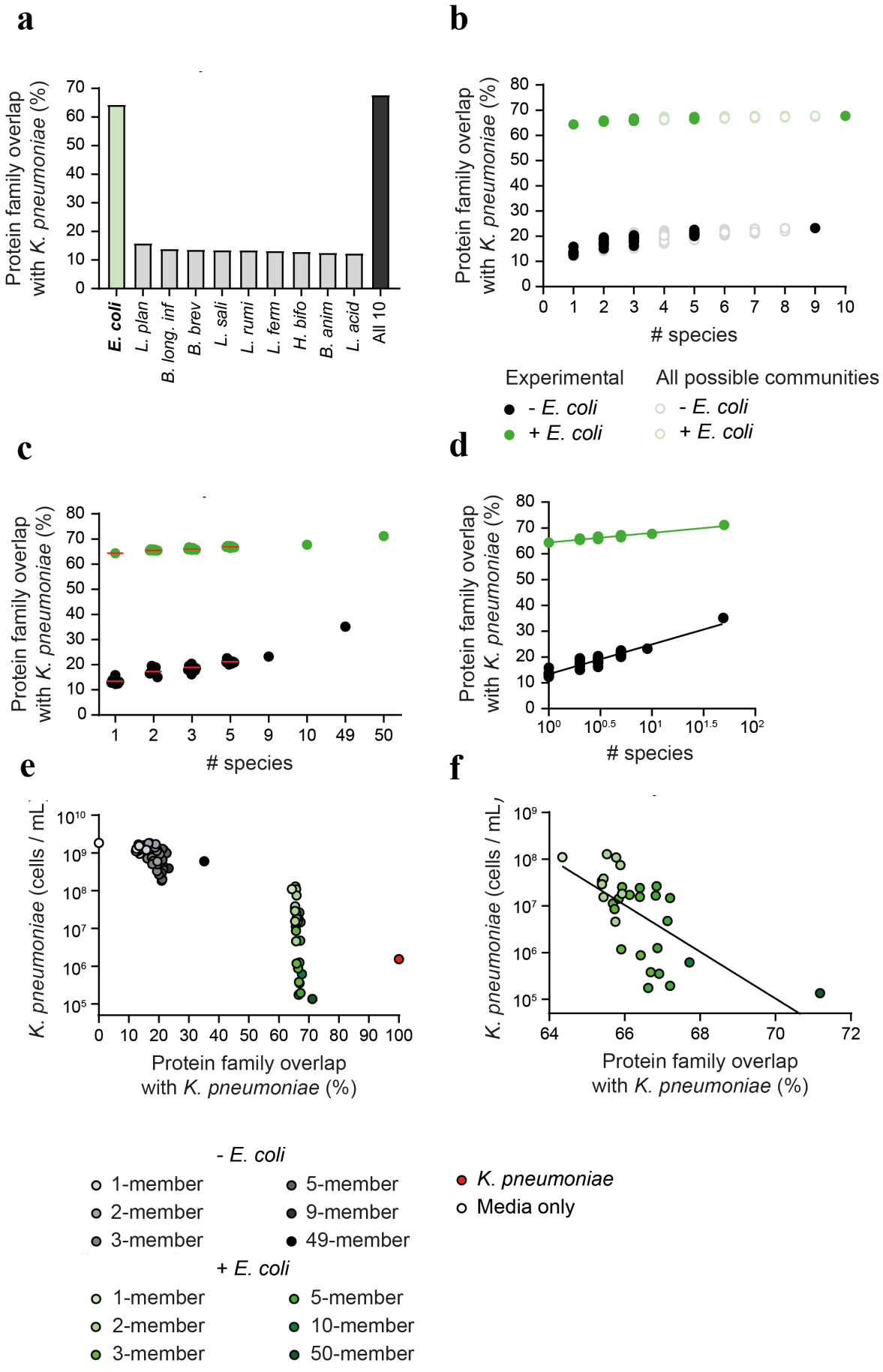

a
Protein family overlap with K. pneumoniae (%)
E. coli
L. plan
B. long. inf
B. brev
L. sali
L. rumi
L. ferm
H. bifo
B. anim
L. acid
All 10
b
Protein family overlap with K. pneumoniae (%)
species
Experimental
- E. coli
+ E. coli
All possible communities
- E. coli
+ E. coli
c
Protein family overlap with K. pneumoniae (%)
species
d
Protein family overlap with K. pneumoniae (%)
species
e
K. pneumoniae (cells / mL)
Protein family overlap with K. pneumoniae (%)
f
K. pneumoniae (cells / mL)
Protein family overlap with K. pneumoniae (%)
- E. coli
1-member
2-member
3-member
5-member
9-member
49-member
+ E. coli
1-member
2-member
3-member
5-member
10-member
50-member
K. pneumoniae
Media only

Figure 5. Protein family overlap between the symbionts and the pathogen explains which communities display the highest colonisation resistance to *K. pneumoniae*. (a) Bar chart showing the protein family overlap with the pathogen for the individual 10 best-ranked species. The bar for *E. coli* IAI1 is shown in green and the other strains in grey. The predicted protein family overlap for all 10 species is shown in dark grey. See Table S1 for species name abbreviations. (b) Experimental communities contain representative protein family overlap to the pathogens compared to all possible combinations of the 10 best-ranked species. All possible combinations of communities are depicted by unfilled circles, experimentally tested communities are shown as filled circles. Communities in green contain *E. coli* IAI1 while communities in black do not contain *E. coli* IAI1. (c) The percentage of protein families overlapping with the pathogens increases as more species are added to a community. Protein family overlap is calculated using an additive approach from protein family overlap of individual strains contained within the community. Communities containing *E. coli* IAI1 are shown in green; communities without *E. coli* IAI1 shown in black. The identities of the communities are the same as in Fig. 1c-f in Chapter 4. A linear regression is performed on log-transformed data in (d). R^2=0.9350, non-zero slope for *E. coli* communities (F test, $p<0.0001$). R^2=0.9182, non-zero slope for communities without *E. coli* (F test, $p<0.0001$). (e) As community cluster overlap with the pathogen increases, the pathogen abundance on Day 2 of the extended competition decreases. Green circles depict communities containing *E. coli*, while black circles represent communities without *E. coli* (data same as in Fig. 1d in Chapter 4). The darker the shade of the symbol, the more diverse the community. The red circles represent the isogenic wild type pathogens. (f) Protein family overlap is compared to the median pathogen abundance values for each community containing *E. coli* from Fig. 1d in Chapter 4. Diversity is visualised by a shade gradient of green circles. A line of best fit is shown from a linear regression on log transformed data: $R^2 = 0.4255$, non-zero slope (F-test, $p<0.0001$).

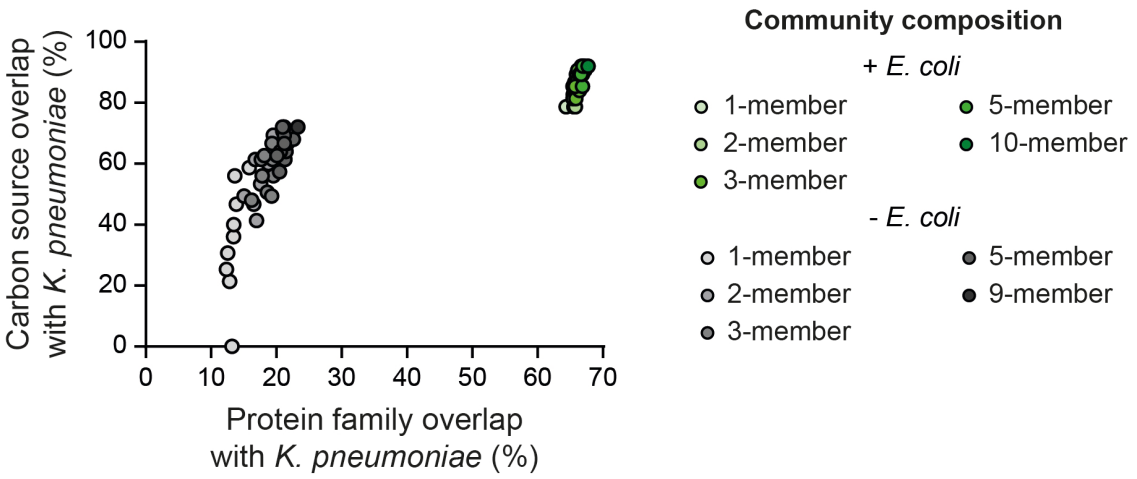


Figure 6. The nutrient use (phenotypic) and protein overlap (genotypic) methods correlate with one another. Correlation between protein cluster percentage. Communities shown in green contain *E. coli* and those in black do not. Gradients of colour intensity show community diversity. R^2=0.6119, slope significantly different than 0 by an F test for communities with *E. coli* ($p<0.0001$). R^2=0.6838, slope significantly different than 0 by an F test for communities without *E. coli* ($p<0.0001$).). The communities are the same as those in Fig. 1c-f, Chapter 4. Percentage overlap calculated as the proportion of shared carbon source use or shared protein families with the pathogen. Values for communities calculated in an additive way based on the profiles of individual strains.

5.3.4 Nutrient blocking can be used to predict colonisation resistance to a novel strain

We find that two overlap measures, one based on carbon source use and the other on protein families, predict the ability of a community to limit growth of the pathogen *K. pneumoniae*. Moreover, these two overlap measures, one phenotypic and one genotypic, themselves are positively correlated (Fig. 6). Along with the evidence that nutrient competition is key to our findings, these observations again suggest the importance of nutrient niche overlap for colonisation resistance in our experiments. That is, only when a community overlaps sufficiently with the nutrient requirements of a pathogen, is it able to block the latter's growth. If correct, this conclusion suggests that one should be able to predict colonisation resistance based on our measures of nutrient niche overlap.

As a first test of this idea, we selected a clinically important and tractable target strain: a pathogenic ampicillin-resistant AMR *E. coli* urine clinical isolate (provided by Nottingham University Hospitals). We sequenced its genome and its carbon source utilisation profile was measured using the same AN Biolog MicroPlates. Carbon source use overlap with 16 symbiont strains (individually

and collectively) was calculated (Fig. 7a). The 16 symbiont strains profiled included the 10 best-ranked strains from the initial screen, as well as the six additional strains (briefly mentioned earlier) that performed well against a parallel screen of another pathogenic Enterobacteriaceae species, *Salmonella enterica* serovar Typhimurium SL1344 (Olivier Cunrath and Erik Bakkeren, unpublished data). As expected, *E. coli* IAI1 had the highest overlap with the AMR *E. coli*. Together, the 16 strains reached nearly 100% overlap with the AMR *E. coli*.

Based on the nutrient use profiles of the 16 single strains, the carbon source use overlap for *in silico* communities at different diversities was predicted (Fig. 7b). To test our ability to predict colonisation resistance of communities, we used the overlap measure to predict the best and the worst performing *E. coli* IAI1-containing communities at each diversity level. We then experimentally tested the colonisation resistance of these communities in our extended competition assay (Fig. 7c). In support of the power of the approach, the predicted 'best' communities performed significantly better at resisting the AMR *E. coli* than the predicted 'worst' communities at all diversity levels tested (two, three, five-strains). However, we noticed that the difference between the 'best' and 'worst' communities at the five-strain level was smaller than at the other diversity levels. Moreover, if *B. breve* was removed from the 'worst' community, the community performed significantly worse than before (Fig. 7d), which is consistent with earlier evidence that it can play an important role in colonisation resistance. Based on this, we reasoned that a limitation of our approach was that we are selecting among 16 strains that all selected for being relatively good at colonisation resistance. We, therefore, sought a different approach where we could select from a larger set of strains.

To do this, we decided to assess whether one can use genetic overlap to predict communities that can resist AMR *E. coli* growth. This immediately gave us more strains to work with in our predictions because the genomes of all of our 50 focal species are sequenced. Communities formed from the 50 strains were assembled *in silico*, therefore, and their protein overlap with the AMR *E. coli* calculated (Fig. 8a-b). The protein family overlap with AMR *E. coli* ranged from 80.70% for *E. coli* IAI1, to 83.46% for the 50 species community. From the communities containing *E. coli* IAI1, the best and worst communities were again predicted at each diversity level. That is, the communities with the predicted highest and lowest percentage overlap with the pathogen were identified. In some cases, there were multiple *E. coli* IAI1-containing communities at the same diversity level with the highest or lowest overlap. In these instances, the best or worst community was chosen from the multiple options at random. These best and worst predicted communities

were tested experimentally in the extended competition assay (Fig. 8c). As for carbon source utilisation, we see that the predicted best community performed significantly better than the predicted worst community at all levels of diversity, supporting the use of genomes to predict resistant communities. Moreover, at the five-strain level we collected more data and tested the five best and the five worst predicted *E. coli* IAI1-containing communities in the extended competition assay (Fig. 8d). Here, the best predicted communities inhibited AMR *E. coli* growth 100-fold more on average than the worst predicted communities. This result suggests that nutrient blocking is a useful principle with which to identify colonisation resistant communities.

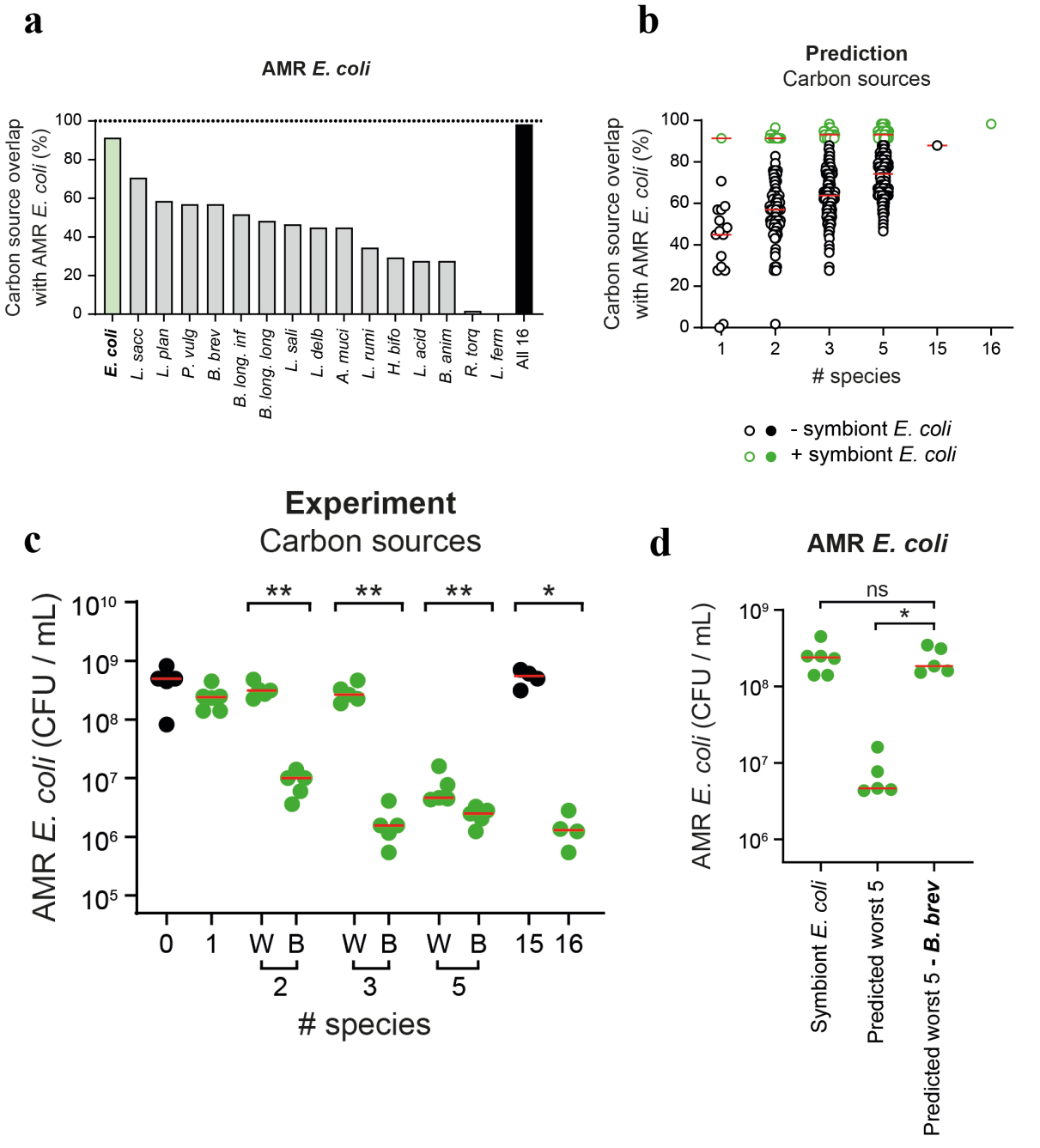


Figure 7. Nutrient use overlap can be used to predict which communities will provide the most and least colonisation resistance to a pathogenic AMR *E. coli* strain. (a) Bar chart showing carbon source utilisation overlap (%) of the 16 best ranked individual strains with the AMR *E. coli* strain. The *E. coli* symbiont is shown in green and the other individual strains in grey. All 16 symbiont strains together are shown in black. The percentage overlap with the pathogen is calculated as the proportion of the number of nutrients that can be used by AMR *E. coli* that can also be used by a particular symbiont strain. (b) *In silico* prediction of carbon source overlap with the AMR *E. coli* strain for all possible combinations of symbiont communities at the indicated diversity levels. Each circle represents a different community. Communities containing the symbiont *E. coli* IAI1 are shown in green and communities without *E. coli* IAI1 are shown in black (predictions as hollow circles; experimental data as solid circles). Predicted carbon source overlap calculated using an additive approach from carbon source use of individual strains measured using AN Biolog MicroPlates. (c) Experimental test of *in silico* predictions in (b). The two *E. coli* IAI1-containing communities predicted to have the best (B) and worst (W) carbon source overlap were picked at each diversity level and competed against AMR *E. coli* in the extended competition assay. A two-tailed Mann-Whitney U test was performed on community pairs ($p>0.05$=ns; $p<0.05$=*; $p<0.01$=**) at the two-, three- and five-strain diversity levels. Red horizontal bars depict the median of each community tested. n=4-5 replicates for each community. (d) AMR *E. coli* density measured by selective plating on Day 2 of the extended competition assay. AMR *E. coli* competed against the predicted worst 5-member community in (c) and against the equivalent drop-out community that is missing *B. breve*. Horizontal red lines show the median of the replicates. n=5-6 replicates for each community. See Table S1 for species name abbreviations.

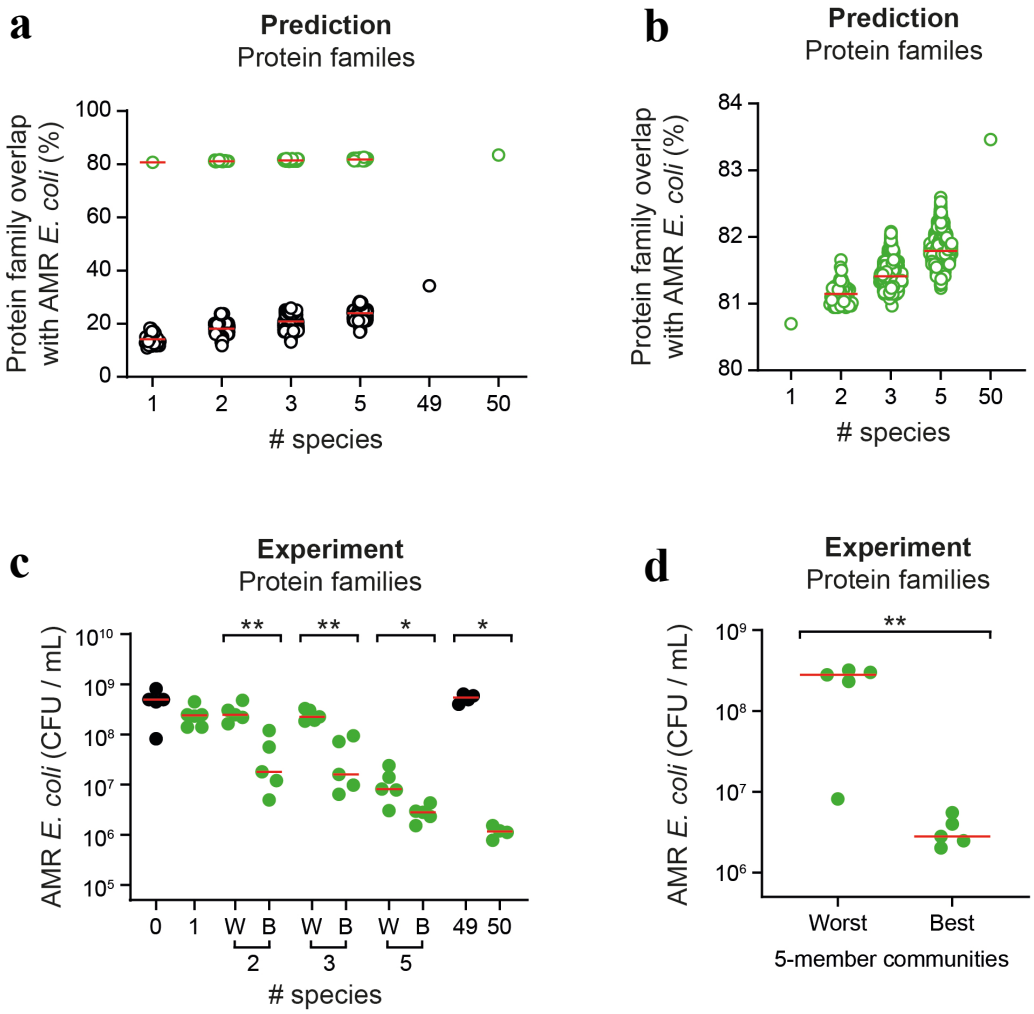


Figure 8. Protein overlap can be used to predict which communities will provide the most and least colonisation resistance to a pathogenic AMR *E. coli* strain. (a) *In silico* prediction of protein family overlap with the AMR *E. coli* strain for a random subset (n=59,043) of all possible symbiont communities at diversity levels two-, three-, and five-strains, as well as all individual strains and the 49- and 50-species communities. Each circle represents a different community. Communities are selected from the strains comprising the 50-member community. Communities containing *E. coli* IAI1 are shown in green and communities without *E. coli* IAI1 are shown in black. (b) Only the *E. coli*-containing communities are plotted to better visualise variation in protein family overlap. (c) Experimental test of *in silico* predictions based on protein cluster overlap in (a-b). The two *E. coli* IAI1-containing communities predicted to have the best (B) and worst (W) protein family overlap were picked at each diversity level (randomly selected, for cases where there were multiple communities with the same overlap) and competed against AMR *E. coli* in the extended competition assay. Red horizontal bars depict the median of each community tested. N=5 replicates for each community. A two-tailed Mann-Whitney test was performed on community pairs (p>0.05=ns; p<0.05=*; p<0.01=**) at the two-, three- and five-strain diversity levels. (d) Experimental test of the predicted five best and five worst communities at the five-strain diversity level, based on protein family overlap with AMR *E. coli*. Each symbol represents the median of n=5 replicates per community. Red horizontal bars depict the median of the best and the worst predicted communities. A two-tailed Mann-Whitney test was performed (p<0.01=**). Community identities for (c-d) are shown in Table S7.

5.4 Discussion

There are multiple potential routes by which symbiotic bacteria can generate colonisation resistance, but there is currently no consensus on which of these mechanisms predominates in the mammalian gut. Here we sought to understand the cause of colonisation resistance in communities of human gut bacteria by first seeking to find evidence for contact-dependent antagonism by growing *K. pneumoniae* in cell-free spent media. We found the spent media was able to inhibit growth of the pathogen, ruling out contact-dependent inhibition as a primary source of colonisation resistance (Fig. 1). Next, we profiled the phenotypic carbon use profiles of the symbiont species and *K. pneumoniae* using Biolog MicroPlates. Calculating the shared carbon sources between the symbiont communities and *K. pneumoniae* revealed that the most resistant communities had the greatest nutrient use overlap with the pathogen (Fig. 2). Moreover, supplementation of the communities with a nutrient private to *K. pneumoniae* abolished colonisation resistance, confirming the central role of nutrients in colonisation resistance (Fig. 3). To colonise the gut, it appears that a nutrient niche must be present for the pathogen (Pereira and Berry 2017). Then, we wanted to find out if we could also use a genomic approach to model niche overlap. The species' genomes were used to calculate protein family overlap between the pathogen and symbionts (Fig. 5) and found that, like when using the carbon sources, the higher the overlap, the greater the colonisation resistance of a community. Our results were consistent with our nutrient blocking hypothesis: that communities block pathogen colonisation by collectively consuming the pathogen's nutrients. We were able to use the nutrient blocking principle to successfully predict which combinations of gut strains would be able to resist growth of another pathogen, an antimicrobial resistant clinical *E. coli* strain. Moreover, these predictions could be made either by using nutrient use profiles (Fig. 7) or genomic information (Fig. 8) from the symbiont strains and the pathogen. Our results have potential for the goal of making probiotic communities, from first principles, that could protect hosts from pathogen colonisation and subsequent infection.

It is important to note that Biolog AN MicroPlates have certain limitations. They only contain 95 different carbon sources, and while these are designed to be representative of anaerobic carbon sources (see biolog.com), they are unlikely to contain the full range of carbon sources present in the nutrient rich mGAM media or in the mammalian gut. However, our aim is to use the Biolog plates in order to obtain a general measure of niche overlap between the symbionts and pathogens. We are not using the Biolog plates to identify which specific nutrients the symbionts and pathogens are competing over in media or in the gut. Furthermore, we have shown that the Biolog overlap calculation is sufficient to explain our results in the extended competition assay (see Fig. 2d) and

make predictions for the AMR *E. coli* strain (see Fig. 7c). However, one cannot usefully make predictions for higher diversity communities (10 strain communities) based on the Biolog MicroPlates, because there are only 95 carbon sources per MicroPlate. Only having 95 carbon sources per MicroPlate means that higher diversity communities reach similarly high carbon source use overlaps with the pathogen, and it is difficult to differentiate them. As such, the genomic prediction method allows more subtle differentiations to be made between communities and going forward, it is arguably the superior method.

Crucially, the data presented in this Chapter do not rule out the potential existence of other mechanisms of colonisation resistance, such as toxin production. The spent media experiments point against the existence of contact-dependent mechanisms of interference competition, because we observed that the cell-free spent media was still able to inhibit growth of *K. pneumoniae*. The nutrient supplementation experiment demonstrates that colonisation resistance can be overcome with supplementation of a private nutrient, suggesting that nutrient competition is the main mechanism at play in our experiments. We find that nutrient blocking is sufficient to explain our results (see Fig. 2d), but it is possible that alternate mechanisms also exist. For example, we sometimes find communities that perform better than expected based on the nutrient use or protein family overlap methods. The original 'worst' predicted five-strain community (Fig. 8c) resists AMR *E. coli* growth more strongly than the four other 'worst' predicted five-strain communities (Fig. 8d). It is possible that some additional underlying mechanism of colonisation resistance such as interference competition plays a role here, allowing the five-strain community to perform better than predicted (for community compositions, see Table S7). In addition, it was found that communities containing *B. breve* performed better than predicted by the Biolog MicroPlates (see *B. breve* dropout experiments, Fig. 7d). Here, it could simply be that there are nutrients present in the media or in the gut that are not represented on the Biolog MicroPlates, and *B. breve* can use some of these nutrients, or it is possible that there is an additional mechanism, such as interference competition, at play. Either way, finding some communities perform better than expected is not a bad thing, indeed, it is preferable to finding communities that perform worse than expected.

The work presented in this Chapter reveals that nutrient blocking plays a central role in colonisation resistance of gut communities. This finding aligns with results from recently published papers that also find nutrient competition is key to pathogen protection in the gut microbiome (Oliveira et al. 2020; Osbelt et al. 2021; Pereira et al. 2020). We also demonstrate two routes, the

first based on phenotype and the second based on genomes, for making predictions about which community combinations will resist a target pathogen. The rational design of potentially probiotic communities will be vastly important for microbiome therapeutics approaches and is largely missing from the commercial probiotics industry. However, this may be beginning to change. A microbiome therapeutics company, Seres Therapeutics, has recently patented an approach for designing communities to prevent or treat *C. difficile* infection based on metabolism of common resources in the gut (see in particular US20220249578A1, publication date August 2022), but this has not been published in the scientific literature and the community compositions and methods of design are undisclosed. Their first product, Vowst, is a prescription medicine approved in the United States in April 2023 to prevent the recurrence of *C. difficile* infection (Jain et al. 2023). This suggests that the role of nutrient competition in colonisation resistance is starting to gain traction in translational microbiome research.

5.5 Materials and Methods

Bacterial strains and plasmids

A full list of bacterial strains used in this study is provided in Table S1. The plasmids used in this study are listed in Table S3. *Klebsiella pneumoniae* subsp. *pneumoniae* purchased from DSMZ (stock number 30104) was used in all experiments containing *K. pneumoniae*. Symbiont strains were chosen based on those commonly isolated from the human gut microbiota. Strains were provided by Nassos Typas (EMBL Heidelberg, Germany), or were ordered from the German Collection of Microorganisms, DSMZ. The *Lactobacillus plantarum* strain was provided by the Department of Food and Nutritional Sciences, University of Reading. The ampicillin-resistant AMR *E. coli* strain is a urine clinical isolate provided by the Pathogen Bank at Nottingham University Hospitals NHS Trust.

Bacterial growth conditions

For engineering of *E. coli* or *K. pneumoniae*, strains were grown aerobically in Lysogeny broth (LB) with the appropriate antibiotics (Table S1) at 37°C, shaking at 220 rpm. All symbionts were cultured under anaerobic conditions (5% H_2, 5% CO_2, 90% N_2, <20ppm O_2) in modified Gifu Anaerobic Medium (mGAM; Nissui Pharmaceuticals) broth buffered to pH 6.2 with 100mM 2-(N-morpholino)ethanesulfonic acid (MES). The redox indicator dye Resazurin (100µg/L media) was added as a quality control check for the presence of oxygen (turns red when conditions are not sufficiently anaerobic). To prepare glycerol stocks, individual strains were first streaked onto mGAM agar and grown under anaerobic conditions (if possible, as not all strains can grow as single colonies on agar-based media). The identity of each strain was confirmed using 16S rRNA sequencing (Sanger sequencing; Source Biosciences) using the universal primers 27F and 1492R for most species, or g-Bifid-F and g-Bifid-R for Bifidobacteria (Table S4). Single colonies were then inoculated in mGAM broth and stored at -70 degrees Celsius in mGAM with a final concentration of 25% glycerol.

Genetic engineering of bacterial strains

The fluorescence plasmid (Cunrath and Bumann 2019) was transformed into *K. pneumoniae* using electroporation. Briefly, 5mL overnight culture was washed 3x with cold milliQ water, before being concentrated in 500µl cold milliQ water. 2µl of plasmid was mixed with 50µl of concentrated cells and electroporated (1.8kV; 0.1cm gap cuvettes) before recovery in 1ml pre-warmed LB (1h at 37°C, shaking at 220rpm) and plating on LB with the appropriate antibiotics.

Gene deletions were generated as described in (Cianfanelli, Cunrath, and Bumann 2020). Briefly, 700 base pairs upstream and downstream of region to be deleted were PCR amplified (Phusion, NEB) and inserted into the suicide vector pFOK, which was linearised using the restriction enzymes BamHI and EcoRI, using the NEBuilder HiFi DNA Assembly (NEB). The plasmid was introduced into a diaminopimelic acid auxotroph *E. coli* strain (JKe201). After 6h of mating between the plasmid-containing donor *E. coli strain* and the recipient *E. coli* strain, trans-conjugants were selected on LB plates containing 50μg/mL kanamycin. Counter-selection was performed on no-salt LB plates supplemented with 0.5μg/mL of anhydrous tetracycline and 20% of sucrose at 30 degrees Celsius. Mutants were screened by colony PCR and the sequence was verified using Sanger sequencing (Eurofins). Primers used for genetic engineering are listed in Table S4.

Extended competition assay

Symbiont strains were grown to stationary phase anaerobically (12-72 hours, depending on the species), in Hungate tubes containing 5mL mGAM broth (HyServe-05433) and 100mM MES (Sigma Aldrich) and buffered to pH 6.2. (225rpm, 37 degrees). *K. pneumoniae* carrying the fluorescence plasmid pBC11 (YPet)(Cunrath and Bumann 2019) was incubated overnight under the same conditions, with the appropriate antibiotics (Table S1).

Once in stationary phase, monocultures of symbionts were passaged (100μL culture into a new 5mL tube of media) and grown for ~17 hours. Communities were assembled under anaerobic conditions into new 5mL Hungate tubes (see section "community preparation") and grown for 24 hours. Once grown, communities were invaded with 100μl of the pathogen (10^6 cells/mL final concentration) in each 5mL Hungate tube. Samples were taken immediately after pathogen invasion and prepared for measurement using flow cytometry (Day 0). Invaded communities were incubated in a shaking incubator (37 degrees Celsius, 225rpm). After 24 hours, the invaded communities were sampled for flow cytometry (Day 1) and 100μL was passaged into new 5mL tubes of mGAM broth. After a further 24 hours, the end-point communities were sampled and measured a final time (Day 2).

For nutrient supplementation experiments (galactitol), 2.5mL mGAM buffered with 100mM MES to pH 6.2 was prepared and autoclaved in hungate tubes. A 2x stock solution of filter-sterilized sugar in miliQ water (e.g. 0.2% or 2% galactitol) was prepared and de-oxygenated in the anaerobic chamber. 2.5mL of the stock solution was added into the hungate tube to generate a 5ml hungate tube with the appropriate concentration of the sugar. The extended competition experiment is performed as described above, except samples were passaged again into tubes with the appropriate

concentration of the sugar. Samples were left to grow for 48h instead of the standard 24h to allow utilisation of low priority sugars, such as galactitol.

For experiments with the AMR *E. coli* clinical isolate, the experiment was performed as described above, except samples were analysed using selective plating instead of flow cytometry (LB + ampicillin to select for the AMR *E. coli* strain; MacConkey agar to enumerate total *E. coli* densities).

Community preparation

Constituent monocultures were grown to stationary phase, passaged into new media and grown overnight for approximately ~17 hours, and then combined into communities. The OD-600 of the single strains was measured and the cultures were streaked anaerobically on mGAM agar to check for contamination. Communities were assembled under anaerobic conditions.

In vitro: For the 10-strain community, equal volumes (100μL) of each overnight were combined in a Hungate tube containing 5mL mGAM to form a community. Communities were grown in the shaking incubator (37 degrees, 225rpm) for 24 hours before being invaded with 10^6 cells/mL of the pathogen.

Flow cytometry

Hungate tubes containing culture to be sampled were de-pressurised under anaerobic conditions using needles. Samples were removed using needles and syringes. 10μL of each sample was diluted in 90μL PBS + chloramphenicol 200μg/ml then 10μL added to a 96-well flat-bottomed plate already containing 80μL PBS + chloramphenicol 200μg/ml. The 96-well plate was left to shake at room temperature on the bench for 15 minutes to allow oxygen-dependent folding of YPet, while preventing further growth of the sample with the bacteriostatic antibiotic chloramphenicol. Next, all bacterial cells were fixed, permeabilised and fluorescently stained by adding 90μL PBS containing 4% paraformaldehyde, 0.4% Triton X-100 and 1μg/mL 4',6-diamidino-2-phenylindole (DAPI) to each sample well and incubating the plate in the dark for 1 hour at room temperature on a microplate shaker. Prior to the measurement, 20μL AccuCheck counting beads (ThermoFisher- PBC100) was added to every sample well. Two wells containing 200μL PBS were left between sample wells, in order to prevent cross-contamination between samples. 96-well plates were run in a flow cytometer set to: acquisition volume 50μL, total draw volume 80μl, total sample volume 200μL, at a speed of 100mL/minute. Relevant spectral parameters were recorded in a flow cytometer (Attune NxT Autosampler) equipped with 405nm, 488nm and 561nm lasers (ThermoFisher). The following channels were used: DAPI staining, excitation 405nm, emission

415-465nm ('blue'); YPet fluorescence, excitation 488nm, emission 505-515nm and 525-555nm ('green').

Flow cytometry data was processed using FlowJo v10.8.1 software. 'Beads' were gated on a linear (FSC-H; SSC-H) axis. 'Bacteria' were gated on a logarithmic (FSC-H; SSC-H) axis. DAPI was gated within the 'Bacteria' gate, on a logarithmic (Ex405-417; Ex405-495) axis. Within the DAPI gate, YPet was gated on a logarithmic (Ex488-503; Ex488-555) axis. Count statistics for beads, DAPI and YPet were exported to Microsoft Excel and pathogen density (cells/mL) was calculated.

Spent media assay

Strains were anaerobically inoculated, grown, passaged and assembled into communities as described above. Communities were grown anaerobically in the shaking incubator (225rpm, 37 degrees) for 96 hours to maximize depletion of nutrients utilisable by the community. Supernatants were prepared by centrifuging the 96-hour cultures (10 minutes, 4400rpm, room temperature) and filter-sterilising the supernatant (0.2μm filter). All preparation of supernatants was done under anaerobic conditions. Two of each of the communities were assembled so that, for each community, one Hungate tube containing 5mL supernatant and another Hungate tube containing 2.5mL supernatant and 2.5mL mGAM (the re-supplemented treatment) were prepared. The supernatants were invaded with 10^6 cells/mL of fluorescent pathogen, sampled and incubated for 24 hours as before. Samples were taken on Days 0 and 1.

Nutrient utilisation overlap using biolog assays

Utilisation of carbon sources by symbionts and the pathogens were assessed using Biolog AN MicroPlates™ according to the protocol of the manufacturer. Briefly, strains were grown in mGAM and passaged (as detailed above). The cultures were centrifuged anaerobically and washed twice in anaerobic PBS. The samples were concentrated and an aliquot was taken to measure the OD600. The cells were diluted or concentrated such that a 200μl aliquot of the cells would correspond to 65% transmittance (OD 0.187; the density outlined by the manufacturer) in the 14ml volume of AN inoculating fluid provided. The concentrated cells were added to the inoculating fluid aerobically (a small amount of oxygen is needed to oxidise the buffer) and 100μl was aliquoted into each well of the MicroPlate. After 10min in aerobic conditions, the plates were put in an air-tight container with a GasPak EZ Container System Sachet to generate hydrogen-free anaerobic conditions. Samples were incubated at 35°C for 24h before measurement at 590nm.

For each plate, the absorbance reading at 590nm was subtracted from the blank (no carbon source control in well A1). Each strain generates a different background signal so it is important to do this on each plate individually. Each strain was measured as three independent biological replicates and the median absorbance value was taken for each carbon source. We used a thresholding approach to determine if a strain can metabolise a given carbon source (defined as Abs590nm >0.1 after median, after blank subtraction; Fig. 2).

To predict overlap with the pathogens, whether a given strain can use a carbon source was compared to the pathogen. We assessed which percentage of carbon sources that the pathogen can use can also be used by the symbiont. To calculate overlap between pathogens and communities, we assumed used an additive calculation approach where if a strain is contained in a community that can use a carbon source, the entire community can use the carbon source. For simplicity, we did not treat cases where multiple species use the same nutrients within the community differently than if a given nutrient is only covered by one species.

Genomic analysis using protein overlap

Genomic information from 50 symbiont strains and *K. pneumoniae* were retrieved from the PATRIC database. On this set, we applied a cluster-based analysis that groups proteins encoded in genomes into PATRIC global protein families. A majority of symbiont strain proteins obtained a protein family designation (clustering rate of 97.83%; 172 848 of 176 675) with protein families being populated by proteins from on average 2.44 genomes (Fig. 4).

Based on this set, we drew protein family designations for focal symbiont communities and calculated pathogen/community overlap using the same approach as for the Biolog plates above. That is, for each protein family encoded in the pathogen's genome, we checked if it overlapped with any protein families encoded in the community.

Whole-genome sequencing

An overnight culture of *E. coli* 19Y000018 (the AMR clinical urine isolate) was prepared in LB containing the appropriate antibiotics. A 1ml pellet was taken and DNA was extracted using the same ethanol precipitation and AMPure clean-up protocol used in DNA isolation from faeces for metagenomics (see Chapter 4, Materials and Methods).

Source Biosciences performed whole-genome Illumina sequencing on a NovaSeq 600 to generate 10M 150bp paired end reads.

Predictions based on biologs and PGFams

Biolog-based predictions: The carbon source utilisation profile of the AMR *E. coli* clinical isolate was assessed using Biolog AN MicroPlates™ as detailed above.

Next, all possible communities made of one, two, three, and five species were identified from the 16 symbiont strains that were previously analysed for carbon source utilisation. For each community, the carbon source utilisation overlap was calculated (as detailed above; Fig. 7b). At each diversity level, communities were sorted by overlap to the AMR *E. coli* clinical isolate. Given that the symbiont *E. coli* is needed for colonisation resistance in our experiments, we only included communities where the symbiont *E. coli* is present. At each diversity level, we chose the highest ranked community (defined "predicted best") and lowest ranked community (defined "predicted worst"). If there were ties in rank, one community was randomly chosen. These communities were experimentally assessed for colonisation resistance using the extended competition *in vitro* assay as detailed above.

PGFam-based predictions: We used the whole-genome sequence of the AMR *E. coli* isolate to calculate PGFam overlap to communities of symbionts drawn from our 50-species community. As for the biolog-based predictions, we restricted the analysis to communities that contained the symbiont *E. coli* strain. Specifically, we generated 100,000 different communities randomly, each containing the symbiont *E. coli* and a total of two, three, five, or 10 species from the 50 species pool. We ranked the communities according to their pathogen overlap at each diversity level and selected the highest and lowest ranked communities for experimental validation. If ties occurred, we chose the communities at random, as for the biolog-based predictions.

Statistical analysis

All graphs were made and statistical analysis carried out in Prism v9.4.1. Protein family overlap analyses and protein family-based predictions were computed in R version v4.0.5. Figure legends indicate the statistical test used and the sample sizes.

6. Conclusion

My thesis explores one of the key benefits of the gut microbiome to the host, colonisation resistance, or the ability of the resident microbes in the gut to protect against incoming species of bacteria. Colonisation resistance provides the host with a degree of natural protection against harmful, pathogenic bacteria such as the species *Klebsiella pneumoniae*, which I have focused on in my DPhil, but also *Salmonella enterica* serovar Typhimurium, *Escherichia coli* and *Clostridium difficile*. It is well known that, when the natural microbial residents of the gut are eliminated, for instance due to antibiotic treatment or by the creation of germ-free lines of mice, the host becomes much more susceptible to infectious disease (de Nies, Kobras, and Stracy 2023; Stecher et al. 2005). However, while the importance of colonisation resistance has been recognised for decades, we have lacked an understanding of why some microbial communities are more resistant to pathogens than others. Specifically, we previously had no knowledge of the general principles that determine whether a community confers pathogen-protection, or understanding of where these principles came from. Multiple mechanisms of colonisation resistance have previously been identified, but are often studied one at a time and with limited ecological context (Buffie et al. 2015; Kim et al. 2019; Jacobson et al. 2018; Pereira et al. 2020; Oliveira et al. 2020; Osbelt et al. 2021; Sequeira et al. 2020; Byndloss et al. 2017). Alternatively, the beneficial effects of diversity have been studied but with no investigation of the mechanism (Heiman and Greenway 2016; Lozupone et al. 2012). I believe it is vital that we identify and understand general ecological principles of colonisation resistance if we are to achieve the ultimate goal of rationally engineering human gut communities to resist infection.

To this end, in Chapter 3, I developed a screen of 100 human gut symbiont strains for their individual ability to resist the growth of *K. pneumoniae*, and found that, although single strains were poor inhibitors of pathogen growth both *in vitro* and in gnotobiotic mice, when combined they can have an effect on suppressing pathogen growth. I explored this striking community effect in Chapter 4. By systematically changing the composition and diversity of communities of human gut microbes, I uncovered two ecological principles of colonisation resistance. Firstly, ecological diversity is in general an important factor that promotes colonisation resistance. Secondly, some species contribute much more to colonisation resistance against a given pathogen than others.

These principles hold true *in vivo* as well as *in vitro*. Importantly, a community needs both diversity and a key member to achieve the greatest colonisation resistance potential. Moreover, I have been able to identify the primary mechanism, nutrient blocking, that underlies these principles. In Chapter 5, I found that the greater the degree of nutrient-use overlap between a gut community and the pathogen, the greater the colonisation resistance of the community. The nutrient blocking ability of a community can be assessed with a phenotypic assay measuring the nutrient use of individual species, or by calculating protein family overlap *in silico* using a genomic approach. Moreover, a parallel set of experiments performed by other lab members, found these patterns hold true for a second pathogen, *Salmonella enterica* Typhimurium, suggesting they are general across pathogen species. Furthermore, I have presented experimentally validated predictions on which combinations of gut species will be most protective against another pathogen, a clinical *E. coli* isolate. This work takes us one step closer to the aim of manipulating the gut microbiome to protect against pathogens.

The importance of diversity in ecology

My work shows that, by depleting available nutrients in the gut, specifically, those that overlap with the metabolic requirements of a pathogen, species-rich communities containing a key competitor can suppress pathogen growth. In doing so, it provides strong experimental evidence for the nutrient niche hypothesis in the gut, as developed by the microbial ecologist Rolf Freter in 1983. Freter's theory postulates that competition for available niches in the environment determines whether an exogenous species can establish. While often difficult to define in practice, a niche is often conceptualised as a multidimensional space encapsulating all environmental factors that impact species survival (Ashby et al. 2017). In the gut, these factors include the environmental gradients discussed in the Introduction, such as pH, oxygen and antimicrobial peptides, as well as nutrients. The findings in Chapter 5 suggest that it is the nutrient landscape of the gut in particular that plays a critical role in dictating competition and carving out niches (Pereira and Berry 2017; Reese et al. 2018). My work suggests that the simple definition of a niche in the gut for a microbe is the ability to use at least one, unique nutrient, that has not been appropriated by another microbial strain.

My work underlines the importance of species diversity for gut functioning and good health. This mirrors a wide range of studies in ecology showing that species diversity is important for ecosystems (Tilman 2014; Weisser 2017). Many of these studies on diversity-ecosystem functioning relationships focus on plant communities, where diversity is thought to promote

overall productivity (Jochum et al. 2020). In addition, diversity has been shown to produce decreased susceptibility to invasion by exotic species (Jochum et al. 2020; Kennedy et al. 2002). Using small experimental grassland plots in Minnesota, it was demonstrated that, compared with plots containing single grassland species, in the most species-rich plots (24 grassland species) the area covered by invading plants decreased by 94% (Kennedy et al. 2002). It was suggested that the reduced invasion was due to biotic factors, namely increased density and crowding in the more species-diverse plots. The finding that more diverse grassland communities exhibit reduced species invasion is analogous to my finding that pathogen growth is reduced in diverse gut communities, suggesting that the underlying ecological principles are similar between plant and microbial ecosystems.

There are also studies looking at the impacts of diversity on microbial communities. For instance, high diversity has often been linked with greater community stability (McCann 2000). Importantly, stability is complex to define and often refers to the ability of a community to remain unchanged over time, which can relate to either community composition or function. A recent study on soil microbes found that higher diversity can stabilise ecosystem functions such as litter decomposition and plant biomass production over time, due to different taxa promoting different functions at different times (Wagg et al. 2021). Despite finding that diversity gives rise to stability, some studies have highlighted that increased stability is not directly caused by high diversity (Ratzke, Barrere, and Gore 2020). However, it is important to note that not all studies find a positive correlation between diversity and stability (Yonatan et al. 2022; Glasl et al. 2018). For example, a recent study that tracked the stability of a range of sponge-associated microbial communities that were subjected to natural levels of salinity disturbance, found that compositional stability was unaffected by diversity (Glasl et al. 2018). Invasion into microbial ecosystems as a function of microbial diversity has also been studied. Experiments on naturally occurring microbial ecosystems obtained from puddles at the roots of trees found that productivity is a key factor underlying invasion resistance in these communities. High productivity is linked to depletion of resources and the occupation of physical space, which are functions of diversity, and, in general, more diverse communities are found to be more productive (M.L. Jones et al. 2021; Bell et al. 2005). These results from natural microbial communities show the importance of diversity for resisting invasion.

In my thesis, I have found that diversity correlates with the ability of a microbial community to resist pathogens and identified nutrient blocking as the underlying explanation. In the context of human health, a diverse microbiome is considered healthy, but mechanistic links between

microbial diversity and host health have not, until now, been demonstrated (Manor et al. 2020). Species composition (type of species) and richness (number of species) are variables which are often confounded in studies on biodiversity (Bell et al. 2005). Diversity may be important for ecosystem functioning because diverse communities are statistically more likely to contain key member species, or because diversity itself plays a role. By independently manipulating species composition at similar levels of diversity in the dropout experiments in Chapter 4, I have managed to separate out the key contributions of species composition and species richness to the colonisation resistance ability of a community. I illustrated the importance of composition by showing that a diverse community of 50 gut species provides much greater colonisation resistance than its otherwise identical 49-species counterpart that lacks *E. coli* (see Chapter 4, Fig. 1d and Fig. 6a). I also demonstrated the role of species richness by showing that the same diverse community of 50 gut species is much more resistant to colonisation than the key competitor strain *E. coli* when it is alone (see Chapter 4, Fig. 1d and Fig. 6a).

From community ecology to new treatments for disease

In light of the antimicrobial resistance crisis, innovative alternatives to antimicrobials are needed. My study species *K. pneumoniae* is one of the top three pathogens on the WHO's priority pathogens list for research and development of new antibiotics, because it is a major cause of mortality for immunocompromised patients in healthcare settings, and strains have developed resistance to last resort antibiotics such as carbapenems (Karampatakis, Tsergouli, and Behzadi 2023). Increasing the colonisation resistance of the gut microbiota is one such alternative approach that has the potential to reduce the need to use antimicrobials, thereby helping to slow the spread and reduce the burden of antimicrobial resistance. In addition, a possible, but still theoretical, advantage of probiotics is that, unlike antibiotics, they are living organisms that can evolve in response to pathogen evolution of resistance, which would circumvent the problem of resistance (King et al. 2016). Broadly speaking, there are two routes by which one might use living bacteria to reduce disease burdens, either prophylactically or as a treatment for an existing disease. My work is clearly most relevant for the former, where one might hope to prevent initial colonisation by pathogens as a prophylactic strategy. While we are clearly some way from real medical interventions, such a strategy might have value in the clinic. One scenario would be the use of a microbiome prophylactic to prevent *K. pneumoniae* colonisation and subsequent infection for immunocompromised patients upon hospital admission. Antimicrobial resistant strains of *K. pneumoniae* are prevalent in hospitals and colonisation risk is much higher than in a community setting (Gorrie et al. 2018; Gorrie et al. 2022).

An important question for such strategies is what level of pathogen is acceptable to achieve sufficient protection from infection in the clinic. In my experiments I did not observe complete absence of *K. pneumoniae* from any community. Rather, we managed to prevent the pathogen's growth. It is likely that this result is, to some extent, dependent on the initial dose of the pathogen. If the dose were lower, elimination of *K. pneumoniae* would more likely be achieved. Varying pathogen load is, therefore, another avenue for future research. However, total elimination of the pathogen from the gut may not be necessary as it could be that controlling pathogen abundance to a low level is enough to lower the risk of infection. Moreover, the host immune system may be able to clear the pathogen if it is brought to a low enough density by the microbiota (Slack and Diard 2022).

However, even if a prophylactic treatment were fully effective at preventing colonisation, some individuals will already be colonised with *K. pneumoniae* and face an increased risk of infection. More generally, there are many other situations where there is a need to treat an existing infection such that a prophylactic strategy is not suitable. To focus again on *K. pneumoniae*, a therapeutic treatment that clears *K. pneumoniae* from the gastrointestinal tract is a desirable prospect. Such a treatment would be particularly useful for immunocompromised individuals, for example those on courses of chemotherapy, or patients undergoing surgery or on ventilators in intensive care, as these are the people most at risk from *K. pneumoniae* infection. One strategy to achieve total elimination of *K. pneumoniae* may be to introduce a competitor of *K. pneumoniae* that suppresses it using antibacterial toxins. The effects of such toxins appeared to be weak or absent in my data. However, some species, including *E. coli*, do naturally make toxins that can target *K. pneumoniae*. A challenge with such a strategy is that one now has to introduce a new beneficial strain into a system that may naturally provide colonisation resistance against it. Here, my work suggests that providing the therapeutic strain with a novel nutrient that it can use may be the way to overcome this (Chapter 5, Fig. 1b). This strategy is also supported by an earlier study that enabled engraftment of a probiotic strain into a complex gut microbiota using a strain of *Bacteroides* engineered to metabolise a marine polysaccharide found in seaweed (Shepherd et al. 2018). Further hope for using bacteria as treatments for disease come from the study of *C. difficile*. Here, the start-up company Seres Therapeutics has recently published encouraging results for treating recurrent *C. difficile* infections with probiotic bacteria, with their newly approved oral microbiome therapeutic, Vowst (Jain et al. 2023). The clinical success of Vowst suggests that using probiotics as therapeutics to treat infections is possible, even if it has not been demonstrated for *K. pneumoniae* yet.

A potential alternative to the addition of novel microbial species to the gut microbiome is to seek to modulate the abundances of those already present. Here, similar to trying to introduce a new therapeutic strain, the addition of specific nutrients (prebiotics) to the host diet may be the answer. Prebiotics are non-digestible compounds in food that are metabolised by beneficial bacteria. To identify potential prebiotics, an *in vivo* metabolomics approach could help to pin-point compounds that are metabolised by the probiotic species and used to supplement the host diet. Another potential way to further reduce or eliminate a pathogen is by combining a microbiome therapeutic approach with other alternatives to antibiotics. One possible way of increasing the beneficial impact of gut microbiome manipulation is to combine it with oral vaccination. This two-pronged approach could improve the effectiveness of probiotic treatments (Slack and Diard 2022). Another potential strategy that could be used in combination with microbiome therapeutics is phage therapy, which involves using viruses to target bacterial pathogens (Lin, Koskella, and Lin 2017). A major advantage of phage therapy is that it is highly specific to the target pathogen, unlike antibiotics, which wreak collateral damage on the resident microbiota (Maier et al. 2021). Despite not yet being licensed for use in the United Kingdom, phage therapy may be used as an unlicensed medicinal product where licensed alternatives are unable to treat a patient. In the past two years, 12 patients in the United Kingdom have received phage therapy and interest in its therapeutic potential is increasing (J.D. Jones et al. 2023).

My thesis has drawn on an ecological perspective to study the effects of diversity in the gut and gain a mechanistic insight into the benefit of a diverse gut microbiome on the health of a host. The concept of ecological diversity was first studied in plant ecosystems and more recently in microbial communities, and here I show that similar principles apply in the gut microbiota, with important consequences for host health. I have found that increased community diversity leads to greater colonisation resistance to pathogens, and that both species composition and species richness are key to this resistance. Improving our understanding of the ecology of the gut microbiota and how it relates to colonisation resistance will be crucial in advancing the aim of engineering the microbiome, as an evolving ecological system, to prevent or treat infectious disease.

Appendices

Table S1. Strains.

Strain	Relevant genotype*	Internal ID	PATRIC ID	Collection ID	Hazard group**	100-strain screen	50-strain community	10 best-ranked	Source
Actinomyces odontolyticus		NT5039	411466.7	DSM43331	2	+			Nassos Typas
Akkermansia muciniphila		F3	349741.6	DSM22959	1	+	+		DSMZ***
Anaerostipes caccae		F2	105841.35	DSM14662	1	+	+		DSMZ
Bacteroides caccae		B1	411901.7	DSM19024	2	+			DSMZ
Bacteroides cellulosilyticus		B2	537012.5	DSM14838	1	+	+		DSMZ
Bacteroides clarus		NT5052	762984.10	DSM22519	1	+	+		Nassos Typas
Bacteroides eggerthii		B13	483216.6	DSM20697	2	+			DSMZ
Bacteroides fragilis enterotoxigenic 20656-2-1		NT5033	817.95	ATCC43860	2	+			Nassos Typas
Bacteroides fragilis 3_1_12		NT5057	457424.5	HM-20	2	+			Nassos Typas
Bacteroides fragilis CL07T12C05		NT5059	997883.3	HM-710	2	+			Nassos Typas
Bacteroides fragilis CL05T00C42		NT5060	997880.3	HM-711	2	+			Nassos Typas

Strain	Relevant genotype*	Internal ID	PATRIC ID	Collection ID	Hazard group**	100-strain screen	50-strain community	10 best-ranked	Source
Bacteroides fragilis CL05T12C13		NT5062	997881.3	HM-712	2	+			Nassos Typas
Bacteroides fragilis CL03T00C08		NT5063	997878.3	HM-713	2	+			Nassos Typas
Bacteroides fragilis CL03T12C07		NT5061	997879.7	HM-714	2	+			Nassos Typas
Bacteroides fragilis nontoxigenic		B4	272559.17	DSM2151	2	+			DSMZ
Bacteroides ovatus		B6	411476.11	DSM1896	2	+			DSMZ
Bacteroides stercoris VPI B5-21		B8	46506.1562	DSM19555	1	+	+		DSMZ
Bacteroides stercoris CC31F		NT5055	1073351.3	HM-1036	2	+			Nassos Typas
Bacteroides thetaiotaomicron		B9	226186.12	DSM2079	2	+			DSMZ
Bacteroides uniformis		B10	820.37	DSM6597	2	+			DSMZ
Bacteroides uniformis CL03T12C37		NT5066	997890.6	HM-716	2	+			Nassos Typas
Bacteroides xylanisolvens XB1A		B12	657309.4	DSM18836	1	+	+		DSMZ
Bacteroides xylanisolvens CL03T12C04		NT5064	997892.50	DSM2079	2	+			Nassos Typas

Strain	Relevant genotype*	Internal ID	PATRIC ID	Collection ID	Hazard group**	100-strain screen	50-strain community	10 best-ranked	Source
Bifidobacterium adolescentis		NT5022	367928.6	DSM20083	1	+	+		Nassos Typas
Bifidobacterium animalis		A2	555970.3	DSM10140	1	+	+	+	DSMZ
Bifidobacterium animalis subsp. lactis Bi-04		NT5043	580050.3		1	+			Nassos Typas
Bifidobacterium animalis subsp. lactis Bi-07		NT5044	742729.3	DGCC2908	1	+	+		Nassos Typas
Bifidobacterium bifidum		A1	500634.6	DSM20456	1	+	+		DSMZ
Bifidobacterium breve		A3	518634.19	DSM20213	1	+	+	+	DSMZ
Bifidobacterium longum subsp. infantis		A4	391904.8	DSM20088	1	+	+	+	DSMZ
Bifidobacterium longum subsp. longum		A5	565042.3	DSM20219	1	+	+		DSMZ
Blautia hansenii		NT5005	537007.6	DSM20583	1	+	+		Nassos Typas
Blautia hydrogenotrophica		F4	476272.21	DSM10507	1	+	+		DSMZ
Christensenella minuta		F7	626937.8	DSM22607	1	+	+		DSMZ
Clostridium difficile 630		NT23006	272563.8	DSM27543	2	+			Nassos Typas
Clostridium leptum		F12	428125.8	DSM753	1	+	+		DSMZ
Clostridium perfringens		NT5031	195103.10	DSM756	2	+			Nassos Typas

Strain	Relevant genotype*	Internal ID	PATRIC ID	Collection ID	Hazard group**	100-strain screen	50-strain community	10 best-ranked	Source
Clostridium perfringens		NT5032	451754.18	DSM11782	2	+			Nassos Typas
Collinsella aerofaciens		A6	411903.6	DSM3979	2	+			DSMZ
Coprococcus comes		NT5048	470146.3	ATCC27758	1	+	+		Nassos Typas
Dorea formicigenerans		NT5076	411461.20	DSM3992	1	+	+		Nassos Typas
Dorea longicatena		F13	411462.6	DSM13814	1	+	+		DSMZ
Eggerthella lenta		NT5024	479437.5	DSM2243	2	+			Nassos Typas
Enterocloster bolteae		NT5026	208479.10	DSM15670	1	+	+		Nassos Typas
Erysipelatoclostridium ramosum		NT5006	445974.19	DSM1402	2	+			Nassos Typas
AMR *Escherichia coli*	Wild type (Ampicillin)	19Y000018		-	2				Nottingham University Hospital Pathogen Bank
Escherichia coli ED1a		NT5078	585397.9		1	+			Nassos Typas
Escherichia coli HS		e-OPC-323	331112.6		1	+			(Formal et al. 1958)
Escherichia coli IAI1		NT5077	585034.5		1	+	+	+	Nassos Typas
Escherichia coli IAI1	*ΔgatABC*	eOPC-364			1				This study
Escherichia coli JKE201		eOPC-362			1				This study
Escherichia coli JKe201		eOPC-363			1				This study
Escherichia coli MG1655		e-OPC-292	511145.12		1	+			(Blattner et al. 1997)

Strain	Relevant genotype*	Internal ID	PATRIC ID	Collection ID	Hazard group**	100-strain screen	50-strain community	10 best-ranked	Source
Escherichia coli Z1269		Z1269		-	1				(Wotzka et al. 2018)
Escherichia coli Z1331		Z1331		-	1				(Wotzka et al. 2018)
Eubacterium rectale		NT5009	657318.12	DSM17629	1	+	+		Nassos Typas
Eubacterium siraeum		NT5040	428128.19	DSM15702	1	+	+		Nassos Typas
Faecalibacterium prausnitzii		F25	411483.3	DSM17677	1		+		DSMZ
Fusobacterium nucleatum CTI-01		NT24006	1204474.3		2	+			Nassos Typas
Fusobacterium nucleatum MJR7757B		NT24015	851.8		2	+			Nassos Typas
Fusobacterium nucleatum subsp. nucleatum		NT5025	190304.8	DSM15643	2	+			Nassos Typas
Fusobacterium nucleatum subsp. vincentii		NT24005	155615.5	DSM19508	2	+			Nassos Typas
Fusobacterium nucleatum subsp. vincentii		NT5030	209882.4	DSM19507	2	+			Nassos Typas
Fusobacterium periodonticum 1_A_54/D10		NT24011	546275.3	ATCC33693	1	+	+		Nassos Typas
Fusobacterium periodonticum 2_1_31		NT24012	469599.3		2	+			Nassos Typas
Gemella morbillorum		NT24013	562982.3		2	+			Nassos Typas

Strain	Relevant genotype*	Internal ID	PATRIC ID	Collection ID	Hazard group**	100-strain screen	50-strain community	10 best-ranked	Source
Holdemanella biformis		F15	518637.5	DSM3989	1	+	+	+	DSMZ
Intestinibacter bartletti		NT5086	261299.118	DSM16795	1	+			Nassos Typas
Klebsiella pneumoniae		K1	272620.9	ATCC 700721	2	+			Modernising Medical Microbiology, Nuffield Department of Medicine
Klebsiella pneumoniae subsp. pneumoniae	Wild type (Carbenicillin)	bFS-26	1162296.3	DSM 30104	2	+			DSMZ
Klebsiella pneumoniae subsp. pneumoniae	+ pRSJ-p_{nptII}::ilux	bFS-29		DSM 30104	2				This study
Klebsiella pneumoniae subsp. pneumoniae	+pBC11	bFS-34		DSM 30104	2				This study
Lachnoclostridium symbiosum WAL-14163		NT24007	742740.3		2	+			Nassos Typas
Lachnoclostridium symbiosum WAL-14673		NT24014	742741.3		2	+			Nassos Typas
Lachnoclostridium hylemonae		NT27002	553973.19	DSM15053	1	+	+		Nassos Typas
Lachnoclostridium scindens		F9	411468.41	DSM5676	1	+	+		DSMZ
Lachnoclostridium symbiosum		F8	411472.5	DSM934	2	+			DSMZ

Strain	Relevant genotype*	Internal ID	PATRIC ID	Collection ID	Hazard group**	100-strain screen	50-strain community	10 best-ranked	Source
Lacrimispora saccharolytica		NT5037	610130.3	DSM2544	1	+	+		Nassos Typas
Lacticaseibacillus casei		F16	219334.4	DSM20011	1	+	+		DSMZ
Lacticaseibacillus paracasei		NT5042	1226298.3	ATCCSD5275	1	+	+		Nassos Typas
Lactiplantibacillus plantarum JDM1		F14	644042.3	-	1	+	+	+	Department of Food and Nutritional Sciences, University of Reading
Lactobacillus acidophilus		NT5041	272621.13	ATCC700936	1	+	+	+	Nassos Typas
Lactobacillus delbrueckii subsp. Delbrueckii		NT14075	1423823.4	DSM20074	1	+	+		Nassos Typas
Lactobacillus gasseri		F18	324831.13	DSM20243	1	+	+		DSMZ
Ligilactobacillus ruminis		F17	1423798.5	DSM20403	1	+	+	+	DSMZ
Ligilactobacillus salivarius		NT14072	1423799.3	DSM20555	1	+	+	+	Nassos Typas
Limosilactobacillus fermentum		NT14076	1613.547	DSM20052	1	+	+	+	Nassos Typas
Mediterraneibacter gnavus		NT5046	411470.47	ATCC29149	1	+	+		Nassos Typas
Mediterraneibacter torques		NT5047	411460.6	ATCC27756	1	+	+		Nassos Typas
Odoribacter splanchnicus		NT5081	709991.142	DSM20712	2	+			Nassos Typas
Parabacteroides distasonis		NT5074	435591.48	DSM20701	2	+			Nassos Typas

Strain	Relevant genotype*	Internal ID	PATRIC ID	Collection ID	Hazard group**	100-strain screen	50-strain community	10 best-ranked	Source
Parabacteroides merdae		NT5071	411477.88	DSM19495	1	+			Nassos Typas
Peptostreptococcus stomatis		NT24002	596315.3	DSM17678	2	+			Nassos Typas
Phocaeicola coprocola		B3	470145.69	DSM17136	1	+	+		DSMZ
Phocaeicola dorei		NT5049	357276.1035	DSM17855	1	+	+		Nassos Typas
Phocaeicola massiliensis		B5	1121098.3	DSM17679	1	+	+		DSMZ
Phocaeicola vulgatus		B11	435590.9	DSM1447	1	+	+		DSMZ
Phocaeicola vulgatus CL09T03C04		NT5056	997891.3		1	+			Nassos Typas
Prevotella buccae		B14	873513.3	DSM19025	2	+			DSMZ
Prevotella copri		B15	537011.439	DSM18205	1	+	+		DSMZ
Roseburia faecis		F24	301302.4	DSM16840	1	+	+		DSMZ
Roseburia hominis		F22	585394.18	DSM16839	1	+	+		DSMZ
Roseburia intestinalis		NT5011	536231.75	DSM14610	1	+	+		Nassos Typas
Roseburia inulinivorans		NT5012	622312.48	DSM16841	1	+	+		Nassos Typas
Salmonella enterica Typhimurium SL1344	Wild type (Streptomycin)	SB300	216597.6	DSM24522	2	+			(Hoiseth and Stocker 1981)

Strain	Relevant genotype*	Internal ID	PATRIC ID	Collection ID	Hazard group**	100-strain screen	50-strain community	10 best-ranked	Source
Staphylococcus epidermis		bOPC-105	176280.85	DSM1798	2	+			ATCC****
Streptococcus parasanguinis		NT5072	760570.3	DSM6778	2	+			Nassos Typas
Streptococcus salivarius		NT5038	1304.1829	DSM20560	2	+			Nassos Typas
Veillonella parvula		NT5017	479436.6	DSM2008	2	+			Nassos Typas

Table S2. Time to grow, average OD-600 measurements at stationary phase and OD corresponding to 10^8 cells/mL of the 50-strain subset.

Strain	Internal ID	Days to grow	Median OD-600	OD for 10^8 cells/mL	Additional comments
Akkermansia muciniphila	F3	3	0.20	0.011	
Anaerostipes caccae	F2	2	0.28	0.034	
Bacteroides cellulosilyticus	B2	2	2.00	0.023	
Bacteroides clarus	NT5052	1	2.00	0.049	
Bacteroides stercoris VPI B5-21	B8	2	2.00	0.021	
Bacteroides xylanisolvens XB1A	B12	2	2.00	0.038	
*Bifidobacterium adolescentis**	NT5022	2	0.83	0.041	
Bifidobacterium animalis	A2	1	0.78	0.041	
Bifidobacterium animalis subsp. lactis Bi-07	NT5044	2	0.60	0.041	
*Bifidobacterium bifidum**	A1	3		0.072	
Bifidobacterium breve	A3	1	2.00	0.101	
Bifidobacterium longum subsp. infantis	A4	1	0.57	0.085	
Bifidobacterium longum subsp. longum	A5	2	0.42	0.072	
Blautia hansenii	NT5005	2	0.37	0.040	
Blautia hydrogenotrophica	F4	2	0.24	0.040	
*Christensenella minuta**	F7	3	0.02	0.020	
*Clostridium leptum**	F12	2	0.03	0.034	
Coprococcus comes	NT5048	1	1.18	0.050	
Dorea formicigenerans	NT5076	2	0.47	0.050	
Dorea longicatena	F13	2	0.88	0.050	Clumpy, shake before measuring
*Enterocloster bolteae**	NT5026	2	1.03	0.050	
Escherichia coli IAI1	NT5077	1	1.40	0.048	
Eubacterium rectale	NT5009	2	2.00	0.050	
*Eubacterium siraeum**	NT5040	3	0.05	0.050	
Faecalibacterium prausnitzii	F25	1	0.05	0.050	
Fusobacterium periodonticum 1_A_54/D10*	NT24011	3	0.02	0.082	
Holdemanella biformis	F15	1	0.92	0.078	
*Lachnoclostridium hylemonae**	NT27002	2	0.20	0.030	
Lachnoclostridium scindens	F9	2	0.33	0.020	
Lacrimispora saccharolytica	NT5037	2	0.87	0.030	
Lacticaseibacillus casei	F16	2	0.55	0.118	
*Lacticaseibacillus paracasei**	NT5042	2	0.62	0.118	

Strain	Internal ID	Days to grow	Median OD-600	OD for 10^8 cells/mL	Additional comments
Lactiplantibacillus plantarum JDM1	F14	1	0.85	0.075	
Lactobacillus acidophilus	NT5041	1	0.74	0.118	
Lactobacillus delbrueckii subsp. Delbrueckii	NT14075	2	0.45	0.118	
Lactobacillus gasseri	F18	1	0.92	0.103	
Ligilactobacillus ruminis	F17	1	0.77	0.079	
Ligilactobacillus salivarius	NT14072	1	0.73	0.118	
Limosilactobacillus fermentum	NT14076	1	0.63	0.118	
Mediterraneibacter gnavus	NT5046	2	0.81	0.050	
Mediterraneibacter torques	NT5047	3	0.40	0.050	
Phocaeicola coprocola	B3	2	1.95	0.100	
Phocaeicola dorei	NT5049	2	2.00	0.036	
Phocaeicola massiliensis	B5	1	2.00	0.049	
Phocaeicola vulgatus	B11	1	2.00	0.036	
Prevotella copri	B15	2	1.90	0.027	
*Roseburia faecis**	F24	2	1.80	0.103	
*Roseburia hominis**	F22	2	1.09	0.027	
Roseburia intestinalis	NT5011	2	1.74	0.103	
*Roseburia inulinivorans**	NT5012	2	0.04	0.103	

*These strains can be difficult to grow, so for these it is recommended to inoculate multiple tubes as back-ups, and inoculate with a large amount of freezer stock.

Table S3. Plasmids.

Plasmid name	Relevant genotype	Resistance*	Source
pRSJ-p_{nptII}::ilux	*lux*CDBAE-*frp* expression	Tetracycline	(Soldan et al. 2021)
pBC11	YPet expression	Kanamycin	(Cunrath and Bumann 2019)
pOPC-231	SV-*aphT-tetR-sceI-sacB-S*Tm-*Δ*gatABC	Kanamycin	This study
pOPC-232	SV-*aphT-tetR-sceI-sacB-Ec*IAI-*Δ*gatABC	Kanamycin	This study

*Relevant resistances only. Streptomycin= >50 ug/mL; carbenicillin=>50µg/mL; ampicillin=>100µg/mL; kanamycin=>50µg/mL; tetracycline=>50µg/mL.
**According to European biosafety designation.
*** Leibniz Institute DSMZ-German Collection of Microorganisms and Cell Cultures, Inhoffenstraße 7, 38124 Braunschwe, Science Campus Braunschweig-Süd, Germany.
**** ATCC (American Type Culture Collection), 10801 University Boulevard, Manassas, Virginia 20110-2209, United States.

Table S4. Primers.

Primer name	Sequence	Purpose	Source
oOPC-953	AGAGTTTGATCCTGGCTCAG	16S sequencing (27F)	(J.S. Johnson et al. 2019)
oOPC-954	TACGGYTACCTTGTTACGACTT	16S sequencing (1492R)	(J.S. Johnson et al. 2019)
g-Bifid-F	5'-CTCCTGGAAACGGGTGG-3'	16S sequencing for Bifidobacteria	(Matsuki et al. 2002)
g-Bifid-R	5'-GGTGTTCTTCCCGATATCTACA-3'		(Matsuki et al. 2002)
oOPC-981	CCCAGTCTCGAGGTCGACGGTATCGATAAGCTTGATATCGAATTCctactgttaaatgtttgcatcgcacc	amplify 700 upstream *gatABC* for deletion - *E.coli* IAI1	This study
oOPC-982	ggtatatgactaacctgtttgttctcgcagaataatttttacctgaggg		This study
oOPC-983	aaaaattattctgcgagaacaaacaggttagtcatataccgtccttattccg	amplify 700 downstream *gatABC* for deletion - *E.coli* IAI1	This study
oOPC-984	CTGGAGCTCCACCGCGGTGGCGGCCGCTCTAGAACTAGTGGATCCtttacgtacgcatcaaaaggcctttattgcc		This study
oOPC-985	aaacgctctgcatttgcggc	check *gatABC* deletion - *E.coli* IAI1	This study
oOPC-986	cccatgttgaagatgccgcc		This study

Table S5. Species compositions of communities used for *in vitro* experiments with *Klebsiella pneumoniae* DSM 30104.

Community ID	Community members	No. replicates	Median Day 2 pathogen density (cells/mL)
No commensals	N/A	15	1.84E+09
KTS1	A3	5	9.45E+08
KTS2	F15	3	1.11E+09
KTS3	F17	3	1.19E+09
KTS4	A4	3	1.29E+09
KTS5	NT5077	3	1.10E+08
KTS6	NT5041	3	1.12E+09
KTS7	A2	3	1.28E+09
KTS8	F14	3	1.21E+09
KTS9	NT14076	3	1.68E+09
KTS10	NT14072	3	1.53E+09
KTD1	A4, NT5041	3	1.33E+09
KTD2	NT5041, F14	3	1.29E+09
KTD3	A3, NT5077	4	4.58E+06
KTD4	F15, F14	3	1.40E+09
KTD5	F15, A2	3	1.83E+09
KTD6	A2, F14	3	1.70E+09
KTD7	F17, NT14072	3	1.59E+09
KTD8	NT5077, NT14076	4	1.28E+08
KTD9	A3, F14	3	5.96E+08
KTD10*	NT5077, F14	3	1.82E+07
KTD11*	F15, NT5077	3	1.09E+08
KTD12*	F17, NT5077	3	3.42E+07
KTD13*	A4, NT5077	3	7.44E+07
KTD14*	NT5077, NT5041	3	1.55E+07
KTD15*	NT5077, A2	3	3.84E+07
KTD16*	NT5077, NT14072	3	2.90E+07
KTD17*	NT5041, A2	3	1.81E+09
KTT1	A3, F15, NT5041	3	3.30E+08
KTT2	A3, F15, A2	3	7.44E+08
KTT3	A2, NT14076, NT14072	3	6.56E+08
KTT4	F17, NT5077, NT14072	3	1.12E+07
KTT5	NT5041, NT14076, NT14072	3	7.11E+08
KTT6	F17, NT5077, A2	3	2.52E+07
KTT7	F17, A4, NT14076	3	1.07E+09
KTT8	A3, F15, F17	4	5.03E+08
KTT9	A3, NT5041, A2	3	7.59E+08
KTT10	A3, A4, NT5041	3	6.13E+08
KTT11	A2, F14, NT14072	3	1.19E+09
KTT12	A4, NT5041, F14	3	9.36E+08
KTT13	F15, F14, NT14072	3	1.13E+09
KTT14	A3, NT5077, F14	3	3.81E+05
KTT15	A3, F17, A2	3	5.07E+08
KTT16	NT5077, F14, NT14072	3	1.72E+07
KTT17	NT5077, NT14076, NT14072	3	1.43E+07
KTT23*	A3, F15, NT5077	2	8.73E+05
KTT24*	A4, NT5077, NT14072	3	1.29E+07

Community ID	Community members	No. replicates	Median Day 2 pathogen density (cells/mL)
KTT25*	A3, NT5077, A2	3	6.53E+05
KTT26*	NT5077, NT5041, NT14072	3	6.20E+06
KTP1	A3, F15, F17, NT5041, NT14076	4	4.77E+08
KTP2	A3, F15, NT5041, A2, NT14072	4	2.98E+08
KTP3	NT5077, A2, F14, NT14076, NT14072	4	1.66E+07
KTP4	F17, NT5077, NT5041, A2, NT14072	4	2.42E+07
KTP5	A3, F15, NT5041, NT14076, NT14072	4	3.63E+08
KTP6	A3, F15, F17, A4, A2	4	5.33E+08
KTP7	F17, A4, NT5077, A2, NT14076	4	2.63E+07
KTP8	A3, F15, F17, NT5077, NT5041	4	1.25E+06
KTP9	A3, A4, NT5041, A2, F14	4	1.85E+08
KTP10	A3, A4, NT5041, F14, NT14072	4	1.99E+08
KTP11	F15, NT5041, A2, F14, NT14072	4	1.19E+09
KTP12	F17, NT5041, A2, F14, NT14076	4	9.19E+08
KTP13	F15, A4, F14, NT14076, NT14072	4	9.89E+08
KTP14	A3, A4, A2, F14, NT14076	4	6.60E+08
KTP15	F17, A4, F14, NT14076, NT14072	4	1.28E+09
KTP16	A3, F17, A4, F14, NT14072	4	2.95E+08
KTP17	A3, A4, A2, NT14076, NT14072	4	2.67E+08
KTP18*	F15, NT5077, NT5041, A2, F14	3	2.72E+06
KTP19*	F17, A4, NT5077, F14, NT14076	3	1.28E+07
KTP20*	A3, NT5077, NT5041, A2, NT14076	3	2.82E+05
KTP21*	A3, F15, NT5077, NT5041, F14	3	3.26E+05
KTP22*	A3, F17, NT5077, NT5041, F14	3	3.08E+05
KALLTOP	A3, F15, F17, A4, NT5077, NT5041, A2, F14, NT14076, NT14072	11	6.17E+05

*Communities that were additionally selected to contain *E. coli* IAI1, but otherwise were selected at random.

Table S6. Species compositions of communities used for gnotobiotic mouse experiments.

Pathogen gavaged	**No. symbionts in community**	**Community members**	***E. coli* IAI1 present**	**No. replicates**	**Median pathogen faecal density 24 hours p.i. (CFU/g)**
K. pneumoniae	0	N/A	No	7	4.0375e+09
K. pneumoniae	1	NT5077	Yes	7	2.28846e+08
K. pneumoniae	5	KTP8 (see Table S4)	Yes	8	4.35148e+07
K. pneumoniae	10	KALLTOP (see Table S4)	Yes	7	4.07019e+07
K. pneumoniae	50	See Table S1	Yes	7	134667
K. pneumoniae	9	KALLTOP minus NT5077	No	7	4.4e+08
K. pneumoniae	49	50 minus NT5077	No	7	2.32e+07

Table S7. Species compositions of communities used for prediction experiments with the AMR *E. coli* strain 19Y000018.

Community ID	Community members	No. replicates	Median Day 2 pathogen density (CFU/mL)
No commensals	N/A	5	4.96E+08
Best 2 Biolog	NT5077, NT5037	5	1.00E+07
Worst 2 Biolog	NT5077, A2	5	3.12E+08
Best 3 Biolog	NT5077, B11, NT5037	5	1.56E+06
Worst 3 Biolog	NT5077, F17, NT5041	5	2.64E+08
Best 5 Biolog	NT5077, NT5037, NT14075, NT5041, B11	5	2.48E+06
Worst 5 Biolog	NT5077, NT14075, A5, A3, F17	5	4.64E+06
Best 2 protein family	NT5077, NT5026	5	1.80E+07
Worst 2 protein family	NT5077, F3	5	2.48E+08
Best 3 protein family	NT5077, NT5026, F2	5	1.60E+07
Worst 3 protein family	NT5077, A2, NT5044	5	2.24E+08
Best 5 protein family	NT5077, NT5026, F2, NT5049, NT24011	5	2.80E+06
Worst 5 protein family	NT5077, NT14072, NT5041, F24, NT5040	5	8.16E+06
Best 10 protein family	NT5077, F2, NT14076, NT5026, NT5049, NT5047, F25, NT24011, NT5037, NT5012	5	1.60E+06
Worst 10 protein family	NT5077, F17, NT5041, NT5076, NT5048, A1, F15, A2, NT5009, NT5044	5	3.40E+06
Best 5 protein family #2	NT5077, NT5026, NT24011, NT5037, NT5052	5	4.00E+06
Best 5 protein family #3	NT5077, NT5026, NT24011, NT5037, NT5049	5	2.02E+06
Best 5 protein family #4	NT5077, F2, NT24011, NT5037, NT5052	5	5.52E+06
Best 5 protein family #5	NT5077, F2, NT5026, F16, NT5049	5	2.48E+06
Worst 5 protein family #2	NT5077, F17, F15, A2, NT5044	5	3.00E+08
Worst 5 protein family #3	NT5077, NT5048, F15, A2, NT5044	5	2.32E+08
Worst 5 protein family #4	NT5077, NT14072, NT5040, A2, NT5044	5	3.20E+08
Worst 5 protein family #5	NT5077, F17, A1, A2, NT5044	5	2.80E+08

References

Albenberg, L., T. V. Esipova, C. P. Judge, K. Bittinger, J. Chen, A. Laughlin, S. Grunberg, R. N. Baldassano, J. D. Lewis, H. Li, S. R. Thom, F. D. Bushman, S. A. Vinogradov, and G. D. Wu. 2014. "Correlation between intraluminal oxygen gradient and radial partitioning of intestinal microbiota." *Gastroenterology* 147 (5): 1055-63 e8. https://doi.org/10.1053/j.gastro.2014.07.020. https://www.ncbi.nlm.nih.gov/pubmed/25046162.

Alegre, M. L. 2019. "Mouse microbiomes: overlooked culprits of experimental variability." *Genome Biol* 20 (1): 108. https://doi.org/10.1186/s13059-019-1723-2. https://www.ncbi.nlm.nih.gov/pubmed/31142368.

Annunziato, G. 2019. "Strategies to Overcome Antimicrobial Resistance (AMR) Making Use of Non-Essential Target Inhibitors: A Review." *Int J Mol Sci* 20 (23). https://doi.org/10.3390/ijms20235844. https://www.ncbi.nlm.nih.gov/pubmed/31766441.

Anthony, W. E., B. Wang, K. V. Sukhum, A. W. D'Souza, T. Hink, C. Cass, S. Seiler, K. A. Reske, C. Coon, E. R. Dubberke, C. D. Burnham, G. Dantas, and J. H. Kwon. 2022. "Acute and persistent effects of commonly used antibiotics on the gut microbiome and resistome in healthy adults." *Cell Rep* 39 (2): 110649. https://doi.org/10.1016/j.celrep.2022.110649. https://www.ncbi.nlm.nih.gov/pubmed/35417701.

Antimicrobial Resistance, Collaborators. 2022. "Global burden of bacterial antimicrobial resistance in 2019: a systematic analysis." *Lancet* 399 (10325): 629-655. https://doi.org/10.1016/S0140-6736(21)02724-0. https://www.ncbi.nlm.nih.gov/pubmed/35065702.

Arnoldini, M., J. Cremer, and T. Hwa. 2018. "Bacterial growth, flow, and mixing shape human gut microbiota density and composition." *Gut Microbes* 9 (6): 559-566. https://doi.org/10.1080/19490976.2018.1448741. https://www.ncbi.nlm.nih.gov/pubmed/29533125.

Ashby, B., E. Watkins, J. Lourenco, S. Gupta, and K. R. Foster. 2017. "Competing species leave many potential niches unfilled." *Nat Ecol Evol* 1 (10): 1495-1501. https://doi.org/10.1038/s41559-017-0295-3. https://www.ncbi.nlm.nih.gov/pubmed/28983517.

Ashurst, J. V., and A. Dawson. 2023. "Klebsiella Pneumonia." In *StatPearls*. Treasure Island (FL).

Assoni, L., R. Girardello, T. R. Converso, and M. Darrieux. 2021. "Current Stage in the Development of Klebsiella pneumoniae Vaccines." *Infect Dis Ther* 10 (4): 2157-2175. https://doi.org/10.1007/s40121-021-00533-4. https://www.ncbi.nlm.nih.gov/pubmed/34476772.

Attar, N. 2016. "Bacterial toxins: Strain competition keeps a lid on gut pathogens." *Nat Rev Microbiol* 14 (9): 546. https://doi.org/10.1038/nrmicro.2016.121. https://www.ncbi.nlm.nih.gov/pubmed/27477299.

Bagdasarian, N., K. Rao, and P. N. Malani. 2015. "Diagnosis and treatment of Clostridium difficile in adults: a systematic review." *JAMA* 313 (4): 398-408. https://doi.org/10.1001/jama.2014.17103. https://www.ncbi.nlm.nih.gov/pubmed/25626036.

Barthels, C., A. Ogrinc, V. Steyer, S. Meier, F. Simon, M. Wimmer, A. Blutke, T. Straub, U. Zimber-Strobl, E. Lutgens, P. Marconi, C. Ohnmacht, D. Garzetti, B. Stecher, and T. Brocker. 2017. "CD40-signalling abrogates induction of RORgammat(+) Treg cells by intestinal CD103(+) DCs and causes fatal colitis." *Nat Commun* 8: 14715. https://doi.org/10.1038/ncomms14715. https://www.ncbi.nlm.nih.gov/pubmed/28276457.

Barthow, C., F. Hood, J. Crane, M. Huthwaite, M. Weatherall, A. Parry-Strong, and J. Krebs. 2022. "A randomised controlled trial of a probiotic and a prebiotic examining metabolic and mental health outcomes in adults with pre-diabetes." *BMJ Open* 12 (3): e055214. https://doi.org/10.1136/bmjopen-2021-055214. https://www.ncbi.nlm.nih.gov/pubmed/35332040.

Behzadi, P., E. Behzadi, H. Yazdanbod, R. Aghapour, M. Akbari Cheshmeh, and D. Salehian Omran. 2010. "A survey on urinary tract infections associated with the three most common uropathogenic bacteria." *Maedica (Bucur)* 5 (2): 111-5. https://www.ncbi.nlm.nih.gov/pubmed/21977133.

Belkaid, Y., and T. W. Hand. 2014. "Role of the microbiota in immunity and inflammation." *Cell* 157 (1): 121-41. https://doi.org/10.1016/j.cell.2014.03.011. https://www.ncbi.nlm.nih.gov/pubmed/24679531.

Bell, T., J. A. Newman, B. W. Silverman, S. L. Turner, and A. K. Lilley. 2005. "The contribution of species richness and composition to bacterial services." *Nature* 436 (7054): 1157-60. https://doi.org/10.1038/nature03891. https://www.ncbi.nlm.nih.gov/pubmed/16121181.

Bellmann, S., D. Carlander, A. Fasano, D. Momcilovic, J. A. Scimeca, W. J. Waldman, L. Gombau, L. Tsytsikova, R. Canady, D. I. Pereira, and D. E. Lefebvre. 2015. "Mammalian gastrointestinal tract parameters modulating the integrity, surface properties, and absorption of food-relevant nanomaterials." *Wiley Interdiscip Rev Nanomed Nanobiotechnol* 7 (5): 609-22. https://doi.org/10.1002/wnan.1333. https://www.ncbi.nlm.nih.gov/pubmed/25641962.

Bello, M. G. D., R. Knight, J. A. Gilbert, and M. J. Blaser. 2018. "Preserving microbial diversity." *Science* 362 (6410): 33-34. https://doi.org/10.1126/science.aau8816. https://www.ncbi.nlm.nih.gov/pubmed/30287652.

Bertrand, R. L. 2019. "Lag Phase Is a Dynamic, Organized, Adaptive, and Evolvable Period That Prepares Bacteria for Cell Division." *J Bacteriol* 201 (7). https://doi.org/10.1128/JB.00697-18. https://www.ncbi.nlm.nih.gov/pubmed/30642990.

Bevins, C. L., and N. H. Salzman. 2011. "Paneth cells, antimicrobial peptides and maintenance of intestinal homeostasis." *Nat Rev Microbiol* 9 (5): 356-68. https://doi.org/10.1038/nrmicro2546. https://www.ncbi.nlm.nih.gov/pubmed/21423246.

Blaser, M. J. 2016. "Antibiotic use and its consequences for the normal microbiome." *Science* 352 (6285): 544-5. https://doi.org/10.1126/science.aad9358. https://www.ncbi.nlm.nih.gov/pubmed/27126037.

---. 2017. "The theory of disappearing microbiota and the epidemics of chronic diseases." *Nat Rev Immunol* 17 (8): 461-463. https://doi.org/10.1038/nri.2017.77. https://www.ncbi.nlm.nih.gov/pubmed/28749457.

Blaser, M. J., and S. Falkow. 2009. "What are the consequences of the disappearing human microbiota?" *Nat Rev Microbiol* 7 (12): 887-94.

https://doi.org/10.1038/nrmicro2245.
https://www.ncbi.nlm.nih.gov/pubmed/19898491.

Blattner, F. R., G. Plunkett, 3rd, C. A. Bloch, N. T. Perna, V. Burland, M. Riley, J. Collado-Vides, J. D. Glasner, C. K. Rode, G. F. Mayhew, J. Gregor, N. W. Davis, H. A. Kirkpatrick, M. A. Goeden, D. J. Rose, B. Mau, and Y. Shao. 1997. "The complete genome sequence of Escherichia coli K-12." *Science* 277 (5331): 1453-62. https://doi.org/10.1126/science.277.5331.1453. https://www.ncbi.nlm.nih.gov/pubmed/9278503.

Borbet, T. C., M. B. Pawline, X. Zhang, M. F. Wipperman, S. Reuter, T. Maher, J. Li, T. Iizumi, Z. Gao, M. Daniele, C. Taube, S. B. Koralov, A. Muller, and M. J. Blaser. 2022. "Influence of the early-life gut microbiota on the immune responses to an inhaled allergen." *Mucosal Immunol* 15 (5): 1000-1011. https://doi.org/10.1038/s41385-022-00544-5. https://www.ncbi.nlm.nih.gov/pubmed/35842561.

Brisse, S., S. Issenhuth-Jeanjean, and P. A. Grimont. 2004. "Molecular serotyping of Klebsiella species isolates by restriction of the amplified capsular antigen gene cluster." *J Clin Microbiol* 42 (8): 3388-98. https://doi.org/10.1128/JCM.42.8.3388-3398.2004. https://www.ncbi.nlm.nih.gov/pubmed/15297473.

Brugiroux, S., M. Beutler, C. Pfann, D. Garzetti, H. J. Ruscheweyh, D. Ring, M. Diehl, S. Herp, Y. Lotscher, S. Hussain, B. Bunk, R. Pukall, D. H. Huson, P. C. Munch, A. C. McHardy, K. D. McCoy, A. J. Macpherson, A. Loy, T. Clavel, D. Berry, and B. Stecher. 2016. "Genome-guided design of a defined mouse microbiota that confers colonization resistance against Salmonella enterica serovar Typhimurium." *Nat Microbiol* 2: 16215. https://doi.org/10.1038/nmicrobiol.2016.215. https://www.ncbi.nlm.nih.gov/pubmed/27869789.

Buffie, C. G., V. Bucci, R. R. Stein, P. T. McKenney, L. Ling, A. Gobourne, D. No, H. Liu, M. Kinnebrew, A. Viale, E. Littmann, M. R. van den Brink, R. R. Jenq, Y. Taur, C. Sander, J. R. Cross, N. C. Toussaint, J. B. Xavier, and E. G. Pamer. 2015. "Precision microbiome reconstitution restores bile acid mediated resistance to Clostridium difficile." *Nature* 517 (7533): 205-8. https://doi.org/10.1038/nature13828. https://www.ncbi.nlm.nih.gov/pubmed/25337874.

Bull, M. J., and N. T. Plummer. 2014. "Part 1: The Human Gut Microbiome in Health and Disease." *Integr Med (Encinitas)* 13 (6): 17-22. https://www.ncbi.nlm.nih.gov/pubmed/26770121.

Byndloss, M. X., E. E. Olsan, F. Rivera-Chavez, C. R. Tiffany, S. A. Cevallos, K. L. Lokken, T. P. Torres, A. J. Byndloss, F. Faber, Y. Gao, Y. Litvak, C. A. Lopez, G. Xu, E. Napoli, C. Giulivi, R. M. Tsolis, A. Revzin, C. B. Lebrilla, and A. J. Baumler. 2017. "Microbiota-activated PPAR-gamma signaling inhibits dysbiotic Enterobacteriaceae expansion." *Science* 357 (6351): 570-575. https://doi.org/10.1126/science.aam9949. https://www.ncbi.nlm.nih.gov/pubmed/28798125.

Caballero, S., R. Carter, X. Ke, B. Susac, I. M. Leiner, G. J. Kim, L. Miller, L. Ling, K. Manova, and E. G. Pamer. 2015. "Distinct but Spatially Overlapping Intestinal Niches for Vancomycin-Resistant Enterococcus faecium and Carbapenem-Resistant Klebsiella pneumoniae." *PLoS Pathog* 11 (9): e1005132. https://doi.org/10.1371/journal.ppat.1005132. https://www.ncbi.nlm.nih.gov/pubmed/26334306.

Caballero-Flores, G., J. M. Pickard, and G. Nunez. 2022. "Microbiota-mediated colonization resistance: mechanisms and regulation." *Nat Rev Microbiol*.

https://doi.org/10.1038/s41579-022-00833-7. https://www.ncbi.nlm.nih.gov/pubmed/36539611.

Calderon-Gonzalez, R., A. Lee, G. Lopez-Campos, S. J. Hancock, J. Sa-Pessoa, A. Dumigan, R. McMullan, E. L. Campbell, and J. A. Bengoechea. 2023. "Modelling the Gastrointestinal Carriage of Klebsiella pneumoniae Infections." *mBio* 14 (1): e0312122. https://doi.org/10.1128/mbio.03121-22. https://www.ncbi.nlm.nih.gov/pubmed/36598189.

Caneiras, C., L. Lito, J. Melo-Cristino, and A. Duarte. 2019. "Community- and Hospital-Acquired Klebsiella pneumoniae Urinary Tract Infections in Portugal: Virulence and Antibiotic Resistance." *Microorganisms* 7 (5). https://doi.org/10.3390/microorganisms7050138. https://www.ncbi.nlm.nih.gov/pubmed/31100810.

Cavaillon, J. M., and J. Levin. 2022. "Revisiting Metchnikoff's work in light of the COVID-19 pandemic." *Innate Immun* 28 (2): 57-66. https://doi.org/10.1177/17534259211070663. https://www.ncbi.nlm.nih.gov/pubmed/35040340.

Chang, D. E., D. J. Smalley, D. L. Tucker, M. P. Leatham, W. E. Norris, S. J. Stevenson, A. B. Anderson, J. E. Grissom, D. C. Laux, P. S. Cohen, and T. Conway. 2004. "Carbon nutrition of Escherichia coli in the mouse intestine." *Proc Natl Acad Sci U S A* 101 (19): 7427-32. https://doi.org/10.1073/pnas.0307888101. https://www.ncbi.nlm.nih.gov/pubmed/15123798.

Chen, J., A. Zaman, B. Ramakrishna, and S. W. Olesen. 2021. "Stool Banking for Fecal Microbiota Transplantation: Methods and Operations at a Large Stool Bank." *Front Cell Infect Microbiol* 11: 622949. https://doi.org/10.3389/fcimb.2021.622949. https://www.ncbi.nlm.nih.gov/pubmed/33937092.

Cheng, A. G., P. Y. Ho, A. Aranda-Diaz, S. Jain, F. B. Yu, X. Meng, M. Wang, M. Iakiviak, K. Nagashima, A. Zhao, P. Murugkar, A. Patil, K. Atabakhsh, A. Weakley, J. Yan, A. R. Brumbaugh, S. Higginbottom, A. Dimas, A. L. Shiver, A. Deutschbauer, N. Neff, J. L. Sonnenburg, K. C. Huang, and M. A. Fischbach. 2022. "Design, construction, and in vivo augmentation of a complex gut microbiome." *Cell* 185 (19): 3617-3636 e19. https://doi.org/10.1016/j.cell.2022.08.003. https://www.ncbi.nlm.nih.gov/pubmed/36070752.

Cheng, W. Y., C. Y. Wu, and J. Yu. 2020. "The role of gut microbiota in cancer treatment: friend or foe?" *Gut* 69 (10): 1867-1876. https://doi.org/10.1136/gutjnl-2020-321153. https://www.ncbi.nlm.nih.gov/pubmed/32759302.

Chikina, A., and D. Matic Vignjevic. 2021. "At the right time in the right place: How do luminal gradients position the microbiota along the gut?" *Cells Dev* 168: 203712. https://doi.org/10.1016/j.cdev.2021.203712. https://www.ncbi.nlm.nih.gov/pubmed/34174490.

Choby, J. E., J. Howard-Anderson, and D. S. Weiss. 2020. "Hypervirulent Klebsiella pneumoniae - clinical and molecular perspectives." *J Intern Med* 287 (3): 283-300. https://doi.org/10.1111/joim.13007. https://www.ncbi.nlm.nih.gov/pubmed/31677303.

Choi, H. H., and Y. S. Cho. 2016. "Fecal Microbiota Transplantation: Current Applications, Effectiveness, and Future Perspectives." *Clin Endosc* 49 (3): 257-65. https://doi.org/10.5946/ce.2015.117. https://www.ncbi.nlm.nih.gov/pubmed/26956193.

Cianfanelli, F. R., O. Cunrath, and D. Bumann. 2020. "Efficient dual-negative selection for bacterial genome editing." *BMC Microbiol* 20 (1): 129. https://doi.org/10.1186/s12866-020-01819-2. https://www.ncbi.nlm.nih.gov/pubmed/32448155.

Cleary, D. F. R., T. Swierts, Fjrc Coelho, A. R. M. Polonia, Y. M. Huang, M. R. S. Ferreira, S. Putchakarn, L. Carvalheiro, E. van der Ent, J. P. Ueng, N. C. M. Gomes, and N. J. de Voogd. 2019. "The sponge microbiome within the greater coral reef microbial metacommunity." *Nat Commun* 10 (1): 1644. https://doi.org/10.1038/s41467-019-09537-8. https://www.ncbi.nlm.nih.gov/pubmed/30967538.

Conlan, S., H. H. Kong, and J. A. Segre. 2012. "Species-level analysis of DNA sequence data from the NIH Human Microbiome Project." *PLoS One* 7 (10): e47075. https://doi.org/10.1371/journal.pone.0047075. https://www.ncbi.nlm.nih.gov/pubmed/23071716.

Coyte, K. Z., J. Schluter, and K. R. Foster. 2015. "The ecology of the microbiome: Networks, competition, and stability." *Science* 350 (6261): 663-6. https://doi.org/10.1126/science.aad2602. https://www.ncbi.nlm.nih.gov/pubmed/26542567.

Cunrath, O., and D. Bumann. 2019. "Host resistance factor SLC11A1 restricts Salmonella growth through magnesium deprivation." *Science* 366 (6468): 995-999. https://doi.org/10.1126/science.aax7898. https://www.ncbi.nlm.nih.gov/pubmed/31753999.

Davis, J. J., S. Gerdes, G. J. Olsen, R. Olson, G. D. Pusch, M. Shukla, V. Vonstein, A. R. Wattam, and H. Yoo. 2016. "PATtyFams: Protein Families for the Microbial Genomes in the PATRIC Database." *Front Microbiol* 7: 118. https://doi.org/10.3389/fmicb.2016.00118. https://www.ncbi.nlm.nih.gov/pubmed/26903996.

de Groot, P. F., M. N. Frissen, N. C. de Clercq, and M. Nieuwdorp. 2017. "Fecal microbiota transplantation in metabolic syndrome: History, present and future." *Gut Microbes* 8 (3): 253-267. https://doi.org/10.1080/19490976.2017.1293224. https://www.ncbi.nlm.nih.gov/pubmed/28609252.

de Jonge, N., B. Carlsen, M. H. Christensen, C. Pertoldi, and J. L. Nielsen. 2022. "The Gut Microbiome of 54 Mammalian Species." *Front Microbiol* 13: 886252. https://doi.org/10.3389/fmicb.2022.886252. https://www.ncbi.nlm.nih.gov/pubmed/35783446.

de Nies, L., C. M. Kobras, and M. Stracy. 2023. "Antibiotic-induced collateral damage to the microbiota and associated infections." *Nat Rev Microbiol*. https://doi.org/10.1038/s41579-023-00936-9. https://www.ncbi.nlm.nih.gov/pubmed/37542123.

De Oliveira, D. M. P., B. M. Forde, T. J. Kidd, P. N. A. Harris, M. A. Schembri, S. A. Beatson, D. L. Paterson, and M. J. Walker. 2020. "Antimicrobial Resistance in ESKAPE Pathogens." *Clin Microbiol Rev* 33 (3). https://doi.org/10.1128/CMR.00181-19. https://www.ncbi.nlm.nih.gov/pubmed/32404435.

den Besten, G., K. van Eunen, A. K. Groen, K. Venema, D. J. Reijngoud, and B. M. Bakker. 2013. "The role of short-chain fatty acids in the interplay between diet, gut microbiota, and host energy metabolism." *J Lipid Res* 54 (9): 2325-40. https://doi.org/10.1194/jlr.R036012. https://www.ncbi.nlm.nih.gov/pubmed/23821742.

Deng, F., Y. Li, and J. Zhao. 2019. "The gut microbiome of healthy long-living people." *Aging (Albany NY)* 11 (2): 289-290. https://doi.org/10.18632/aging.101771. https://www.ncbi.nlm.nih.gov/pubmed/30648974.

Depommier, C., A. Everard, C. Druart, H. Plovier, M. Van Hul, S. Vieira-Silva, G. Falony, J. Raes, D. Maiter, N. M. Delzenne, M. de Barsy, A. Loumaye, M. P. Hermans, J. P. Thissen, W. M. de Vos, and P. D. Cani. 2019. "Supplementation with Akkermansia muciniphila in overweight and obese human volunteers: a proof-of-concept exploratory study." *Nat Med* 25 (7): 1096-1103. https://doi.org/10.1038/s41591-019-0495-2. https://www.ncbi.nlm.nih.gov/pubmed/31263284.

Derrien, M., and J. E. van Hylckama Vlieg. 2015. "Fate, activity, and impact of ingested bacteria within the human gut microbiota." *Trends Microbiol* 23 (6): 354-66. https://doi.org/10.1016/j.tim.2015.03.002. https://www.ncbi.nlm.nih.gov/pubmed/25840765.

Donaldson, G. P., S. M. Lee, and S. K. Mazmanian. 2016. "Gut biogeography of the bacterial microbiota." *Nat Rev Microbiol* 14 (1): 20-32. https://doi.org/10.1038/nrmicro3552. https://www.ncbi.nlm.nih.gov/pubmed/26499895.

Dronkers, T. M. G., A. C. Ouwehand, and G. T. Rijkers. 2020. "Global analysis of clinical trials with probiotics." *Heliyon* 6 (7): e04467. https://doi.org/10.1016/j.heliyon.2020.e04467. https://www.ncbi.nlm.nih.gov/pubmed/32715136.

Dupont, A., L. Heinbockel, K. Brandenburg, and M. W. Hornef. 2014. "Antimicrobial peptides and the enteric mucus layer act in concert to protect the intestinal mucosa." *Gut Microbes* 5 (6): 761-5. https://doi.org/10.4161/19490976.2014.972238. https://www.ncbi.nlm.nih.gov/pubmed/25483327.

Eisenhauer, N.; Schulz, W.; Scheu, S.; Jousset, A. 2012. "Niche dimensionality links biodiversity and invasibility of microbial communities." *Functional Ecology*.

El Aidy, S., G. Hooiveld, V. Tremaroli, F. Backhed, and M. Kleerebezem. 2013. "The gut microbiota and mucosal homeostasis: colonized at birth or at adulthood, does it matter?" *Gut Microbes* 4 (2): 118-24. https://doi.org/10.4161/gmic.23362. https://www.ncbi.nlm.nih.gov/pubmed/23333858.

Elinav, E., W. S. Garrett, G. Trinchieri, and J. Wargo. 2019. "The cancer microbiome." *Nat Rev Cancer* 19 (7): 371-376. https://doi.org/10.1038/s41568-019-0155-3. https://www.ncbi.nlm.nih.gov/pubmed/31186547.

Ermund, A., A. Schutte, M. E. Johansson, J. K. Gustafsson, and G. C. Hansson. 2013. "Studies of mucus in mouse stomach, small intestine, and colon. I. Gastrointestinal mucus layers have different properties depending on location as well as over the Peyer's patches." *Am J Physiol Gastrointest Liver Physiol* 305 (5): G341-7. https://doi.org/10.1152/ajpgi.00046.2013. https://www.ncbi.nlm.nih.gov/pubmed/23832518.

Ersoy, S. C., D. M. Heithoff, L. th Barnes, G. K. Tripp, J. K. House, J. D. Marth, J. W. Smith, and M. J. Mahan. 2017. "Correcting a Fundamental Flaw in the Paradigm for Antimicrobial Susceptibility Testing." *EBioMedicine* 20: 173-181. https://doi.org/10.1016/j.ebiom.2017.05.026. https://www.ncbi.nlm.nih.gov/pubmed/28579300.

Espenhain, L., S. B. Jorgensen, T. M. Leegaard, M. M. Lelek, S. H. Hansgen, B. Nakstad, M. Sunde, and M. Steinbakk. 2018. "Travel to Asia is a strong predictor for carriage of cephalosporin resistant E. coli and Klebsiella spp. but does not explain everything;

prevalence study at a Norwegian hospital 2014-2016." *Antimicrob Resist Infect Control* 7: 146. https://doi.org/10.1186/s13756-018-0429-7. https://www.ncbi.nlm.nih.gov/pubmed/30534366.

Fallingborg, J. 1999. "Intraluminal pH of the human gastrointestinal tract." *Dan Med Bull* 46 (3): 183-96. https://www.ncbi.nlm.nih.gov/pubmed/10421978.

Formal, S. B., G. J. Dammin, E. H. Labrec, and H. Schneider. 1958. "Experimental Shigella infections: characteristics of a fatal infection produced in guinea pigs." *J Bacteriol* 75 (5): 604-10. https://doi.org/10.1128/jb.75.5.604-610.1958. https://www.ncbi.nlm.nih.gov/pubmed/13538931.

Foster, K. R., and T. Bell. 2012. "Competition, not cooperation, dominates interactions among culturable microbial species." *Curr Biol* 22 (19): 1845-50. https://doi.org/10.1016/j.cub.2012.08.005. https://www.ncbi.nlm.nih.gov/pubmed/22959348.

Foster, K. R., J. Schluter, K. Z. Coyte, and S. Rakoff-Nahoum. 2017. "The evolution of the host microbiome as an ecosystem on a leash." *Nature* 548 (7665): 43-51. https://doi.org/10.1038/nature23292. https://www.ncbi.nlm.nih.gov/pubmed/28770836.

Friedman, E. S., K. Bittinger, T. V. Esipova, L. Hou, L. Chau, J. Jiang, C. Mesaros, P. J. Lund, X. Liang, G. A. FitzGerald, M. Goulian, D. Lee, B. A. Garcia, I. A. Blair, S. A. Vinogradov, and G. D. Wu. 2018. "Microbes vs. chemistry in the origin of the anaerobic gut lumen." *Proc Natl Acad Sci U S A* 115 (16): 4170-4175. https://doi.org/10.1073/pnas.1718635115. https://www.ncbi.nlm.nih.gov/pubmed/29610310.

Fujimori, S. 2020. "Gastric acid level of humans must decrease in the future." *World J Gastroenterol* 26 (43): 6706-6709. https://doi.org/10.3748/wjg.v26.i43.6706. https://www.ncbi.nlm.nih.gov/pubmed/33268958.

Gabanyi, I., G. Lepousez, R. Wheeler, A. Vieites-Prado, A. Nissant, G. Chevalier, S. Wagner, C. Moigneu, S. Dulauroy, S. Hicham, B. Polomack, F. Verny, P. Rosenstiel, N. Renier, I. G. Boneca, G. Eberl, and P. M. Lledo. 2022. "Bacterial sensing via neuronal Nod2 regulates appetite and body temperature." *Science* 376 (6590): eabj3986. https://doi.org/10.1126/science.abj3986. https://www.ncbi.nlm.nih.gov/pubmed/35420957.

Galland, Thomas, Guillaume Adeux, Hana Dvořáková, Anna E-Vojtkó, Ildikó Orbán, Michele Lussu, Javier Puy, Petr Blažek, Vojtěch Lanta, Jan Lepš, Francesco Bello, Carlos Pérez Carmona, Enrique Valencia, and Lars Götzenberger. 2019. "Colonization resistance and establishment success along gradients of functional and phylogenetic diversity in experimental plant communities." *Journal of Ecology* 107 (5): 2090-2104. https://doi.org/10.1111/1365-2745.13246. https://dx.doi.org/10.1111/1365-2745.13246.

Gensollen, T., and R. S. Blumberg. 2017. "Correlation between early-life regulation of the immune system by microbiota and allergy development." *J Allergy Clin Immunol* 139 (4): 1084-1091. https://doi.org/10.1016/j.jaci.2017.02.011. https://www.ncbi.nlm.nih.gov/pubmed/28390575.

Gilbert, J. A., M. J. Blaser, J. G. Caporaso, J. K. Jansson, S. V. Lynch, and R. Knight. 2018. "Current understanding of the human microbiome." *Nat Med* 24 (4): 392-400. https://doi.org/10.1038/nm.4517. https://www.ncbi.nlm.nih.gov/pubmed/29634682.

Glasl, B., C. E. Smith, D. G. Bourne, and N. S. Webster. 2018. "Exploring the diversity-stability paradigm using sponge microbial communities." *Sci Rep* 8 (1): 8425. https://doi.org/10.1038/s41598-018-26641-9. https://www.ncbi.nlm.nih.gov/pubmed/29849034.

Glover, J. S., T. D. Ticer, and M. A. Engevik. 2022. "Characterizing the mucin-degrading capacity of the human gut microbiota." *Sci Rep* 12 (1): 8456. https://doi.org/10.1038/s41598-022-11819-z. https://www.ncbi.nlm.nih.gov/pubmed/35589783.

Gomes, M. Z. R., E. M. de Lima, C. A. Martins Aires, P. S. Pereira, J. Yim, F. H. Silva, C. A. S. Rodrigues, Trte Oliveira, P. P. da Silva, C. M. Eller, C. M. R. de Souza, M. J. Rybak, R. M. Albano, A. B. de Miranda, E. Machado, M. Catanho, and collaborators Nucleus of Hospital Research study. 2023. "Outbreak report of polymyxin-carbapenem-resistant Klebsiella pneumoniae causing untreatable infections evidenced by synergy tests and bacterial genomes." *Sci Rep* 13 (1): 6238. https://doi.org/10.1038/s41598-023-31901-4. https://www.ncbi.nlm.nih.gov/pubmed/37069157.

Gorrie, C. L., M. Mirceta, R. R. Wick, D. J. Edwards, N. R. Thomson, R. A. Strugnell, N. F. Pratt, J. S. Garlick, K. M. Watson, D. V. Pilcher, S. A. McGloughlin, D. W. Spelman, A. W. J. Jenney, and K. E. Holt. 2017. "Gastrointestinal Carriage Is a Major Reservoir of Klebsiella pneumoniae Infection in Intensive Care Patients." *Clin Infect Dis* 65 (2): 208-215. https://doi.org/10.1093/cid/cix270. https://www.ncbi.nlm.nih.gov/pubmed/28369261.

Gorrie, C. L., M. Mirceta, R. R. Wick, L. M. Judd, M. M. C. Lam, R. Gomi, I. J. Abbott, N. R. Thomson, R. A. Strugnell, N. F. Pratt, J. S. Garlick, K. M. Watson, P. C. Hunter, D. V. Pilcher, S. A. McGloughlin, D. W. Spelman, K. L. Wyres, A. W. J. Jenney, and K. E. Holt. 2022. "Genomic dissection of Klebsiella pneumoniae infections in hospital patients reveals insights into an opportunistic pathogen." *Nat Commun* 13 (1): 3017. https://doi.org/10.1038/s41467-022-30717-6. https://www.ncbi.nlm.nih.gov/pubmed/35641522.

Gorrie, C. L., M. Mirceta, R. R. Wick, L. M. Judd, K. L. Wyres, N. R. Thomson, R. A. Strugnell, N. F. Pratt, J. S. Garlick, K. M. Watson, P. C. Hunter, S. A. McGloughlin, D. W. Spelman, A. W. J. Jenney, and K. E. Holt. 2018. "Antimicrobial-Resistant Klebsiella pneumoniae Carriage and Infection in Specialized Geriatric Care Wards Linked to Acquisition in the Referring Hospital." *Clin Infect Dis* 67 (2): 161-170. https://doi.org/10.1093/cid/ciy027. https://www.ncbi.nlm.nih.gov/pubmed/29340588.

Gould, A. L., V. Zhang, L. Lamberti, E. W. Jones, B. Obadia, N. Korasidis, A. Gavryushkin, J. M. Carlson, N. Beerenwinkel, and W. B. Ludington. 2018. "Microbiome interactions shape host fitness." *Proc Natl Acad Sci U S A* 115 (51): E11951-E11960. https://doi.org/10.1073/pnas.1809349115. https://www.ncbi.nlm.nih.gov/pubmed/30510004.

Granato, E. T., T. A. Meiller-Legrand, and K. R. Foster. 2019. "The Evolution and Ecology of Bacterial Warfare." *Curr Biol* 29 (11): R521-R537. https://doi.org/10.1016/j.cub.2019.04.024. https://www.ncbi.nlm.nih.gov/pubmed/31163166.

Gu, D., N. Dong, Z. Zheng, D. Lin, M. Huang, L. Wang, E. W. Chan, L. Shu, J. Yu, R. Zhang, and S. Chen. 2018. "A fatal outbreak of ST11 carbapenem-resistant hypervirulent Klebsiella pneumoniae in a Chinese hospital: a molecular epidemiological study."

Lancet Infect Dis 18 (1): 37-46. https://doi.org/10.1016/S1473-3099(17)30489-9. https://www.ncbi.nlm.nih.gov/pubmed/28864030.

Guillemard, E., F. Tondu, F. Lacoin, and J. Schrezenmeir. 2010. "Consumption of a fermented dairy product containing the probiotic Lactobacillus casei DN-114001 reduces the duration of respiratory infections in the elderly in a randomised controlled trial." *Br J Nutr* 103 (1): 58-68. https://doi.org/10.1017/S0007114509991395. https://www.ncbi.nlm.nih.gov/pubmed/19747410.

Hapfelmeier, S., M. A. Lawson, E. Slack, J. K. Kirundi, M. Stoel, M. Heikenwalder, J. Cahenzli, Y. Velykoredko, M. L. Balmer, K. Endt, M. B. Geuking, R. Curtiss, 3rd, K. D. McCoy, and A. J. Macpherson. 2010. "Reversible microbial colonization of germ-free mice reveals the dynamics of IgA immune responses." *Science* 328 (5986): 1705-9. https://doi.org/10.1126/science.1188454. https://www.ncbi.nlm.nih.gov/pubmed/20576892.

Hasani, A., E. Soltani, M. Ahangarzadeh Rezaee, T. Pirzadeh, M. Ahangar Oskouee, A. Hasani, P. Gholizadeh, A. Noie Oskouie, and E. Binesh. 2020. "Serotyping of Klebsiella pneumoniae and Its Relation with Capsule-Associated Virulence Genes, Antimicrobial Resistance Pattern, and Clinical Infections: A Descriptive Study in Medical Practice." *Infect Drug Resist* 13: 1971-1980. https://doi.org/10.2147/IDR.S243984. https://www.ncbi.nlm.nih.gov/pubmed/32606843.

Hecht, A. L., B. W. Casterline, Z. M. Earley, Y. A. Goo, D. R. Goodlett, and J. Bubeck Wardenburg. 2016. "Strain competition restricts colonization of an enteric pathogen and prevents colitis." *EMBO Rep* 17 (9): 1281-91. https://doi.org/10.15252/embr.201642282. https://www.ncbi.nlm.nih.gov/pubmed/27432285.

Heiman, M. L., and F. L. Greenway. 2016. "A healthy gastrointestinal microbiome is dependent on dietary diversity." *Mol Metab* 5 (5): 317-320. https://doi.org/10.1016/j.molmet.2016.02.005. https://www.ncbi.nlm.nih.gov/pubmed/27110483.

Helander, H. F., and L. Fandriks. 2014. "Surface area of the digestive tract - revisited." *Scand J Gastroenterol* 49 (6): 681-9. https://doi.org/10.3109/00365521.2014.898326. https://www.ncbi.nlm.nih.gov/pubmed/24694282.

Hoiseth, S. K., and B. A. Stocker. 1981. "Aromatic-dependent Salmonella typhimurium are non-virulent and effective as live vaccines." *Nature* 291 (5812): 238-9. http://www.ncbi.nlm.nih.gov/pubmed/7015147.

Huynh, B. T., V. Passet, A. Rakotondrasoa, T. Diallo, A. Kerleguer, M. Hennart, A. Lauzanne, P. Herindrainy, A. Seck, R. Bercion, L. Borand, M. Pardos de la Gandara, E. Delarocque-Astagneau, D. Guillemot, M. Vray, B. Garin, J. M. Collard, C. Rodrigues, and S. Brisse. 2020. "Klebsiella pneumoniae carriage in low-income countries: antimicrobial resistance, genomic diversity and risk factors." *Gut Microbes* 11 (5): 1287-1299. https://doi.org/10.1080/19490976.2020.1748257. https://www.ncbi.nlm.nih.gov/pubmed/32404021.

Iwasaki, A., and B. L. Kelsall. 1999. "Freshly isolated Peyer's patch, but not spleen, dendritic cells produce interleukin 10 and induce the differentiation of T helper type 2 cells." *J Exp Med* 190 (2): 229-39. https://doi.org/10.1084/jem.190.2.229. https://www.ncbi.nlm.nih.gov/pubmed/10432286.

Jacobson, A., L. Lam, M. Rajendram, F. Tamburini, J. Honeycutt, T. Pham, W. Van Treuren, K. Pruss, S. R. Stabler, K. Lugo, D. M. Bouley, J. G. Vilches-Moure, M. Smith, J. L.

Sonnenburg, A. S. Bhatt, K. C. Huang, and D. Monack. 2018. "A Gut Commensal-Produced Metabolite Mediates Colonization Resistance to Salmonella Infection." *Cell Host Microbe* 24 (2): 296-307 e7. https://doi.org/10.1016/j.chom.2018.07.002. https://www.ncbi.nlm.nih.gov/pubmed/30057174.

Jain, N., T. P. Umar, A. F. Fahner, and V. Gibietis. 2023. "Advancing therapeutics for recurrent clostridioides difficile infections: an overview of vowst's FDA approval and implications." *Gut Microbes* 15 (1): 2232137. https://doi.org/10.1080/19490976.2023.2232137. https://www.ncbi.nlm.nih.gov/pubmed/37431860.

Jochum, M., M. Fischer, F. Isbell, C. Roscher, F. van der Plas, S. Boch, G. Boenisch, N. Buchmann, J. A. Catford, J. Cavender-Bares, A. Ebeling, N. Eisenhauer, G. Gleixner, N. Holzel, J. Kattge, V. H. Klaus, T. Kleinebecker, M. Lange, G. Le Provost, S. T. Meyer, R. Molina-Venegas, L. Mommer, Y. Oelmann, C. Penone, D. Prati, P. B. Reich, A. Rindisbacher, D. Schafer, S. Scheu, B. Schmid, D. Tilman, T. Tscharntke, A. Vogel, C. Wagg, A. Weigelt, W. W. Weisser, W. Wilcke, and P. Manning. 2020. "The results of biodiversity-ecosystem functioning experiments are realistic." *Nat Ecol Evol* 4 (11): 1485-1494. https://doi.org/10.1038/s41559-020-1280-9. https://www.ncbi.nlm.nih.gov/pubmed/32839545.

Johnson, J. S., D. J. Spakowicz, B. Y. Hong, L. M. Petersen, P. Demkowicz, L. Chen, S. R. Leopold, B. M. Hanson, H. O. Agresta, M. Gerstein, E. Sodergren, and G. M. Weinstock. 2019. "Evaluation of 16S rRNA gene sequencing for species and strain-level microbiome analysis." *Nat Commun* 10 (1): 5029. https://doi.org/10.1038/s41467-019-13036-1. https://www.ncbi.nlm.nih.gov/pubmed/31695033.

Johnson, K. V. 2020. "Gut microbiome composition and diversity are related to human personality traits." *Hum Microb J* 15: None. https://doi.org/10.1016/j.humic.2019.100069. https://www.ncbi.nlm.nih.gov/pubmed/34435164.

Jones, J. D., C. Trippett, M. Suleman, M. R. J. Clokie, and J. R. Clark. 2023. "The Future of Clinical Phage Therapy in the United Kingdom." *Viruses* 15 (3). https://doi.org/10.3390/v15030721. https://www.ncbi.nlm.nih.gov/pubmed/36992430.

Jones, M. L., D. W. Rivett, A. Pascual-Garcia, and T. Bell. 2021. "Relationships between community composition, productivity and invasion resistance in semi-natural bacterial microcosms." *Elife* 10. https://doi.org/10.7554/eLife.71811. https://www.ncbi.nlm.nih.gov/pubmed/34662276.

Karampatakis, T., K. Tsergouli, and P. Behzadi. 2023. "Carbapenem-Resistant Klebsiella pneumoniae: Virulence Factors, Molecular Epidemiology and Latest Updates in Treatment Options." *Antibiotics (Basel)* 12 (2). https://doi.org/10.3390/antibiotics12020234. https://www.ncbi.nlm.nih.gov/pubmed/36830145.

Kennedy, T. A., S. Naeem, K. M. Howe, J. M. Knops, D. Tilman, and P. Reich. 2002. "Biodiversity as a barrier to ecological invasion." *Nature* 417 (6889): 636-8. https://doi.org/10.1038/nature00776. https://www.ncbi.nlm.nih.gov/pubmed/12050662.

Khoruts, A. 2017. "Fecal microbiota transplantation-early steps on a long journey ahead." *Gut Microbes* 8 (3): 199-204. https://doi.org/10.1080/19490976.2017.1316447. https://www.ncbi.nlm.nih.gov/pubmed/28394706.

Kim, S. G., S. Becattini, T. U. Moody, P. V. Shliaha, E. R. Littmann, R. Seok, M. Gjonbalaj, V. Eaton, E. Fontana, L. Amoretti, R. Wright, S. Caballero, Z. X. Wang, H. J. Jung, S. M. Morjaria, I. M. Leiner, W. Qin, Rjjf Ramos, J. R. Cross, S. Narushima, K. Honda, J. U. Peled, R. C. Hendrickson, Y. Taur, M. R. M. van den Brink, and E. G. Pamer. 2019. "Microbiota-derived lantibiotic restores resistance against vancomycin-resistant Enterococcus." *Nature* 572 (7771): 665-669. https://doi.org/10.1038/s41586-019-1501-z. https://www.ncbi.nlm.nih.gov/pubmed/31435014.

King, K. C., M. A. Brockhurst, O. Vasieva, S. Paterson, A. Betts, S. A. Ford, C. L. Frost, M. J. Horsburgh, S. Haldenby, and G. D. Hurst. 2016. "Rapid evolution of microbe-mediated protection against pathogens in a worm host." *ISME J* 10 (8): 1915-24. https://doi.org/10.1038/ismej.2015.259. https://www.ncbi.nlm.nih.gov/pubmed/26978164.

Kobayashi, K. S., M. Chamaillard, Y. Ogura, O. Henegariu, N. Inohara, G. Nunez, and R. A. Flavell. 2005. "Nod2-dependent regulation of innate and adaptive immunity in the intestinal tract." *Science* 307 (5710): 731-4. https://doi.org/10.1126/science.1104911. https://www.ncbi.nlm.nih.gov/pubmed/15692051.

Kristensen, N. B., T. Bryrup, K. H. Allin, T. Nielsen, T. H. Hansen, and O. Pedersen. 2016. "Alterations in fecal microbiota composition by probiotic supplementation in healthy adults: a systematic review of randomized controlled trials." *Genome Med* 8 (1): 52. https://doi.org/10.1186/s13073-016-0300-5. https://www.ncbi.nlm.nih.gov/pubmed/27159972.

Kruis, W., P. Fric, J. Pokrotnieks, M. Lukas, B. Fixa, M. Kascak, M. A. Kamm, J. Weismueller, C. Beglinger, M. Stolte, C. Wolff, and J. Schulze. 2004. "Maintaining remission of ulcerative colitis with the probiotic Escherichia coli Nissle 1917 is as effective as with standard mesalazine." *Gut* 53 (11): 1617-23. https://doi.org/10.1136/gut.2003.037747. https://www.ncbi.nlm.nih.gov/pubmed/15479682.

Kwon, Y. J., H. J. Kwak, H. K. Lee, H. C. Lim, and D. H. Jung. 2021. "Comparison of bacterial community profiles from large intestine specimens, rectal swabs, and stool samples." *Appl Microbiol Biotechnol* 105 (24): 9273-9284. https://doi.org/10.1007/s00253-021-11650-y. https://www.ncbi.nlm.nih.gov/pubmed/34773153.

Langenheder, S., and A. J. Szekely. 2011. "Species sorting and neutral processes are both important during the initial assembly of bacterial communities." *ISME J* 5 (7): 1086-94. https://doi.org/10.1038/ismej.2010.207. https://www.ncbi.nlm.nih.gov/pubmed/21270841.

Larsson, D. G. J., and C. F. Flach. 2022. "Antibiotic resistance in the environment." *Nat Rev Microbiol* 20 (5): 257-269. https://doi.org/10.1038/s41579-021-00649-x. https://www.ncbi.nlm.nih.gov/pubmed/34737424.

Lau, H. Y., G. B. Huffnagle, and T. A. Moore. 2008. "Host and microbiota factors that control Klebsiella pneumoniae mucosal colonization in mice." *Microbes Infect* 10 (12-13): 1283-90. https://doi.org/10.1016/j.micinf.2008.07.040. https://www.ncbi.nlm.nih.gov/pubmed/18762269.

Lee, J. H., I. S. Cheon, B. S. Shim, D. W. Kim, S. W. Kim, J. Chun, and M. Song. 2012. "Draft genome sequence of Klebsiella pneumoniae subsp. pneumoniae DSM 30104T." *J Bacteriol* 194 (20): 5722-3. https://doi.org/10.1128/JB.01388-12. https://www.ncbi.nlm.nih.gov/pubmed/23012294.

Lee, K., S. Raguideau, K. Siren, F. Asnicar, F. Cumbo, F. Hildebrand, N. Segata, C. J. Cha, and C. Quince. 2023. "Population-level impacts of antibiotic usage on the human gut microbiome." *Nat Commun* 14 (1): 1191. https://doi.org/10.1038/s41467-023-36633-7. https://www.ncbi.nlm.nih.gov/pubmed/36864029.

Lee, Y. Y., A. Erdogan, and S. S. Rao. 2014. "How to assess regional and whole gut transit time with wireless motility capsule." *J Neurogastroenterol Motil* 20 (2): 265-70. https://doi.org/10.5056/jnm.2014.20.2.265. https://www.ncbi.nlm.nih.gov/pubmed/24840380.

Leite, G. G. S., S. Weitsman, G. Parodi, S. Celly, R. Sedighi, M. Sanchez, W. Morales, M. J. Villanueva-Millan, G. M. Barlow, R. Mathur, S. K. Lo, L. H. Jamil, S. Paski, A. Rezaie, and M. Pimentel. 2020. "Mapping the Segmental Microbiomes in the Human Small Bowel in Comparison with Stool: A REIMAGINE Study." *Dig Dis Sci* 65 (9): 2595-2604. https://doi.org/10.1007/s10620-020-06173-x. https://www.ncbi.nlm.nih.gov/pubmed/32140945.

Lepuschitz, S., K. Hauser, A. Schriebl, C. Schlagenhaufen, A. Stoger, A. Chakeri, K. Votsch, S. Pekard-Amenitsch, B. Springer, F. Allerberger, and W. Ruppitsch. 2020. "Fecal Klebsiella pneumoniae Carriage Is Intermittent and of High Clonal Diversity." *Front Microbiol* 11: 581081. https://doi.org/10.3389/fmicb.2020.581081. https://www.ncbi.nlm.nih.gov/pubmed/33324367.

Lerminiaux, N. A., and A. D. S. Cameron. 2019. "Horizontal transfer of antibiotic resistance genes in clinical environments." *Can J Microbiol* 65 (1): 34-44. https://doi.org/10.1139/cjm-2018-0275. https://www.ncbi.nlm.nih.gov/pubmed/30248271.

Lerner, A., Y. Shoenfeld, and T. Matthias. 2019. "Probiotics: If It Does Not Help It Does Not Do Any Harm. Really?" *Microorganisms* 7 (4). https://doi.org/10.3390/microorganisms7040104. https://www.ncbi.nlm.nih.gov/pubmed/30979072.

Leshem, A., T. Liwinski, and E. Elinav. 2020. "Immune-Microbiota Interplay and Colonization Resistance in Infection." *Mol Cell* 78 (4): 597-613. https://doi.org/10.1016/j.molcel.2020.03.001. https://www.ncbi.nlm.nih.gov/pubmed/32208169.

Lewis, B. B., C. G. Buffie, R. A. Carter, I. Leiner, N. C. Toussaint, L. C. Miller, A. Gobourne, L. Ling, and E. G. Pamer. 2015. "Loss of Microbiota-Mediated Colonization Resistance to Clostridium difficile Infection With Oral Vancomycin Compared With Metronidazole." *J Infect Dis* 212 (10): 1656-65. https://doi.org/10.1093/infdis/jiv256. https://www.ncbi.nlm.nih.gov/pubmed/25920320.

Ley, R. E., D. A. Peterson, and J. I. Gordon. 2006. "Ecological and evolutionary forces shaping microbial diversity in the human intestine." *Cell* 124 (4): 837-48. https://doi.org/10.1016/j.cell.2006.02.017. https://www.ncbi.nlm.nih.gov/pubmed/16497592.

Liao, C. H., Y. T. Huang, C. C. Lai, C. Y. Chang, F. Y. Chu, M. S. Hsu, H. S. Hsu, and P. R. Hseuh. 2011. "Klebsiella pneumoniae bacteremia and capsular serotypes, Taiwan." *Emerg*

Infect Dis 17 (6): 1113-5. https://doi.org/10.3201/eid/1706.100811. https://www.ncbi.nlm.nih.gov/pubmed/21749784.

Lim, J. J., C. Diener, J. Wilson, J. J. Valenzuela, N. S. Baliga, and S. M. Gibbons. 2023. "Growth phase estimation for abundant bacterial populations sampled longitudinally from human stool metagenomes." *Nat Commun* 14 (1): 5682. https://doi.org/10.1038/s41467-023-41424-1. https://www.ncbi.nlm.nih.gov/pubmed/37709733.

Lin, D. M., B. Koskella, and H. C. Lin. 2017. "Phage therapy: An alternative to antibiotics in the age of multi-drug resistance." *World J Gastrointest Pharmacol Ther* 8 (3): 162-173. https://doi.org/10.4292/wjgpt.v8.i3.162. https://www.ncbi.nlm.nih.gov/pubmed/28828194.

Llor, C., and L. Bjerrum. 2014. "Antimicrobial resistance: risk associated with antibiotic overuse and initiatives to reduce the problem." *Ther Adv Drug Saf* 5 (6): 229-41. https://doi.org/10.1177/2042098614554919. https://www.ncbi.nlm.nih.gov/pubmed/25436105.

Lozupone, C. A., J. I. Stombaugh, J. I. Gordon, J. K. Jansson, and R. Knight. 2012. "Diversity, stability and resilience of the human gut microbiota." *Nature* 489 (7415): 220-30. https://doi.org/10.1038/nature11550. https://www.ncbi.nlm.nih.gov/pubmed/22972295.

M. Schultz, J.P. Burton. 2017. "The Microbiota in Gastrointestinal Pathophysiology." 11.

Mackowiak, P. A. 2013. "Recycling metchnikoff: probiotics, the intestinal microbiome and the quest for long life." *Front Public Health* 1: 52. https://doi.org/10.3389/fpubh.2013.00052. https://www.ncbi.nlm.nih.gov/pubmed/24350221.

Magne, F., M. Gotteland, L. Gauthier, A. Zazueta, S. Pesoa, P. Navarrete, and R. Balamurugan. 2020. "The Firmicutes/Bacteroidetes Ratio: A Relevant Marker of Gut Dysbiosis in Obese Patients?" *Nutrients* 12 (5). https://doi.org/10.3390/nu12051474. https://www.ncbi.nlm.nih.gov/pubmed/32438689.

Maier, L., C. V. Goemans, J. Wirbel, M. Kuhn, C. Eberl, M. Pruteanu, P. Muller, S. Garcia-Santamarina, E. Cacace, B. Zhang, C. Gekeler, T. Banerjee, E. E. Anderson, A. Milanese, U. Lober, S. K. Forslund, K. R. Patil, M. Zimmermann, B. Stecher, G. Zeller, P. Bork, and A. Typas. 2021. "Unravelling the collateral damage of antibiotics on gut bacteria." *Nature* 599 (7883): 120-124. https://doi.org/10.1038/s41586-021-03986-2. https://www.ncbi.nlm.nih.gov/pubmed/34646011.

Maier, L., M. Pruteanu, M. Kuhn, G. Zeller, A. Telzerow, E. E. Anderson, A. R. Brochado, K. C. Fernandez, H. Dose, H. Mori, K. R. Patil, P. Bork, and A. Typas. 2018. "Extensive impact of non-antibiotic drugs on human gut bacteria." *Nature* 555 (7698): 623-628. https://doi.org/10.1038/nature25979. https://www.ncbi.nlm.nih.gov/pubmed/29555994.

Maier, L., and A. Typas. 2017. "Systematically investigating the impact of medication on the gut microbiome." *Curr Opin Microbiol* 39: 128-135. https://doi.org/10.1016/j.mib.2017.11.001. https://www.ncbi.nlm.nih.gov/pubmed/29169088.

Maltby, R., M. P. Leatham-Jensen, T. Gibson, P. S. Cohen, and T. Conway. 2013. "Nutritional basis for colonization resistance by human commensal Escherichia coli strains HS and Nissle 1917 against E. coli O157:H7 in the mouse intestine." *PLoS One* 8 (1): e53957.

https://doi.org/10.1371/journal.pone.0053957. https://www.ncbi.nlm.nih.gov/pubmed/23349773.

Mamoon, L., and S. W. Olesen. 2020. "Fecal Microbiota Transplants Annually and Their Positive Clinical Impact." *Clin Transl Gastroenterol* 11 (11): e00247. https://doi.org/10.14309/ctg.0000000000000247. https://www.ncbi.nlm.nih.gov/pubmed/33259159.

Manor, O., C. L. Dai, S. A. Kornilov, B. Smith, N. D. Price, J. C. Lovejoy, S. M. Gibbons, and A. T. Magis. 2020. "Health and disease markers correlate with gut microbiome composition across thousands of people." *Nat Commun* 11 (1): 5206. https://doi.org/10.1038/s41467-020-18871-1. https://www.ncbi.nlm.nih.gov/pubmed/33060586.

Mark Welch, J. L., Y. Hasegawa, N. P. McNulty, J. I. Gordon, and G. G. Borisy. 2017. "Spatial organization of a model 15-member human gut microbiota established in gnotobiotic mice." *Proc Natl Acad Sci U S A* 114 (43): E9105-E9114. https://doi.org/10.1073/pnas.1711596114. https://www.ncbi.nlm.nih.gov/pubmed/29073107.

Marteau, P., P. Pochart, J. Dore, C. Bera-Maillet, A. Bernalier, and G. Corthier. 2001. "Comparative study of bacterial groups within the human cecal and fecal microbiota." *Appl Environ Microbiol* 67 (10): 4939-42. https://doi.org/10.1128/AEM.67.10.4939-4942.2001. https://www.ncbi.nlm.nih.gov/pubmed/11571208.

Matlock, W., S. Lipworth, K. K. Chau, M. AbuOun, L. Barker, J. Kavanagh, M. Andersson, S. Oakley, M. Morgan, D. W. Crook, D. S. Read, M. Anjum, L. P. Shaw, N. Stoesser, and Rehab Consortium. 2023. "Enterobacterales plasmid sharing amongst human bloodstream infections, livestock, wastewater, and waterway niches in Oxfordshire, UK." *Elife* 12. https://doi.org/10.7554/eLife.85302. https://www.ncbi.nlm.nih.gov/pubmed/36961866.

Matsuki, T., K. Watanabe, J. Fujimoto, Y. Miyamoto, T. Takada, K. Matsumoto, H. Oyaizu, and R. Tanaka. 2002. "Development of 16S rRNA-gene-targeted group-specific primers for the detection and identification of predominant bacteria in human feces." *Appl Environ Microbiol* 68 (11): 5445-51. https://doi.org/10.1128/AEM.68.11.5445-5451.2002. https://www.ncbi.nlm.nih.gov/pubmed/12406736.

Mayfield, M. M., and D. B. Stouffer. 2017. "Higher-order interactions capture unexplained complexity in diverse communities." *Nat Ecol Evol* 1 (3): 62. https://doi.org/10.1038/s41559-016-0062. https://www.ncbi.nlm.nih.gov/pubmed/28812740.

McCann, K. S. 2000. "The diversity-stability debate." *Nature* 405 (6783): 228-33. https://doi.org/10.1038/35012234. https://www.ncbi.nlm.nih.gov/pubmed/10821283.

McDonald, D., E. Hyde, J. W. Debelius, J. T. Morton, A. Gonzalez, G. Ackermann, A. A. Aksenov, B. Behsaz, C. Brennan, Y. Chen, L. DeRight Goldasich, P. C. Dorrestein, R. R. Dunn, A. K. Fahimipour, J. Gaffney, J. A. Gilbert, G. Gogul, J. L. Green, P. Hugenholtz, G. Humphrey, C. Huttenhower, M. A. Jackson, S. Janssen, D. V. Jeste, L. Jiang, S. T. Kelley, D. Knights, T. Kosciolek, J. Ladau, J. Leach, C. Marotz, D. Meleshko, A. V. Melnik, J. L. Metcalf, H. Mohimani, E. Montassier, J. Navas-Molina, T. T. Nguyen, S. Peddada, P. Pevzner, K. S. Pollard, G. Rahnavard, A. Robbins-Pianka, N. Sangwan, J. Shorenstein, L. Smarr, S. J. Song, T. Spector, A. D. Swafford, V. G. Thackray, L. R.

Thompson, A. Tripathi, Y. Vazquez-Baeza, A. Vrbanac, P. Wischmeyer, E. Wolfe, Q. Zhu, Consortium American Gut, and R. Knight. 2018. "American Gut: an Open Platform for Citizen Science Microbiome Research." *mSystems* 3 (3). https://doi.org/10.1128/mSystems.00031-18. https://www.ncbi.nlm.nih.gov/pubmed/29795809.

McFarland, L. V. 2021. "Efficacy of Single-Strain Probiotics Versus Multi-Strain Mixtures: Systematic Review of Strain and Disease Specificity." *Dig Dis Sci* 66 (3): 694-704. https://doi.org/10.1007/s10620-020-06244-z. https://www.ncbi.nlm.nih.gov/pubmed/32274669.

McLaren, M. R., and B. J. Callahan. 2020. "Pathogen resistance may be the principal evolutionary advantage provided by the microbiome." *Philos Trans R Soc Lond B Biol Sci* 375 (1808): 20190592. https://doi.org/10.1098/rstb.2019.0592. https://www.ncbi.nlm.nih.gov/pubmed/32772671.

McLoughlin, K., J. Schluter, S. Rakoff-Nahoum, A. L. Smith, and K. R. Foster. 2016. "Host Selection of Microbiota via Differential Adhesion." *Cell Host Microbe* 19 (4): 550-9. https://doi.org/10.1016/j.chom.2016.02.021. https://www.ncbi.nlm.nih.gov/pubmed/27053168.

Meier, K. H. U., J. Trouillon, H. Li, M. Lang, T. Fuhrer, N. Zamboni, S. Sunagawa, A. J. Macpherson, and U. Sauer. 2023. "Metabolic landscape of the male mouse gut identifies different niches determined by microbial activities." *Nat Metab*. https://doi.org/10.1038/s42255-023-00802-1. https://www.ncbi.nlm.nih.gov/pubmed/37217759.

Merrill, B. D., M. M. Carter, M. R. Olm, D. Dahan, S. Tripathi, S. P. Spencer, B. Yu, S. Jain, N. Neff, A. R. Jha, E. D. Sonnenburg, and J. L. Sonnenburg. 2022. "Ultra-deep Sequencing of Hadza Hunter-Gatherers Recovers Vanishing Gut Microbes." *bioRxiv*. https://doi.org/10.1101/2022.03.30.486478. https://www.ncbi.nlm.nih.gov/pubmed/36238714.

Mikolasevic, I., G. Hauser, M. Abram, T. Filipec Kanizaj, M. Radic, and I. Krznaric Zrnic. 2021. "Fecal microbiota transplantation - where are we?" *Croat Med J* 62 (1): 52-58. https://doi.org/10.3325/cmj.2021.62.52. https://www.ncbi.nlm.nih.gov/pubmed/33660961.

Morais, L. H., H. L. th Schreiber, and S. K. Mazmanian. 2021. "The gut microbiota-brain axis in behaviour and brain disorders." *Nat Rev Microbiol* 19 (4): 241-255. https://doi.org/10.1038/s41579-020-00460-0. https://www.ncbi.nlm.nih.gov/pubmed/33093662.

Mosca, A., M. Leclerc, and J. P. Hugot. 2016. "Gut Microbiota Diversity and Human Diseases: Should We Reintroduce Key Predators in Our Ecosystem?" *Front Microbiol* 7: 455. https://doi.org/10.3389/fmicb.2016.00455. https://www.ncbi.nlm.nih.gov/pubmed/27065999.

Mukherjee, S., and L. V. Hooper. 2015. "Antimicrobial defense of the intestine." *Immunity* 42 (1): 28-39. https://doi.org/10.1016/j.immuni.2014.12.028. https://www.ncbi.nlm.nih.gov/pubmed/25607457.

Naito, Y., K. Uchiyama, and T. Takagi. 2018. "A next-generation beneficial microbe: Akkermansia muciniphila." *J Clin Biochem Nutr* 63 (1): 33-35. https://doi.org/10.3164/jcbn.18-57. https://www.ncbi.nlm.nih.gov/pubmed/30087541.

Nguyen, N., B. Zhang, S. D. Holubar, D. S. Pardi, and S. Singh. 2019. "Treatment and prevention of pouchitis after ileal pouch-anal anastomosis for chronic ulcerative colitis." *Cochrane Database Syst Rev* 11 (11): CD001176. https://doi.org/10.1002/14651858.CD001176.pub5. https://www.ncbi.nlm.nih.gov/pubmed/31785173.

Nicholson, M. R., P. D. Mitchell, E. Alexander, S. Ballal, M. Bartlett, P. Becker, Z. Davidovics, M. Docktor, M. Dole, G. Felix, J. Gisser, S. K. Hourigan, M. K. Jensen, J. L. Kaplan, J. Kelsen, M. Kennedy, S. Khanna, E. Knackstedt, M. Leier, J. Lewis, A. Lodarek, S. Michail, M. Oliva-Hemker, T. Patton, K. Queliza, G. H. Russell, N. Singh, A. Solomon, D. L. Suskind, S. Werlin, R. Kellermayer, and S. A. Kahn. 2020. "Efficacy of Fecal Microbiota Transplantation for Clostridium difficile Infection in Children." *Clin Gastroenterol Hepatol* 18 (3): 612-619 e1. https://doi.org/10.1016/j.cgh.2019.04.037. https://www.ncbi.nlm.nih.gov/pubmed/31009795.

Nysten, J., and P. Van Dijck. 2023. "Can we microbe-manage our vitamin acquisition for better health?" *PLoS Pathog* 19 (5): e1011361. https://doi.org/10.1371/journal.ppat.1011361. https://www.ncbi.nlm.nih.gov/pubmed/37200232.

Oliphant, K., and E. Allen-Vercoe. 2019. "Macronutrient metabolism by the human gut microbiome: major fermentation by-products and their impact on host health." *Microbiome* 7 (1): 91. https://doi.org/10.1186/s40168-019-0704-8. https://www.ncbi.nlm.nih.gov/pubmed/31196177.

Oliveira, R. A., K. M. Ng, M. B. Correia, V. Cabral, H. Shi, J. L. Sonnenburg, K. C. Huang, and K. B. Xavier. 2020. "Klebsiella michiganensis transmission enhances resistance to Enterobacteriaceae gut invasion by nutrition competition." *Nat Microbiol* 5 (4): 630-641. https://doi.org/10.1038/s41564-019-0658-4. https://www.ncbi.nlm.nih.gov/pubmed/31959968.

Osbelt, L., M. Wende, E. Almasi, E. Derksen, U. Muthukumarasamy, T. R. Lesker, E. J. C. Galvez, M. C. Pils, E. Schalk, P. Chhatwal, J. Farber, M. Neumann-Schaal, T. Fischer, D. Schluter, and T. Strowig. 2021. "Klebsiella oxytoca causes colonization resistance against multidrug-resistant K. pneumoniae in the gut via cooperative carbohydrate competition." *Cell Host Microbe* 29 (11): 1663-1679 e7. https://doi.org/10.1016/j.chom.2021.09.003. https://www.ncbi.nlm.nih.gov/pubmed/34610293.

Paczosa, M. K., and J. Mecsas. 2016. "Klebsiella pneumoniae: Going on the Offense with a Strong Defense." *Microbiol Mol Biol Rev* 80 (3): 629-61. https://doi.org/10.1128/MMBR.00078-15. https://www.ncbi.nlm.nih.gov/pubmed/27307579.

Palmer, J. D., and K. R. Foster. 2022a. "Bacterial species rarely work together." *Science* 376 (6593): 581-582. https://doi.org/10.1126/science.abn5093. https://www.ncbi.nlm.nih.gov/pubmed/35511986.

---. 2022b. "The evolution of spectrum in antibiotics and bacteriocins." *Proc Natl Acad Sci U S A* 119 (38): e2205407119. https://doi.org/10.1073/pnas.2205407119. https://www.ncbi.nlm.nih.gov/pubmed/36099299.

Park, S. Y., and G. S. Seo. 2021. "Fecal Microbiota Transplantation: Is It Safe?" *Clin Endosc* 54 (2): 157-160. https://doi.org/10.5946/ce.2021.072. https://www.ncbi.nlm.nih.gov/pubmed/33827154.

Patangia, D. V., C. Anthony Ryan, E. Dempsey, R. Paul Ross, and C. Stanton. 2022. "Impact of antibiotics on the human microbiome and consequences for host health." *Microbiologyopen* 11 (1): e1260. https://doi.org/10.1002/mbo3.1260. https://www.ncbi.nlm.nih.gov/pubmed/35212478.

Pereira, F. C., and D. Berry. 2017. "Microbial nutrient niches in the gut." *Environ Microbiol* 19 (4): 1366-1378. https://doi.org/10.1111/1462-2920.13659. https://www.ncbi.nlm.nih.gov/pubmed/28035742.

Pereira, F. C., K. Wasmund, I. Cobankovic, N. Jehmlich, C. W. Herbold, K. S. Lee, B. Sziranyi, C. Vesely, T. Decker, R. Stocker, B. Warth, M. von Bergen, M. Wagner, and D. Berry. 2020. "Rational design of a microbial consortium of mucosal sugar utilizers reduces Clostridiodes difficile colonization." *Nat Commun* 11 (1): 5104. https://doi.org/10.1038/s41467-020-18928-1. https://www.ncbi.nlm.nih.gov/pubmed/33037214.

Perez, M., A. Ntemiri, H. Tan, H. M. B. Harris, H. M. Roager, C. Ribiere, and P. W. O'Toole. 2021. "A synthetic consortium of 100 gut commensals modulates the composition and function in a colon model of the microbiome of elderly subjects." *Gut Microbes* 13 (1): 1-19. https://doi.org/10.1080/19490976.2021.1919464. https://www.ncbi.nlm.nih.gov/pubmed/33993839.

Perry, J., N. Waglechner, and G. Wright. 2016. "The Prehistory of Antibiotic Resistance." *Cold Spring Harb Perspect Med* 6 (6). https://doi.org/10.1101/cshperspect.a025197. https://www.ncbi.nlm.nih.gov/pubmed/27252395.

Podolsky, S. H. 2012. "Metchnikoff and the microbiome." *Lancet* 380 (9856): 1810-1. https://doi.org/10.1016/s0140-6736(12)62018-2. https://www.ncbi.nlm.nih.gov/pubmed/23189332.

Pope, J. L., Y. Yang, R. C. Newsome, W. Sun, X. Sun, M. Ukhanova, J. Neu, J. P. Issa, V. Mai, and C. Jobin. 2019. "Microbial Colonization Coordinates the Pathogenesis of a Klebsiella pneumoniae Infant Isolate." *Sci Rep* 9 (1): 3380. https://doi.org/10.1038/s41598-019-39887-8. https://www.ncbi.nlm.nih.gov/pubmed/30833613.

Rao, A., R. L. Jump, N. J. Pultz, M. J. Pultz, and C. J. Donskey. 2006. "In vitro killing of nosocomial pathogens by acid and acidified nitrite." *Antimicrob Agents Chemother* 50 (11): 3901-4. https://doi.org/10.1128/AAC.01506-05. https://www.ncbi.nlm.nih.gov/pubmed/17065628.

Ratzke, C., J. Barrere, and J. Gore. 2020. "Strength of species interactions determines biodiversity and stability in microbial communities." *Nat Ecol Evol* 4 (3): 376-383. https://doi.org/10.1038/s41559-020-1099-4. https://www.ncbi.nlm.nih.gov/pubmed/32042124.

Reese, A. T., F. C. Pereira, A. Schintlmeister, D. Berry, M. Wagner, L. P. Hale, A. Wu, S. Jiang, H. K. Durand, X. Zhou, R. T. Premont, A. M. Diehl, T. M. O'Connell, S. C. Alberts, T. R. Kartzinel, R. M. Pringle, R. R. Dunn, J. P. Wright, and L. A. David. 2018. "Microbial nitrogen limitation in the mammalian large intestine." *Nat Microbiol* 3 (12): 1441-1450. https://doi.org/10.1038/s41564-018-0267-7. https://www.ncbi.nlm.nih.gov/pubmed/30374168.

Remya, P., M. Shanthi, and U. Sekar. 2018. "Occurrence and characterization of hyperviscous K1 and K2 serotype in Klebsiella pneumoniae." *J Lab Physicians* 10 (3): 283-288. https://doi.org/10.4103/JLP.JLP_48_18. https://www.ncbi.nlm.nih.gov/pubmed/30078963.

Rendueles, O. 2020. "Deciphering the role of the capsule of Klebsiella pneumoniae during pathogenesis: A cautionary tale." *Mol Microbiol* 113 (5): 883-888. https://doi.org/10.1111/mmi.14474. https://www.ncbi.nlm.nih.gov/pubmed/31997409.

Rohlke, F., and N. Stollman. 2012. "Fecal microbiota transplantation in relapsing Clostridium difficile infection." *Therap Adv Gastroenterol* 5 (6): 403-20. https://doi.org/10.1177/1756283X12453637. https://www.ncbi.nlm.nih.gov/pubmed/23152734.

Roselli, M., F. Natella, P. Zinno, B. Guantario, R. Canali, E. Schifano, M. De Angelis, O. Nikoloudaki, M. Gobbetti, G. Perozzi, and C. Devirgiliis. 2021. "Colonization Ability and Impact on Human Gut Microbiota of Foodborne Microbes From Traditional or Probiotic-Added Fermented Foods: A Systematic Review." *Front Nutr* 8: 689084. https://doi.org/10.3389/fnut.2021.689084. https://www.ncbi.nlm.nih.gov/pubmed/34395494.

Russo, T. A., and C. M. Marr. 2019. "Hypervirulent Klebsiella pneumoniae." *Clin Microbiol Rev* 32 (3). https://doi.org/10.1128/CMR.00001-19. https://www.ncbi.nlm.nih.gov/pubmed/31092506.

Sachs, R. E., and C. A. Edelstein. 2015. "Ensuring the safe and effective FDA regulation of fecal microbiota transplantation." *J Law Biosci* 2 (2): 396-415. https://doi.org/10.1093/jlb/lsv032. https://www.ncbi.nlm.nih.gov/pubmed/27774199.

Sampson, T. R., J. W. Debelius, T. Thron, S. Janssen, G. G. Shastri, Z. E. Ilhan, C. Challis, C. E. Schretter, S. Rocha, V. Gradinaru, M. F. Chesselet, A. Keshavarzian, K. M. Shannon, R. Krajmalnik-Brown, P. Wittung-Stafshede, R. Knight, and S. K. Mazmanian. 2016. "Gut Microbiota Regulate Motor Deficits and Neuroinflammation in a Model of Parkinson's Disease." *Cell* 167 (6): 1469-1480 e12. https://doi.org/10.1016/j.cell.2016.11.018. https://www.ncbi.nlm.nih.gov/pubmed/27912057.

Sbahi, H., and J. A. Di Palma. 2016. "Faecal microbiota transplantation: applications and limitations in treating gastrointestinal disorders." *BMJ Open Gastroenterol* 3 (1): e000087. https://doi.org/10.1136/bmjgast-2016-000087. https://www.ncbi.nlm.nih.gov/pubmed/27239328.

Scheithauer, T. P., G. M. Dallinga-Thie, W. M. de Vos, M. Nieuwdorp, and D. H. van Raalte. 2016. "Causality of small and large intestinal microbiota in weight regulation and insulin resistance." *Mol Metab* 5 (9): 759-70. https://doi.org/10.1016/j.molmet.2016.06.002. https://www.ncbi.nlm.nih.gov/pubmed/27617199.

Schluter, J., and K. R. Foster. 2012. "The evolution of mutualism in gut microbiota via host epithelial selection." *PLoS Biol* 10 (11): e1001424. https://doi.org/10.1371/journal.pbio.1001424. https://www.ncbi.nlm.nih.gov/pubmed/23185130.

Seddik, H. A., F. Bendali, F. Gancel, I. Fliss, G. Spano, and D. Drider. 2017. "Lactobacillus plantarum and Its Probiotic and Food Potentialities." *Probiotics Antimicrob Proteins* 9 (2): 111-122. https://doi.org/10.1007/s12602-017-9264-z. https://www.ncbi.nlm.nih.gov/pubmed/28271469.

Seedorf, H., N. W. Griffin, V. K. Ridaura, A. Reyes, J. Cheng, F. E. Rey, M. I. Smith, G. M. Simon, R. H. Scheffrahn, D. Woebken, A. M. Spormann, W. Van Treuren, L. K. Ursell, M.

Pirrung, A. Robbins-Pianka, B. L. Cantarel, V. Lombard, B. Henrissat, R. Knight, and J. I. Gordon. 2014. "Bacteria from diverse habitats colonize and compete in the mouse gut." *Cell* 159 (2): 253-66. https://doi.org/10.1016/j.cell.2014.09.008. https://www.ncbi.nlm.nih.gov/pubmed/25284151.

Sender, R., S. Fuchs, and R. Milo. 2016. "Revised Estimates for the Number of Human and Bacteria Cells in the Body." *PLoS Biol* 14 (8): e1002533. https://doi.org/10.1371/journal.pbio.1002533. https://www.ncbi.nlm.nih.gov/pubmed/27541692.

Sequeira, R. P., J. A. K. McDonald, J. R. Marchesi, and T. B. Clarke. 2020. "Commensal Bacteroidetes protect against Klebsiella pneumoniae colonization and transmission through IL-36 signalling." *Nat Microbiol* 5 (2): 304-313. https://doi.org/10.1038/s41564-019-0640-1. https://www.ncbi.nlm.nih.gov/pubmed/31907407.

Serapio-Palacios, A., S. E. Woodward, S. L. Vogt, W. Deng, A. Creus-Cuadros, K. E. Huus, M. Cirstea, M. Gerrie, W. Barcik, H. Yu, and B. B. Finlay. 2022. "Type VI secretion systems of pathogenic and commensal bacteria mediate niche occupancy in the gut." *Cell Rep* 39 (4): 110731. https://doi.org/10.1016/j.celrep.2022.110731. https://www.ncbi.nlm.nih.gov/pubmed/35476983.

Sharon, G., N. J. Cruz, D. W. Kang, M. J. Gandal, B. Wang, Y. M. Kim, E. M. Zink, C. P. Casey, B. C. Taylor, C. J. Lane, L. M. Bramer, N. G. Isern, D. W. Hoyt, C. Noecker, M. J. Sweredoski, A. Moradian, E. Borenstein, J. K. Jansson, R. Knight, T. O. Metz, C. Lois, D. H. Geschwind, R. Krajmalnik-Brown, and S. K. Mazmanian. 2019. "Human Gut Microbiota from Autism Spectrum Disorder Promote Behavioral Symptoms in Mice." *Cell* 177 (6): 1600-1618 e17. https://doi.org/10.1016/j.cell.2019.05.004. https://www.ncbi.nlm.nih.gov/pubmed/31150625.

Shepherd, E. S., W. C. DeLoache, K. M. Pruss, W. R. Whitaker, and J. L. Sonnenburg. 2018. "An exclusive metabolic niche enables strain engraftment in the gut microbiota." *Nature* 557 (7705): 434-438. https://doi.org/10.1038/s41586-018-0092-4. https://www.ncbi.nlm.nih.gov/pubmed/29743671.

Shoubridge, A. P., J. M. Choo, A. M. Martin, D. J. Keating, M. L. Wong, J. Licinio, and G. B. Rogers. 2022. "The gut microbiome and mental health: advances in research and emerging priorities." *Mol Psychiatry* 27 (4): 1908-1919. https://doi.org/10.1038/s41380-022-01479-w. https://www.ncbi.nlm.nih.gov/pubmed/35236957.

Shrestha, J., F. Zahra, and Jr P. Cannady. 2023. "Antimicrobial Stewardship." In *StatPearls*. Treasure Island (FL).

Shumaker, A. M., V. Laclare McEneany, M. J. Coyne, P. A. Silver, and L. E. Comstock. 2019. "Identification of a Fifth Antibacterial Toxin Produced by a Single Bacteroides fragilis Strain." *J Bacteriol* 201 (8). https://doi.org/10.1128/JB.00577-18. https://www.ncbi.nlm.nih.gov/pubmed/30692177.

Sicard, J. F., G. Le Bihan, P. Vogeleer, M. Jacques, and J. Harel. 2017. "Interactions of Intestinal Bacteria with Components of the Intestinal Mucus." *Front Cell Infect Microbiol* 7: 387. https://doi.org/10.3389/fcimb.2017.00387. https://www.ncbi.nlm.nih.gov/pubmed/28929087.

Singh, A., A. N. Sarangi, A. Goel, R. Srivastava, R. Bhargava, P. Gaur, A. Aggarwal, and R. Aggarwal. 2018. "Effect of administration of a probiotic preparation on gut microbiota and immune response in healthy women in India: an open-label, single-

arm pilot study." *BMC Gastroenterol* 18 (1): 85. https://doi.org/10.1186/s12876-018-0819-6. https://www.ncbi.nlm.nih.gov/pubmed/29907093.

Slack, E., and M. Diard. 2022. "Resistance is futile? Mucosal immune mechanisms in the context of microbial ecology and evolution." *Mucosal Immunol* 15 (6): 1188-1198. https://doi.org/10.1038/s41385-022-00574-z. https://www.ncbi.nlm.nih.gov/pubmed/36329192.

Soldan, R., N. Sanguankiattichai, M. Bach-Pages, I. Bervoets, W. E. Huang, and G. M. Preston. 2021. "From macro to micro: a combined bioluminescence-fluorescence approach to monitor bacterial localization." *Environ Microbiol* 23 (4): 2070-2085. https://doi.org/10.1111/1462-2920.15296. https://www.ncbi.nlm.nih.gov/pubmed/33103833.

Sonnenborn, U. 2016. "Escherichia coli strain Nissle 1917-from bench to bedside and back: history of a special Escherichia coli strain with probiotic properties." *FEMS Microbiol Lett* 363 (19). https://doi.org/10.1093/femsle/fnw212. https://www.ncbi.nlm.nih.gov/pubmed/27619890.

Sonnenburg, E. D., S. A. Smits, M. Tikhonov, S. K. Higginbottom, N. S. Wingreen, and J. L. Sonnenburg. 2016. "Diet-induced extinctions in the gut microbiota compound over generations." *Nature* 529 (7585): 212-5. https://doi.org/10.1038/nature16504. https://www.ncbi.nlm.nih.gov/pubmed/26762459.

Sonnenburg, E. D., and J. L. Sonnenburg. 2019. "The ancestral and industrialized gut microbiota and implications for human health." *Nat Rev Microbiol* 17 (6): 383-390. https://doi.org/10.1038/s41579-019-0191-8. https://www.ncbi.nlm.nih.gov/pubmed/31089293.

Sorbara, M. T., and E. G. Pamer. 2019. "Interbacterial mechanisms of colonization resistance and the strategies pathogens use to overcome them." *Mucosal Immunol* 12 (1): 1-9. https://doi.org/10.1038/s41385-018-0053-0. https://www.ncbi.nlm.nih.gov/pubmed/29988120.

Soto, S. M. 2013. "Role of efflux pumps in the antibiotic resistance of bacteria embedded in a biofilm." *Virulence* 4 (3): 223-9. https://doi.org/10.4161/viru.23724. https://www.ncbi.nlm.nih.gov/pubmed/23380871.

Stecher, B., A. J. Macpherson, S. Hapfelmeier, M. Kremer, T. Stallmach, and W. D. Hardt. 2005. "Comparison of Salmonella enterica serovar Typhimurium colitis in germfree mice and mice pretreated with streptomycin." *Infect Immun* 73 (6): 3228-41. https://doi.org/10.1128/IAI.73.6.3228-3241.2005. https://www.ncbi.nlm.nih.gov/pubmed/15908347.

Steeb, B., B. Claudi, N. A. Burton, P. Tienz, A. Schmidt, H. Farhan, A. Maze, and D. Bumann. 2013. "Parallel exploitation of diverse host nutrients enhances Salmonella virulence." *PLoS Pathog* 9 (4): e1003301. https://doi.org/10.1371/journal.ppat.1003301. https://www.ncbi.nlm.nih.gov/pubmed/23633950.

Steele, M. I., E. V. S. Motta, T. Gattu, D. Martinez, and N. A. Moran. 2021. "The Gut Microbiota Protects Bees from Invasion by a Bacterial Pathogen." *Microbiol Spectr* 9 (2): e0039421. https://doi.org/10.1128/Spectrum.00394-21. https://www.ncbi.nlm.nih.gov/pubmed/34523998.

Suez, J., N. Zmora, E. Segal, and E. Elinav. 2019. "The pros, cons, and many unknowns of probiotics." *Nat Med* 25 (5): 716-729. https://doi.org/10.1038/s41591-019-0439-x. https://www.ncbi.nlm.nih.gov/pubmed/31061539.

Tang, Q., G. Jin, G. Wang, T. Liu, X. Liu, B. Wang, and H. Cao. 2020. "Current Sampling Methods for Gut Microbiota: A Call for More Precise Devices." *Front Cell Infect Microbiol* 10: 151. https://doi.org/10.3389/fcimb.2020.00151. https://www.ncbi.nlm.nih.gov/pubmed/32328469.

Teng, C., K. R. Reveles, O. O. Obodozie-Ofoegbu, and C. R. Frei. 2019. "Clostridium difficile Infection Risk with Important Antibiotic Classes: An Analysis of the FDA Adverse Event Reporting System." *Int J Med Sci* 16 (5): 630-635. https://doi.org/10.7150/ijms.30739. https://www.ncbi.nlm.nih.gov/pubmed/31217729.

Theriot, C. M., M. J. Koenigsknecht, P. E. Carlson, Jr., G. E. Hatton, A. M. Nelson, B. Li, G. B. Huffnagle, Z. Li J, and V. B. Young. 2014. "Antibiotic-induced shifts in the mouse gut microbiome and metabolome increase susceptibility to Clostridium difficile infection." *Nat Commun* 5: 3114. https://doi.org/10.1038/ncomms4114. https://www.ncbi.nlm.nih.gov/pubmed/24445449.

Tilman, D.; Isbell, F. and Cowles, J.M. 2014. "Biodiversity and Ecosystem Functioning." *Annual Review of Ecology, Evolution, and Systematics* 45: 471-493.

Torres, A., N. Zhong, J. Pachl, J. F. Timsit, M. Kollef, Z. Chen, J. Song, D. Taylor, P. J. Laud, G. G. Stone, and J. W. Chow. 2018. "Ceftazidime-avibactam versus meropenem in nosocomial pneumonia, including ventilator-associated pneumonia (REPROVE): a randomised, double-blind, phase 3 non-inferiority trial." *Lancet Infect Dis* 18 (3): 285-295. https://doi.org/10.1016/S1473-3099(17)30747-8. https://www.ncbi.nlm.nih.gov/pubmed/29254862.

Tropini, C., K. A. Earle, K. C. Huang, and J. L. Sonnenburg. 2017. "The Gut Microbiome: Connecting Spatial Organization to Function." *Cell Host Microbe* 21 (4): 433-442. https://doi.org/10.1016/j.chom.2017.03.010. https://www.ncbi.nlm.nih.gov/pubmed/28407481.

Turnbull, Lindsay A., Jonathan M. Levine, Alexander J. F. Fergus, and Jana S. Petermann. 2010. "Species diversity reduces invasion success in pathogen-regulated communities." *Oikos* 119 (6): 1040-1046. http://www.jstor.org/stable/25700338.

Umesaki, Y., H. Setoyama, S. Matsumoto, and Y. Okada. 1993. "Expansion of alpha beta T-cell receptor-bearing intestinal intraepithelial lymphocytes after microbial colonization in germ-free mice and its independence from thymus." *Immunology* 79 (1): 32-7. https://www.ncbi.nlm.nih.gov/pubmed/8509140.

Valdes, A. M., J. Walter, E. Segal, and T. D. Spector. 2018. "Role of the gut microbiota in nutrition and health." *BMJ* 361: k2179. https://doi.org/10.1136/bmj.k2179. https://www.ncbi.nlm.nih.gov/pubmed/29899036.

van Nood, E., A. Vrieze, M. Nieuwdorp, S. Fuentes, E. G. Zoetendal, W. M. de Vos, C. E. Visser, E. J. Kuijper, J. F. Bartelsman, J. G. Tijssen, P. Speelman, M. G. Dijkgraaf, and J. J. Keller. 2013. "Duodenal infusion of donor feces for recurrent Clostridium difficile." *N Engl J Med* 368 (5): 407-15. https://doi.org/10.1056/NEJMoa1205037. https://www.ncbi.nlm.nih.gov/pubmed/23323867.

van Oppen, M. J. H., and L. L. Blackall. 2019. "Coral microbiome dynamics, functions and design in a changing world." *Nat Rev Microbiol* 17 (9): 557-567. https://doi.org/10.1038/s41579-019-0223-4. https://www.ncbi.nlm.nih.gov/pubmed/31263246.

Velazquez, E. M., H. Nguyen, K. T. Heasley, C. H. Saechao, L. M. Gil, A. W. L. Rogers, B. M. Miller, M. R. Rolston, C. A. Lopez, Y. Litvak, M. J. Liou, F. Faber, D. N. Bronner, C. R.

Tiffany, M. X. Byndloss, A. J. Byndloss, and A. J. Baumler. 2019. "Endogenous Enterobacteriaceae underlie variation in susceptibility to Salmonella infection." *Nat Microbiol* 4 (6): 1057-1064. https://doi.org/10.1038/s41564-019-0407-8. https://www.ncbi.nlm.nih.gov/pubmed/30911125.

Velazquez-Meza, M. E., M. Galarde-Lopez, B. Carrillo-Quiroz, and C. M. Alpuche-Aranda. 2022. "Antimicrobial resistance: One Health approach." *Vet World* 15 (3): 743-749. https://doi.org/10.14202/vetworld.2022.743-749. https://www.ncbi.nlm.nih.gov/pubmed/35497962.

Wagg, C., Y. Hautier, S. Pellkofer, S. Banerjee, B. Schmid, and M. G. van der Heijden. 2021. "Diversity and asynchrony in soil microbial communities stabilizes ecosystem functioning." *Elife* 10. https://doi.org/10.7554/eLife.62813. https://www.ncbi.nlm.nih.gov/pubmed/33755017.

Walker, K. A., and V. L. Miller. 2020. "The intersection of capsule gene expression, hypermucoviscosity and hypervirulence in Klebsiella pneumoniae." *Curr Opin Microbiol* 54: 95-102. https://doi.org/10.1016/j.mib.2020.01.006. https://www.ncbi.nlm.nih.gov/pubmed/32062153.

Walker, K. A., T. A. Miner, M. Palacios, D. Trzilova, D. R. Frederick, C. A. Broberg, V. E. Sepulveda, J. D. Quinn, and V. L. Miller. 2019. "A Klebsiella pneumoniae Regulatory Mutant Has Reduced Capsule Expression but Retains Hypermucoviscosity." *mBio* 10 (2). https://doi.org/10.1128/mBio.00089-19. https://www.ncbi.nlm.nih.gov/pubmed/30914502.

Wang, Q., M. Nute, and T. J. Treangen. 2023. "Bakdrive: identifying a minimum set of bacterial species driving interactions across multiple microbial communities." *Bioinformatics* 39 (39 Suppl 1): i47-i56. https://doi.org/10.1093/bioinformatics/btad236. https://www.ncbi.nlm.nih.gov/pubmed/37387148.

Wareth, G., and H. Neubauer. 2021. "The Animal-foods-environment interface of Klebsiella pneumoniae in Germany: an observational study on pathogenicity, resistance development and the current situation." *Vet Res* 52 (1): 16. https://doi.org/10.1186/s13567-020-00875-w. https://www.ncbi.nlm.nih.gov/pubmed/33557913.

Wasan, H., D. Singh, K. H. Reeta, and Y. K. Gupta. 2023. "Landscape of Push Funding in Antibiotic Research: Current Status and Way Forward." *Biology (Basel)* 12 (1). https://doi.org/10.3390/biology12010101. https://www.ncbi.nlm.nih.gov/pubmed/36671792.

Weersma, R. K., A. Zhernakova, and J. Fu. 2020. "Interaction between drugs and the gut microbiome." *Gut* 69 (8): 1510-1519. https://doi.org/10.1136/gutjnl-2019-320204. https://www.ncbi.nlm.nih.gov/pubmed/32409589.

Weisser, W. W. 2017. "Biodiversity effects on ecosystem functioning in a 15-year grassland experiment: Patterns, mechanisms and open questions."

Wheeler, R., P. A. D. Bastos, O. Disson, A. Rifflet, I. Gabanyi, J. Spielbauer, M. Berard, M. Lecuit, and I. G. Boneca. 2023. "Microbiota-induced active translocation of peptidoglycan across the intestinal barrier dictates its within-host dissemination." *Proc Natl Acad Sci U S A* 120 (4): e2209936120. https://doi.org/10.1073/pnas.2209936120. https://www.ncbi.nlm.nih.gov/pubmed/36669110.

Whitaker, W. R., E. S. Shepherd, and J. L. Sonnenburg. 2017. "Tunable Expression Tools Enable Single-Cell Strain Distinction in the Gut Microbiome." *Cell* 169 (3): 538-546 e12. https://doi.org/10.1016/j.cell.2017.03.041. https://www.ncbi.nlm.nih.gov/pubmed/28431251.

Whitman, W. B., D. C. Coleman, and W. J. Wiebe. 1998. "Prokaryotes: the unseen majority." *Proc Natl Acad Sci U S A* 95 (12): 6578-83. https://doi.org/10.1073/pnas.95.12.6578. https://www.ncbi.nlm.nih.gov/pubmed/9618454.

WHO. 2017. "WHO Global Priority List of Antibiotic-Resistant Bacteria to Guide Research, Discovery and Development of New Antibiotics."

Wotzka, S. Y., M. Kreuzer, L. Maier, M. Arnoldini, B. D. Nguyen, A. O. Brachmann, D. L. Berthold, M. Zund, A. Hausmann, E. Bakkeren, D. Hoces, E. Gul, M. Beutler, T. Dolowschiak, M. Zimmermann, T. Fuhrer, K. Moor, U. Sauer, A. Typas, J. Piel, M. Diard, A. J. Macpherson, B. Stecher, S. Sunagawa, E. Slack, and W. D. Hardt. 2019. "Escherichia coli limits Salmonella Typhimurium infections after diet shifts and fat-mediated microbiota perturbation in mice." *Nat Microbiol* 4 (12): 2164-2174. https://doi.org/10.1038/s41564-019-0568-5. https://www.ncbi.nlm.nih.gov/pubmed/31591555.

Wotzka, S. Y., M. Kreuzer, L. Maier, M. Zund, M. Schlumberger, B. Nguyen, M. Fox, D. Pohl, H. Heinrich, G. Rogler, L. Biedermann, M. Scharl, S. Sunagawa, W. D. Hardt, and B. Misselwitz. 2018. "Microbiota stability in healthy individuals after single-dose lactulose challenge-A randomized controlled study." *PLoS One* 13 (10): e0206214. https://doi.org/10.1371/journal.pone.0206214. https://www.ncbi.nlm.nih.gov/pubmed/30359438.

Yang, J., J. Pu, S. Lu, X. Bai, Y. Wu, D. Jin, Y. Cheng, G. Zhang, W. Zhu, X. Luo, R. Rossello-Mora, and J. Xu. 2020. "Species-Level Analysis of Human Gut Microbiota With Metataxonomics." *Front Microbiol* 11: 2029. https://doi.org/10.3389/fmicb.2020.02029. https://www.ncbi.nlm.nih.gov/pubmed/32983030.

Yang, Z. Q., Y. L. Huang, H. W. Zhou, R. Zhang, and K. Zhu. 2018. "Persistent carbapenem-resistant Klebsiella pneumoniae: a Trojan horse." *Lancet Infect Dis* 18 (1): 22-23. https://doi.org/10.1016/S1473-3099(17)30627-8. https://www.ncbi.nlm.nih.gov/pubmed/29102519.

Yonatan, Y., G. Amit, J. Friedman, and A. Bashan. 2022. "Complexity-stability trade-off in empirical microbial ecosystems." *Nat Ecol Evol* 6 (6): 693-700. https://doi.org/10.1038/s41559-022-01745-8. https://www.ncbi.nlm.nih.gov/pubmed/35484221.

Young, T. M., A. S. Bray, R. K. Nagpal, D. L. Caudell, H. Yadav, and M. A. Zafar. 2020. "Animal Model To Study Klebsiella pneumoniae Gastrointestinal Colonization and Host-to-Host Transmission." *Infect Immun* 88 (11). https://doi.org/10.1128/IAI.00071-20. https://www.ncbi.nlm.nih.gov/pubmed/32839189.

Zeng, M. Y., N. Inohara, and G. Nunez. 2017. "Mechanisms of inflammation-driven bacterial dysbiosis in the gut." *Mucosal Immunol* 10 (1): 18-26. https://doi.org/10.1038/mi.2016.75. https://www.ncbi.nlm.nih.gov/pubmed/27554295.

Zhang, L., C. Liu, Q. Jiang, and Y. Yin. 2021. "Butyrate in Energy Metabolism: There Is Still More to Learn." *Trends Endocrinol Metab* 32 (3): 159-169.

https://doi.org/10.1016/j.tem.2020.12.003. https://www.ncbi.nlm.nih.gov/pubmed/33461886.

Zheng, D., T. Liwinski, and E. Elinav. 2020. "Interaction between microbiota and immunity in health and disease." *Cell Res* 30 (6): 492-506. https://doi.org/10.1038/s41422-020-0332-7. https://www.ncbi.nlm.nih.gov/pubmed/32433595.